

# Summer School on GNSS CORE TECHNOLOGIES

## July 2-4, 2012

### Lecture Notes

Joint Research Centre,  
Ispra (VA), Italy

#### Speakers:

Jahshan Bhatti  
Daniele Borio  
Joaquim Fortuny  
Olivier Julien  
Heidi Kuusniemi  
Gérard Lachapelle  
Letizia Lo Presti  
Cillian O'Driscoll



[www.jrc.ec.europa.eu](http://www.jrc.ec.europa.eu)

Joaquim Fortuny-Guasch  
European Commission • Joint Research Centre  
Institute for the Protection and Security of the Citizen (IPSC)  
Tel. +39 0332 785104  
Email: Joaquim.Fortuny@jrc.ec.europa.eu





# Joint Research Centre

The European Commission's in-house science service



Geel



Karlsruhe



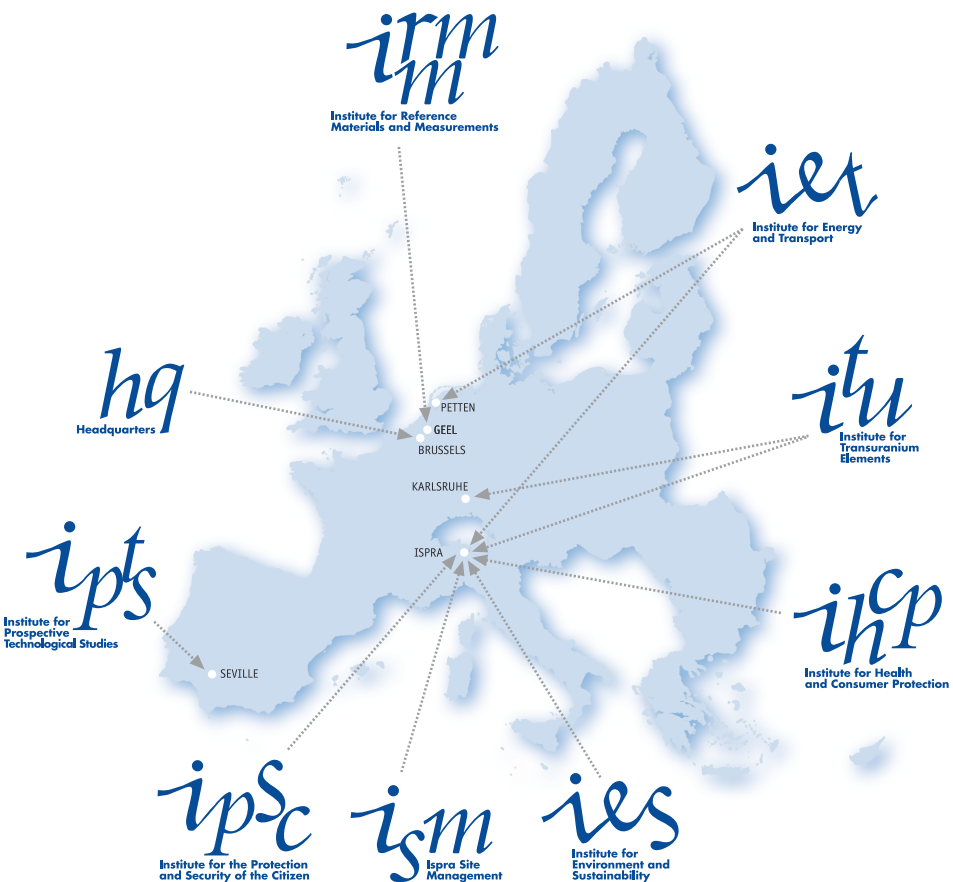
Petten



Ispra



Seville



## For further information

European Commission  
Joint Research Centre  
External Communication Unit  
SDME 10/78  
B-1049 Brussels  
  
E-mail: [jrc-info@ec.europa.eu](mailto:jrc-info@ec.europa.eu)

Brussels  
Tel. +32 (0)2 29 74181  
Fax +32 (0)2 29 96322  
Ispra  
Tel. +39 0332 78 9889  
Fax +39 0332 78 5409

## Mission

The mission of the Joint Research Centre (JRC) is to provide customer-driven scientific and technical support for the conception, development, implementation and monitoring of European Union policies. As a service of the European Commission, the JRC functions as a reference centre of science and technology for the Union. Close to the policy-making process, it serves the common interest of the Member States, while being independent of special interests, whether private or national.

[www.jrc.ec.europa.eu](http://www.jrc.ec.europa.eu)

*Serving society,  
stimulating innovation,  
supporting legislation*



# GNSS

## Summer School

# GNSS

## Summer School

# GNSS

## Summer School

### Monday July, 2

10:00	Opening section, Joaquim Fortuny <ul style="list-style-type: none"> <li>The JRC and his mission, brief summary of the JRC activities on GNSS and Galileo</li> <li>Introduction: motivations, objectives and contents of the summer school</li> </ul>
10:45	Coffee break
11:00	Introduction to GNSS, Cillian O'Driscoll <ul style="list-style-type: none"> <li>GNSS System architecture</li> <li>GNSS signal structure</li> </ul>
12:30	Lunch break
14:00	GNSS Receiver Architecture, Daniele Borio <ul style="list-style-type: none"> <li>Antennas, Receiver Front-end, Local oscillators and frequency synthesis, etc.</li> </ul>
15:30	Coffee break
15:45	GNSS signal acquisition, Letizia Lo Presti
17:30	End of the day
18:00	Bus for the hotel

### Tuesday July, 3

9:30	GNSS Signal Tracking, Daniele Borio <ul style="list-style-type: none"> <li>Summary of the previous day</li> <li>Tracking Overview</li> <li>Tracking Loop Structure</li> <li>Tracking performance: Linear and Non-linear Analysis</li> </ul>
10:45	Coffee break
11:00	Signal processing utilities, Cillian O'Driscoll <ul style="list-style-type: none"> <li>C/N0 estimation, Bit synchronization, etc.</li> </ul>
11:30	Tracking loop demo, Cillian O'Driscoll
12:00	Lunch break
13:30	From signal tracking to the navigation solution, Heidi Kuusniemi <ul style="list-style-type: none"> <li>GNSS Measurements</li> <li>Computation of the navigation solution</li> </ul>
14:30	Carrier phase positioning, Gérard Lachapelle
15:30	Coffee break
15:45	New Galileo Signals, Olivier Julien <ul style="list-style-type: none"> <li>New GNSS modulations (BOC and derived mod)</li> <li>Changes in the receiver architecture</li> </ul>
16:45	Galileo and EGNOS programme update, DG ENTR
17:30	End of the day
18:00	Bus for the hotel
19:30	Bus pick up
20:00	Social dinner

### Wednesday July, 4

9:30	GNSS interference, Heidi Kuusniemi <ul style="list-style-type: none"> <li>Introduction: type of interference</li> <li>CW, Pulsed, Chirp, etc.</li> <li>GNSS jammers</li> </ul>
10:45	Interference detection and mitigation, Daniele Borio <ul style="list-style-type: none"> <li>Interference cancellation</li> <li>Notch filters</li> <li>Pulse blanking</li> <li>Transformed domain excision</li> </ul>
12:30	Lunch break
13:30	Jamming Location and Spoofing, Jahshan Bhatti
14:00	Pseudolites, Cillian O'Driscoll <ul style="list-style-type: none"> <li>Issues and opportunities</li> <li>Signal and system design</li> <li>Coexistence analysis</li> </ul>
15:30	Coffee break
15:45	Open discussion <ul style="list-style-type: none"> <li>For the students requiring ECTS accreditation: final examination</li> </ul>
17:00	End of the day and of the workshop



# JRC Summer School on GNSS Core Technologies

## KEYNOTE SPEAKERS

### **Jahshan Bhatti**

Jahshan A. Bhatti is pursuing a Ph.D. in the Department of Aerospace Engineering and Engineering Mechanics at the University of Texas at Austin, where he also received his M.S. and B.S. He is a member of the UT Radionavigation Laboratory. His research interests are in the development of small satellites, software-defined radio applications, space weather, and GNSS security and integrity.

### **Daniele Borio**

Daniele Borio received the M.S. degree in Communications Engineering from Politecnico di Torino, Italy, the M.S. degree in Electronics Engineering from ENSERG/INPG de Grenoble, France, in 2004, and the doctoral degree in electrical engineering from Politecnico di Torino in April 2008. From January 2008 to September 2010 he was a senior research associate in the PLAN group of the University of Calgary, Canada. Since October 2010 he has been a post-doctoral fellow at the Joint Research Centre of the European Commission. His research interests include the fields of digital and wireless communications, location and navigation.

### **Joaquim Fortuny-Guasch**

Joaquim Fortuny-Guasch received the Engineering degree in telecommunications from the Technical University of Catalonia (UPC), Barcelona, Spain, in 1988, and the Dr.-Ing. degree in electrical engineering from the Universität Karlsruhe (TH), Karlsruhe, Germany, in 2001. Since 1993, he has been working for the Joint Research Centre (JRC) of the European Commission, Ispra, Italy, as senior scientific officer. He is the head of the European Microwave Signature Laboratory and leads the JRC research group on GNSS and wireless communications systems.

### **Olivier Julien**

Olivier Julien is the head of the Signal Processing and Navigation (SIGNAV) research group of the ENAC (Ecole Nationale de l'Aviation Civile), Toulouse, France. His research interests are GNSS receiver design, GNSS multipath and interference mitigation and GNSS interoperability.

He received his engineering degree in 2001 in civil aviation with major in digital communications from ENAC and his PhD in 2005 from the Department of Geomatics Engineering of the University of Calgary, Canada.

### **Heidi Kuusniemi**

Dr. Heidi Kuusniemi is a Research Manager at the Department of Navigation and Positioning at the Finnish Geodetic Institute, where she leads the research group on satellite and radio navigation. She is also a Lecturer at the Department of Surveying Sciences at Aalto University, Finland. She received her M.Sc. degree in 2002 and D.Sc.(Tech.) degree in 2005 from Tampere University of Technology, Finland. Her doctoral studies on personal satellite navigation were partly conducted at the Department of Geomatics Engineering at the University of Calgary, Canada. From 2005 to 2009 she worked as a GPS Software Engineer in research and development at Fastrax Ltd. Now, her research interests cover various aspects of GNSS navigation, quality control, software defined receivers, multi-sensor fusion algorithms for seamless outdoor/indoor positioning, and GNSS interference mitigation methods. She is the President of the Nordic Institute of Navigation since May 2011, and a member of the IEEE and the ION.

### **Gérard Lachapelle**

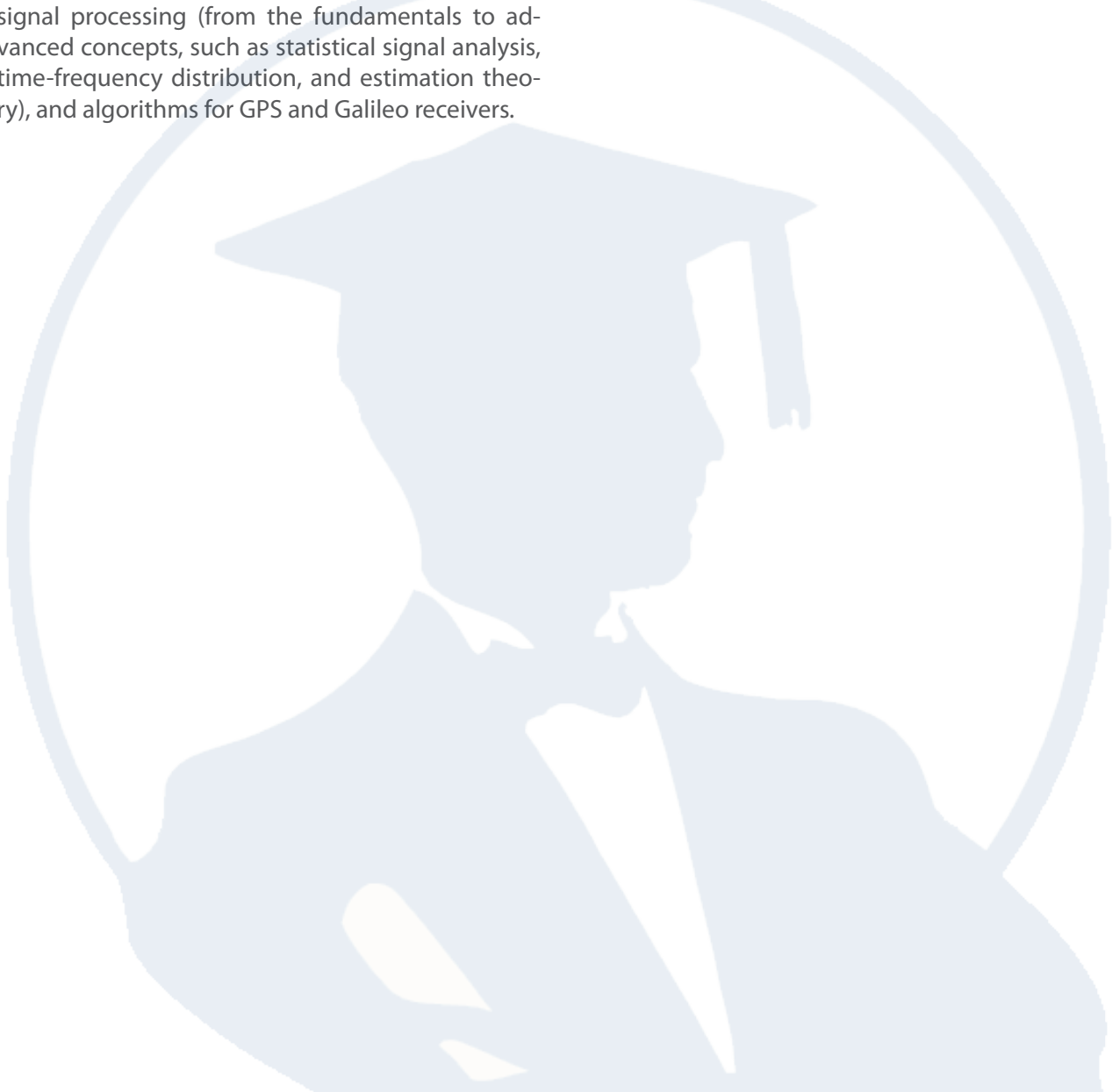
Professor Gérard Lachapelle has been involved in GNSS R&D since 1980, first in industry and, since 1988, at the University of Calgary in the Dept of Geomatics Engineering where holds a research Chair in wireless location and is a member of the PLAN Group. He has contributed to numerous aspects of ground and satellite-based navigation and has received scores of awards and other recognitions for his work. He and his research colleagues have developed algorithms and software related to GNSS carrier phase-based positioning, GNSS signal enhancements, augmentation with self-contained sensors, software receivers, pedestrian navigation, and interference and spoofing mitigation, many of which are patented. Professor Lachapelle holds degrees for Laval University, the University of Oxford, the University of Helsinki and the Technical University at Graz.

## **Letizia Lo Presti**

Letizia Lo Presti, is a full professor with the Information Engineering Faculty of Politecnico di Torino, working in the Electronics Department. She is the head of the NavSAS group, focused on research activities in the field of Global Navigation Satellite Systems, and she is the scientific coordinator of the Master on Navigation and Related Applications held by Politecnico di Torino (since 2003). Her research activities cover the field of digital signal processing, simulation of telecommunication systems, and the technology of navigation and positioning systems. Her teaching activity is mainly focused on signal processing (from the fundamentals to advanced concepts, such as statistical signal analysis, time-frequency distribution, and estimation theory), and algorithms for GPS and Galileo receivers.

## **Cillian O'Driscoll**

Cillian O'Driscoll received his M.Eng.Sc. and Ph.D. degrees from the Department of Electrical and Electronic Engineering, University College Cork, Ireland. He was a senior research engineer with the Position, Location and Navigation (PLAN) group at the Department of Geomatics Engineering in the University of Calgary from 2007 to 2010. Since January 2011 he has been a post-doctoral researcher in the Institute for the Protection and Security of the Citizen (IPSC) at the Joint Research Centre (JRC) of the European Commission. His research interests are in all areas of GNSS signal processing.





# Overview of JRC GNSS Activities

Joaquim Fortuny

Joint Research Centre,  
Ispra (VA), Italy



Joint Research Centre



## Outline

- Pseudolites**
- GNSS Timing**
- Space Weather**
- Interference**

Joint Research Centre

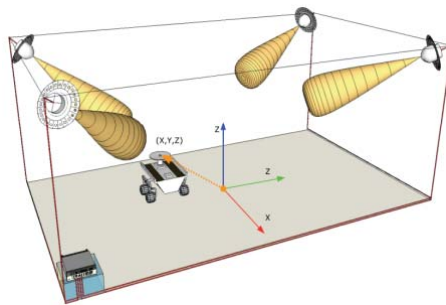


## Pseudolites

Ground-based transmitters playing the role of satellites when satellites are not available

Ground-based extension of a GNSS

Non-Participating Receivers:  
GNSS receivers not designed or not able to process a pseudolite signal



Pseudolite signals can severely affect the performance of non-participating GNSS receivers

Issues:

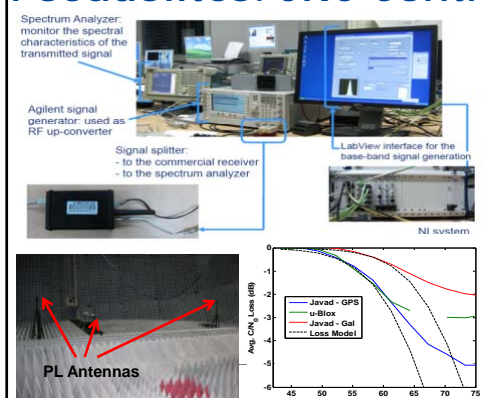
- Regulatory
- **Interference**
- Monitoring
- Technical

**JRC Contribution:**  
**Support to DG-ENTR**  
**Support to CEPT**

Joint Research Centre



## Pseudolites: JRC Contribution



Experimental Work

Development of a model for predicting the loss caused by pulsed pseudolites:

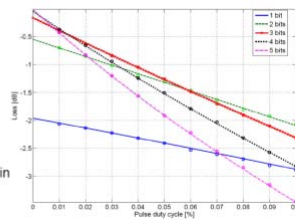
criteria for setting safeguard distances

(input to **CEPT**)

Theoretical Analysis

$$\frac{L_q \cdot (1 - d)}{1 + g(B, A_q) \frac{d}{1-d}}$$

Quantization loss  
Pulse duty cycle  
ADC: number of bits  
AGC gain

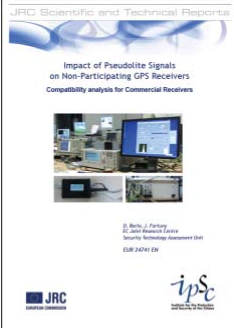




## JRC Reports on Pseudolites

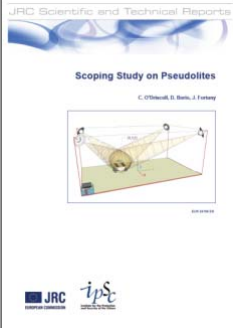
Available at: <http://publications.jrc.ec.europa.eu/repository>

Preliminary analysis  
for EC meeting on  
PL



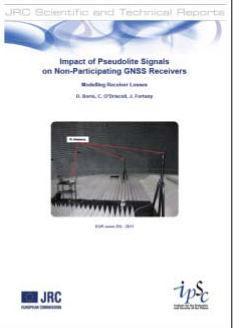
**JRC**  
Joint Research  
Centre

Scoping study  
mandated by  
DG-ENTR



**JRC**  
Joint Research  
Centre

Contribution to  
CEPT SE40  
activities



**JRC**  
Joint Research  
Centre

**Joint Research Centre**

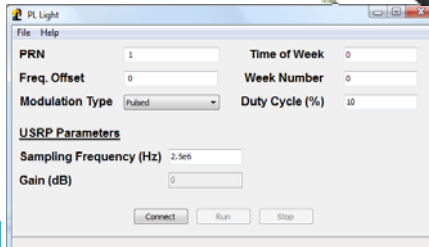


## Current and Future Activities

**EPCIP 2010:**  
Analysis on participating receivers

- ✓ Mitigation techniques:
  - Successive interference cancellation (SIC)
  - Pulse blanking
  - Time-Frequency excision
- ✓ Pulse synchronization techniques
- ✓ Development of PL receiver

Development of an USRP II pseudolite prototype

**Joint Research Centre**



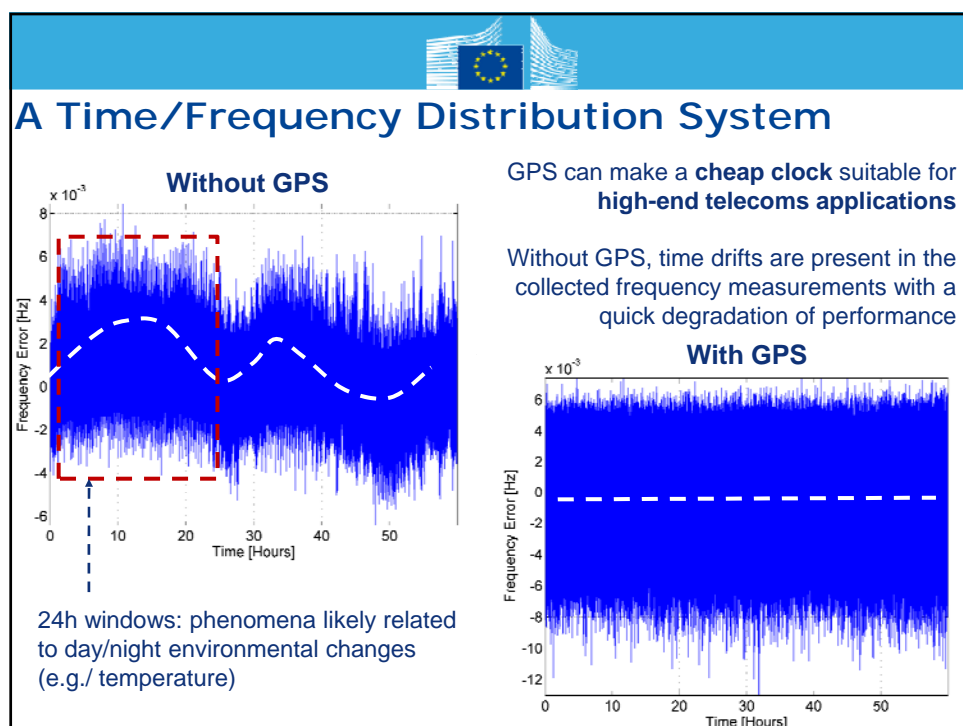
## GNSS Timing

**GNSS:**  
time and frequency distribution  
for critical infrastructures

- ✓ Power plants and power distribution
- ✓ Telecommunication network
- ✓ Financial Infrastructures (Bank transactions)

In general: over-reliance on GPS and GNSS

Vulnerability with respect to several sources of interference



## Timing: JRC Contribution

- ✓ Impact of **RF interference** on GNSS timing receivers  
(Agreement with DG-HOME)
- ✓ Seven different GPS clocks of different quality
- ✓ From the experiments: GPS can be **easily denied**



Anechoic chamber experiments:  
different types and levels of  
interference



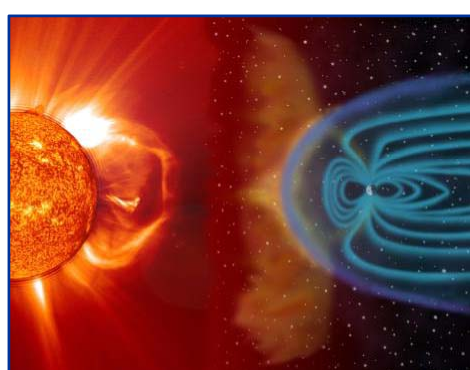
## Space Weather

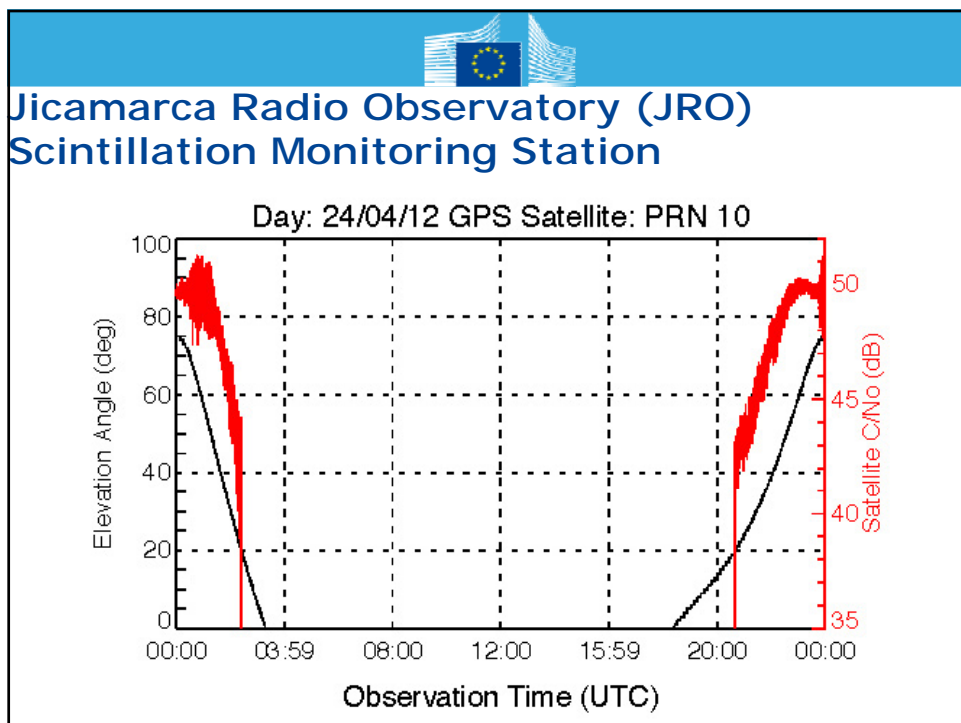
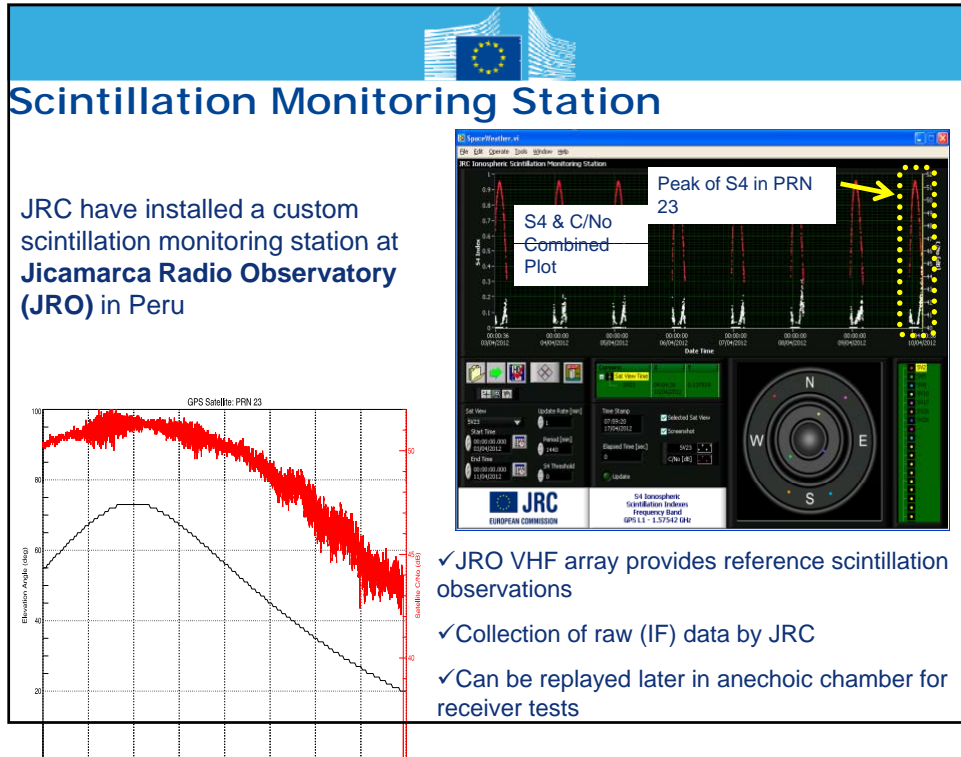
GNSS and RF signals pass through a region of atmosphere called **ionosphere**. In the ionosphere, free ions interact with RF signals potentially disturbing their propagation

Solar activity can cause instabilities in the ionosphere leading to **scintillation**

Severe scintillation can cause **disruption of satellite services**

**GNSS signals:** effective way for monitoring scintillation







## Scintillation Data

Summary of Scintillation Events observed at the EC Joint Research Centre Monitoring Station at the Iquitos Radio Observatory (Peru)

Satellite PRNs	UTC Time Window	Observations
1-Apr-12	0,6,10,22	0-4 AM
2-Apr-12	0,10,22	Around 2 AM
3-Apr-12	None	
4-Apr-12	None	
5-Apr-12	None	
6-Apr-12	None	
7-Apr-12	None	
8-Apr-12	0,6,12,22	2-4 AM
9-Apr-12	0,10,12,22	1-4 AM
10-Apr-12	12	1-4 AM
11-Apr-12	None	Unclear
12-Apr-12	No Data Available	
13-Apr-12	0,10,12,22	1-4 AM
14-Apr-12	12	1-4 AM Unclear
15-Apr-12	6,12,22	0-4 AM
16-Apr-12	None	
17-Apr-12	Datasets not confirmed	
18-Apr-12	0,10,22	0-4 AM
19-Apr-12	None	
20-Apr-12	None	
21-Apr-12	None	
22-Apr-12	None	
23-Apr-12	None	
24-Apr-12	0,10,16,19	1-1:30 AM Clear and short event
25-Apr-12	0,10	0-0:30 Clear and short event
26-Apr-12	None	
27-Apr-12	None	
28-Apr-12	None	
29-Apr-12	None	
30-Apr-12	None	
1-May-12	None	
2-May-12	None	
3-May-12	None	
4-May-12	None	
5-May-12	None	
6-May-12	None	
7-May-12	None	
8-May-12	None	
9-May-12	None	
10-May-12	None	

JOINT RESEARCH CENTRE  
Institute for the Protection and Security of the Citizen  
Security Technology Assessment Unit

Joint Research Centre

Live data have been collected since April 2012

The aim is to create a library of raw scintillation data which will be made available by JRC for receiver testing

Towards the establishment of new standards for receiver operation under scintillation

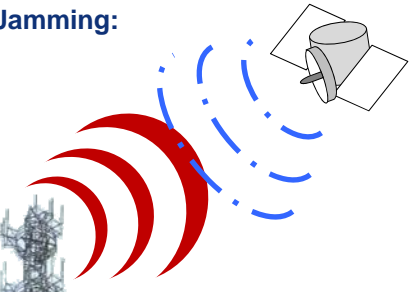
Depending on the success of the current campaign, new stations may be deployed





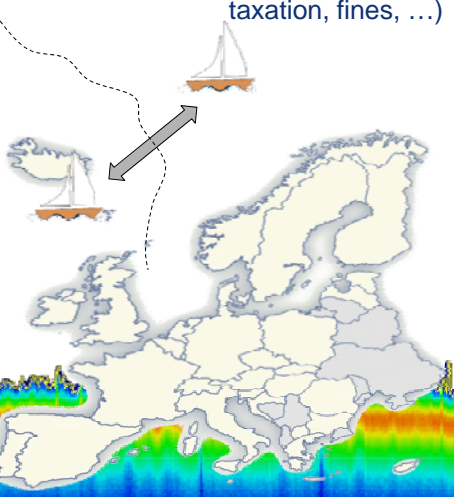
## GNSS Interference

Jamming:



Overpowering the weak GNSS signal (intentionally or unintentionally)

Spoofing:  
fool a GNSS receiver providing the wrong user position (for example to avoid taxation, fines, ...)



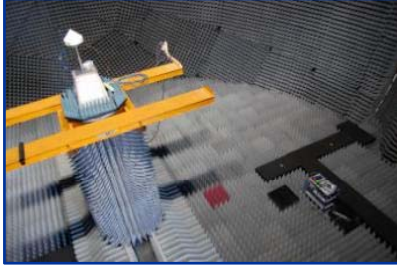
JOINT RESEARCH CENTRE  
Institute for the Protection and Security of the Citizen  
Security Technology Assessment Unit



## LightSquared Tests

Testing impact of LightSquared on GPS and Galileo O/S signals

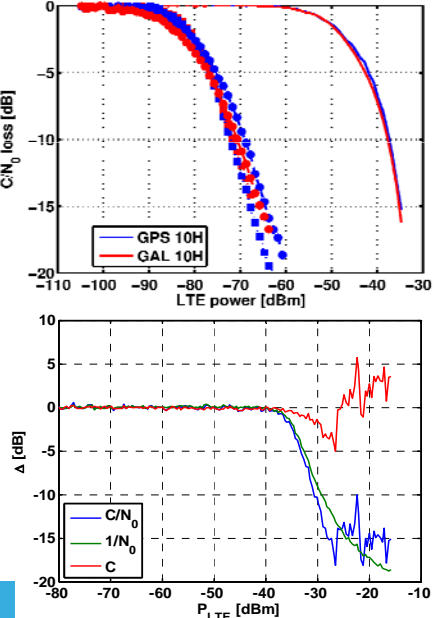
- Radiated tests in anechoic chamber
- Commercial Receivers



Also leverage structure of PRS using codeless processing

- Conducted mode tests
- Custom software receiver

Joint Research Centre

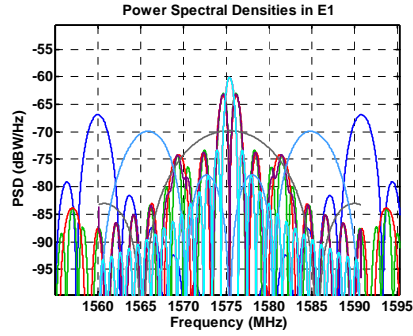
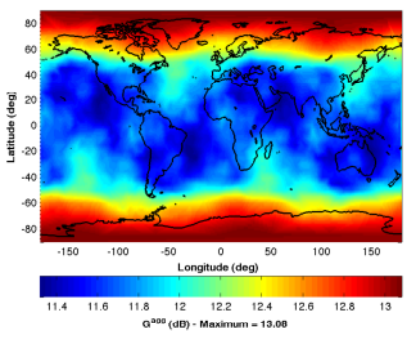




## Inter-System Compatibility Studies

JRC provides support to DG-ENTR in inter-system signal compatibility

- ✓ Participation in CSI-WG
- ✓ Participation at WG-A 13

Development of models for dealing with C/A code structure

Joint Research Centre

In-house development of software for Radio Frequency Compatibility (RFC)

- ✓ Follows ITU recommendations
- ✓ Independent development for cross-checking with other groups



# GNSS Signals Workshop Systems and Signals

Cillian O'Driscoll

[www.jrc.ec.europa.eu](http://www.jrc.ec.europa.eu)



*Serving society  
Stimulating innovation  
Supporting legislation*

Joint Research Center



## Overview

- Global Satellite Navigation Systems (GNSS)
  - What is GNSS?
  - Principles of Operation
  - Current GNSS: GPS, GLONASS, Galileo, Compass
- GNSS Signals
  - Basic Principles and Signal Model
  - The Propagation channel
  - Overview of current signals



Joint Research Center

2



Part I:

## GLOBAL SATELLITE NAVIGATION SYSTEMS

Joint  
Research  
Centre

3



### What is GNSS?

Global Navigation Satellite System

- Global : Worldwide system
- Navigation: For providing **position, velocity** and **time** (PVT)
- Satellite System: Using signals transmitted from satellites in orbit

Current GNSS

- Global Positioning System (GPS): U.S. system
  - GLONASS: Russian System
  - Galileo : European system
  - Compass: Chinese system
- } Fully operational      } Under development

Joint  
Research  
Centre

4



## Purpose of GNSS

- GNSS are deployed to enable **users** to compute **Position, Velocity and Time (PVT)** at their current location
  - GNSS is **not** a tracking system – contrary to most public opinion
  - GNSS is **not just** a positioning system – important to remember V and T!
- Almost unlimited range of applications:
  - Commercial, recreational, military, scientific, network synchronisation, autonomous navigation, collision avoidance, etc, etc, etc
- Some applications are sensitive:
  - Aviation, military, time synchronisation in telecommunications and power networks



## Basic Principle: Positioning

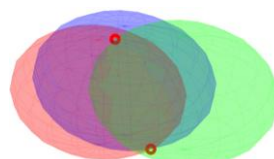
The basic principle of GNSS positioning is very simple:

**Knowing the distance (range) to 4 objects at known locations, the user position can be unambiguously calculated in 3 dimensions**

Yields 4 equations in 3 unknowns

- One unknown per dimension ( $x_u, y_u, z_u$ )
- One equation per range ( $D_i$ )

$$D_i = \sqrt{(x_u - x_i)^2 + (y_u - y_i)^2 + (z_u - z_i)^2} = \|\mathbf{r}_u - \mathbf{r}_i\|$$



- Each equation is non-linear
  - 3 equations leads to two valid solutions for 3 unknowns
    - Intersection of 3 spheres
  - Typically only one solution is near the earth's surface, so we can usually use 3 equations (Earth acts like 4<sup>th</sup> sphere)
- This principle is called **trilateration**



## Trilateration in GNSS

- The application of this basic principle to GNSS is straightforward:
  - The satellites are the **objects at known locations**
  - The **range** is computed by measuring the “**time of flight**” of an electromagnetic signal from the satellite
- $D_i = c \cdot t_i = c \cdot (t_i^{rx} - t_i^{tx})$
- Difficulties arise due to the complexity in:
  - **Accurately** determining the satellite positions  $[x_i, y_i, z_i]$  at a **precise** time  $t_i^{tx}$
  - **Accurately** determining the **precise** time at which the signal is received  $t_i^{rx}$
- Note that timing errors are scaled by the speed of light:  $1 \text{ ns} \approx 30 \text{ cm}$

Joint  
Research  
Centre

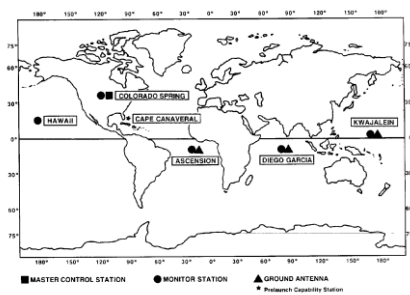
7



## Problem 1: Accurate Satellite Positions

- To solve the problem of accurate satellite positioning each GNSS contains a **ground segment** consisting of **monitoring stations** distributed around the globe

### GPS Monitor Stations c. 1996



- Satellite positions and clocks are constantly monitored
- Orbit model and clock error model parameters are uploaded to the satellites (at least daily)
- These parameters are re-transmitted by the satellites
- User computes satellite position using these parameters

Joint  
Research  
Centre

8



## Problem 2: Accurate Receiver Time

- A GNSS receiver must have an on-board “clock” to measure  $t^{rx}$
- But this is usually of low quality → it will have a time varying error  

$$t^{rx} = t^{sys} + t_u^b$$
- Range measurements will be **biased** by  $c \cdot t_u^b$
- Solution:** Treat the receiver clock bias as another parameter to be estimated
- There are now **four** parameters:  $x_u, y_u, z_u, t_u^b$
- Can be solved using measurements to at least **four** satellites
- The receiver in fact measures the so-called **pseudorange** defined as:

$$\rho_i = D_i + c \cdot (t_u^b - t_i^b)$$



9

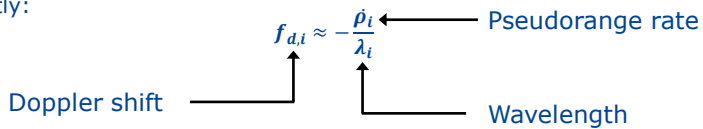


## Trilateration and Velocity

- We have seen how GNSS provides estimates of **position** and **time**
  - What of the **velocity** component of the **PVT**?
- The situation is analogous to the positioning case:
  - The rate of change of range (**range rate**) is given by:  

$$\dot{D}_i = \sqrt{(\dot{x}_i - \dot{x}_u)^2 + (\dot{y}_i - \dot{y}_u)^2 + (\dot{z}_i - \dot{z}_u)^2} = \|\dot{r}_i - \dot{r}_u\|$$
  - The **pseudorange rate** is given by:  

$$\dot{\rho}_i = \dot{D}_i + c \cdot (t_u^b - \dot{t}_i^b)$$
  - GNSS make use of the **Doppler** effect to measure the pseudorange rate directly:



10



## Recap: Principles of PVT

- A GNSS receiver needs to solve for 8 unknowns
$$\begin{matrix} x_w, y_w, z_w, t_w^b \\ \dot{x}_w, \dot{y}_w, \dot{z}_w, \dot{t}_w^b \end{matrix}$$
- To do so it needs pairs of **measurements** ( $\rho_i, p_i$ ) from at least 4 satellites – these measurements are also called the **observations** or **observables**
- The satellite positions must be known with sufficient accuracy
- The time at which the signals are transmitted from the satellites must be known with sufficient accuracy
- **However:** There are some further (significant) sources of error which we have not yet considered

11



## Current GNSS Systems

There are currently 4 GNSS systems with active signals in space

- **GPS**
  - Technically the full title is **NAVSTAR GPS: Navigation by Satellite Tracking And Ranging Global Positioning System**
  - The first and, at present, still the best
- **GLONASS**
  - **Global Navigation Satellite System: The Russian GNSS** (technically: *Globalnaya Navigatsionnaya Sputnikovaya Sistema*)
  - Fully operational in the last year – under development since the late '70s
- **Galileo**
  - European GNSS – conceived in the late '90s
  - First two satellites are now in orbit
- **Compass**
  - Chinese system – also called **Beidou**
  - 11 Active satellites in orbit – of which 3 have global coverage

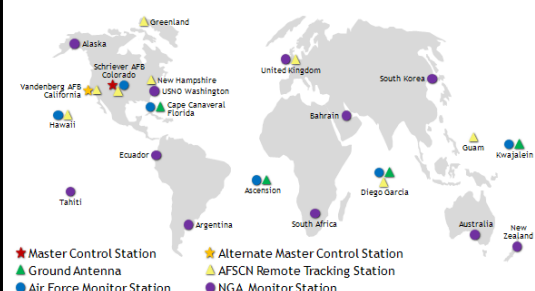
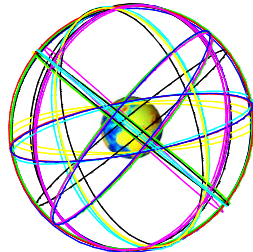
12





## NAVSTAR GPS:

- Space Segment:
  - 6 Orbital planes: spaced by  $60^\circ$  around equator
  - Inclined at  $\approx 55^\circ$  with respect to the equatorial plane
  - Nominal 4 satellites per plane (total of 31 svs today!)
  - Orbital radius  $\approx 26,500$  km  
→ speed  $\approx 3.8$  km/s ( $> 13,000$  km/hr)



- Ground Segment
  - 16 monitoring stations
  - 12 command antennas
  - 1 master station
  - 1 alternate master

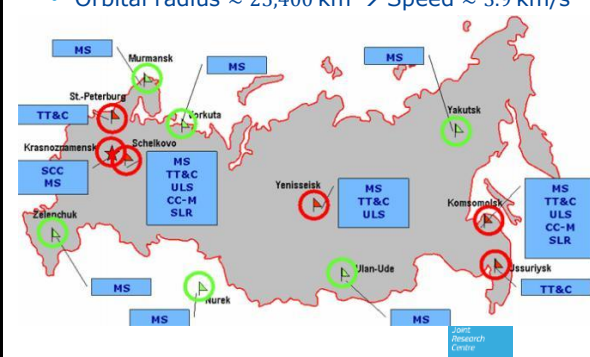
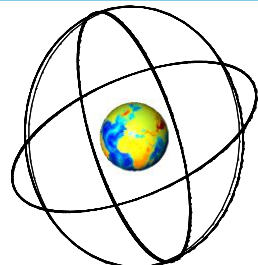
(source: [www.gps.gov](http://www.gps.gov))

13



## GLONASS

- Space Segment:
  - 3 Orbital planes spaced by  $120^\circ$  around equator
  - Inclined at  $64.8^\circ$  wrt equatorial plane
  - Nominally 8 satellites per plane
  - Orbital radius  $\approx 25,400$  km → Speed  $\approx 3.9$  km/s



- Ground Segment
  - 10 monitoring stations
  - 3 command antennas
  - 1 master station
- All in Russia
  - Reduced accuracy in other parts of the world
  - Two stations now in Antarctica

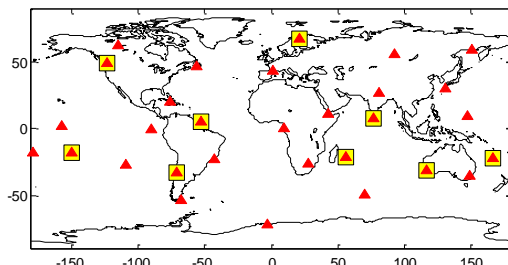
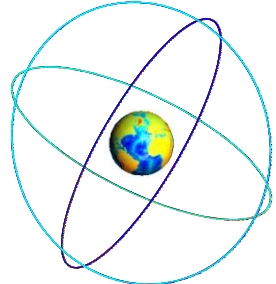
(source: CGSIC 2008)

14



## Galileo

- Space Segment:
  - 3 orbital planes: 9 satellites per plane + 3 spares
  - Only 2 active satellites today
  - Inclined at  $\approx 56^\circ$  wrt the equatorial plane
  - Orbital radius  $\approx 29,600$  km  $\rightarrow$  Speed  $\approx 3.7$  km/s
  - Constellation repeats every 10 days



- Ground Segment
  - 30 monitoring stations (planned)
  - 5 command antennas
  - 2 control stations

(source: [www.esa.int](http://www.esa.int))

Source: <http://www.cesah.de/>

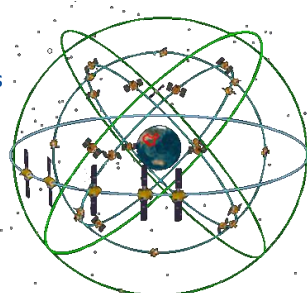
15

Joint  
Research  
Centre



## Compass (Beidou-2)

- Space Segment
  - Unusual in that it consists of both Geosynchronous Earth Orbit (GEO,IGSO) and Medium Earth Orbit (MEO) components
  - Few details available
  - Latest constellation plans (ICG 2010):
    - 5 Geostationary satellites (GEO)
    - 3 Inclined Geosynchronous satellites (IGSO)
      - Inclined at  $55^\circ$
    - 27 Medium Earth Orbit Satellites (MEO)
      - Inclined at  $55^\circ$
      - 3 Orbital planes, 8 satellites per plane (7 active + 1 spare)
      - Radius  $\approx 27878$  km
  - Currently there are 3 MEO, 4 GEO and 5 IGSO in orbit
  - Sources:
    - International Committee on GNSS (ICG)
    - Official compass website: [beidou.gov.cn](http://beidou.gov.cn)
    - Inside GNSS magazine [insidegnss.com](http://insidegnss.com)



Joint  
Research  
Centre

16



Part II:  
**GNSS SIGNALS**

Joint  
Research  
Centre

17



## **GNSS Signals:**

Recall – the purpose of a GNSS is to provide PVT to the user using the principle of trilateration

The GNSS signal must, therefore, provide the user with the ability to:

1. Determine the pseudorange to the satellite
2. Determine the pseudorange rate to the satellite
3. Determine the satellite position and velocity

Other practical considerations must also be taken into account:

- Multiple signals from the same system must be visible at the same time
  - ➔ need to limit interference between these signals
- Satellites from multiple systems will be visible at the same time
  - ➔ need to limit inter-system interference
- Signals must pass through the earth's atmosphere ➔ limited choice of frequencies

Joint  
Research  
Centre

18



## Ranging Principles

Ranging is a common application

**Active** ranging systems (e.g. radar, sonar) operate by transmitting a signal then detecting reflections.

- Range is obtained by measuring the “round trip” time
- Not appropriate in GNSS context



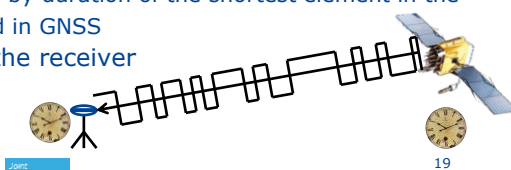
**Passive** ranging systems: measuring device does not transmit any signal

- No “round trip” → timing must be encoded in the transmitted signal

By transmitting a known sequence: each element of sequence transmitted at a particular time:

→ ranging precision determined by duration of the shortest element in the sequence. This approach is used in GNSS

- By “reading” the sequence the receiver determines the **time of transmission  $t_{tx}$**



Joint  
Research  
Centre

19



## Ranging: Achievable Accuracy

Assuming that the ranging signal is broadcast in an Additive White Gaussian Noise (AWGN) channel → it can be shown that the so-called **Cramer-Rao Lower Bound** (CRLB) on the accuracy of the delay estimation is given by:

$$\sigma_\tau^2 \geq \frac{1}{2 \frac{C}{N_0} B_g^2}$$

where:

- $C/N_0$  is the carrier power to noise Power Spectral Density (PSD) ratio
- $B_g$  is the so-called Gabor Bandwidth, or rms bandwidth

$$B_g^2 = \int_{-\infty}^{\infty} f^2 G(f) df = -R''(0)$$

Signal PSD                      Second derivative of the signal auto-correlation function

Desirable properties for ranging signals:

- Wide bandwidth
- Most power towards **edge** of the bandwidth

Joint  
Research  
Centre

20



## PROPAGATION EFFECTS

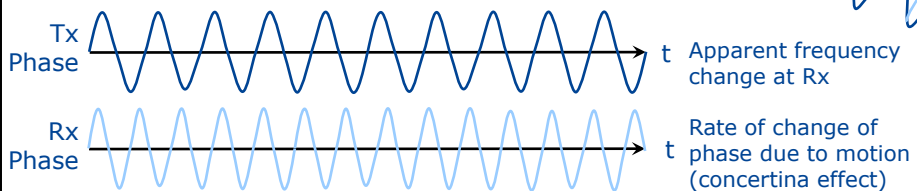
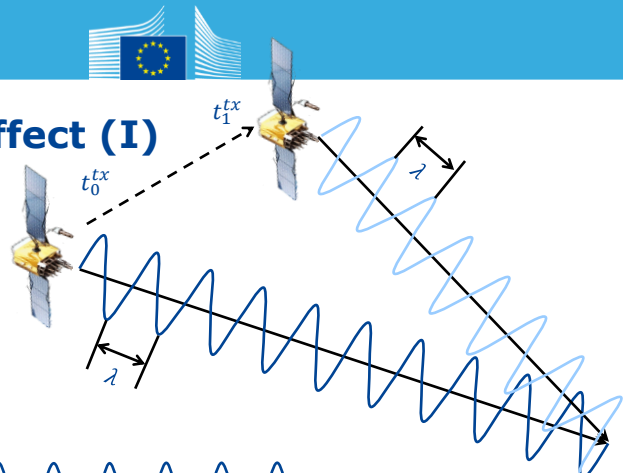
Joint  
Research  
Centre

21

### The Doppler Effect (I)

Relative motion  
between transmitter  
and receiver →  
**apparent frequency  
shift**

- **Wavelength** in  
space is not affected



Joint  
Research  
Centre

22

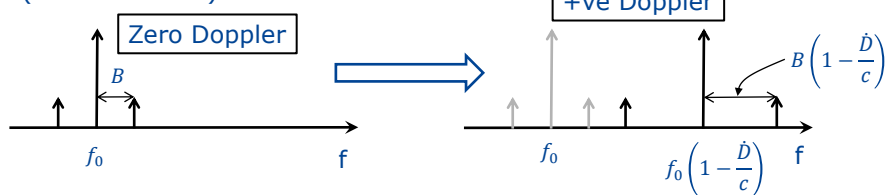


## The Doppler Effect (II)

$$\text{Mathematically: } \Delta f = -\frac{\dot{D}}{\lambda} = -\frac{\dot{D}}{c} f$$

This is a **frequency dependent** frequency shift

- Higher frequencies are shifted by larger amounts for the same relative velocity
- Concertina effect in frequency domain
- Compression in time domain ➔ expansion in frequency domain (and vice versa)



Summary: Doppler has **no effect** on wavelength; **compression** in time domain ➔ **expansion** in frequency domain and vice versa



## Accumulated Doppler

The Doppler shift can be measured with an accuracy of  $\approx 1\%$  of a cycle per second

- For GNSS frequencies (1 – 2 GHz) – very accurate velocity measurements

By integrating (accumulating) the Doppler measurements

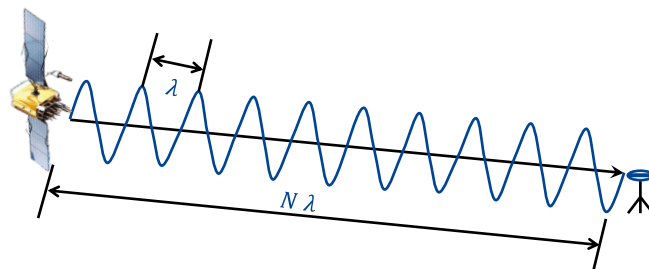
- Accurate measure of **change** in range
- Can be used to **smooth** the pseudorange measurements over time
- This is commonly implemented in three ways:
  1. **Aiding** of the code tracking using the Doppler estimates
  2. **Smoothing** of the code measurements using the phase estimates
  3. **Filtering** the navigation solution: the velocity solution “drives” the position solution



## Carrier Phase Measurement

In addition: carrier phase of received signal is (**ambiguous**) measure of pseudorange

- Very high precision positioning can be achieved using carrier phase measurements
- Not originally foreseen when GNSS was first proposed ➔ widely used now



Joint  
Research  
Centre

25



## Atmospheric Effects

Signal passes through the Earth's atmosphere en route to the receiver

Leads to signal **diffraction**

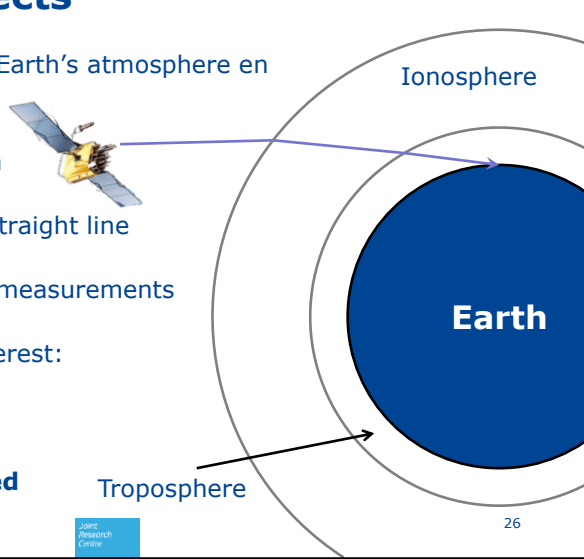
Propagation path is not a straight line

Leading to errors in range measurements

Two primary regions of interest:

1. The **ionosphere**
2. The **troposphere**

Signals are also **attenuated**



Joint  
Research  
Centre

26



## Ionospheric Effects (I)

The ionosphere is a region of free electrons in the upper atmosphere (from about 50 to about 1000 km)

Mostly formed by Ultra Violet (UV) radiation from the sun

- Degree of ionization varies with latitude, time of day, time of year and degree of solar activity

It is **frequency dispersive** (refractive index is a function of frequency)

$$n \approx 1 - \frac{40.3}{f^2} \int N dl$$

This leads to a **carrier phase advance** and **group delay** of the signal

$$\Delta x^{phase} = -\frac{40.3}{f^2} \int N dl \quad \Delta x^{group} = \frac{40.3}{f^2} \int N dl$$



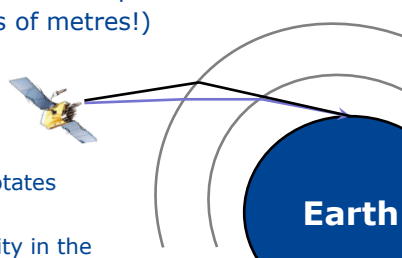
## Ionospheric Effects (II)

Due to frequency dispersive nature → Use of two frequencies allows compensation of the ionospheric delay (10's of metres!)

$$\Delta D^{iono} = \left( \frac{f_2^2}{f_2^2 - f_1^2} \right) [\rho_1 - \rho_2]$$

Additional ionospheric effects:

- Faraday Rotation: direction of polarization rotates as the signal passes through the ionosphere
- Scintillation: rapid variation in electron density in the ionosphere → causes interference pattern on the ground.  
Like passing signal through a diffraction grating. This most often occurs when the ionosphere is disturbed by solar storms, or just after sunset near the equator
- Second order effects: the previous model is first order





## Tropospheric Effects

The troposphere is that part of the atmosphere from the surface up to about 50 km

For GNSS frequencies, it is not frequency dispersive

Consists of **dry** and **wet** components:

- Dry component accounts for about 90 % of the tropospheric delay: stable
- Wet component is highly variable, hard to predict
- Total contribution is about 2-3 m at zenith (more at lower angles)



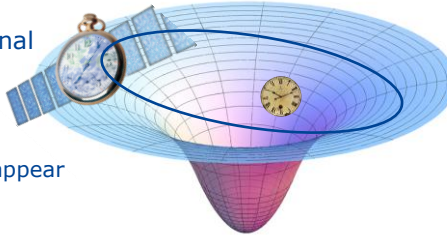
## OTHER ERROR SOURCES



## Relativistic Effects

GNSS are among the few systems which must account for relativistic effects

- Time runs slower at higher gravitational potential
- Satellite clocks are tuned to **lower frequencies** on the ground
  - Once they reach orbital altitude signals appear at the correct frequency
- GNSS orbits are typically **elliptical** :
  - Clocks run slower in some parts of the orbit than in others (up to 20 m)
  - This can be compensated for using:  
$$\Delta t_r = 2 \frac{r \cdot v}{c^2}$$
- In GPS and Galileo this is done at the user side (different but equivalent formula). In Glonass this is done on board the satellite.



Joint  
Research  
Centre

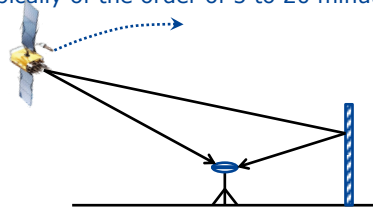
31



## Multipath

As the signal propagates from satellite to earth, it may reflect off of surfaces such as buildings, cars, the ground

- The signal can reach the receiver through **multiple paths** → **multipath**
- This results in constructive/destructive interference between the **line-of-sight** (LOS) and the reflections
- As the geometry changes, the relative phase between LOS and reflections changes → **fluctuations** in apparent received power, indicative of multipath (typically of the order of 5 to 20 minute period for GPS L1 C/A)



Multipath is one of the largest error sources for most GNSS receivers

**Local** phenomenon: must be handled by receivers

Joint  
Research  
Centre

32



## Hardware Delays

As signals pass through the transmitter and receiver front-ends there can be significant delays

Typically these delays are very similar for **signals of the same type**

For signals with differing spectra: there can be significant differences in the delays

The inter-signal delays due to the satellite hardware are usually broadcast as part of the navigation message

May need to be calibrated out at the receiver side

Note that delays that are common to all signals → will enter into the clock bias estimate



## GNSS SIGNAL STRUCTURE



## GNSS Signal Structure

The general model of GNSS signal is as follows:

$$y_i(t) = \sqrt{2C_i} d_i(t) s_i(t) c_i(t) \cos(2\pi f_i t + \varphi_i)$$

Carrier Power      ↓  
 Navigation Data    ↑  
 Secondary code    ↑  
 Ranging code        ↓

Relative phase      ↓  
 Centre frequency    ↓

**Navigation Data:** Contains satellite orbit and clock parameters, plus other information

**Secondary Code:** Not always present. Used to aid synchronization.

**Ranging Code:** Consists of two components:

1. A pseudorandom sequence (**PRN**: PseudoRandom Noise code)
  - Provides timing & **spreads** the spectrum of the data signal
2. A **sub-carrier**
  - The PRN is just a sequence – the sub-carrier maps this to a real signal



35



## Pseudorandom Sequences (I)

The basic idea is to use a binary sequence to measure time.

Terminology: The current element of a sequence is referred to as the **phase** of the sequence.



The transmitted sequence must be synchronized with the satellite clock, such that a given sequence phase corresponds to a precise time of transmission

At a given time the receiver measures the phase of the received sequence (giving  $t^{rx}$ ) and simultaneously records time according to the receiver clock ( $t^{rx}$ )

This is the basis for forming the pseudorange:  $\rho = c \cdot (t^{rx} - t^{tx})$

But how can the phase of the sequence be measured?

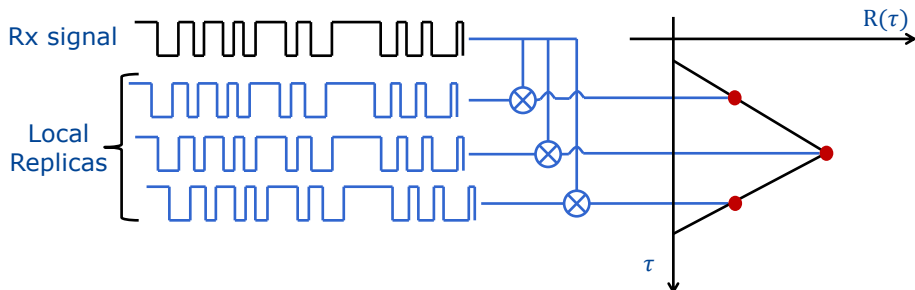


36



## Pseudorandom Sequences (II)

The receiver generates a local copy of the sequence and **correlates** this local replica with the received signal



By reading the “phase” of the local replica when correlation is maximised  
→ obtain estimate of the transmit time

Requires that the PRN sequence have good **auto-correlation** properties



## Pseudorandom Sequences (III)

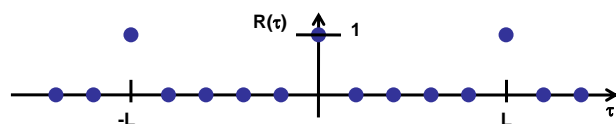
The ranging sequence should be chosen to have “good” **auto-correlation** properties

$$R(\tau) = \sum_{i=1}^L s_i s_{i-\tau}$$

Sequence Length

Sequence Elements

The optimal auto-correlation shape is noise-like in structure, consisting of a peak at zero delay and zeros elsewhere



Another desirable property may be to have low **cross-correlation** between sequences transmitted by different satellites

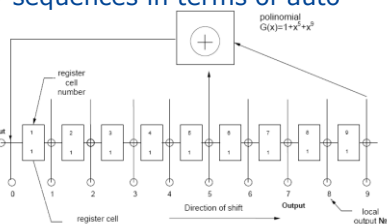
- Allows all satellites to transmit at the same frequency
- Referred to as **code division multiple access (CDMA)**
- Used by all GNSS except for Glonass (plans to use CDMA in GLONASS in future)



## Sample Pseudorandom Sequences

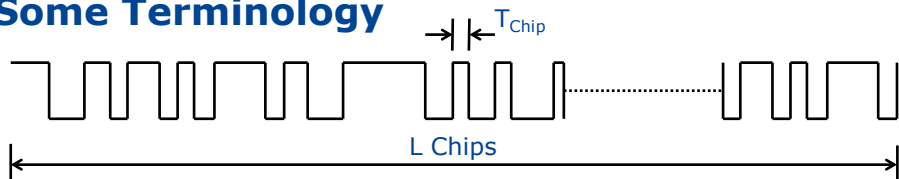
- **M-Sequences:** These are optimal binary sequences in terms of auto-correlation.
  - Very easy to generate
  - Excellent auto-correlation properties
  - Generally poor cross-correlation properties
  - Used in GLONASS (signals from different satellites are broadcast on different frequencies – FDMA)
- **Gold Codes:** Sub-optimal auto-correlation, but excellent cross-correlation for a large family of codes
  - Also very easy to generate (XOR of two m-sequences)
  - Used in GPS and Galileo
- **Memory codes:** Codes with no simple structure
  - Highly optimised, but must be stored in entirety in receiver
  - Used in Galileo

Joint  
Research  
Centre



39

## Some Terminology



Each element in a binary sequence is referred to as a **chip**

The chip duration is  $T_{\text{chip}}$  and the duration of the code is  $L T_{\text{chip}}$  seconds

The frequency is referred to as the **chip rate** and is denoted  $f_c = 1/ T_{\text{chip}}$ .

The entire sequence is usually referred to as the **PRN code**, **PN code**, **spreading code**, or simply the **code**.

The phase of the sequence is called the **code phase**

Joint  
Research  
Centre

40



## Broadcasting the Signal: The sub-carrier

The PRN code, while of vital importance, is simply a sequence of +/- 1 values

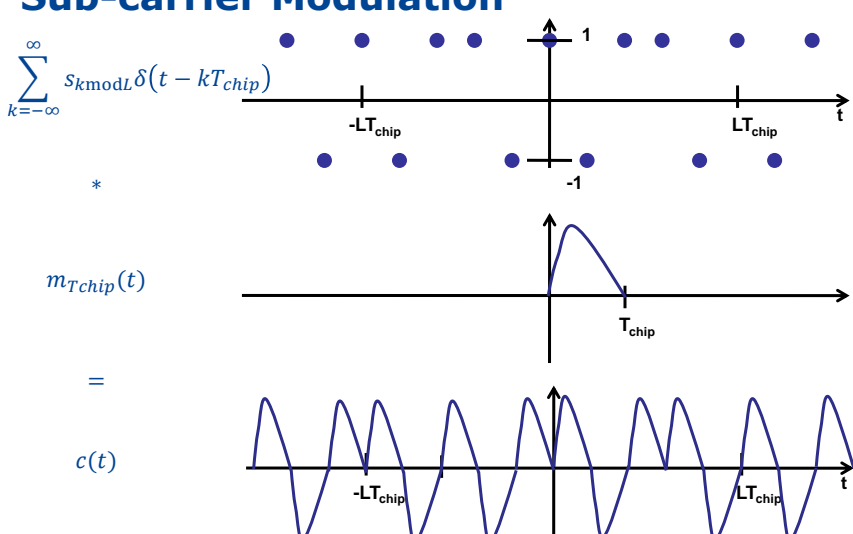
$$s(t) = \sum_{n=-\infty}^{\infty} s_{n \bmod L} \delta(t - n T_{chip})$$

To be broadcast, the sequence must be **modulated** by a real signal to form the **ranging code**:

$$c(t) = s(t) * m_{Tchip}(t)$$

In communications this is called the **chip shaping**, in navigation we refer to it as the **sub-carrier**

## Sub-carrier Modulation





## Properties of the Sub-Carrier

The sub-carrier must be constrained to be zero outside of the range:

$$0 \leq t < T_{Chip}$$

It is **desirable** that the sub-carrier (or the sum of all sub-carriers in the same frequency band) have a constant envelope

- This is due to efficiency considerations on the satellites – constant envelope ensures that the transmit filter operates in saturation mode at all times, leading to greater efficiency

To a large extent the sub-carrier determines the **spectral characteristics** of the broadcast signal

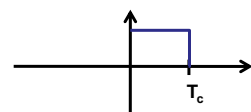
The **auto-correlation properties** are also largely determined by the sub-carrier



## Sample Sub-Carriers

All the original GNSS signals used the so-called **BPSK** sub-carrier

- Simplest sub-carrier
- Also called a Non-Return to Zero (NRZ) pulse
- Denoted by BPSK(fc)

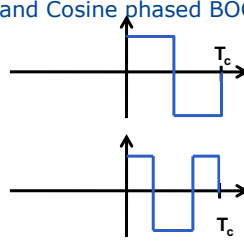


In the late 1990's a new sub-carrier, called Binary Offset Carrier (**BOC**) modulation was introduced:

- Consists of a square wave with frequency  $f_s$  and is denoted BOC( $f_s$ ,  $f_c$ )
- Comes in two "flavours": Sine phased BOC and Cosine phased BOC

$$m_{BOC(f_c, f_s)}(t) = \begin{cases} \text{sgn}(\sin 2\pi f_s t) & 0 \leq t \leq 1/f_c \\ 0 & \text{otherwise} \end{cases}$$

$$m_{BOC_{cos}(f_c, f_s)}(t) = \begin{cases} \text{sgn}(\cos 2\pi f_s t) & 0 \leq t \leq 1/f_c \\ 0 & \text{otherwise} \end{cases}$$





## Alternative Formulation: Periodic Subcarrier

The convolutional model does not hold when the sub-carrier is longer than the chip period.

In this case we use a multiplicative model:

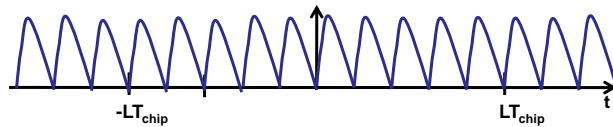
$$c(t) = s_{BPSK}(t) \cdot \tilde{m}(t)$$

Where:

- $s_{BPSK}(t) = s(t) * m_{BPSK, T_{chip}}(t)$  is a BPSK realisation of the PRN code



- $\tilde{m}(t) = \sum_{i=-\infty}^{\infty} m_{T_{chip}}(t) \delta(t - iT_{chip})$  is the period extension of the subcarrier



45



## Subcarrier Nomenclature

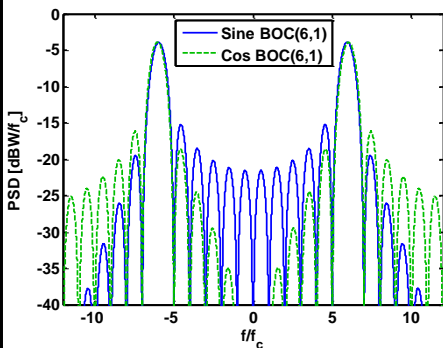
With the exception of GLONASS, all GNSS signals have chip rates which are multiples of the base rate:  $f_0 = 1.023$  MHz

Thus the shorthand notation BPSK(1) denotes a BPSK subcarrier with a chipping rate of  $1 \cdot f_0 = 1.023$  MHz

Similarly BOC modulation is typically denoted by BOC(M,N) for integer values M and N such that  $f_s = M \cdot f_0$  and  $f_c = N \cdot f_0$



## Notes on BOC Sub-Carriers: PSD



Properties of BOC(fs,fc) sub-carriers' PSD:

- Two main lobes centred at  $\approx \pm f_c$
- Each main lobe has a width of  $2f_c$
- For **sine** phased BOC: energy is mostly in the **centre** between the two lobes
- For **cosine** phased BOC: energy is mostly to the **edges**, away from the two lobes

Recall: more power at higher frequencies → better delay estimation

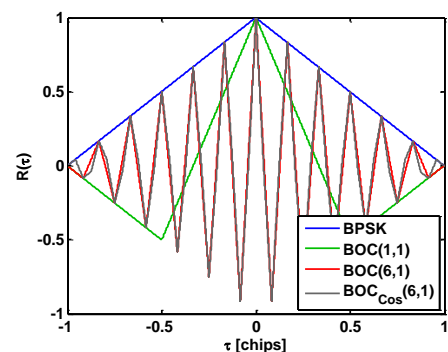
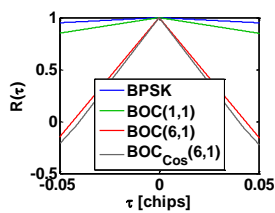
**But:** requires larger bandwidth in the receiver → more expensive



## Notes on BOC Sub-Carriers: Correlation

The BOC correlation function:

- Has  $4\frac{f_s}{f_c} - 1$  peaks (+ve and -ve)  
Extra peaks lead to potential tracking biases
- Care must be taken to ensure the correct peak is tracked
- Cosine phased version has sharper correlation peak (marginally)



Higher ratio  $f_s/f_c$  gives sharper main peak  
→ At expense of more side-peaks



## Multiplexed BOC (MBOC)

Following an EU-U.S. agreement on common signal structures a **signal task force** was established

In 2006 the task force recommended a **multiplexed BOC** signal consisting of a power split between a BOC(1,1) and a BOC(6,1) sub-carrier, with 1/11 of the power in the BOC(6,1) component

$$G_{MBOC}(f) = \frac{10}{11} G_{BOC(1,1)}(f) + \frac{1}{11} G_{BOC(6,1)}(f)$$

While the U.S. signal (L1C) and the EU signal (E1 OS) have the same spectrum, they use different **realisations** of the signal

- **L1C:** Consists of a BOC(1,1) data channel and a time multiplexed pilot channel (TMBOC)
- **E1 OS:** Consists of a weighted sum of BOC(1,1) and BOC(6,1) in both data and pilot channels (CBOC)

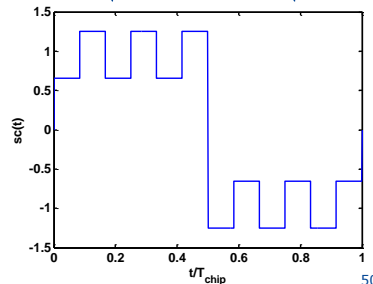
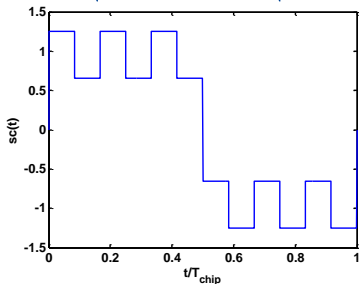


## Galileo E1 OS: Composite BOC (CBOC)

The Galileo E1 Open Service (OS) signal consists of data (E1b) and pilot (E1c) components

- 50/50 power split between the components
- Subcarriers formed as follows:

$$sc_{E1b}(t) = \sqrt{\frac{11}{10}} sc_{BOC(1,1)}(t) + \sqrt{\frac{1}{11}} sc_{BOC(6,1)}(t) \quad sc_{E1c}(t) = \sqrt{\frac{11}{10}} sc_{BOC(1,1)}(t) - \sqrt{\frac{1}{11}} sc_{BOC(6,1)}(t)$$

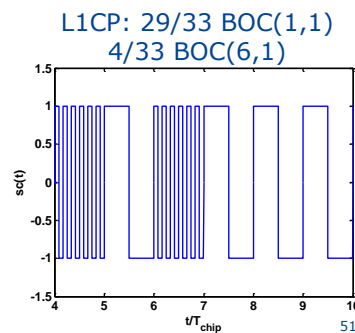
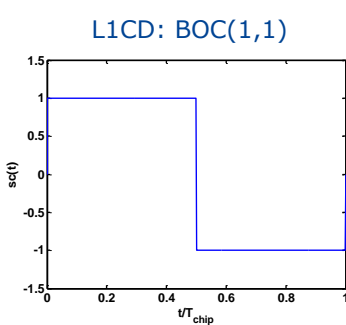




## GPS L1C: Time-Multiplexed BOC (TMBOC)

GPS also contains data (L1CD) and pilot (L1CP) components

- Data channel is simply BOC(1,1) with 1/4 of the power
- 3/4 of the signal power is in the pilot
- Pilot consists of a time multiplexing of BOC(1,1) and BOC(6,1)
- 29 out of every 33 chips are BOC(1,1) while 4 are BOC(6,1)



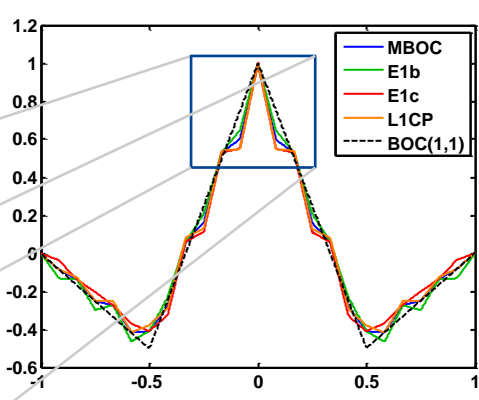
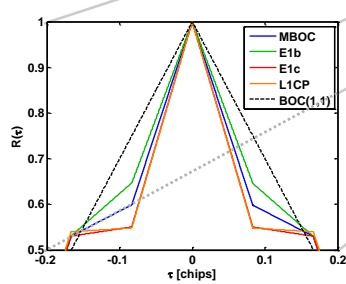
Joint Research Centre



## MBOC Comparison:

E1c and L1CP have marginally narrower correlation peaks

Ultimately quite similar



Joint Research Centre



## Signal Multiplexing (I/II)

All GNSS transmit multiple signals → providing different **services** on each signal

Signals on the **same frequency** must be **multiplexed** (combined) in some way. Possible approaches:

- Different antennas – not commonly used, but possibly used for the new GPS M-code
- Orthogonal carriers: two signals can be multiplexed by transmitting them with a 90° phase offset – one is **in-phase** (I) the other in **quadrature** (Q). Used for the original GPS and GLONASS L1 signals
- Time multiplexing: one signal is set to zero while the other transmits and vice versa (used for the GPS L2 Civil signal for example)
- When three or more signals are combined, more advanced techniques:  
→ **Interplexing**  
→ **AltBOC**



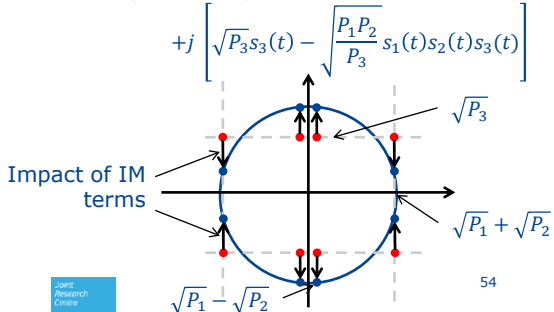
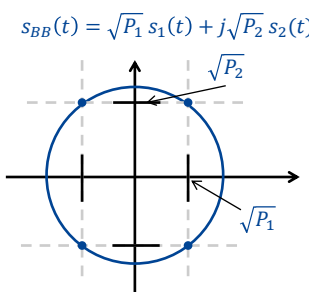
## Signal Multiplexing (II/II)

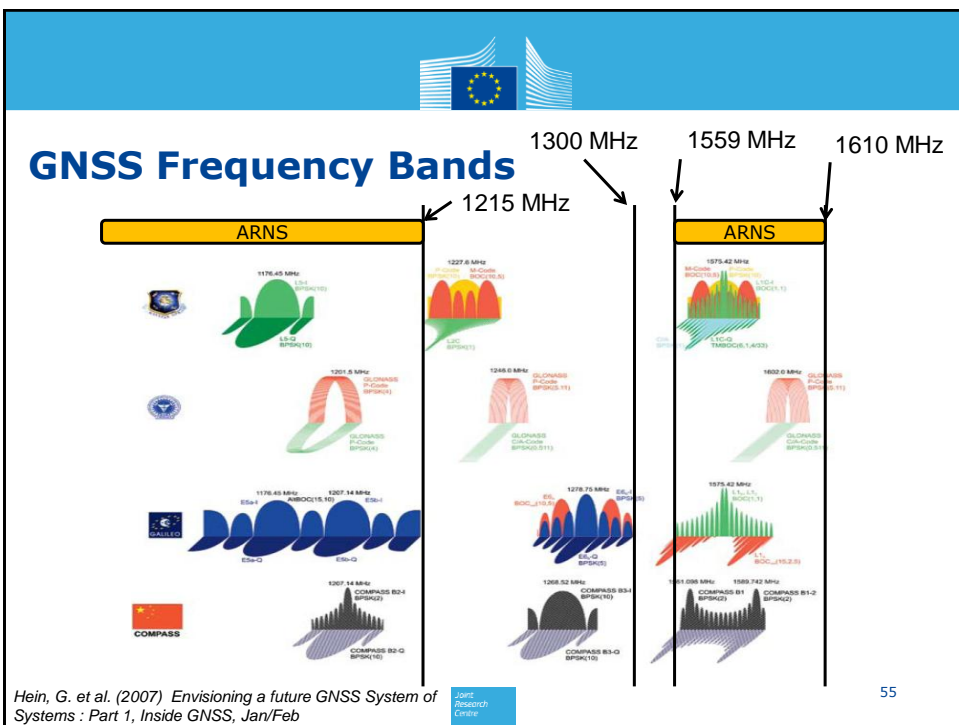
The driving forces behind multiplexing are the desire to:

- Minimise interference between the components
- Maintain a **constant envelope** - this keeps the satellite power amplifier operating in its saturation region → maximises efficiency

In general: two signals can be combined using I/Q modulation, three or more signals require the addition of **intermodulation (IM) products** to maintain a constant envelope

$$s_{BB}(t) = \sqrt{P_1} s_1(t) + \sqrt{P_2} s_2(t)$$







## Legacy GPS Signals

The original GPS signals consisted of a civil, or **Coarse/Acquisition (C/A)** signal at L1 and a military **Precise (P)** signal on both L1 and L2 where: L1 = 1575.42 MHz and L2 = 1227.6 MHz

Note: L1 = 10.23 MHz x 154

L2 = 10.23 MHz x 120

The military signal is reserved for use by authorized users and is generally **encrypted** to provide the **Y** signal – in general the military signal is referred to as P(Y)

The C/A signal has a BPSK(1) sub-carrier  $f_c = 1.023 \text{ MHz}$

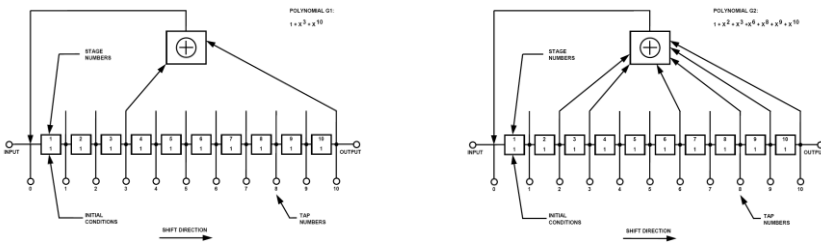
The P(Y) signal has a BPSK(10) sub-carrier  $f_c = 10.23 \text{ MHz}$



## The GPS C/A Signal

The C/A signal consists of a **Gold Code** of length 1023 chips and  $f_c = 1.023 \text{ MHz}$  for a code period of 1 ms

This is modulated by a navigation message with a data rate of 50 bps  
→ there are 20 repetitions of the C/A code in each data bit period of 20 ms



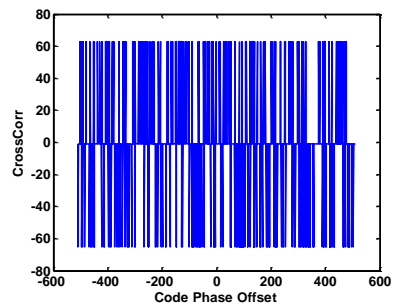
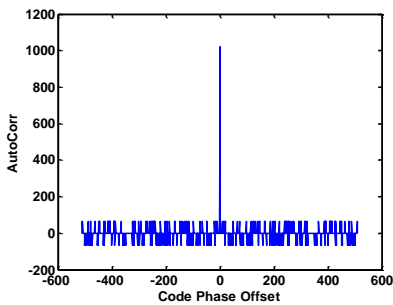


## Properties of the C/A code (I/II)

Good **cyclic** auto-correlation properties: side-lobes  $\in \{-65, -1, 63\}$

Family of 1025 possible codes (36 of which are reserved for GPS use)

Excellent **cyclic** cross-correlation properties: side-lobes  $\in \{-65, -1, 63\}$



Joint  
Research  
Centre

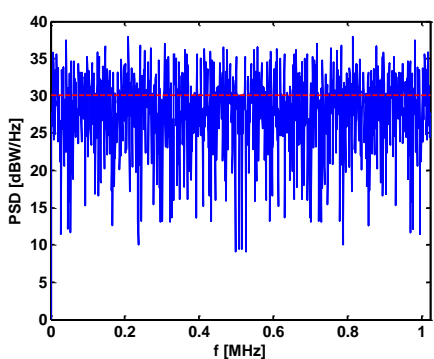
59



## Properties of the C/A code (II/II)

The spectral properties of the code are illustrated below

The dashed red line indicates the spectrum of an **ideal** random code



### Notes:

- The C/A **code** is discrete and periodic  $\rightarrow$  its spectrum is discrete (1 kHz) and periodic (1.023 MHz)
- The spectrum of the C/A **signal** must also account for the sub-carrier and the navigation data

Joint  
Research  
Centre

60



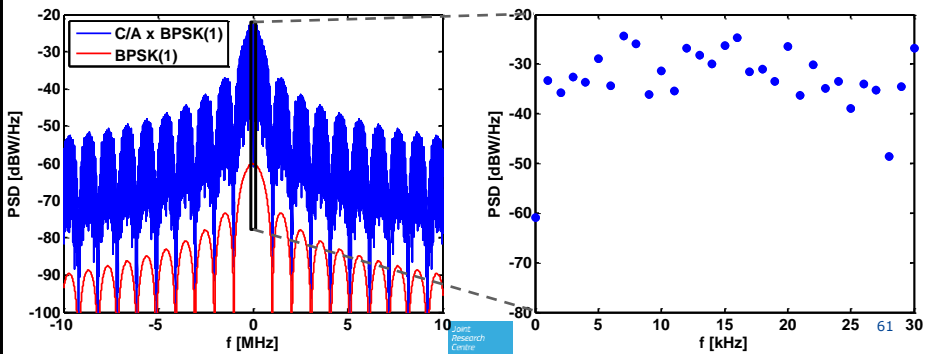
## Impact of the Subcarrier on C/A Signal

Model the subcarrier contribution as:  $c_{CA}(t) * s_{BPSK(1)}(t)$

So the PSD is given by the product of the PSDs:  $G_{CA}(f) \cdot G_{BPSK(1)}(f)$

Note that the C/A code is **periodic** → PSD is **discrete**

**Result:** BPSK controls the “envelope” and C/A code provides fine structure



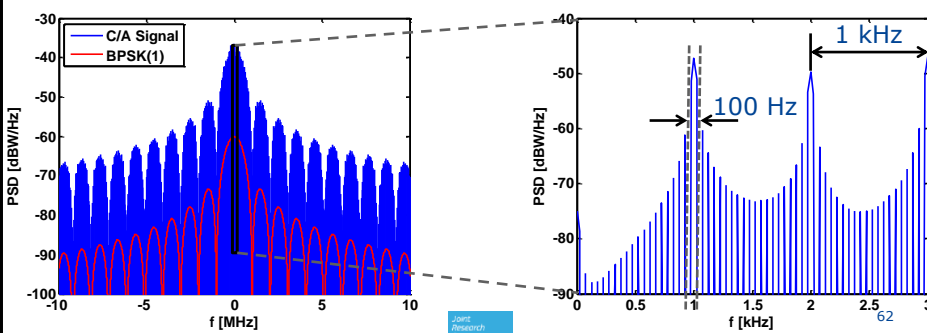
Joint Research Center

## Impact of Navigation Data on C/A Signal

After the subcarrier, the signal is **multiplied** by a 50 bps navigation message:  $d(t) \cdot [c_{CA}(t) * s_{BPSK(1)}(t)]$

PSD is given by:  $G_d(f) * [G_{CA}(f) \cdot G_{BPSK(1)}(f)]$

The data PSD is a  $\text{sinc}^2$  function with lobe width of 100 Hz

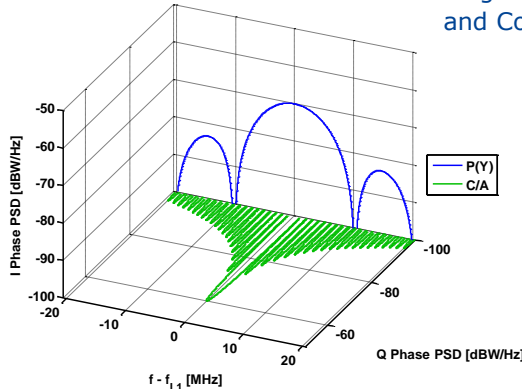


Joint Research Center



## GPS: L1 (Legacy Signals)

Original L1 signals consist of just of P(Y) and Coarse/Acquisition (C/A) signals



	C/A	P(Y)
<b>Sub Carr</b>	BPSK(1)	BPSK(10)
<b>PRN</b>	Gold	Combined m-seqs
<b>L</b>	1023	$6.2 \times 10^{12}$
<b>Data Rate</b>	50 bps	50 bps
<b>Sec. Code</b>	None	None

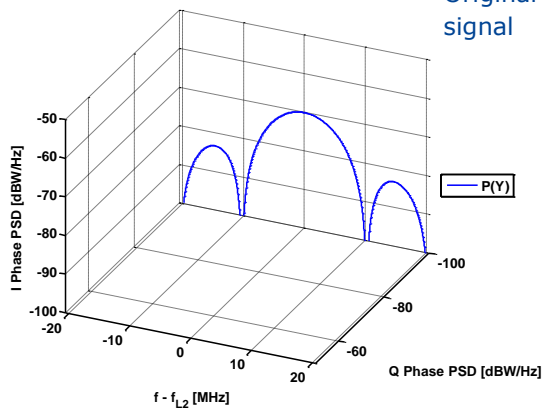


63



## GPS: L2 (Legacy Signals)

Original L1 signals consist of just of P(Y) signal



	P(Y)
<b>Sub Carr</b>	BPSK(10)
<b>PRN</b>	Combined m-seqs
<b>L</b>	$6.2 \times 10^{12}$
<b>Data Rate</b>	50 bps
<b>Sec. Code</b>	None



64



## Legacy Glonass Signals

Current Glonass Signals use Frequency Division Multiple Access (**FDMA**)  
Modernisation plan: move to CDMA

The frequency bands are:

Band	Centre Freq (MHz)	Bandwidth (MHz)
L1	1602.00	~20
L2	1246.00	~20

Glonass operates two services:

1. The Open Service (OS) – available to all
2. The Authorised Service (AS) – available only to military: encrypted

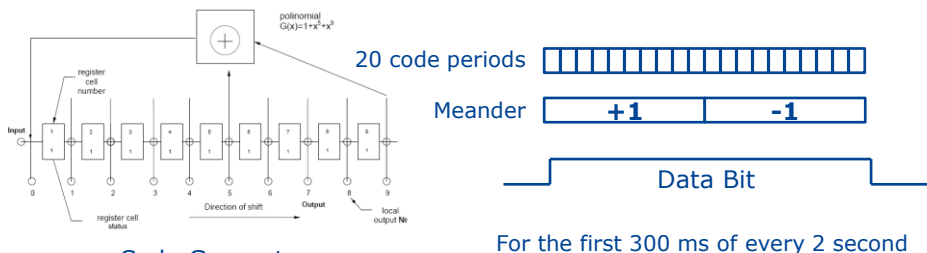


## Glonass C/A Signal

The Glonass C/A signal consists of a BPSK( 511 kHz) modulated by an m-sequence of length 511 chips for a code period of 1 ms

This is subsequently modulated by a secondary code of sorts called the **meander** sequence of ten +1 values followed by ten -1 values

Finally modulated by the data sequence  $\{+1,-1\}$  at 50 bps

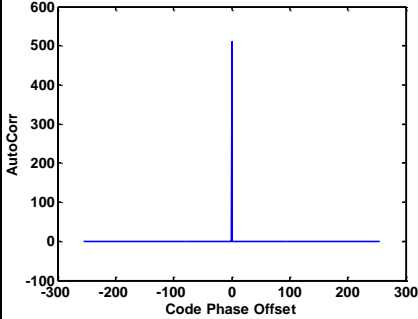




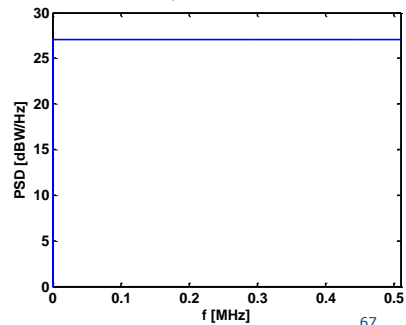
## Properties of the Glonass C/A Code

The Glonass C/A code is an m-sequence. It has ideal auto-correlation and spectral properties

$$R(\tau) = \begin{cases} L, & \tau = 0 \\ -1, & \text{otherwise} \end{cases}$$



$$G_{CA}(f) = \begin{cases} 1, & f = 0 \\ \frac{L^2 - 1}{L - 1}, & \text{otherwise} \end{cases}$$



Joint Research Centre

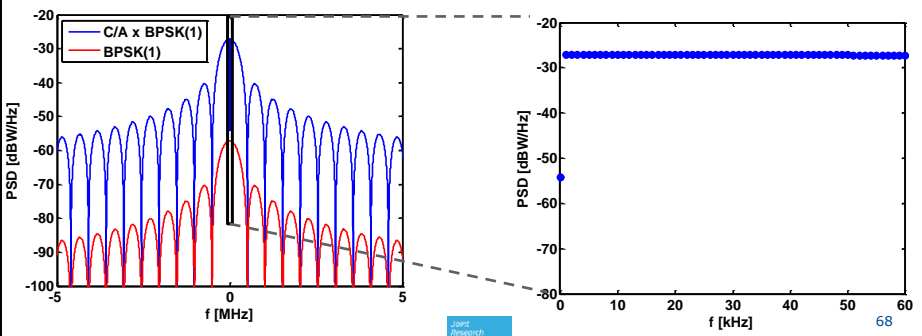
67



## Impact of the Subcarrier

**Result:** BPSK controls the “envelope” and C/A code provides fine structure

Same as for GPS – but in this case the code is **ideal**



Joint Research Centre

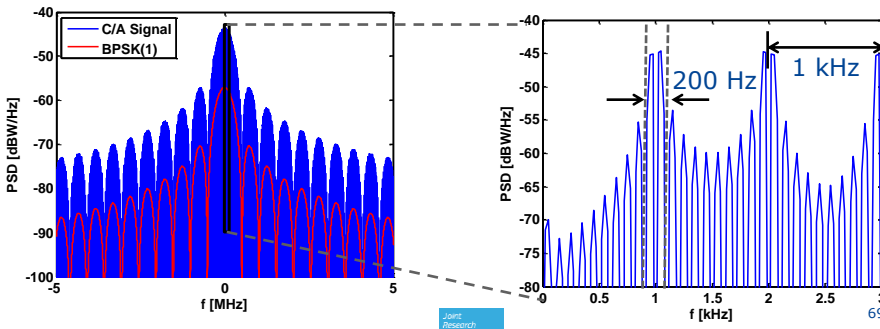
68



## Impact of the Meander and Data

Very similar to the GPS case – but the meander sequence changes the data PSD

The data PSD is equivalent to that of a BOC( 50Hz, 50Hz ) !



Joint Research Centre



## Glonass: L1

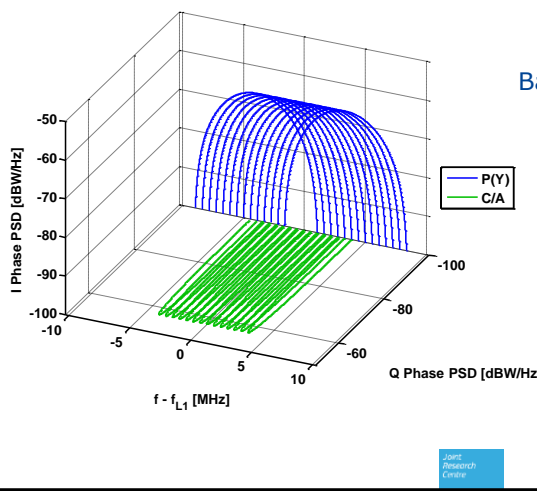
All signals are **FDMA**

14 Channels (-7 to +6)

Kth channel centred at:

$$f_k = 1602 \text{ MHz} + k \cdot 562.5 \text{ kHz}$$

Base frequency:  $f_0 = 0.511 \text{ MHz}$



	C/A	P
<b>Sub Carr</b>	BPSK(1)	BPSK(10)
<b>PRN</b>	M-sequence	N.A.
<b>L</b>	511	N.A.
<b>Data Rate</b>	50 bps	N.A.
<b>Sec. Code</b>	Meander	N.A.

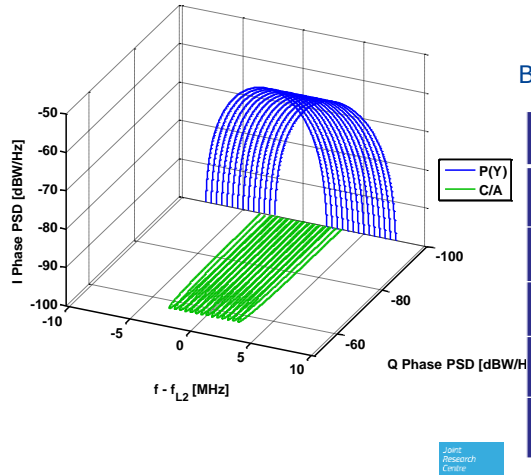
Joint Research Centre



## Glonass: L2

All signals are **FDMA**  
 14 Channels (-7 to +6)  
 Kth channel centred at:  
 $f_k = 1246 \text{ MHz} + k \cdot 437.5 \text{ kHz}$

Base frequency:  $f_0 = 0.511 \text{ MHz}$

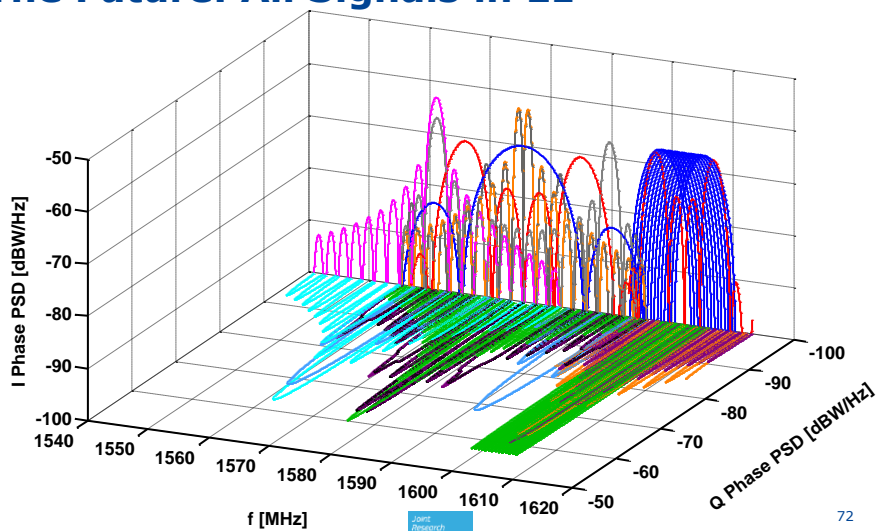


	C/A	P
<b>Sub Carr</b>	BPSK(1)	BPSK(10)
<b>PRN</b>	M-sequence	N.A.
<b>L</b>	511	N.A.
<b>Data Rate</b>	50 bps	N.A.
<b>Sec. Code</b>	Meander	N.A.

Joint Research Centre



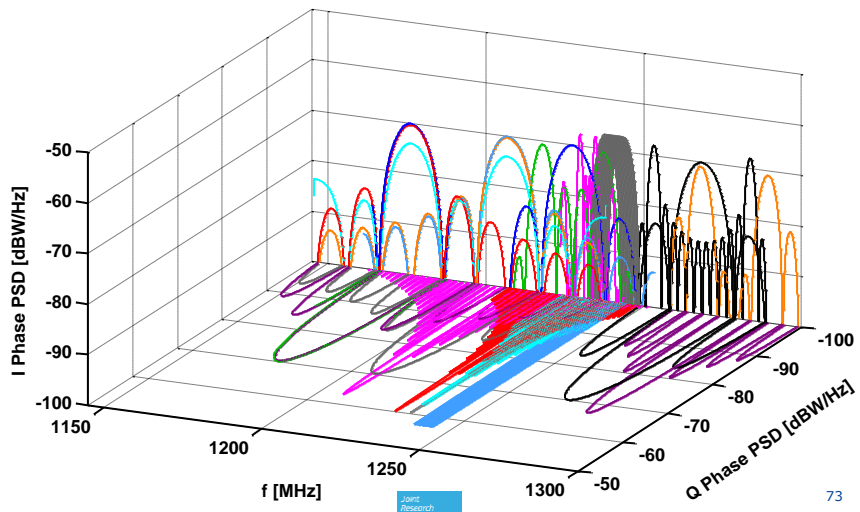
## The Future: All Signals in L1



Joint Research Centre



## The Future: All Signals in 1150 – 1300 MHz



Joint  
Research  
Centre

73



## REFERENCES

Joint  
Research  
Centre

74



## References on System Status

The Interface and Control Documents (ICD) for each system can be found on-line:

- **GPS:** <http://www.gps.gov/technical/icwg/>
- **Galileo:** [http://ec.europa.eu/enterprise/policies/satnav/galileo/open-service/index\\_en.htm](http://ec.europa.eu/enterprise/policies/satnav/galileo/open-service/index_en.htm)
- **Glonass:** <http://facility.unavco.org/kb/questions/727/English+version+of+ICD-GLOASS+version+5.1>
- **Compass:** <http://www.beidou.gov.cn> (in Chinese)

For updates on current and future plans for the various GNSS, look at the website of the International Committee on GNSS:

- <http://www.oosa.unvienna.org/oosa/SAP/gnss/icg/meetings.html>



## Text books

Among the most commonly used textbooks on GNSS are:

- Parkinson, B. W. & Spilker Jr., J. J., ed. (1996), *Global Positioning System: Theory and Applications*, Vol. 1, American Institute of Aeronautics and Astronautics, Washington DC.
- Kaplan, E. D. & Hegarty, C. J., ed. (2006), *Understanding GPS: Principles and Applications*, Artech House Publishers.
- Misra, P. & Enge, P. (2006), *Global Positioning System: Signals, Measurements, and Performance*, Ganga-Jamuna Press.



## References on signal structure

- Ávila-Rodríguez, J. Á. (2008), 'On Generalized Signal Waveforms for Satellite Navigation', PhD thesis, University FAF Munich.
- Lestarquit, L.; Artaud, G. & Issler, J. L. (2008), AltBOC for Dummies or Everything you Always Wanted to Know About AltBOC, in '*Proceedings of the ION GNSS 2008*', pp. 961-970.
- Pratt, A. R. (2009), New Navigation Signals and Future Systems in Evolution, Chapter 17 in Scott Gleason & Demoz Gebre-Egziabher, ed., '*GNSS Methods and Applications*', Artech House.





# GNSS Receiver Architecture

Daniele Borio

Joint Research Centre,  
Ispra (VA), Italy



Summer School on  
GNSS CORE TECHNOLOGIES  
July 2-4, 2012



## Introduction

The purpose of GNSS receivers is to collect the signals transmitted by GNSS satellites, determine ranges and range rates and compute the user PVT.

The analog signal at the receiver antenna can be modeled as (simplified model):

$$y(t) = \sum_{i=0}^{L-1} \sqrt{2C_i} d(t - \tau_i) c_i(t - \tau_i) \cos(2\pi(f_{RF} + f_{d,i})t + \varphi_i)$$

Annotations for the equation:

- Received power
- Navigation message
- PRN code
- code delay
- RF frequency
- Doppler frequency
- Carrier phase

The receiver needs to amplify, filter, down-convert, samples and quantize the received signal before being able to process it

### Content of this part:

- ✓ **receiver architecture:** functional blocks
- ✓ **from the digital to the analog signal**



## C/N<sub>0</sub> (I/II)

A key metric in GNSS receivers is the **Carrier-To-Noise Spectral Density Ratio** (C/N<sub>0</sub>).

The *i*th GNSS signal arriving at the receiver antenna has a total power content denoted C<sub>*i*</sub>. For a given direction of arrival of the signal, this power will be a function of the transmitted power, satellite antenna gain pattern, free-space losses, and any attenuation due to the channel

Additionally, the receiver front-end by its nature generates a coloured Gaussian random noise process (to be explained later). This can be modelled as a white noise process at the output of the antenna, which is subsequently filtered by the RF front-end. This white noise process has a flat power spectral density of N<sub>0</sub>/2 Watts/Hz

Therefore, at the output of the antenna, a measure of the **signal quality** can be given by the ratio of the carrier power to the noise power spectral density: i.e. the C/N<sub>0</sub>



## C/N<sub>0</sub> (II/II)

The C/N<sub>0</sub> is a **quantity independent** from the receiver that should quantify the signal quality independently from any receiver implementation

Each GNSS receiver **estimates** the C/N<sub>0</sub> of its received signals: different estimates can be provided by different receivers

The **receiver sensitivity** is determined by the C/N<sub>0</sub> (or equivalently, signal power) of the weakest signal that the receiver is able to process

The C/N<sub>0</sub> is a ratio, but is usually expressed in log scale (dB-Hz)

$$\left( \left[ \frac{C}{N_0} \right] \right)_{dB} = \left( \left[ \frac{[C]}{[N_0]} \right] \right)_{dB} = \left( \frac{Watt}{Watt / Hz} \right)_{dB} = (Hz)_{dB} = dB \text{ Hz}$$

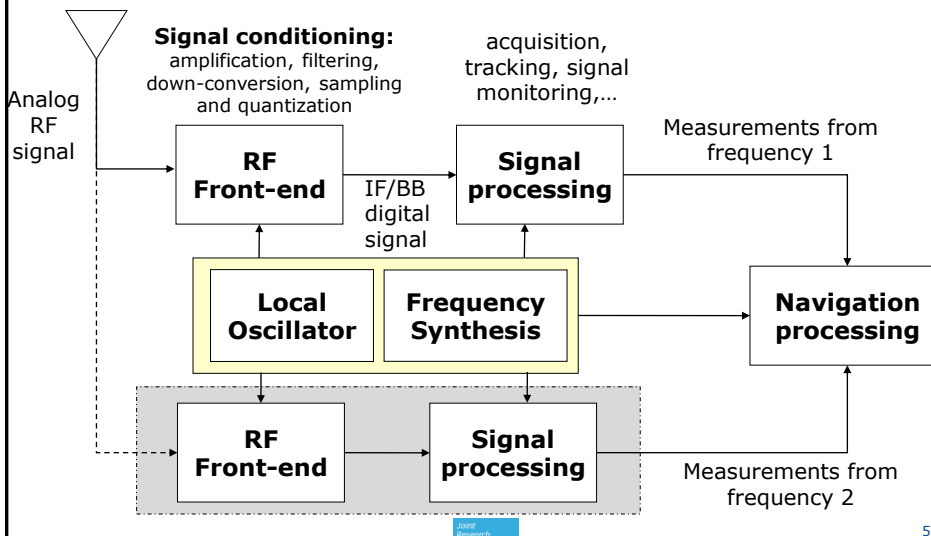
The noise Power Spectral Density (PSD) can be computed as

$$N_0 = k_B T_0$$

where  $k_B = 1.38 \cdot 10^{-23}$  (Jules/Kelvin) is the Boltzmann constant and T<sub>0</sub> is the noise temperature. Assuming T<sub>0</sub> = 290 K, N<sub>0</sub> = -204 dB W/Hz. For the GPS L1 C/A signal, the received power is approximately C=-160 dBW, leading to a nominal C/N<sub>0</sub> of about 44 dB-Hz



## High Level Architecture (I/II)



5



## High Level Architecture (II/II)

- ✓ Modern GNSS receivers are equipped with antennas capable of collecting signals from several frequencies
- ✓ Several front-ends can be present for processing signals from different frequencies
  - careful design to avoid inter-frequencies biases in the GNSS measurements (pseudo-ranges, carrier phase, ...)
- ✓ The local oscillator plays a significant role in the receiver operations
  - used for generating the carriers for the signal down-conversion
  - local clock
- ✓ The 'navigation processing' block combines measurements from all frequencies



## Antenna Considerations

- The antenna is the **interface element** that allows a GNSS receiver to collect RF signals
- It is usually not considered a part of the receiver front-end, but it can contain elements (Low Noise Amplifier (LNA), filters, ...) that are usually part of the front-end

All measurements and the user position are computed with respect to the antenna **phase center**.

The phase center is not a **physical point**, but an **apparent place** at the centre of a sphere on which the signals are received with constant phase.

- vary with the frequency
- Phase Centre Variations (PCV) are distributed by many antenna manufacturers for mm-level applications

Fundamental parameters of a GNSS antenna are:

- ✓ **frequency response/bandwidth**: the antenna acts a first filtering stage and its behavior is frequency dependent
- ✓ **gain pattern**
- ✓ **polarization**

Joint  
Research  
Centre

7

## Gain Pattern and Polarization

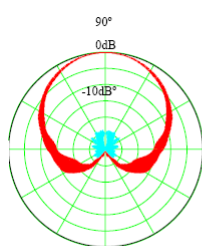
The antenna **gain pattern** describes how the antenna receives energy from space

- it is frequency dependent
- it is polarization dependent

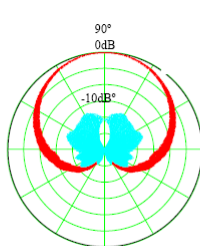
**Polarization** (wave): orientation of the oscillations of an electromagnetic wave  
**Polarization** (antenna): capability to receive waves with a specific polarization

GNSS signals are Right Hand Circularly Polarized (RHCP) and GNSS antennas should be designed to receive this kind of signals

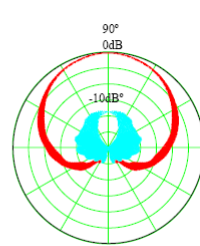
- Multipath rejection (reflections change the wave polarization)



L1 Pattern  
Peak Gain = 6.0 dBiC



L2 Pattern  
Peak Gain = 2.5 dBiC



L5 Pattern  
Peak Gain = 2.0 dBiC

**Red : RHCP**  
**Green: LHCP**

NovAtel Inc. (2009).  
GPS-704X Antenna  
Design and  
Performance, White  
paper.

8



## Antenna Classification

Depending on the application and target performance, GNSS antennas can have very different characteristics.

Also the type of technology (patch, helix, travelling wave antennas) strongly impacts their characteristics

Platform	Applications	Bands*	Instant. Bandwidth*	Gain Pattern	Multipath Rejection*	Interference Rejection*	Phase Center Stability**	Size	Weight	Cost
<b>Large</b>	Geodetic, ships, etc.	2 or more	> 40 MHz	Very strict*	High	High	Good	Diameter > 15 cm	Heavy*	High*
<b>Medium</b>	Car, truck, train, aircraft	1-2	> 10 MHz	Somewhat strict*	Medium	Medium	Fair	Diameter > 3 cm	Medium	Medium
<b>Small</b>	Body-wearable, laptop	1	> 2 MHz	Not strict	Low	Low	Poor	Small and conformal	Light	Low
<b>Handheld</b>	Cellphone, GNSS receiver	1	> 2 MHz	Ignored	None	None	Very poor	Very small	Very light	Very low

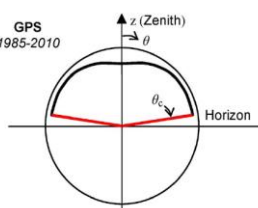
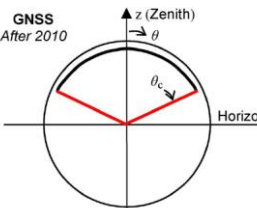
\* Large changes in a few years are expected.

\*\* Some will have serious degradation when bands and bandwidth are expanded.

From Wang, J. J. H.; , "Antennas for Global Navigation Satellite System (GNSS)," *Proceedings of the IEEE* , no.99, pp.1-7



## From GPS to GNSS Antennas

	<b>GPS</b>	<b>GNSS</b>
Frequency	<ul style="list-style-type: none"> <li>✓ single frequency (L1 1575.42 MHz)</li> <li>✓ dual frequency receivers (L1+L2, 1575.42 MHz)</li> </ul>	GNSS spectra across the 1146-1616 MHz frequencies (470 MHz bandwidth) Gap o 259 MHz (1300-1559 MHz)
Maximum Signal bandwidth	About 20 MHz	30.96 MHz (GPS) 40.96 MHz (Galileo and Glonass)
Gain Pattern		

Source: Wang, J. J. H.; , "Antennas for Global Navigation Satellite System (GNSS)," *Proceedings of the IEEE* , 10 no.99, pp.1-7



## The Local Oscillator

The local oscillator plays a fundamental role in a GNSS receiver.  
It is used for

- ✓ **signal down-conversion**
- ✓ **sampling**
- ✓ local code and carrier generation
- ✓ navigation solution (generation of a common time scale, measurements time stamping...)

The output of a local oscillator is usually a sinusoidal (or square) wave at a frequency  $f_o(t)$ .  $f_o(t)$  is time-varying and can introduce distortions in the received GNSS signals

Frequency multipliers can be used to increase the frequency provided by the local oscillator.

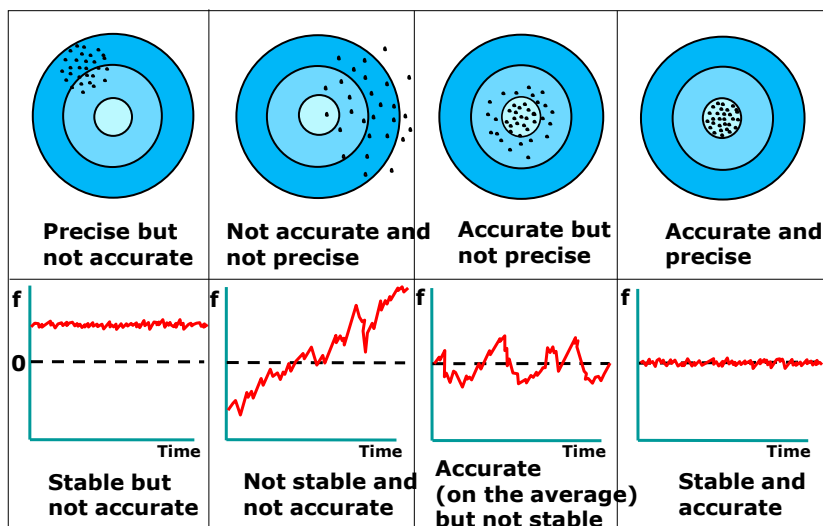
A characterization of the local oscillator is required to properly set the processing parameters of GNSS receivers

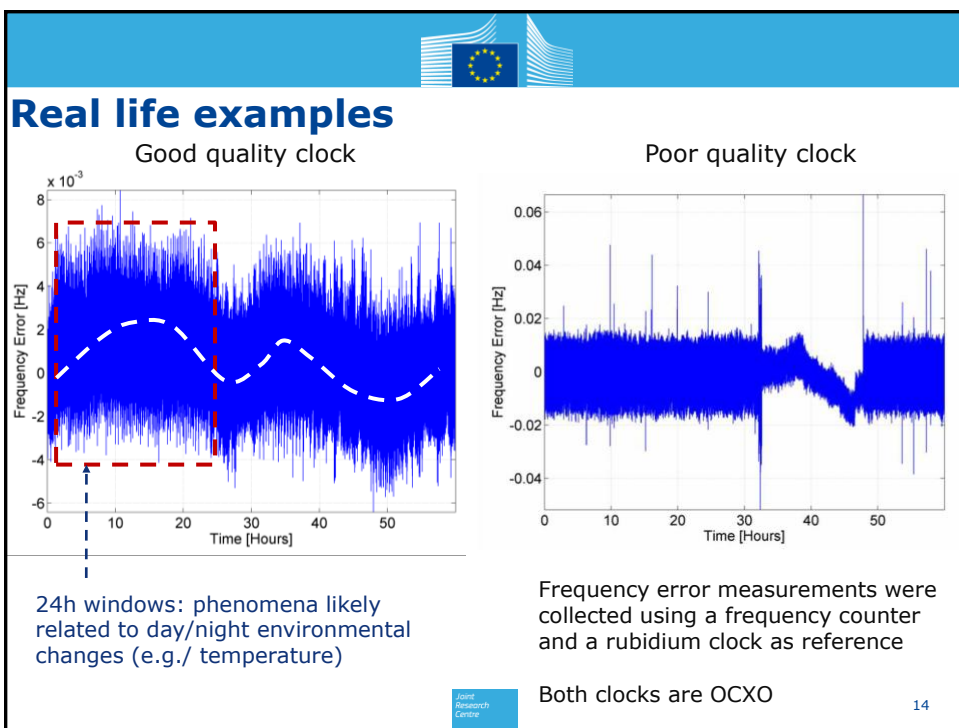
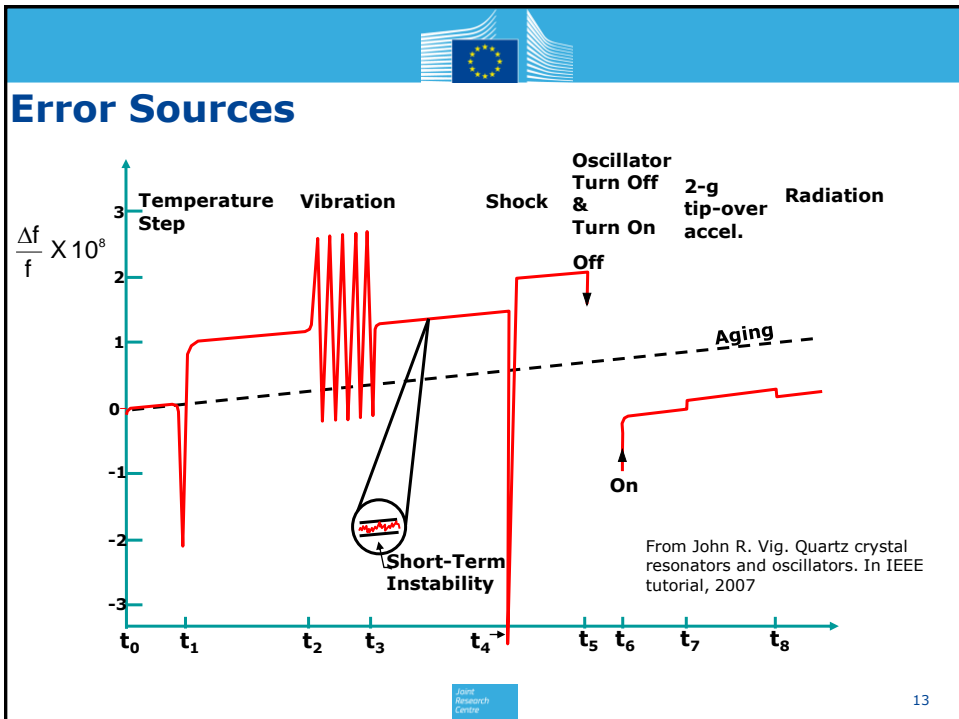
E.g./ Acquisition and tracking parameters  
Nav Solution: Kalman filter parameters

Gaggero P. (2008) Effect of oscillator instability on GNSS signal integration time. Masters Thesis, University of Neuchtel, Switzerland. Available on-line: [http://plan.geomatics.ucalgary.ca/papers/msc\\_thesis\\_gaggero\\_feb08.pdf](http://plan.geomatics.ucalgary.ca/papers/msc_thesis_gaggero_feb08.pdf) 11



## Properties of the Local Oscillator







## Oscillator Errors as a Random Process

The frequency reference provided by the local oscillator is a **non-stationary, scale-dependent** random process:

### **non-stationarity:**

the statistical properties change over time. Mean and variance (when defined) are not constant.

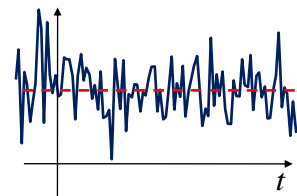
### **scale dependency:**

a continuous time process cannot be observed with an infinite time resolution. The observations are sampled in time: when the process is sampled with different time scales, different phenomena arise

The non-stationary nature of the process means it is not ergodic, therefore statistical properties (such as mean, variance) are a function of time. In fact variance tends to infinity as time scale increases.

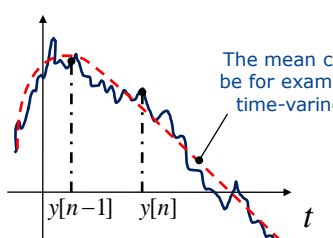


## Non-stationary signals



**Wide Sense Stationary (WSS) signal:**  
mean and variance are constant over time and can be estimated as:

$$\hat{\sigma}^2 = \frac{1}{N-1} \sum_{n=0}^{N-1} (y[n] - \bar{y})^2 \quad \bar{y} = \frac{1}{N} \sum_{n=0}^{N-1} y[n]$$



**Non-stationary signals**  
the mean and variance are no longer constant, even the noise distribution can change over time

Standard empirical mean and variance estimates lose their meaning

New meaningful quantities are required to characterize oscillator noises

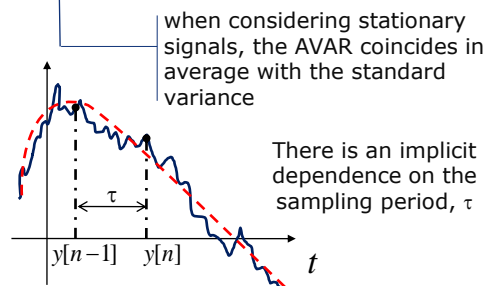


## Allan Variance

The Allan Variance (AVAR) measures the average deviation between frequency measurements taken at subsequent time instants

### Allan variance

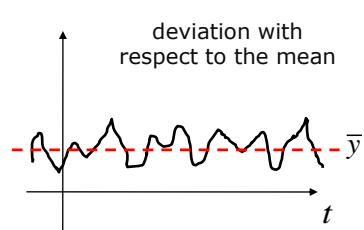
$$\sigma_A^2 = \frac{1}{2(N-1)} \sum_{n=1}^{N-1} (y[n] - y[n-1])^2$$



Joint Research Centre

### Sample variance

$$\hat{\sigma}^2 = \frac{1}{N-1} \sum_{n=0}^{N-1} (y[n] - \bar{y})^2$$



17

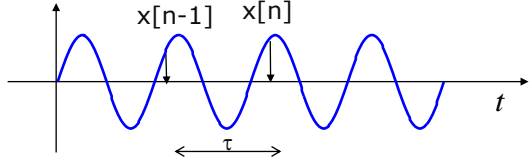
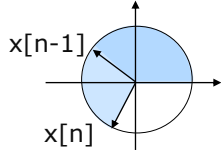
## Allan Variance and Oscillators

The AVAR (and Allan deviation) is a mathematical tool and can be used for the analysis of generic time series ( $y[n]$ ). For example, it has been used for characterization of Inertial Mounted Units (IMUs).

In the case of clocks,  $y[n]$ , is a **frequency measurement** (the frequency of the generated sinusoid) obtained on the reference interval  $\tau$ .

$y[n]$  can be expressed in terms of phase measurements:

$$y[n] = \frac{x[n] - x[n-1]}{\tau}$$



Joint Research Centre

18



## Oscillator PSD

Since the oscillator errors are non-stationary, the power spectral density is **undefined**.

For practical reasons, the PSD can be **defined** as that which would be measured by a **spectrum analyzer**

From a mixture of practical and theoretical considerations, the following model arises for the PSD of the frequency error:

$$S_y(f) = \sum_{\alpha=-2}^2 h_\alpha f^\alpha \quad \text{for } 0 \leq f \leq f_h \quad \begin{matrix} \leftarrow & \text{Upper cut-off} \\ & \text{frequency} \end{matrix}$$

This is a **power-law model** where the coefficients are referred to as the **h-parameters** of the oscillator

Each power of f, represented by  $\alpha$ , corresponds to a different error domain:

- 2 : random walk frequency modulation
- 1: flicker-noise frequency modulation
- 0 : white noise frequency modulation
- 1: flicker noise phase modulation
- 2 : white noise phase modulation

19

IT Research  
Centre

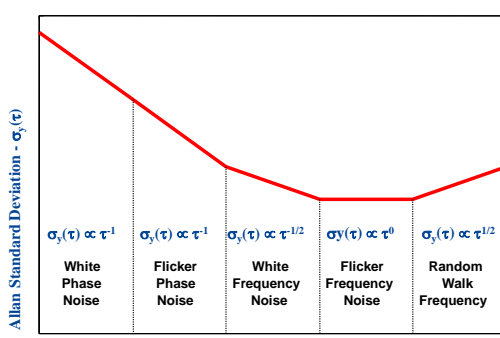
## AVAR and PSD

Each power law region in the PSD model has an equivalent power-law region in the Allan variance model:

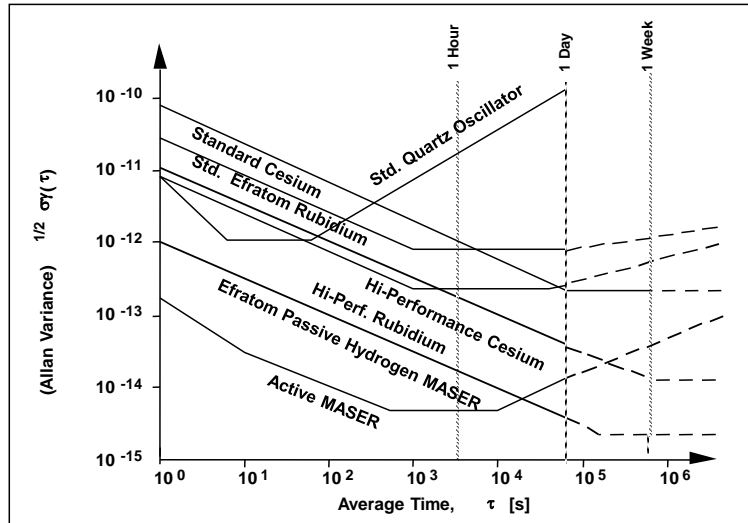
$$S_y(f) \sim f^\alpha \rightarrow \sigma_y^2(\tau) \sim \tau^\alpha$$

Equivalence due to the fact that the AVAR can be expressed as the area under a filtered version of the PSD

$$\sigma_y^2(\tau) = \frac{1}{2} \int_0^{+\infty} S_y(f) \underbrace{\frac{4 \sin^4(\pi f \tau)}{(\pi f \tau)^2} df}_{\text{Filter Transfer Function}}$$



## Oscillator Stability Comparison



21

## Frequency Synthesis

GNSS receivers may require multiple frequency references – for example, during down-conversion, each mixer stage requires a precise reference frequency; the sampling clock must be generated, etc

**Frequency Synthesis** is the process of generating the desired reference frequencies in the receiver from the local oscillator. This is usually achieved by combinations of integer and rational frequency multiplication

This is an important consideration in receiver design, as it affects how oscillator errors propagate through the design. Consider a 10 MHz reference oscillator with a 10 Hz error (1 part per million), after up-conversion to the GPS L1 frequency (1575.42 MHz), this corresponds to a frequency error of approximately 1.5 kHz

22

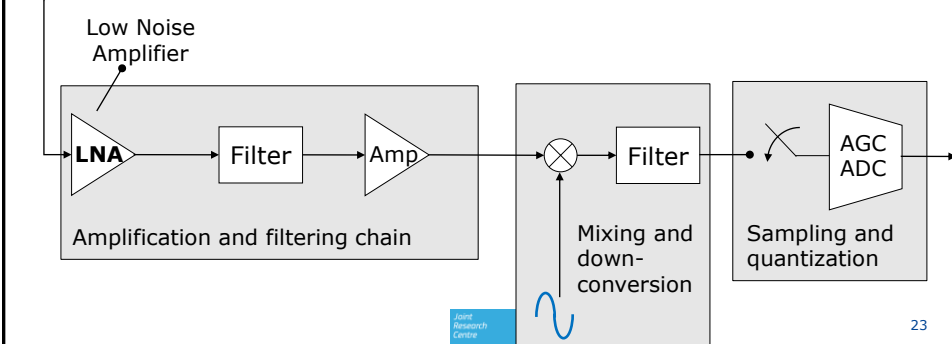


## Front-end structure

The front-end includes all the devices necessary to convert the analog signal captured by the antenna into the digital sequence that will be used by the signal processing and navigation blocks

- ✓ There exists of several front-end architectures
- ✓ Three fundamental operation:
  - amplification and filtering
  - down-conversion
  - sampling and quantization (digitization)

Multi-frequency/channel front-ends must provide synchronous samples from each collected signal



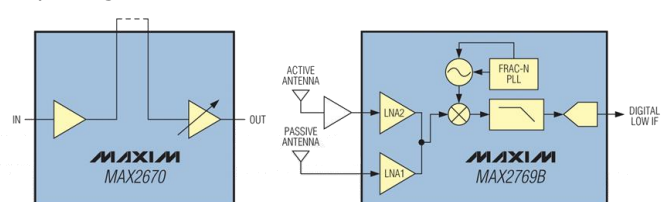
## The Pre-amplifier

The pre-amplifier is usually the first active component in the front-end chain.

- ✓ Usually **integrated** in the antenna (low-cost, better performance)
- ✓ Amplification can be performed using several stages:
  - The first amplifier should be a **Low Noise Amplifier** (LNA): high gain, low noise figure (to be justified using the Friis' formula)
- ✓ The amplifier behavior is **frequency dependent**
  - enhance frequency filtering
  - the amplifier characteristics have to be accounted for the design of multi-band GNSS receivers (multi-band coverage)
- ✓ Typical GNSS amplifier requires gains > 30 dB

### Example:

Maxim MAX2670  
 - Dual stage amplifier  
 - 34.8 dB gain  
 - 1.4 dB Noise Figure



## Amplifier Noise Model

The power of the noise at the output of a (linear) amplifier can be expressed as:

$$\begin{aligned}
 P_{out} &= \int_{-\infty}^{\infty} G_n(f) |H(f)|^2 df + P_{amp} \\
 \text{output power} &\quad \text{PSD of the input noise} \quad \text{Power of the additional noise introduced by the amplifier} \\
 \text{Input noise: thermal noise} &\quad \text{Transfer function of the linear amplifier} \\
 \text{with PSD } G_n(f) = \frac{1}{2} k_B T & \\
 P_{out} &= \frac{1}{2} k_B T \int_{-\infty}^{\infty} |H(f)|^2 df + P_{amp} = k_B T \max_f |H(f)|^2 \left[ \frac{\int_{-\infty}^{\infty} |H(f)|^2 df}{2 \max_f |H(f)|^2} + P_{amp} \right] \\
 &= k_B g_d B_e T + P_{amp} = k_B g_d B_e \left( T + \frac{P_{amp}}{k_B g_d B_e} \right) = k_B g_d B_e (T + T_e) \\
 \text{amplifier gain} &\quad \text{Device bandwidth} \\
 \text{Joint Research Centre} &\quad \text{Effective noise temperature}
 \end{aligned}$$

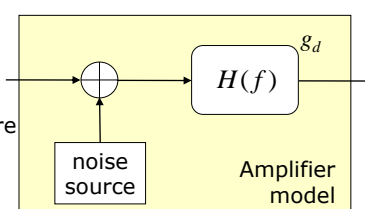
25

## Noise factor and Noise figure

A linear amplifier can be thus modeled as filter with transfer function  $H(f)$  and gain  $g_d$ , with an additional noise source at its input

The additional noise has PSD  $\frac{1}{2} k_B T_e$

$T_e$  describes the increase of noise temperature caused by the amplifier



### Input/Output SNR

$P_s$ : useful signal power at the amplifier input

$$\left( \frac{S}{N} \right)_{out} = \frac{g_d P_s}{k_B g_d B_e (T + T_e)} = \frac{1}{1 + T_e / T} \frac{P_s}{k_B T B_e} = \frac{1}{1 + T_e / T} \left( \frac{S}{N} \right)_{in}$$

$$F = \frac{(S/N)_m}{(S/N)_{out}} = 1 + \frac{T_e}{T}$$

**Noise factor**

$$[F]_{dB} = 10 \log_{10} \left( 1 + \frac{T_e}{T} \right)$$

**Noise figure**

$F$  is usually computed at a reference temperature  $T = 290K$

26



## Friis' Formula

The effective noise temperature of a system of cascaded dipoles (electronic devices) can be computed using Friis' formula:

$$T_e = T_{e,1} + \frac{T_{e,2}}{g_1} + \dots + \frac{T_{e,n}}{g_1 \cdot g_2 \cdots g_{n-1}}$$

$g_i, T_{e,i}$  gain and noise temperature of the  $i$ th device

Friis' formula can be expressed in term of noise factor:

$$F = F_1 + \frac{F_2 - 1}{g_1} + \dots + \frac{F_n - 1}{g_1 \cdot g_2 \cdots g_{n-1}}$$

recall

$$T_{e,i} = (F_i - 1)T$$

### Remarks:

✓ These results are valid when there is **impedance matching**: the impedance of the device input has to be matched to the impedance of the load

✓ An impedance mismatch causes an increase of the noise factor

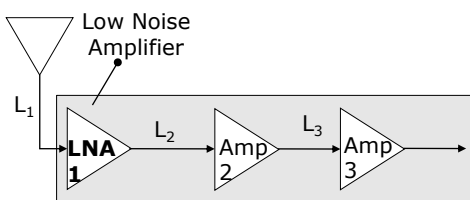
✓ A passive device (e.g., a cable) with a loss  $L$  introduces a noise with power

$$P_n = k_B T B_e \left(1 - \frac{1}{L}\right), \text{ i.e., it is characterized by a noise factor } F = L$$

27



## Friis'Formula and GNSS Receivers



The antenna is connected to the LNA with a short cable with loss  $L_1$ :

$$T_e = T \left[ L_1 - 1 + L_1 \left[ F_1 - 1 + \frac{1}{g_1} [L_2 - 1 + L_2 [\dots]] \right] \right]$$

The gain of a passive component is the inverse of its loss,  $L$

In order to minimize the noise introduced by the receiver it is necessary to:

✓ minimize  $L_1$  (this justifies the choice of integrating the LNA within the antenna)

✓ maximize  $g_1$  (the gain of the first amplifier in the chain)

✓ minimize  $F_1$  (the noise figure of the first amplifier)

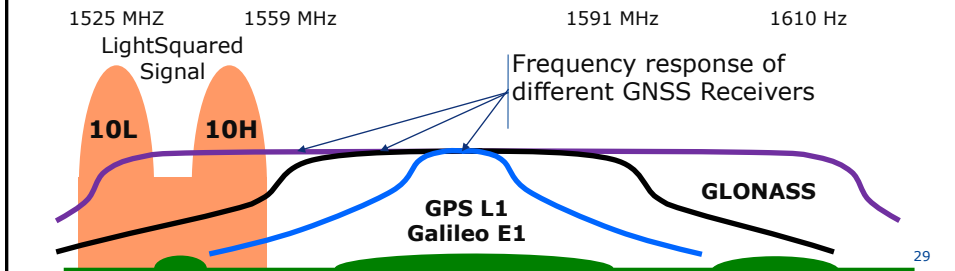


## Front-end Filtering

Front-end filtering is used to:

- ✓ reduce the impact of the input noise and RF interference
- ✓ avoid aliasing during the sampling process.
- ✓ Front-end filtering can be realized using several stages
- ✓ usual are requirements: **constant gain** and **flat group delay** across the GNSS signal bandwidths (avoid measurement biases)
- ✓ **colors** the received noise (correlated noise)
- ✓ new GNSS signals are wide-band in nature: larger front-end filters with respect to the GPS L1 C/A signal
- ✓ GPS L1 C/A signal: from 2 MHz (low-cost) to 20 MHz (high fidelity) filter bandwidths.

The front-end frequency response determine the impact of **RF interference**



29



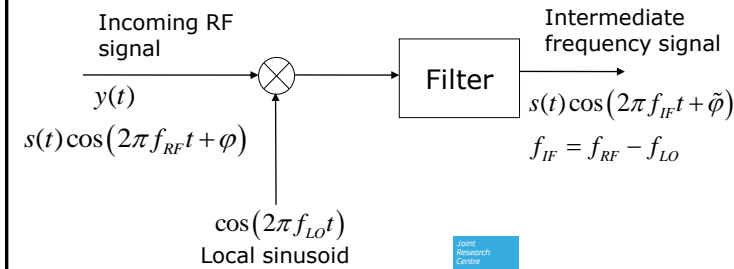
## Down-conversion

Down-conversion is the process of lowering the centre frequency of a narrow band signal.

There exists several down-conversion schemes:

- ✓ to an **intermediate frequency (IF)**
- ✓ to **baseband (BB)** using an I/Q down-conversion scheme
- ✓ **direct sampling**: down-conversion is performed exploiting a frequency replica caused by aliasing, during the sampling process

The simplest down-conversion scheme is based on mixing the input signal with a local sinusoid. Filtering is used to remove the additional frequency components generated by mixing



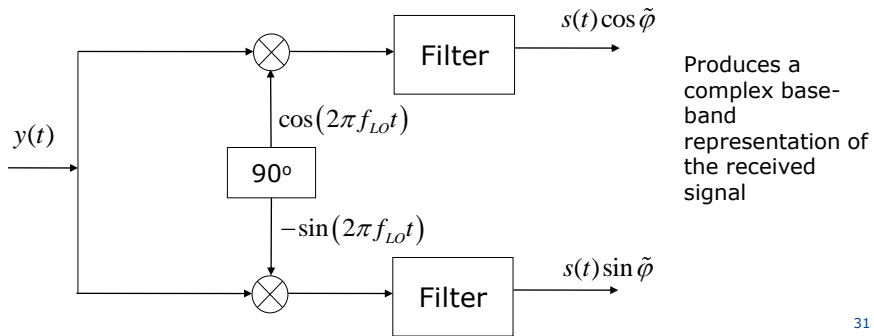


## I/Q down-conversion

I/Q down-conversion is obtained by mixing the input signal with two orthogonal signals.

Oscillator errors (frequency drift, frequency noise, ...) affect the phase and frequency of the down-converted signal (frequency offset causes an apparent Doppler effect on the measurements)

Down-conversion and filtering are usually performed using multiple stages.



31



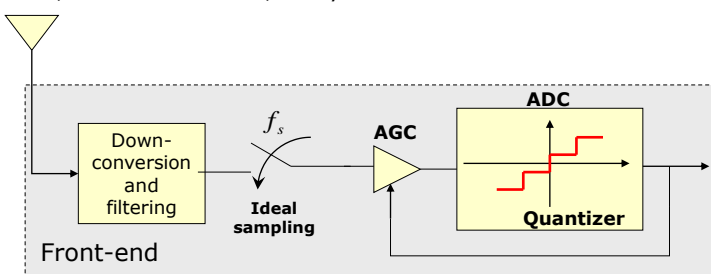
## Sampling and quantization

The function of the digitizer is two-fold:

- 1) It transforms the continuous time signal to a discrete time signal (**sampling**)
- 2) it transforms a continuous valued signal to a discrete valued signal (**quantization**)

By Shannon's sampling theorem sampling can be achieved with no loss of information (the sampling frequency has to be at least twice the signal bandwidth)

Quantization, on the other hand, always leads to some losses.





## AGC and ADC

Quantization is performed using the combination of the

✓ **Automatic Gain Control (AGC)**: properly scales the input signal in order to fully use the ADC dynamics. Strong signals, with an amplitude outside the ADC input range are clipped.

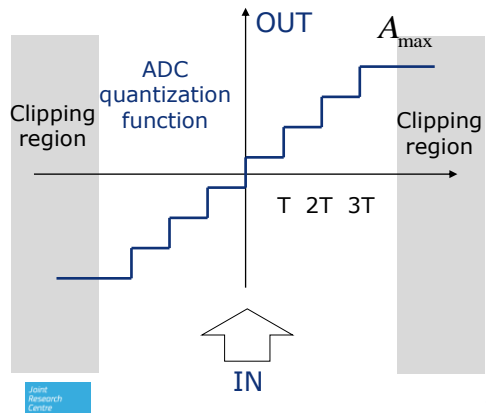
✓ **Analog-to-Digital Converter (ADC)**: map the analog signal into a finite alphabet

ADC are characterized by the quantization function,  $Q(x)$  that defines how analog signals are mapped into a finite alphabet

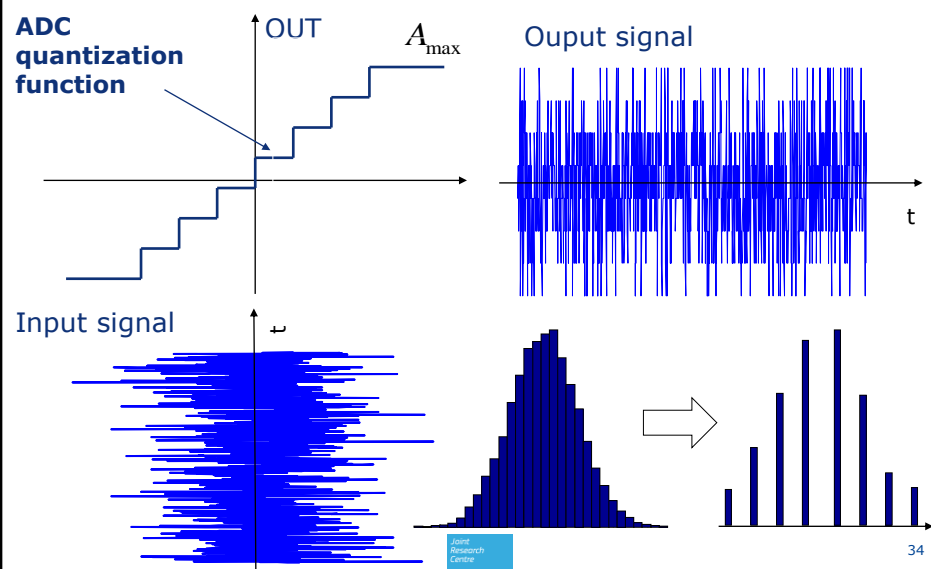
The simple ADC uses only 1 bit for the signal representation and

$$Q(x) = \text{sign}(x)$$

In this case, no AGC is required



## AGC/ADC principles



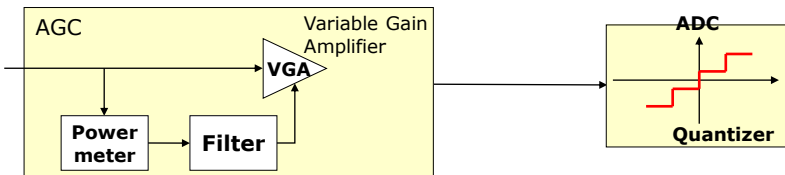


## AGC Control Loop

The AGC gain is determined using a control loop

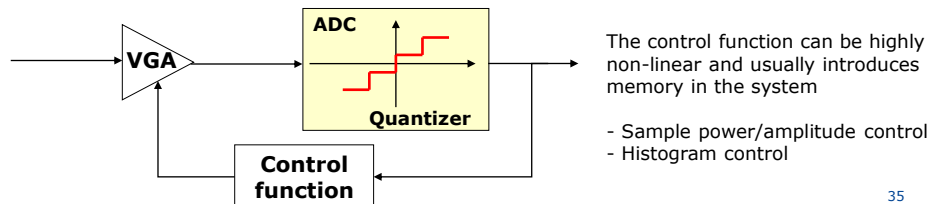
### Analog AGC

The AGC gain is determined using the input analog signal



### Digital AGC

The AGC gain is determined using the digital samples at the ADC output

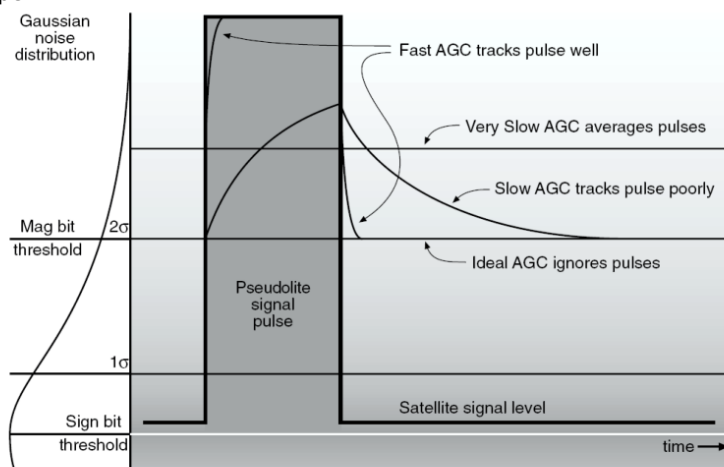


35



## AGC types

The responsiveness of the AGC in changes in the input power determines the AGC type.



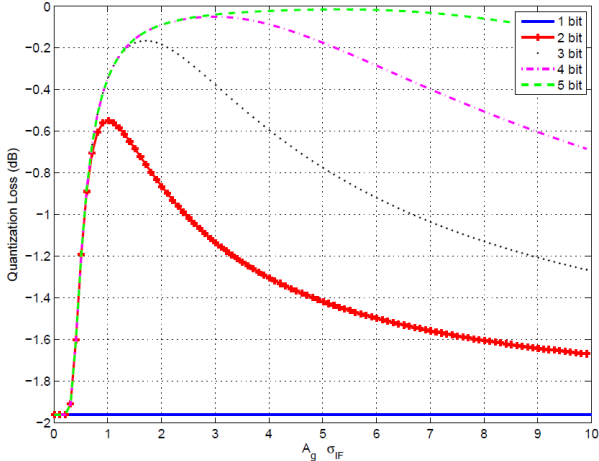
**AGC and ADC**  
plays a  
significant role  
in rejecting/  
amplifying the  
effect of RF  
interference

- ✓ natural immunity with respect to pulsed interference

From H. Stewart Cobb. GPS pseudolites: Theory, Design and Applications. Phd thesis, Stanford University, <http://waas.stanford.edu/www/papers/gps/PDF/StuCobbThesis97.pdf>, September 1997.

36

## Quantization Losses



The signal at the ADC input is made of useful components and noise.

The SNR (to be better explained) defines the ratio between useful and noise components.

Quantization reduces the SNR at the ADC output.

During normal operation of the receiver, the AGC control loop tries to minimize the quantization loss

37

## Signal Model at the Front-End Output (I/II)

### IF model

After amplification, filtering, down-conversion and quantization the received GNSS signal can be expressed as:

$$r[n] = \sum_{i=0}^{L-1} \sqrt{2\tilde{C}_i} \tilde{d}(nT_s - \tilde{\tau}_i) \tilde{c}_i(nT_s - \tilde{\tau}_i) \cos(2\pi(f_{IF} + f_{d,i})nT_s + \tilde{\varphi}_i) + \eta[n]$$

The  $\sim$  is used to indicate the effect of front-end filtering

Amplification, AGC scaling and quantization change the amplitude of the received signal

The front-end can introduce additional delays

$\tilde{\tau}_i$  is time-varying (it contains at least a code rate term)

Intermediate frequency

Sampling interval

Doppler frequency and carrier phase are affected by the errors introduced by the local oscillator

Noise collected by the antenna and introduced by the front-end

Joint Research Centre

38



## Signal Model at the Front-End Output (II/II)

### Base-band model

$$r[n] = \sum_{i=0}^{L-1} \sqrt{\tilde{C}_i} \tilde{d}(nT_s - \tilde{\tau}_i) \tilde{c}_i(nT_s - \tilde{\tau}_i) \exp\left\{j2\pi f_{d,i} nT_s + \tilde{\varphi}_i\right\} + \eta[n]$$

Complex circularly  
symmetric noise

The noise term is **non-Gaussian** (effect of quantization) and **colored** (effect of filtering)

#### However:

for mathematical simplicity and ease of receiver design

IF model

$$\eta[n] \sim \mathcal{N}(0, \sigma^2)$$

BB model

$$\eta[n] \sim C\mathcal{N}(0, I_2 \sigma^2)$$

A more advanced theory accounting for the noise correlation exists: see "Effect of partial-band interference on receiver estimation of C/N0: Theory." J.W. Betz - 2001

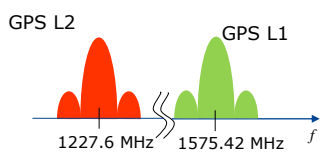
Joint  
Research  
Centre

## Multi-frequency Front-ends

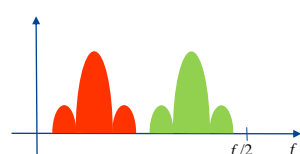
A multi-frequency front-end provides several signals from different bands with a structure similar to that illustrated in the previous slides

- ✓ the noise components can be considered independent
- ✓ signals from different bands pass through different hardware path (different receiver chains): **different delays** through the front-end for each band. These delays need to be **estimated** on the fly or **calibrated** after manufacturing
- ✓ Different signals have different bandwidths and thus can be sampled at **different rates**. Sampling rates should be multiples of some base frequency to ensure **synchronous processing** of signals from all front-end paths.

A possible solution for the GPS L2 signal:



Separate down-conversion to adjacent bands and joint sampling



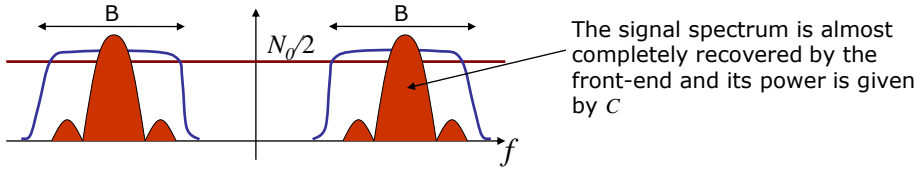
S. Qaisar and A. Dempster (2007) "Receiving the L2C Signal with Namuru GPS L1 Receiver"



## C/N<sub>0</sub> and SNR

The SNR is the ratio between the signal and noise power at a **given receiver stage**. It is a function of the C/N<sub>0</sub> and the receiver bandwidth.

The receiver recovers only a portion of the available spectrum.



Only a portion of the noise power enters the receiver. The collected noise power is proportional to the front-end bandwidth and it is given by:

$$\sigma_{RF}^2 = 2 \frac{N_0}{2} B$$

Thus the SNR is:

$$SNR = \frac{C}{\sigma_{RF}^2} = \frac{C}{N_0 B}$$

B is the receiver bandwidth and depends on front-end filtering

Each receiver stage changes the SNR (implementation losses) [41](#)



## Typical SNR in GNSS Front-Ends

In general, the final noise variance,  $\sigma^2$ , is not simply equal to  $\sigma_{RF}^2$  since it also account for the losses introduced by quantization and filtering.

- ✓ Typical C/N<sub>0</sub> values for the GPS C/A signal are in the region of 45 dB-Hz (High-Sensitivity receivers can process signal with a 25 dB-Hz C/N<sub>0</sub>)
- ✓ GPS receivers usually adopt bandwidths in the range [2 – 20 MHz]
- ✓ Assuming implementation losses equal to 2 dB, the SNR at the front-end output is in the range:

$$SNR_{dB} = C / N_0 - 10 \log_{10} B - L_f \\ = [-30, -20] \text{ dB}$$

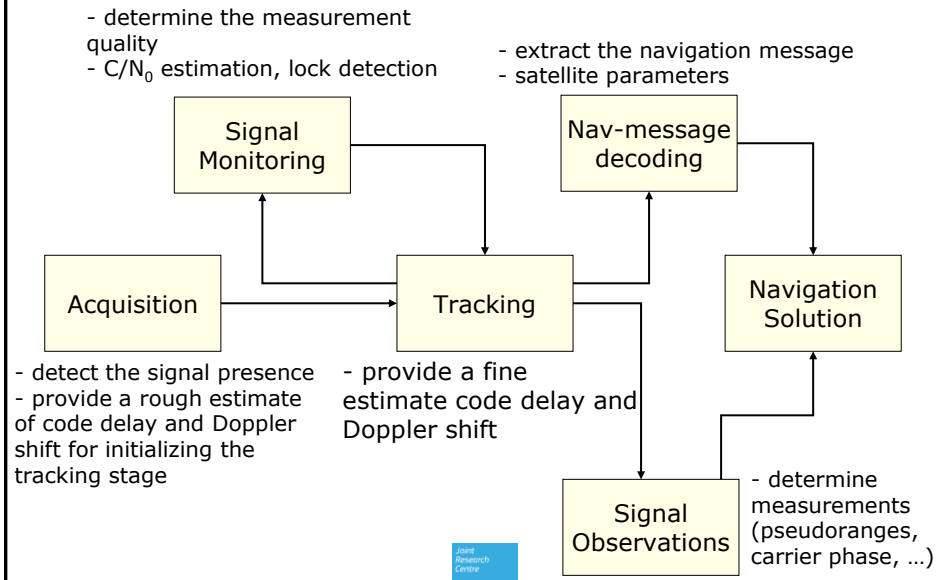
- ✓ These are extremely weak values!

The digital sequences generated by the front-end are passed to the signal processing and navigation blocks that will use them for generating measurements and computing the navigation solution

Digital processing stages are able to increase the SNR and extract the useful signal from noise [42](#)



## Signal Processing Stages





# *The acquisition*



[www.navsas.eu](http://www.navsas.eu)



Istituto Superiore Mario Boella

**Prof. Letizia Lo Presti**

**Politecnico di Torino**

ISPRRA July 2, 2012



## Table of contents

1. Introduction
2. Detection methods
3. Detection in GNSS
4. Search space
5. CAF evaluation schemes
6. Threshold setting
7. Coherent and non-coherent integration
8. Verification phase

ISPRRA July 2, 2012

2



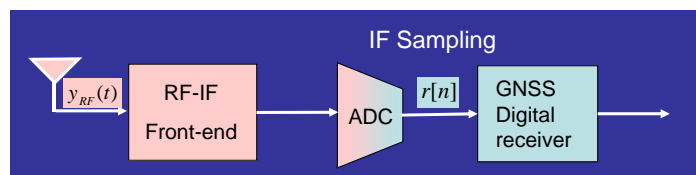
## Table of contents

Sec. 1

1. Introduction
2. Detection methods
3. Detection in GNSS
4. Search space
5. CAF evaluation schemes
6. Threshold setting
7. Coherent and non-coherent integration
8. Verification phase

## The RX chain

Sec. 1

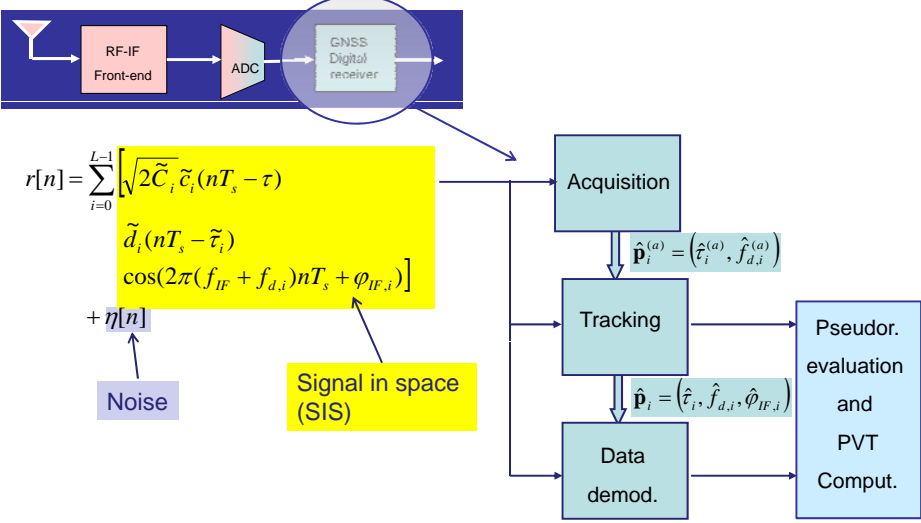


$$y_{RF}(t) = \sum_{i=0}^{L-1} \sqrt{2C_i} c_i(t - \tau_i) d_i(t - \tau_i) \cos(2\pi(f_{RF} + f_{d,i})t + \phi_{RF,i}) + w_{RF}[n]$$

$$r[n] = \sum_{i=0}^{L-1} \sqrt{2\tilde{C}_i} \tilde{c}_i(nT_s - \tilde{\tau}_i) \tilde{d}_i(nT_s - \tilde{\tau}_i) \cos(2\pi(f_{IF} + f_{d,i})nT_s + \varphi_{IF,i}) + \eta[n]$$

## The RX digital section

Sec. 1



ISPRRA July 2, 2012

5



## The acquisition tasks

Sec. 1

- To detect the satellites in view
- To provide coarse estimates of some SIS parameters (details in the next slides)

Let us start with detection

ISPRRA July 2, 2012

6



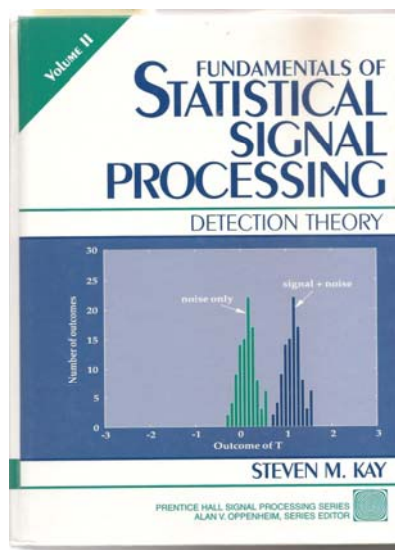
## Table of contents

Sec. 2

1. Introduction
2. Detection methods
3. Detection in GNSS
4. Search space
5. CAF evaluation schemes
6. Threshold setting
7. Coherent and non-coherent integration
8. Verification phase

## Detection theory

Sec. 2



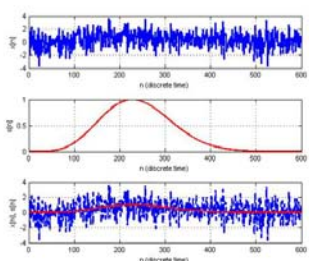
## Detection task

Sec. 2

Starting point: a set of measured data.

### Example:

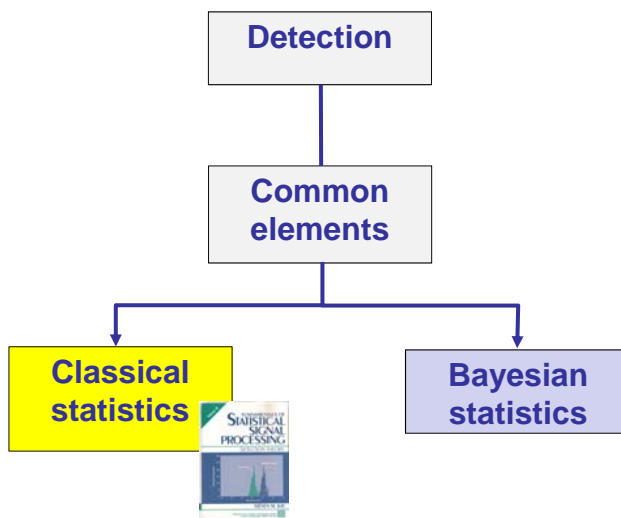
Signal plus noise



1. **Detection theory** (We want to detect the presence of the signal)
2. **Decision theory** (From data analysis, we have to decide if the signal is present)
3. **Hypothesis testing** (we formulate a hypothesis, and test if it is true)

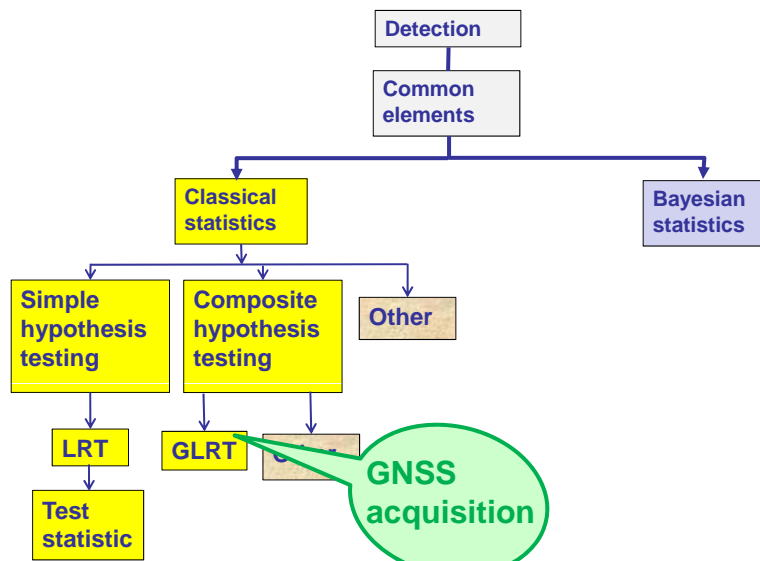
## Detection methods

Sec. 2



## Addressed topics

Sec. 2



ISPRRA July 2, 2012

11



## Simple hypothesis testing: Binary hypothesis

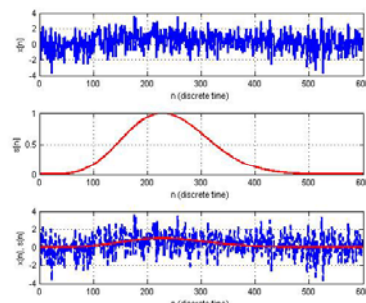
Sec. 2

$H_0$  Null hypothesis

$H_1$  Alternative hypothesis

### Example

$x_m[n] = as[n] + w[n]$   
 $(rp) \Rightarrow X[n] = As[n] + W[n]$   
 $H_0 : A = 0$   
 $H_1 : A = 1$



Note: Multiple hypothesis are possible, but not considered in this presentation

ISPRRA July 2, 2012

12



## Probabilistic model

Sec. 2

World of observables	World of models
Vector of measured data $\mathbf{x}_m = \{x_m[0], x_m[1], \dots, x_m[N-1]\}$	Vector of all possible data $\mathbf{x} = \{x[0], x[1], \dots, x[N-1]\}$
	Vector of random variables $\mathbf{X} = \{X[0], X[1], \dots, X[N-1]\}$
	Probability density function (PDF) Conditional PDF of $\mathbf{X}$ given $H_1$
	$p(\mathbf{x}; H_1)$ Conditional PDF of $\mathbf{X}$ given $H_0$ $p(\mathbf{x}; H_0)$

In our example:

$$H_0 : A = 0$$

$$H_1 : A = 1$$

## Likelihood function

Sec. 2

In our example:

$$p(\mathbf{x}; H_0) = p(\mathbf{x}; A = 0)$$

$$p(\mathbf{x}; H_1) = p(\mathbf{x}; A = 1)$$

$$p(\mathbf{x}; A = a)$$

Likelihood function

$$L(a) = p(\mathbf{x}_m; A = a)$$

Measured Vector!!

## Neyman – Pearson theorem

Sec. 2

From Kay

$$P_D = \Pr(H_1; H_1)$$

Detection probability

$$P_{FA} = \Pr(H_1; H_0)$$

False alarm probability

Theorem 3.1 (Neyman-Pearson) To maximize  $P_D$  for a given  $P_{FA} = \alpha$  decide  $\mathcal{H}_1$  if

$$L(\mathbf{x}_m) = \frac{p(\mathbf{x}_m; H_1)}{p(\mathbf{x}_m; H_0)} > \gamma \quad (3.3)$$

where the threshold  $\gamma$  is found from

$$P_{FA} = \int_{\{\mathbf{x}: L(\mathbf{x}) > \gamma\}} p(\mathbf{x}; \mathcal{H}_0) d\mathbf{x} = \alpha.$$

## Neyman – Pearson (NP) detector: design

Sec. 2

Theorem 3.1 (Neyman-Pearson) To maximize  $P_D$  for a given  $P_{FA} = \alpha$  decide  $\mathcal{H}_1$  if

$$L(\mathbf{x}_m) = \frac{p(\mathbf{x}_m; H_1)}{p(\mathbf{x}_m; H_0)} > \gamma \quad (3.3)$$

where the threshold  $\gamma$  is found from

$$P_{FA} = \int_{\{\mathbf{x}: L(\mathbf{x}) > \gamma\}} p(\mathbf{x}; \mathcal{H}_0) d\mathbf{x} = \alpha.$$

Likelihood ratio test (LRT)

1. Fix the probability of false alarm  $\alpha$
2. Evaluate the region  $\mathbf{x}: L(\mathbf{x}) > \gamma$

## Test statistic

Sec. 2

**Theorem 3.1 (Neyman-Pearson)** To maximize  $P_D$  for a given  $P_{FA} = \alpha$  decide  $\mathcal{H}_1$  if

$$L(\mathbf{x}_m) = \frac{p(\mathbf{x}_m; H_1)}{p(\mathbf{x}_m; H_0)} > \gamma \quad (3.3)$$

where the threshold  $\gamma$  is found from

$$P_{FA} = \int_{\{\mathbf{x}: L(\mathbf{x}) > \gamma\}} p(\mathbf{x}; H_0) d\mathbf{x} = \alpha.$$



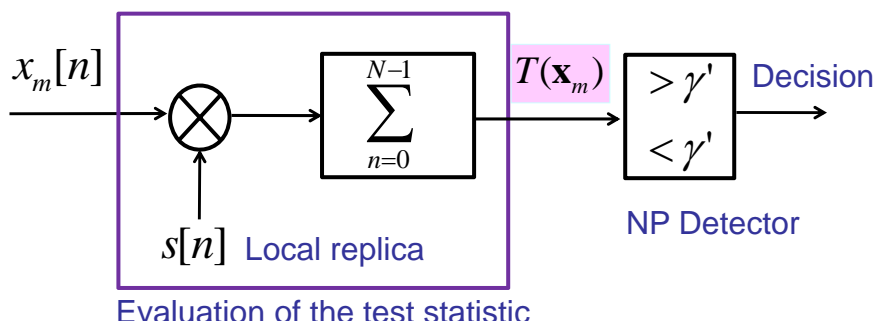
It is possible to transform this test into a test on a function of data: the **test statistic**

## Neyman-Pearson (NP) detector (example)

Sec. 2

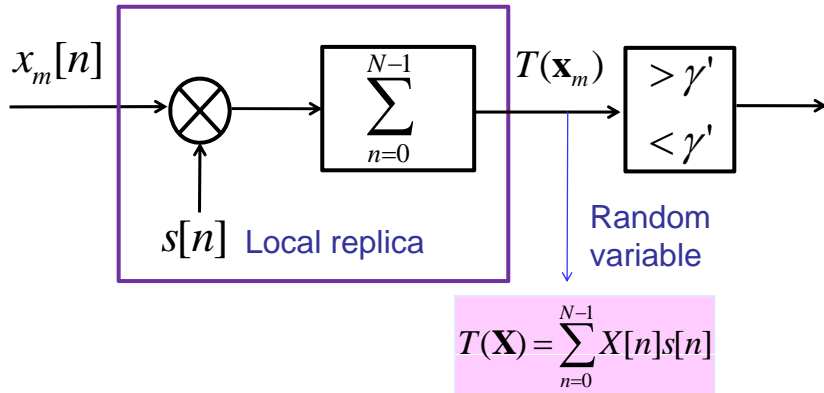
$$X[n] = A s[n] + W[n] \Rightarrow \text{AWGN}$$

$$L(\mathbf{x}_m) = \frac{p(\mathbf{x}_m; H_1)}{p(\mathbf{x}_m; H_0)} > \gamma \longrightarrow T(\mathbf{x}_m) = \sum_{n=0}^{N-1} x_m[n] s[n] > \gamma'$$



## Test statistic and probabilities (example)

Sec. 2



$P_{FA}, P_D$  can be evaluated from  $T(\mathbf{X}; H_i)$

## Summary: Steps of the test

Sec. 2

World of observables	World of models
Vector of measured data $\mathbf{x}_m = \{x_m[0], x_m[1], \dots, x_m[N-1]\}$	Vector of all possible data $\mathbf{x} = \{x[0], x[1], \dots, x[N-1]\}$
	Vector of random variables $\mathbf{X} = \{X[0], X[1], \dots, X[N-1]\}$
	Conditional PDFs $p(\mathbf{x}; H_i)$
Test statistic (from LRT) $T(\mathbf{x}_m)$	Test statistic (RV) $T(\mathbf{X}; H_i)$
	$P_{FA} = \Pr(T(\mathbf{X}) > \gamma'   H_0) = \alpha$
	Evaluation of $\gamma'$
Test $T(\mathbf{x}_m) > \gamma'?$	

## Probabilistic model in Composite hypothesis testing (CHT)

Sec. 2

$$p(\mathbf{x}; H_i) \Rightarrow p(\mathbf{x}; \mathbf{b}_i, H_i)$$

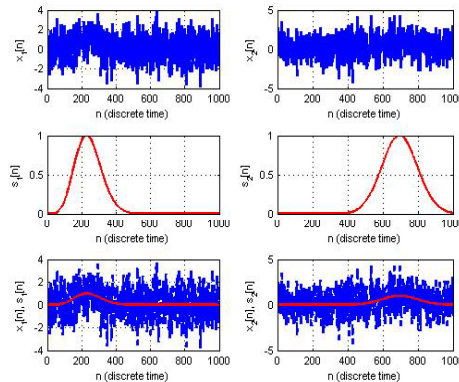
$\mathbf{b}_i$  Vector of **unknown** parameters

### Example

$$x[n] = as[n - b] + w[n]$$

Deterministic with unknown delay

Realization of a random process with known PDF



ISPRA July 2, 2012

21



## GLRT definition

Sec. 2

It is a generalization of LRT

It is a mixture of estimation and detection

$$L(\mathbf{x}_m) = \frac{p(\mathbf{x}_m; \hat{\mathbf{b}}_1, H_1)}{p(\mathbf{x}_m; \hat{\mathbf{b}}_0, H_0)} > \gamma$$

$\hat{\mathbf{b}}_i$  ML estimate of  $\mathbf{b}_i$

- The NP theorem does not apply
- The optimum NP detector cannot be derived
- In most cases it leads to a good approximation of the optimum NP detector

ISPRA July 2, 2012

22



## Table of contents

Sec. 3

1. Introduction
2. Detection methods
3. Detection in GNSS
4. Search space
5. CAF evaluation schemes
6. Threshold setting
7. Coherent and non-coherent integration
8. Verification phase

## GLRT in GNSS

Sec. 3

For the detection of the GNSS SIS, starting from:

$$L(\mathbf{x}_m) = \frac{p(\mathbf{x}_m; \hat{\mathbf{b}}_1, H_1)}{p(\mathbf{x}_m; \hat{\mathbf{b}}_0, H_0)} > \gamma$$

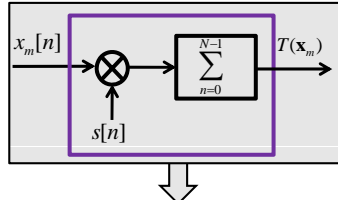
It is possible to find a **test statistic** to be compared against a threshold  $\gamma'$  :

The peak of a 2D function (described in next slide)

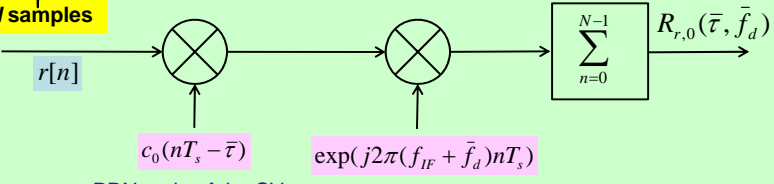
(*The proof is omitted*)

## Test statistic evaluation in GNSS

Sec. 3



$$r[n] = \sum_{i=0}^{L-1} \sqrt{2\tilde{C}_i} \tilde{c}_i(nT_s - \tilde{\tau}_i) \tilde{d}(nT_s - \tilde{\tau}_i) \cos(2\pi(f_{IF} + f_{d,i})nT_s + \varphi_{IF,i}) + \eta[n]$$



PRN code of the SV  
we are looking for (i=0,  
without loss of generality)

ISPRRA July 2, 2012

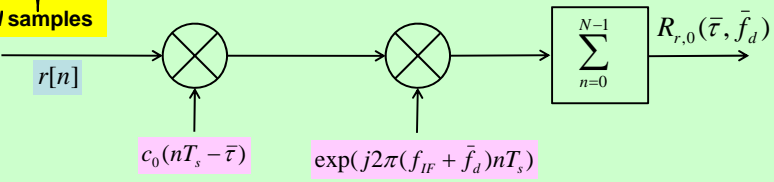
25



## Cross ambiguity function (CAF)

Sec. 3

$$r[n] = \sum_{i=0}^{L-1} \sqrt{2\tilde{C}_i} \tilde{c}_i(nT_s - \tilde{\tau}_i) \tilde{d}(nT_s - \tilde{\tau}_i) \cos(2\pi(f_{IF} + f_{d,i})nT_s + \varphi_{IF,i}) + \eta[n]$$



$$R_{r,0}(\bar{\tau}, \bar{f}_d) = \sum_{n=0}^{N-1} r[n] c_0(nT_s - \bar{\tau}) \exp(j2\pi(f_{IF} + \bar{f}_d)nT_s)$$

Cross Ambiguity  
Function (CAF)

Local sequences

ISPRRA July 2, 2012

26



## CAF with aligned code

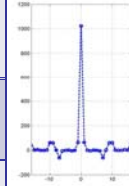
Sec. 3

$$r[n] = \sum_{i=0}^{L-1} \sqrt{2\tilde{C}_i} \tilde{c}_i(nT_s - \tilde{\tau}_i) \tilde{d}(nT_s - \tilde{\tau}_i) \cos(2\pi(f_{IF} + f_{d,i})nT_s + \varphi_{IF,i}) + \eta[n]$$

$$c_0(nT_s - \bar{\tau})$$

$$R_{r,0}(\bar{\tau}, \bar{f}_d) = \sum_{n=0}^{N-1} c_0(nT_s - \bar{\tau}) \sum_{i=0}^{L-1} \tilde{c}_i(nT_s - \tau_i) \alpha[n] + \text{noise}$$

$i = 0, \bar{\tau} = \tau_0$	$\sum_{n=0}^{N-1} c_0(nT_s - \bar{\tau}) \tilde{c}_0(nT_s - \tau_0) = N$	Pseudo-noise correlation (delta-like)
$i = 0, \bar{\tau} \neq \tau_0$	$\sum_{n=0}^{N-1} c_0(nT_s - \bar{\tau}) \tilde{c}_0(nT_s - \tau_0) \cong 0$	Pseudo-noise correlation (delta-like)
$i \neq 0$	$\sum_{n=0}^{N-1} c_0(nT_s - \bar{\tau}) \tilde{c}_{i \neq 0}(nT_s - \tau_i) \cong 0$	PRN code orthogonality



## CAF with $\bar{f}_d = f_{d,0}$

Sec. 3

$$r[n] = \sum_{i=0}^{L-1} \sqrt{2\tilde{C}_i} \tilde{c}_i(nT_s - \tilde{\tau}_i) \tilde{d}(nT_s - \tilde{\tau}_i) \cos(2\pi(f_{IF} + f_{d,i})nT_s + \varphi_{IF,i}) + \eta[n]$$

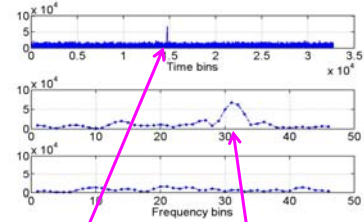
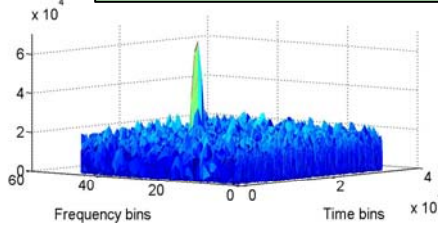
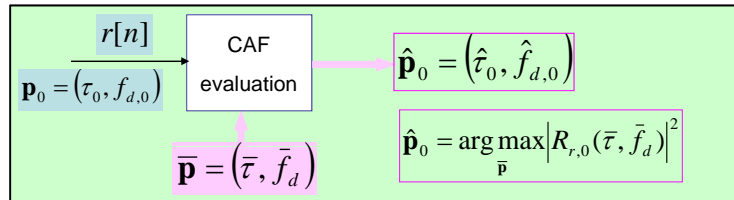
$$\exp(j2\pi(f_{IF} + \bar{f}_d)nT_s)$$

$$R_{r,0}(\bar{\tau}, \bar{f}_d) = \sum_{n=0}^{N-1} \exp(-j2\pi(f_{IF} + \bar{f}_d)nT_s) \sum_{i=0}^{L-1} \cos(2\pi(f_{IF} + f_{d,i})nT_s + \varphi_{IF,i}) \beta[n] + \text{noise}$$

$\bar{\tau} = \tau_0$	$c_0(nT_s - \bar{\tau}) \tilde{c}_0(nT_s - \tau) = 1$	In the term $\beta[n]$
$i = 0, \bar{\tau} = \tau_0, \bar{f}_d = f_{d,0}$	$R_{r,0}(\bar{\tau}, \bar{f}_d) \gg 0$	
$\bar{f}_d \neq f_{d,0}$	$R_{r,0}(\bar{\tau}, \bar{f}_d) \cong 0$	

## Parameter estimation from the CAF envelope

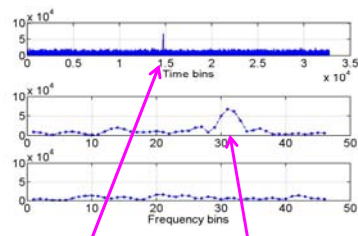
Sec. 3



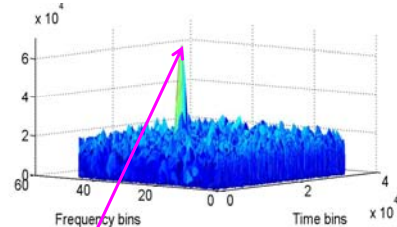
Estimation step:  
Delay and frequency  
estimation

## Estimation and Detection

Sec. 3



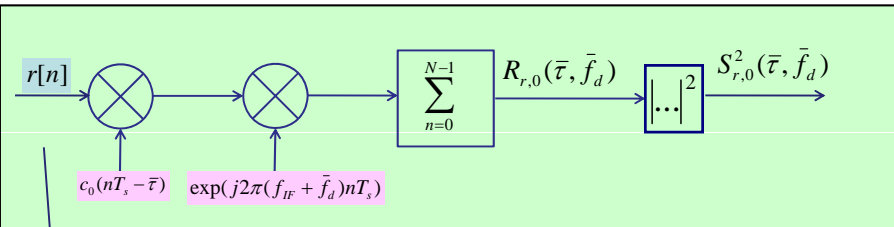
Estimation step:  
Delay and frequency  
estimation



Detection step:  
The peak is compared  
against a threshold

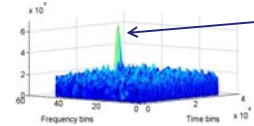
## Despreading gain

Sec. 3



$$\text{SNR}_{\text{IF}} = \frac{C}{N_0 B_{\text{FE}}}$$

$B_{\text{FE}} \rightarrow \text{FE bandwidth}$



$$\text{SNR}_{\text{peak}} = \text{SNR}_{\text{IF}} \frac{N}{2}$$

Despreading gain

Example

SNR <sub>IF</sub>	N	Gain	SNR <sub>peak</sub>
-18 dB	2048	30dB	12dB

## Table of contents

Sec. 4

1. Introduction
2. Detection methods
3. Detection in GNSS
- 4. Search space**
5. CAF evaluation schemes
6. Threshold setting
7. Coherent and non-coherent integration
8. Verification phase

## Search space (SS)

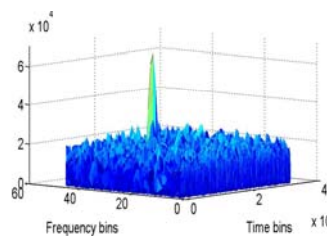
Sec. 4

$$R_{r,0}(\bar{\tau}, \bar{f}_d)$$

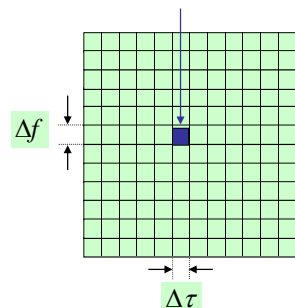


$$\bar{\tau} \Rightarrow i\Delta\tau$$

$$\bar{f}_d \Rightarrow k\Delta f$$



$$S_{r,0}^2(i\Delta\tau, k\Delta f) = |R_{r,0}(i\Delta\tau, k\Delta f)|^2$$



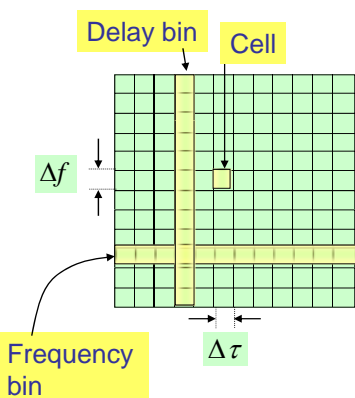
$$R_{r,0}(i\Delta\tau, k\Delta f) = \sum_{n=0}^{N-1} r[n] \cdot$$

$$c_0(nT_s - i\Delta\tau) \cdot$$

$$\exp(j2\pi(f_{IF} + k\Delta f)nT_s)$$

## The bins of the Search space

Sec. 4



How to choose the bin size?

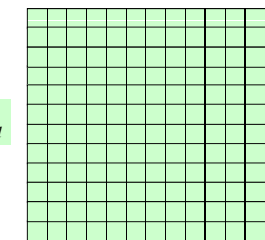
The bin size depends on several parameters:

1. The integration time ( $N$ )
2. The real time constraints
3. The desired performance
4. The HW constraints
5. The constraints imposed by the tracking systems

## Bin ranges

Sec. 4

- Search over a frequency range of (-10kHz,+10kHz) for high-speed aircraft.
- Search over a frequency range of (-5kHz,+5kHz) for low mobility.



Search over a delay range covering the code period:

- 1ms for GPS – OS
- 4ms for Galileo E1-OS (BOC(1,1))

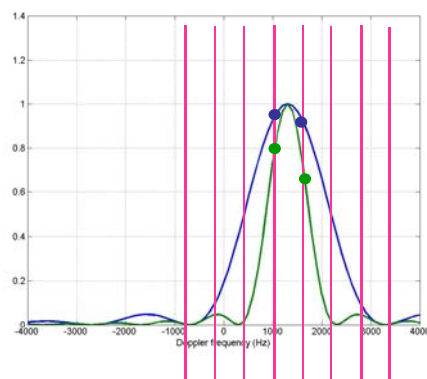
$\bar{\tau}$

## The frequency bin size

Sec. 4

Normalized CAF envelope at the right delay bin.

The green curve is obtained by doubling the integration time (with respect to the blue curve)



$$\Delta f = \frac{2}{3NT_s}$$

□ The peak of the blue curve is nearly represented in the SS (frequency bin suitable)

□ The peak of the green curve is not a point of the SS (frequency bin too large)

## Cold & warm start

Sec. 4

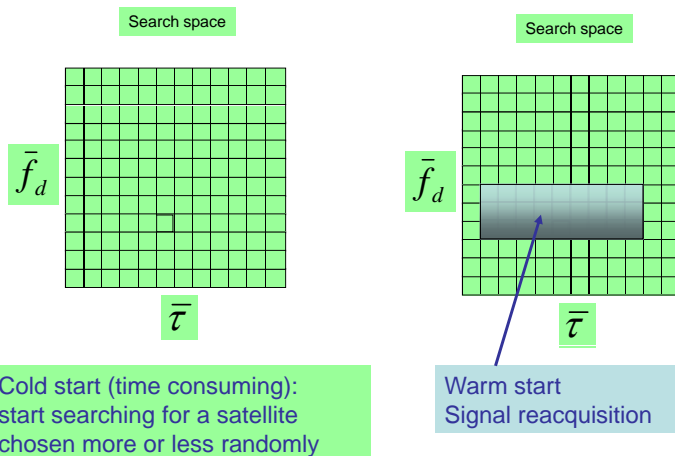


## Table of contents

Sec. 5

1. Introduction
2. Detection methods
3. Detection in GNSS
4. Search space
- 5. CAF evaluation schemes**
6. Threshold setting
7. Coherent and non-coherent integration
8. Verification phase

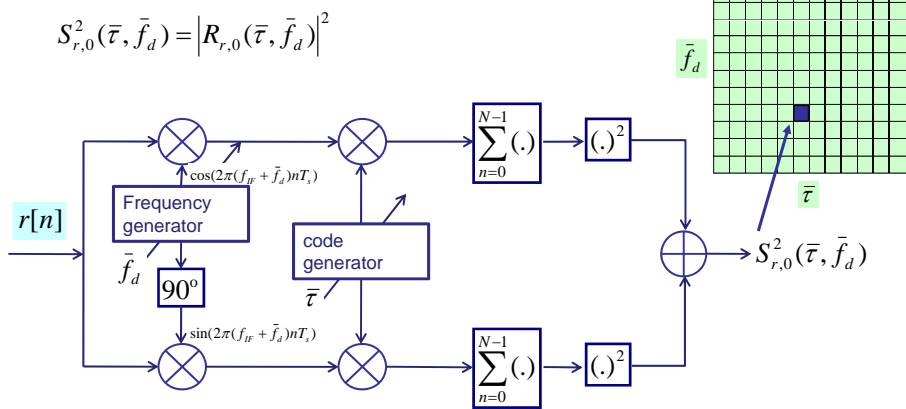
## CAF evaluation: Method 1

Sec. 5

### Serial scheme

$$R_{r,0}(\bar{\tau}, \bar{f}_d) = \sum_{n=0}^{N-1} r[n] c_0(nT_s - \bar{\tau}) \exp(j2\pi(f_{IF} + \bar{f}_d)nT_s)$$

$$S_{r,0}^2(\bar{\tau}, \bar{f}_d) = |R_{r,0}(\bar{\tau}, \bar{f}_d)|^2$$



## CAF and correlation

Sec. 5

### Fast correlation by FFT

$$R_{r,0}(\bar{\tau}, \bar{f}_d) = \sum_{n=0}^{N-1} r[n] c_0(nT_s - \bar{\tau}) \exp(j2\pi(f_{IF} + \bar{f}_d)nT_s)$$

$$R_{r,0}(\bar{\tau}, \bar{f}_d) = \sum_{n=0}^{N-1} r[n] \exp(j2\pi(f_{IF} + \bar{f}_d)nT_s) c_0(nT_s - \bar{\tau})$$

$$R_{r,0}(\bar{\tau}, \bar{f}_d) = \sum_{n=0}^{N-1} r[n] \exp(j2\pi(f_{IF} + \bar{f}_d)nT_s) c_0(nT_s - \bar{\tau})$$

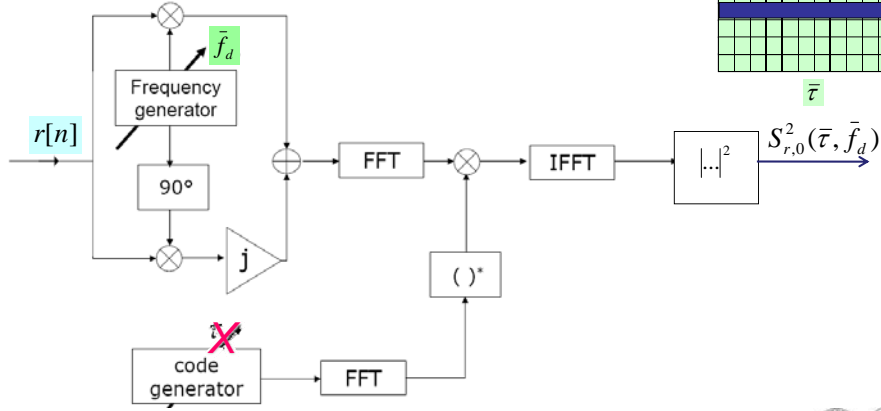
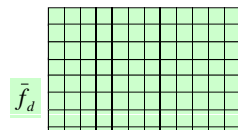
Correlation of two sequences

## CAF evaluation: Method 2

Sec. 5

### FFT in the time domain

$$R_{r,0}(\bar{\tau}, \bar{f}_d) = \sum_{n=0}^{N-1} r[n] \exp(j2\pi(f_{IF} + \bar{f}_d)nT_s) c_0(nT_s - \bar{\tau})$$



ISPRRA July 2, 2012

41

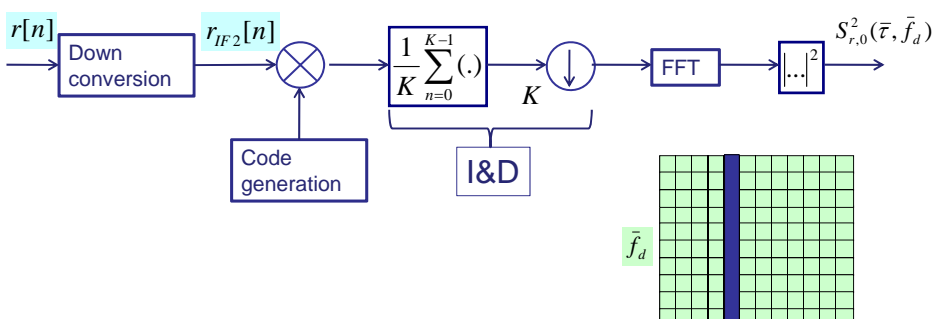


## CAF evaluation: Method 3

Sec. 5

### FFT in the Doppler domain

$$R_{r,0}(\bar{\tau}, \bar{f}_d) = \sum_{n=0}^{N-1} r[n] c_0(nT_s - \bar{\tau}) \exp(j2\pi(f_{IF} + \bar{f}_d)nT_s)$$



ISPRRA July 2, 2012

42



## Table of contents

Sec. 6

1. Introduction
2. Detection methods
3. Detection in GNSS
4. Search space
5. CAF evaluation schemes
6. Threshold setting
7. Coherent and non-coherent integration
8. Verification phase

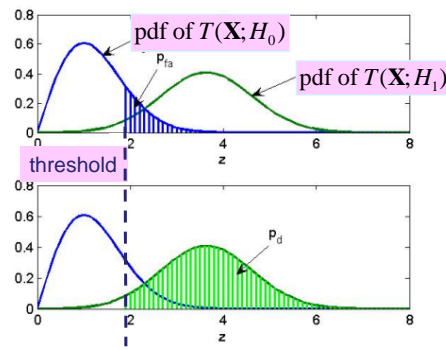
## Test statistic (CAF peak)

Sec. 6

The performance of a generic detector is generally expressed in terms of detection and false alarm probabilities.

### Test statistic (RV)

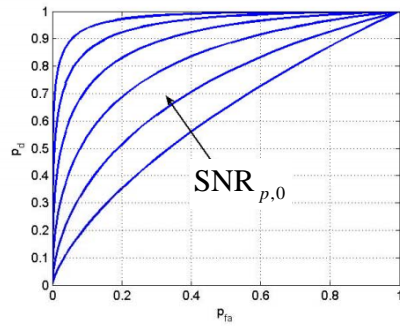
$$T(\mathbf{X}) = \max_{\bar{\mathbf{p}}} |R_{r,0}(\bar{\tau}, \bar{f}_d)|^2$$



## ROC curves

Sec. 6

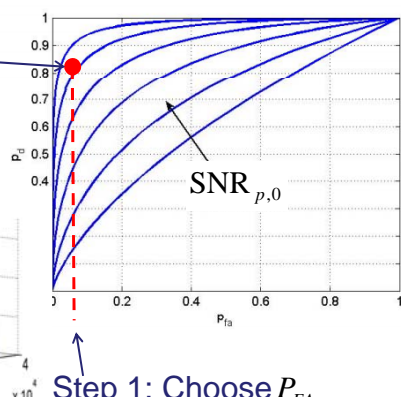
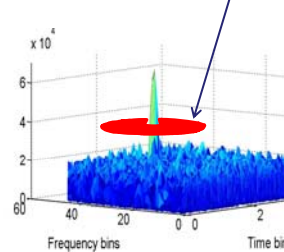
The couples  $(P_D, P_{FA})$  for different values of the threshold are represented in terms of ROC (Receiver Operating characteristics) curves.



## Threshold setting

Sec. 6

Step 2: Find  
the threshold



Step 1: Choose  $P_{FA}$

## More details on ....

Sec. 6

996

IEEE TRANSACTIONS ON AEROSPACE AND ELECTRONIC SYSTEMS VOL. 44, NO. 3 JULY 2008

### Impact of GPS Acquisition Strategy on Decision Probabilities

DANIELE BORIO, Member, IEEE  
Politecnico di Torino  
Italy

LAURA CAMORIANO  
Istituto Superiore Mario Boella  
Italy

LETIZIA LO PRESTI, Member, IEEE  
Politecnico di Torino  
Italy

The first stage of processing within a GPS receiver consists of the signal acquisition process, the output of which provides a rough estimation of code delay and Doppler frequency. The strong dependence of the acquisition performance on the decision strategy is shown, establishing the role of decision probabilities. Three acquisition strategies are analyzed and a new model describing the performance of a hybrid acquisition system is developed. The theoretical models are validated by simulations, and secondary phenomena, generally neglected in the literature, are also discussed.

ISPRA July 2, 2012

47



## Table of contents

Sec. 7

1. Introduction
2. Detection methods
3. Detection in GNSS
4. Search space
5. CAF evaluation schemes
6. Threshold setting
7. Coherent and non-coherent integration
8. Verification phase

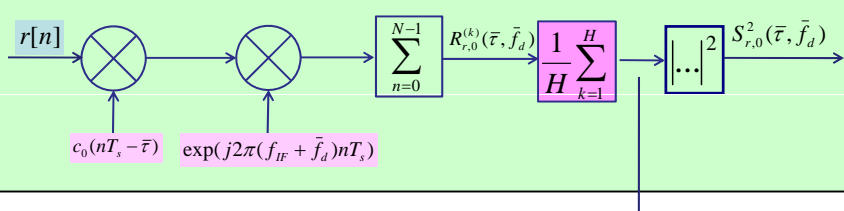
ISPRA July 2, 2012

48



## Coherent integration

Sec. 7



Integration interval	Integration epochs	CAF at each epoch	CAF average (Coherent integration)
$NT_s$	$t_k = t_0 + kNT_s$	$R_{r,0}^{(k)}(\bar{\tau}, \bar{f}_d)$	$\bar{R}_{r,0}(\bar{\tau}, \bar{f}_d) = \frac{1}{H} \sum_{k=1}^H R_{r,0}^{(k)}(\bar{\tau}, \bar{f}_d)$

Integration with phase continuity

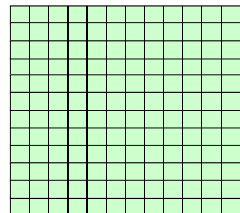
## Bin size with coherent integration

Sec. 7

Integration interval	Integration epochs	CAF at each epoch	CAF average (Coherent integration)
$NT_s$	$t_k = t_0 + kNT_s$	$R_{r,0}^{(k)}(\bar{\tau}, \bar{f}_d)$	$\bar{R}_{r,0}(\bar{\tau}, \bar{f}_d) = \frac{1}{H} \sum_{k=1}^H R_{r,0}^{(k)}(\bar{\tau}, \bar{f}_d)$

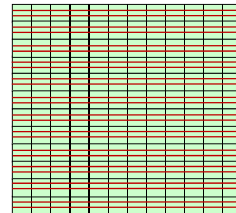
$$\bar{R}_{r,0}(\bar{\tau}, \bar{f}_d) = \sum_{k=1}^{H \cdot N-1} R_{r,0}^{(k)}(\bar{\tau}, \bar{f}_d)$$

$$\Delta f|_{H=1} = \frac{2}{3NT_s}$$



$$\Delta f|_{H>1} = \frac{2}{3HNT_s}$$

Complexity increase!



## Despreading gain with coherent integration

Sec. 7

$$\bar{R}_{r,0}(\bar{\tau}, \bar{f}_d) = \sum_{k=1}^{H \cdot N-1} R_{r,0}^{(k)}(\bar{\tau}, \bar{f}_d)$$

SNR (IF)	SNR at CAF peak (single integration)	SNR after coherent integration
$\text{SNR}_{\text{IF}} = \frac{C}{N_0 B}$	$\text{SNR}_p = \frac{C}{N_0 B} \frac{N}{2}$	$\text{SNR}_{p,H} = \left[ \frac{C}{N_0 B} \frac{N}{2} \right] H$
	$\text{SNR}_p = \text{SNR}_{\text{IF}} \frac{N}{2}$	$\text{SNR}_{p,H} = \text{SNR}_p H$

Despreading  
gain

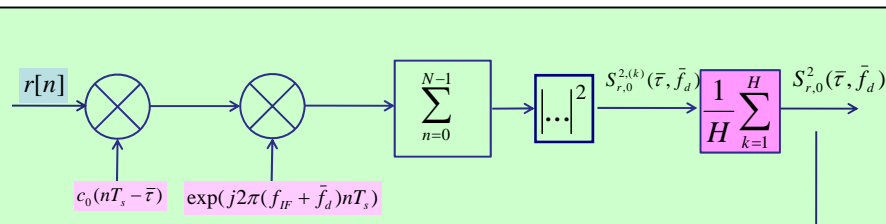
Gain due to  
coherent  
integration

51



## Noncoherent integration

Sec. 7



Integration interval	Integration epochs	CAF envelope at each epoch	CAF envelope average (noncoherent integration)
$NT_s$	$t_k = t_0 + kNT_s$	$S_{r,0}^{2,(k)}(\bar{\tau}, \bar{f}_d)$	$\bar{S}_{r,0}^2(\bar{\tau}, \bar{f}_d) = \frac{1}{H} \sum_{k=1}^H S_{r,0}^{2,(k)}(\bar{\tau}, \bar{f}_d)$

ISPRRA July 2, 2012

52

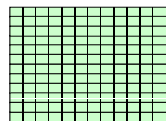


## Bin size and despreading gain with N-C integration

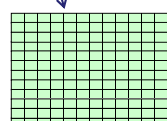
Sec. 7

Integration interval	Integration epochs	CAF envelope at each epoch	CAF envelope average (noncoherent integration)
$NT_s$	$t_k = t_0 + kNT_s$	$S_{r,0}^{2,(k)}(\bar{\tau}, \bar{f}_d)$	$\bar{S}_{r,0}^2(\bar{\tau}, \bar{f}_d) = \frac{1}{H} \sum_{k=1}^H S_{r,0}^{2,(k)}(\bar{\tau}, \bar{f}_d)$

$$\Delta f|_{H=1} = \frac{2}{3NT_s}$$



$$\Delta f|_{H>1} = \frac{2}{3NT_s}$$

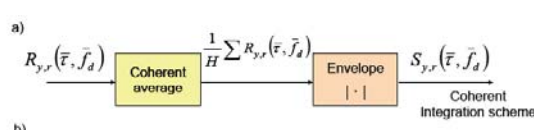


Bin size unchanged

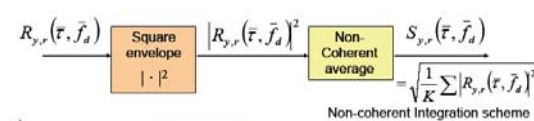
Gain with squaring loss

## Other solutions exist

Sec. 7



- The number of frequency bins increases
- Data transition limits the value of  $H$



Squaring loss

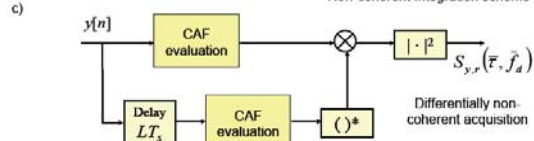


## Table of contents

Sec. 8

1. Introduction
2. Detection methods
3. Detection in GNSS
4. Search space
5. CAF evaluation schemes
6. Threshold setting
7. Coherent and non-coherent integration
8. Verification phase

## Multitrial

Sec. 8

When a first decision about the satellite presence and a first estimation of the code delay and of the Doppler frequency are available, the system can refine these results in a **verification** phase.

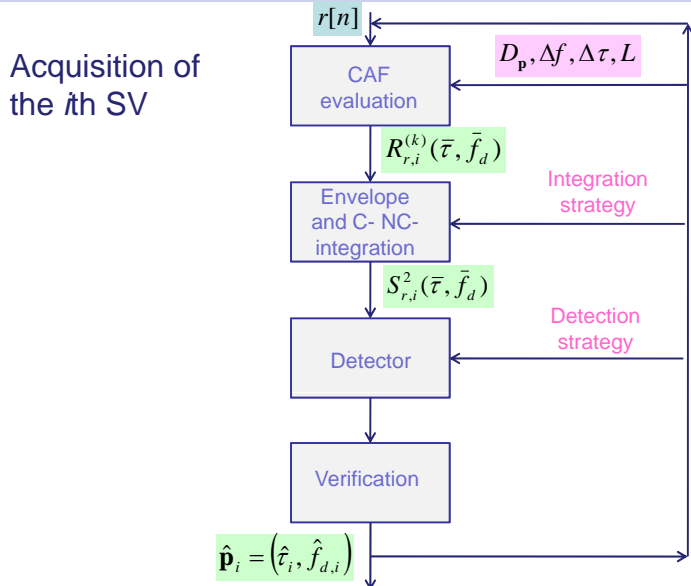
Thus **multitrial** techniques, based on the use of different CAF evaluated over subsequent portions of the input signal, can be employed.

Two examples of these techniques are the **M on N** and the **Tong** methods.

Multitrial techniques generally do not require the computation of more than one complete search space, thus they interact with the other blocks changing the requirements for the subsequent iterations occurring in the process.

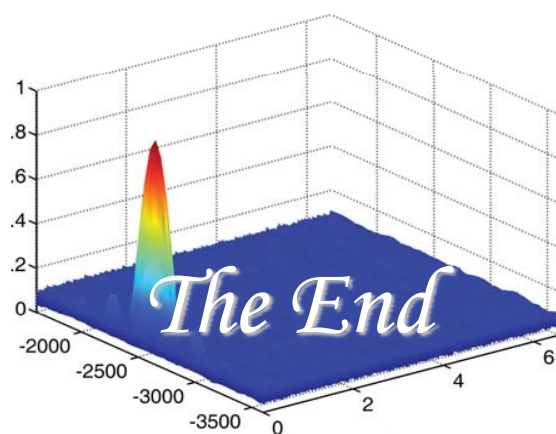
## In summary the acquisition steps are ...

Sec. 8



ISPRRA July 2, 2012

57



ISPRRA July 2, 2012



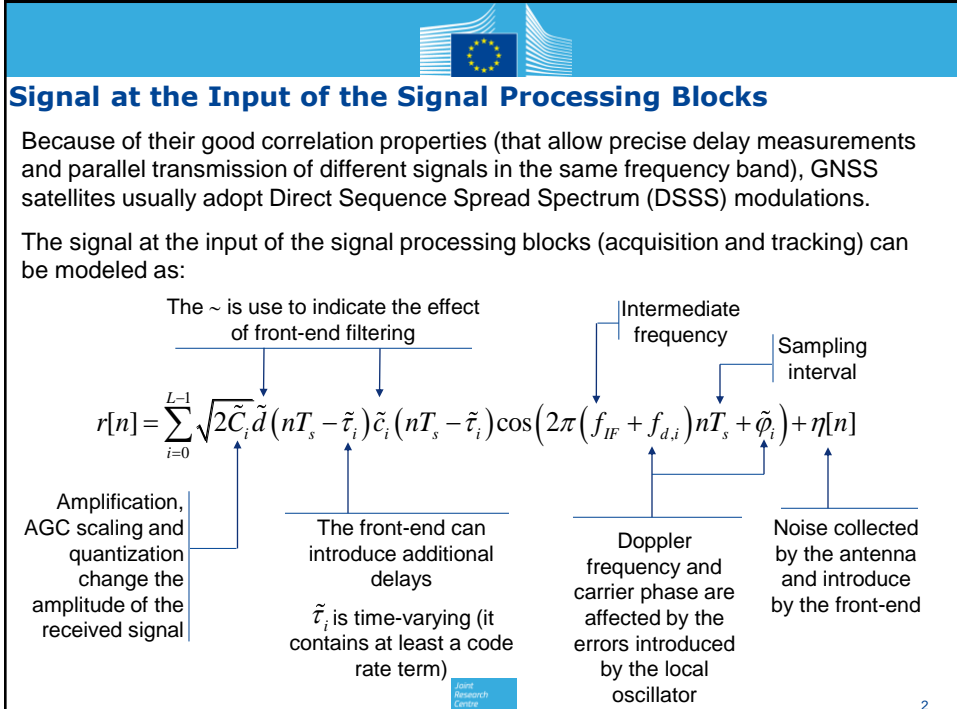




# GNSS Signal Tracking

Daniele Borio

Joint Research Centre,  
Ispra (VA), Italy





## The Maximum Likelihood Equation

The signal parameters can be computed solving the Maximum Likelihood (ML) Equation

$$\begin{aligned}(\hat{\tau}, \hat{f}_d) &= \arg \max_{\tau, f_d} |R(\tau, f_d)|^2 \\ \hat{\phi} &= \angle R(\hat{\tau}, \hat{f}_d)\end{aligned}$$

where  $R(\tau, f_d)$  is the cross-ambiguity function computed for the delay  $\tau$  and the Doppler frequency  $f_d$ .

$$R(\tau, f_d) = \frac{1}{N} \sum_{n=0}^{N-1} r[n] c^*(nT_s - \tau) \exp\{-j2\pi(f_{IF} + f_d)nT_s\}$$

Tracking loops are iterative techniques used for solving the ML equation.

Acquisition can be considered as the initial step used for initializing the optimization process performed by the tracking loops.

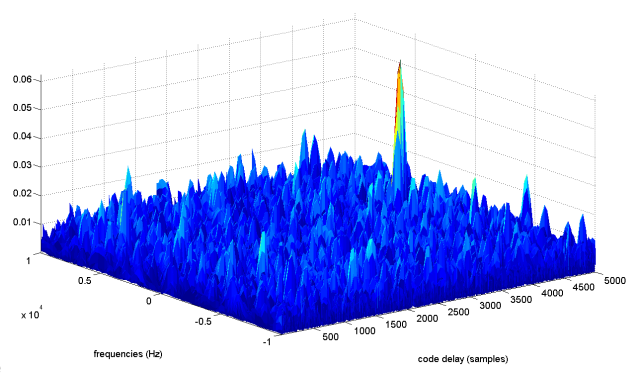


## The Acquisition Process

First “signal processing” stage that provides a rough estimate of the signal Doppler frequency and code delay.

Since no prior information about the signal parameters is available, a brute force (computationally demanding) approach is adopted. Correlator outputs are evaluated over a grid of different code delays and Doppler frequencies.

- ✓ Correlator outputs with the same code delay and Doppler frequency from different epochs are used to form a **decision variable**.
- ✓ If the decision variable passes a threshold, the signal is declared present.
- ✓ The estimated Doppler frequency and code delay are extracted from the decision variable passing the threshold.





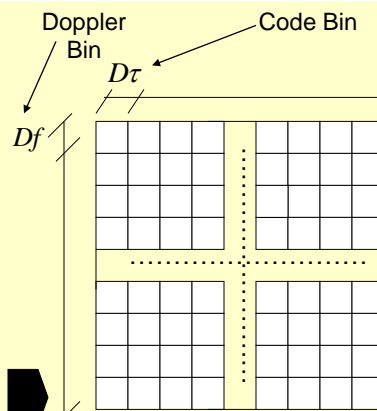
## What Is Left From Acquisition?

- ✓ The Doppler frequency and code delay estimated by the acquisition block are too rough for being used for positioning and navigation
- ✓ The phase information is totally ignored (use of a non-linear operation for removing the phase dependence)
- ✓ The signal parameters change over time whereas acquisition provides a static “one-shot” estimation

### Signal Tracking for:

- fine code phase and Doppler frequency estimation
- track the changes of the signal parameters
- phase estimation

The search grid of the acquisition process is too coarse for precise positioning



5



## Signal Tracking Overview

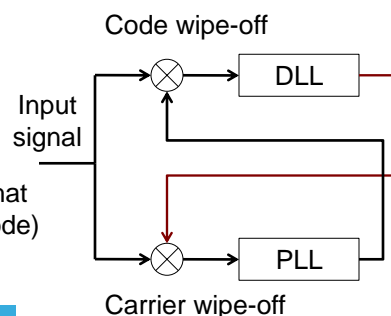
Signal tracking is used to generate precise replicas of the incoming code and carrier. The local code and carrier can be correctly generated only if the signal parameters are correctly tracked.

Use of two separate loops for

- + the local code: code delay → Delay Lock Loop (DLL)
- + the local carrier: phase and frequency → Phase Lock Loop (PLL)

Precise phase estimation is not required for the normal receiver operations and a Frequency Lock Loop (FLL) can be used.

The two loops are coupled in the sense that the DLL (PLL) requires precise carrier (code) wipe-off for operating correctly.





## Gradient Ascent/Descent Algorithms

Let  $f(\theta)$  be a cost function to maximize/minimize:  $f(\theta) = E[g(\theta)]$

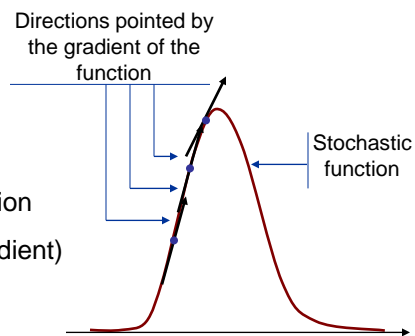
A common example is the Mean Square Error:  $f(\theta) = E[(\theta - \theta_{true})^2]$

The function can be maximized (minimized) by following the (opposite) direction of the gradient of the function.

$$\theta_{k+1} = \theta_k - \mu \frac{\partial f(\theta)}{\partial \theta} \Big|_{\theta=\theta_k} = \theta_k - \mu E \left[ \frac{\partial g(\theta)}{\partial \theta} \right]_{\theta=\theta_k}$$

### 4 steps:

- ✓ Evaluation of the instantaneous cost function
- ✓ Evaluation of the derivative (stochastic gradient)
- ✓ Evaluation of the average of the gradient
- ✓ Update of the parameter estimate



7

Joint Research Centre



## Structure of a Tracking Loop (I/II)

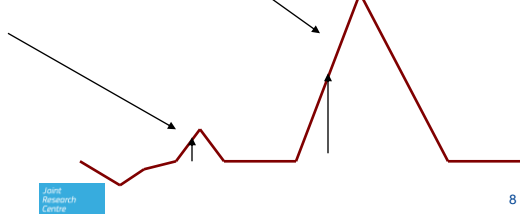
Tracking loops implement gradient ascent (descent) algorithms that maximize (minimize) a specific cost function.

E.g./

- the DLL estimates the code delay by maximizing the correlation between the incoming signal and local code replica
- the PLL tries to minimize the residual phase of the correlator outputs

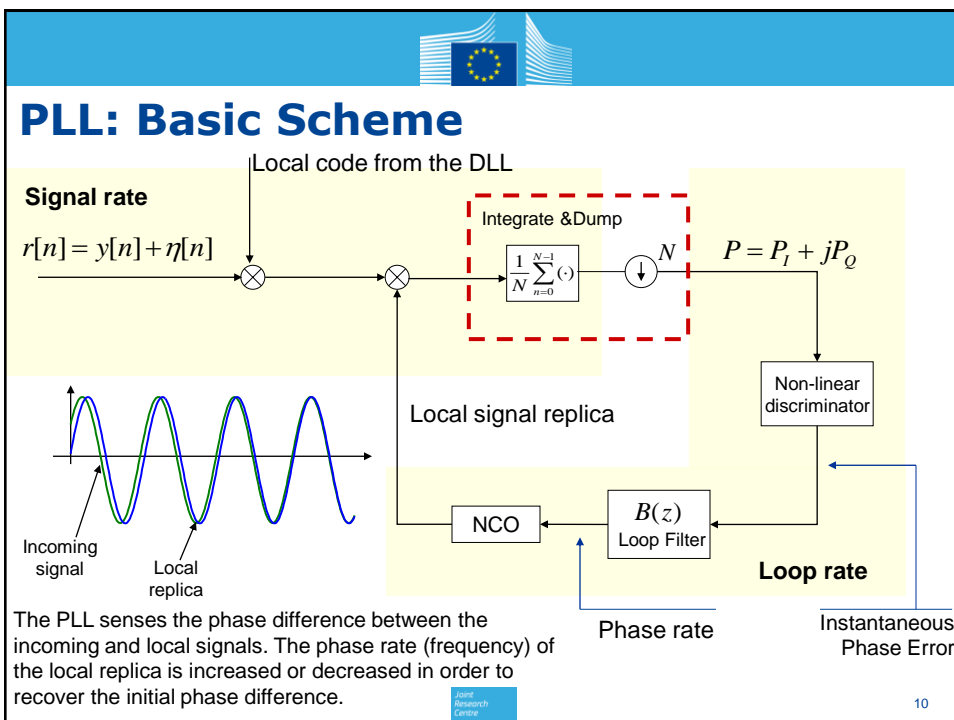
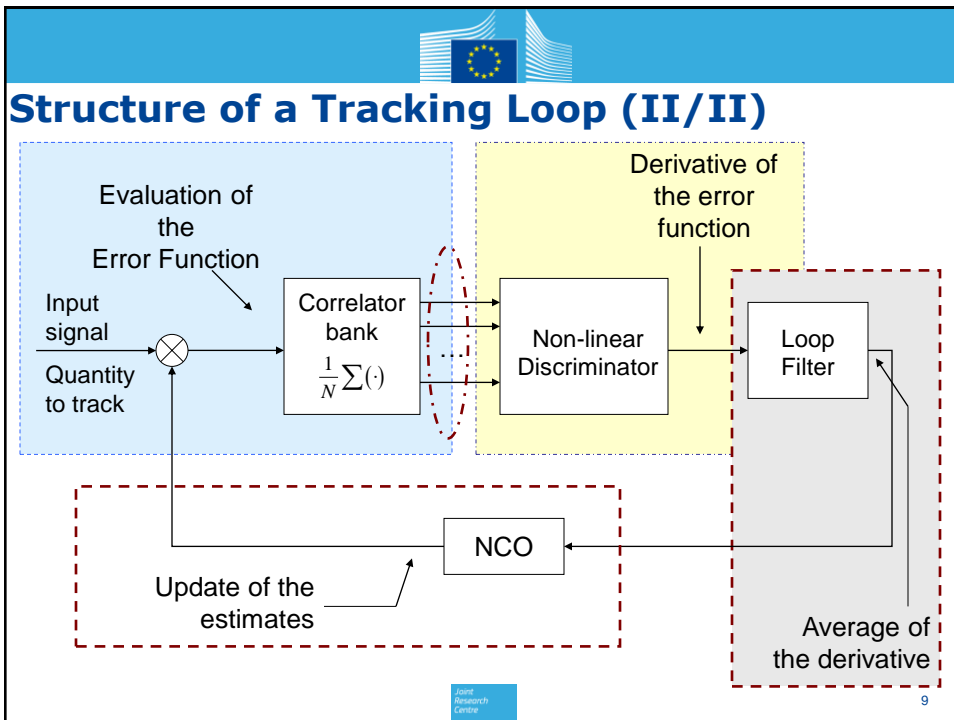
Acquisition has to provide a sufficiently accurate estimate of the signal parameters to avoid lock on local minima/maxima

Correlation function



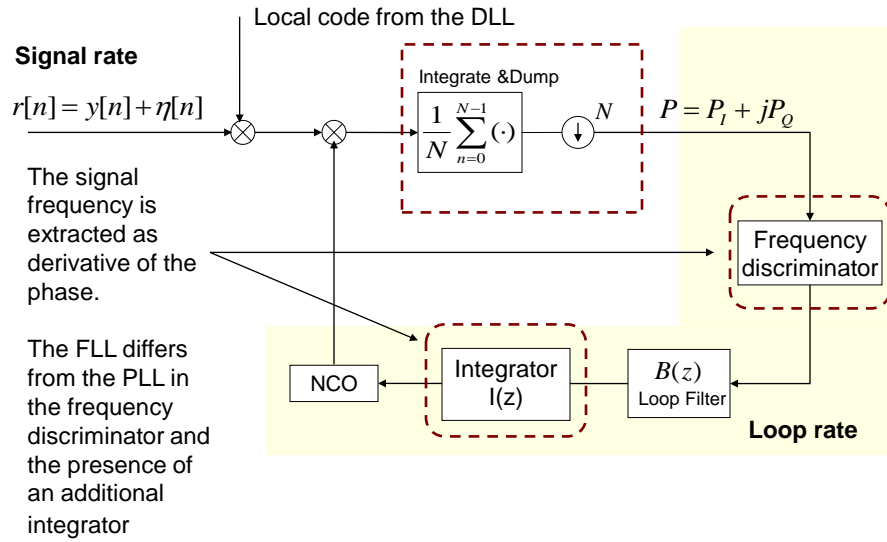
8

Joint Research Centre





## FLL: Basic Scheme

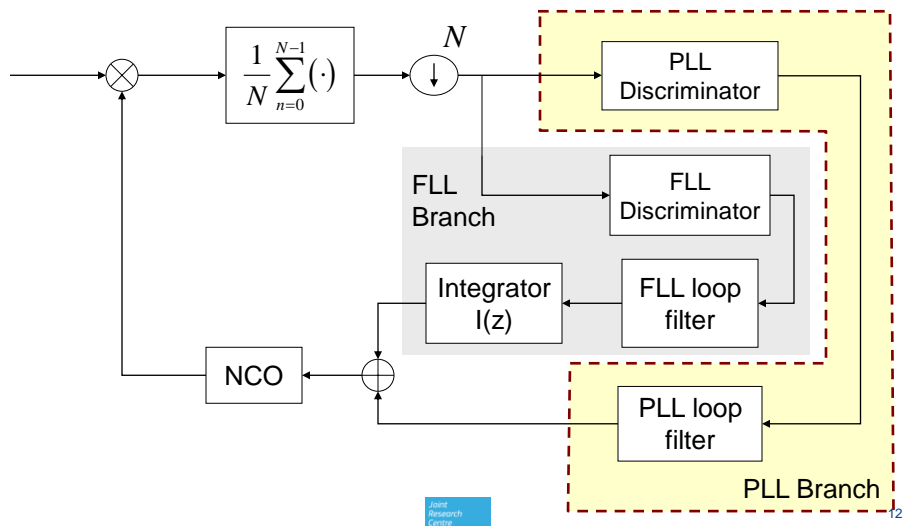


11



## FLL Assisted PLL

FLL and PLL can be jointly used to better track the signal dynamics.



Joint Research Centre

12



## Combined use of FLL and PLL

If the initial frequency estimate (from the acquisition block) is not sufficiently precise, the PLL can fail to lock the signal phase and frequency.

The FLL can usually track higher dynamics and can pull the signal in frequency lock conditions more easily than a PLL (Kaplan & Hegarty, 2006).

→ Combined use of PLL and FLL

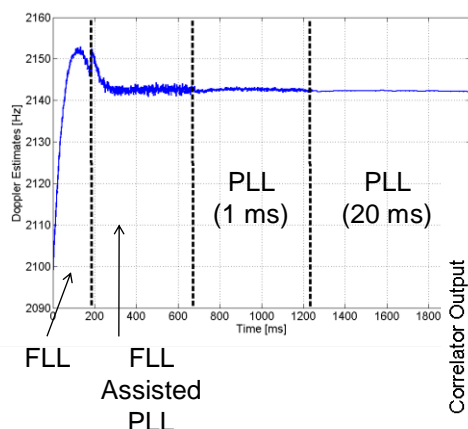
The receiver can start tracking operations using an FLL and progressively move PLL with different bandwidths and integration times.

It requires a decision logic allowing the receiver to transit among different tracking states.

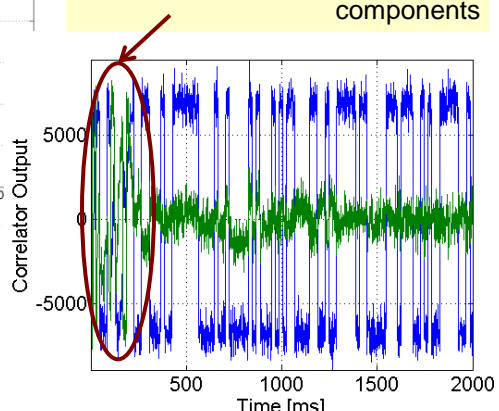
Kaplan E. D. and C.J. Hegarty (2006), "Understanding GPS Principles and Applications", Artech House



## PLL vs. FLL



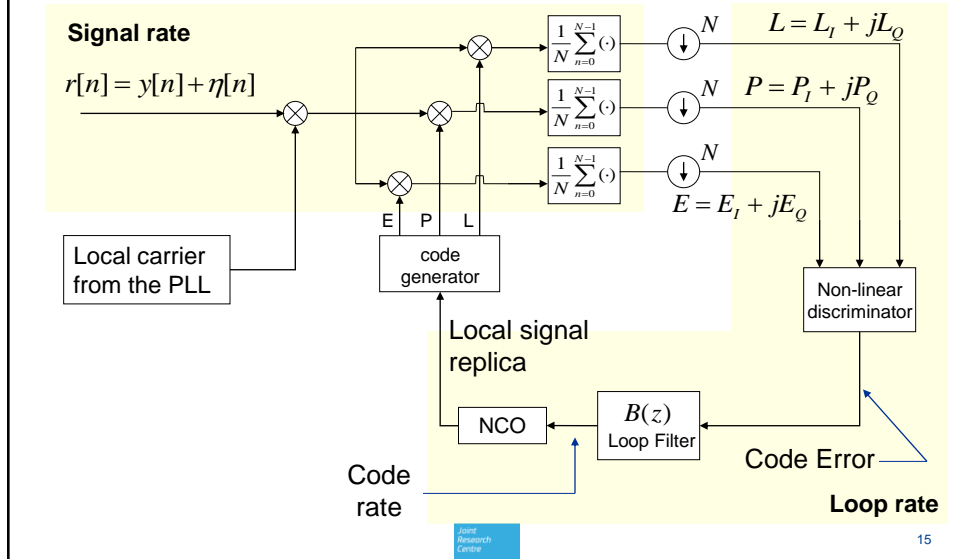
When using the FLL, a residual phase is present and the signal power is split between the I and Q components



The receiver operates in different modes, with different lock properties



## DLL: Basic Scheme



## Carrier Aiding (I/II)

Carrier and code Doppler are both due to the relative motion between receiver and satellite. Without ionosphere, code and carrier would be affected by the same Doppler shift scaled by a constant factor.

► Carrier Doppler can be scaled to aid the code loop

Scaling factor

$$\text{scaling factor} = \frac{R_c}{f_{RF}}$$

Chipping rate of the code

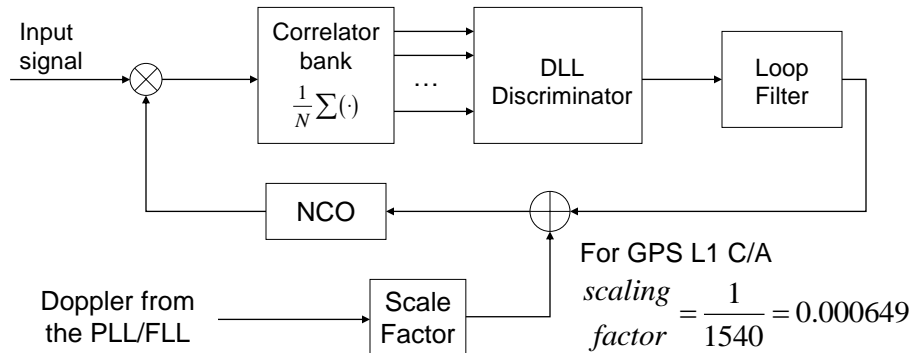
Carrier centre frequency

The Doppler shift is proportional to the signal centre frequency and the scaling factor is given by the ratio of code chipping rate and carrier centre frequency.

Carrier aiding allows removing all the LOS dynamics from the code loop and the DLL has to track only the ionospheric divergence and noise.



## Carrier Aiding (II/II)



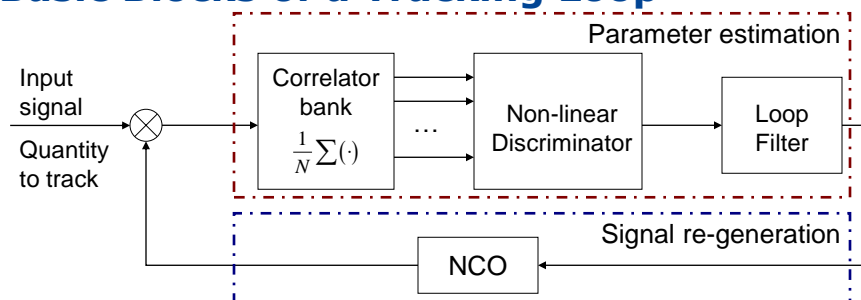
Carrier aiding allows reducing the DLL order and bandwidth.

"Code aiding" is not feasible since the scaling factor would be  $\gg 1$ , leading to a significant noise amplification

17



## Basic Blocks of a Tracking Loop

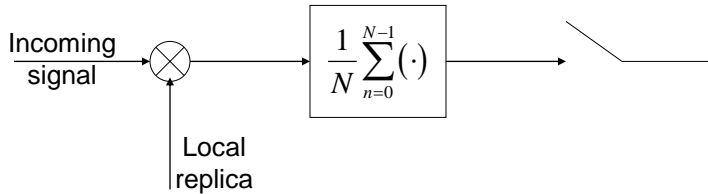


Each tracking loop is made of:

- One or more correlators (Integrate & Dump filters)
- A non-linear discriminator for extracting the quantity to be tracked (phase and delay)
- A loop filter for improving the estimate of the quantity to be tracked
- A carrier/code numerically controlled oscillator (NCO)



## The Integrate and Dump Block



The correlator blocks (Integrate & Dump) evaluate the projection of the incoming signal over its local replica (scalar product).

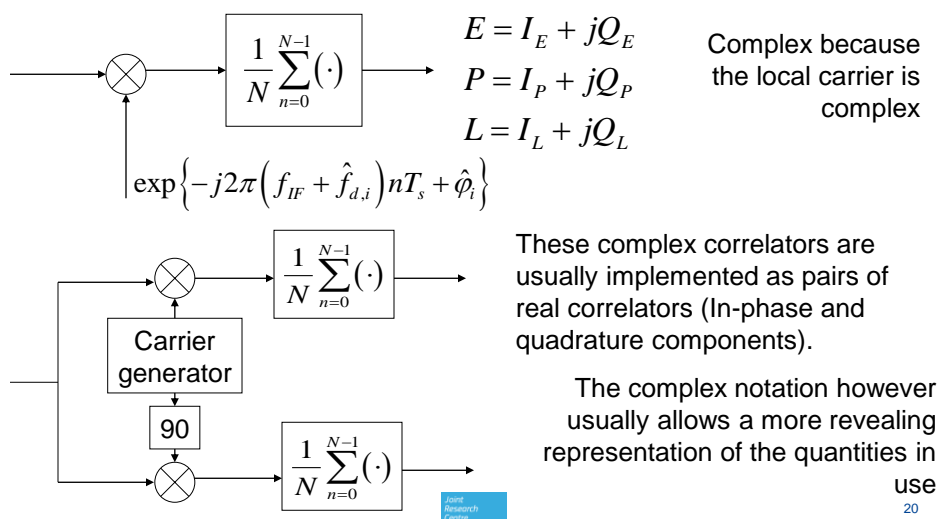
- ➔ measure of how similar the local and incoming signals are.
- ➔ the correlator outputs are a function of code and carrier errors

$$C_R(\Delta\tau, \Delta f, \Delta\varphi) = \frac{\sqrt{C}}{2} dR_s(\Delta\tau) \frac{\sin(\pi\Delta f NT_s)}{N \sin(\pi\Delta f T_s)} \exp\{j2\pi\Delta f(N-1)T_s + j\Delta\varphi\} + w$$



## Real and Complex Correlators

In a standard receiver, at least 3 complex correlators (E, P, L) are required.





## The Non-Linear Discriminator

The non-linear discriminator is responsible for evaluating an error function (an odd function) of the quantity to be tracked. The loop tries to drive to zero the error evaluated by the discriminator (minimization/maximization of the cost function).

The discriminator output can be thought as an approximation of the gradient of the cost function

The discriminator is usually a **non-linear, memory less** function



## Phase Discriminators

The objective of the PLL is to minimize the phase difference between input and local signals

A phase discriminator has to produce an estimate of  $\Delta\varphi$  or an error signal approximately proportional to it.

Odd functions of  $\Delta\varphi$  are valid error signals

$$g(\hat{\varphi}) = |\varphi - \hat{\varphi}|^2$$

↑  
Phase of the local signal      ↑  
Phase of the incoming signal

$$\frac{\partial g(\hat{\varphi})}{\partial \hat{\varphi}} = 2(\hat{\varphi} - \varphi) = 2\Delta\varphi$$

$$f_{odd}(\Delta\varphi) \approx G_d \Delta\varphi + O(\Delta\varphi^3)$$

In GNSS, two types of PLL discriminators are used:

- **pure PLL discriminators:** the input signal is unmodulated and the discriminator does not account for the effect of data bits

- **Costas loop discriminators:** the discriminator is insensitive to bit transitions.



## Standard PLL Discriminators

Complexity ↑	Discriminator Algorithm	Output Phase Error	Characteristics	Amplitude normalization
	$\arctan\left(\frac{P_Q}{P_I}\right)$	$\Delta\varphi$	Two-quadrant arctangent discriminator, MLE	Amplitude independent
	$\frac{P_Q}{P_I}$	$\tan\Delta\varphi$	Suboptimal but good at high and low SNR	Amplitude independent
	$P_I \cdot P_Q$	$\sin 2\Delta\varphi$	Standard Costas discriminator, near optimal at low SNR	$P_I^2 + P_Q^2$
	$P_Q \cdot \text{sign}(P_I)$	$\sin \Delta\varphi$	Decision directed Costas. Near optimal at high SNR	$\sqrt{P_I^2 + P_Q^2}$

From Kaplan E. D. and C.J. Hegarty (2006), "Understanding GPS Principles and Applications", Artech House 23



## Pure PLL Discriminators

In the absence of data bits (for example when using pilot channels), pure PLL discriminators can be used.

The ML phase estimator in the absence of data bit becomes:

$$D(P) = \arctan_2(P_Q, P_I) \quad \text{Four quadrant arctangent}$$

Other pure PLL discriminators can be obtained by opportunely approximating the four quadrant arctangent

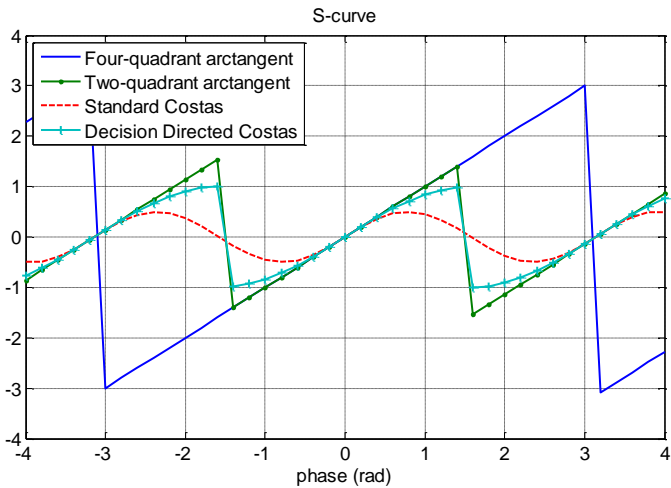
$$D(P) = P_Q \longrightarrow D(P) = \frac{P_Q}{\sqrt{P_I^2 + P_Q^2}}$$



## PLL Discriminators: The S-Curve

The error produced by the discriminator is an odd-function of the input phase (delay). The plot of the discriminator output (in the absence of noise) as a function of the input phase is called S-curve.

The S-curve defines the lock properties of the loop.



Joint Research Centre

25



## The Discriminator Gain

A loop discriminator is usually a non-linear function of the error that the loop is trying to minimize. Thus, for small errors, the discriminator function can be approximated by a constant gain:

$$D(P) = f_{odd}(\Delta\varphi) = G_d \cdot \Delta\varphi + O(\Delta\varphi)$$

where  $G_d$  is the discriminator gain:

$$G_d = \left. \frac{\partial D(P)}{\partial (\Delta\varphi)} \right|_{\Delta\varphi=0} = \left. \frac{\partial f_{odd}(\Delta\varphi)}{\partial (\Delta\varphi)} \right|_{\Delta\varphi=0}$$

The discriminator gain plays a crucial role in the linear analysis of a tracking loop.

Joint Research Centre

26



## Standard FLL Discriminators

Complexity ↑	Discriminator Algorithm	Output Phase Error	Characteristics	Amplitude normalization
	$\frac{1}{2\pi T_c} \arctan\left(\frac{\text{cross}}{\text{dot}}\right)$	$\Delta f$	Two-quadrant arctangent discriminator, MLE	Amplitude independent
	$\frac{1}{2\pi T_c} \frac{\text{cross}}{\text{dot}}$	$\tan\left(2\pi T_c \Delta f\right) / 2\pi T_c$	Suboptimal but good at high and low SNR	Amplitude independent
	$\frac{\text{cross} \cdot \text{dot}}{2\pi T_c}$	$\sin\left(4\pi T_c \Delta f\right) / 4\pi T_c$	Standard Costas discriminator, near optimal at low SNR	$[P_I^2 + P_Q^2]^2$
	$\frac{\text{cross} \cdot \text{sign}(\text{dot})}{2\pi T_c}$	$\sin\left(2\pi T_c \Delta f\right) / 2\pi T_c$	Decision directed Costas. Near optimal at high SNR	$P_I^2 + P_Q^2$



## DLL Discriminator Design

DLL discriminators are designed as approximations of the derivative (gradient) of the correlation function.

The derivative of the correlation function is approximated by the difference quotient:

$$D(\Delta\tau) \propto \frac{\partial R(\Delta\tau)}{\partial(\Delta\tau)} \approx \frac{R(\Delta\tau - d_s/2) - R(\Delta\tau + d_s/2)}{d_s}$$

Early                              Late  
 ↓                                   ↑  
 Correlator spacing

When phase errors are present, a non-linear function is applied to the correlation in order to obtain a phase independent function to maximize



## Standard DLL Discriminators

Complexity ↑	Discriminator Algorithm	Characteristics	Amplitude normalization
	$E_I - L_I$	Coherent Early-minus-Late. It requires phase lock conditions. Most accurate measurements	Amplitude dependent (A)
	$(E_I - L_I)P_I + (E_Q - L_Q)P_Q$	Quasi-coherent dot product. Phase independent	Square amplitude ( $A^2$ )
	$\left[ (E_I^2 + E_Q^2) - (L_I^2 + L_Q^2) \right]$	Non-coherent early-minus-late power. Phase independent	Square amplitude ( $A^2$ )
	$\frac{\sqrt{E_I^2 + E_Q^2} - \sqrt{L_I^2 + L_Q^2}}{\sqrt{E_I^2 + E_Q^2} + \sqrt{L_I^2 + L_Q^2}}$	Normalized non-coherent early-minus-late envelope	Amplitude independent

Joint Research Centre

29



## DLL Discriminators: Complex form

Using the complex notation for the correlators, it is possible to rewrite the loop discriminators in complex form. This usually provides a more intuitive interpretation of the discriminator itself.

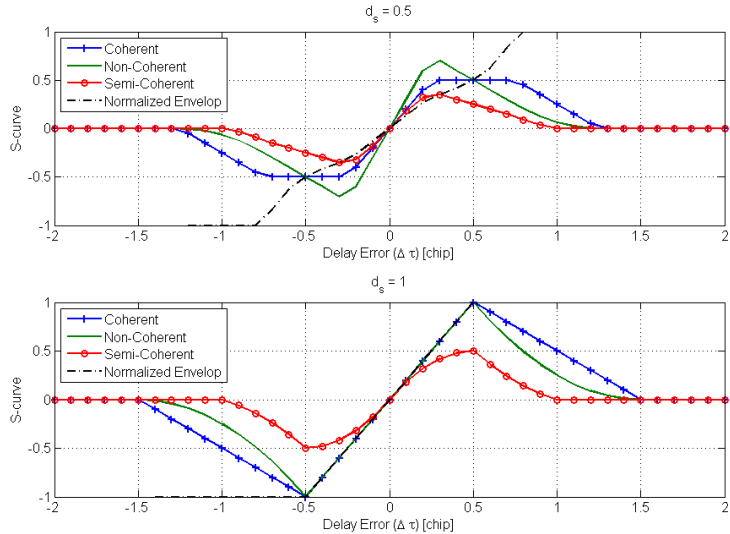
DLL discriminator: real notation	DLL discriminator: complex notation
	$\Re\{E - L\}E_I - L_I$
$(E_I - L_I)P_I + (E_Q - L_Q)P_Q$	$\Re\{(E - L)P^*\}$
$\left[ (E_I^2 + E_Q^2) - (L_I^2 + L_Q^2) \right]$	$\left[  E ^2 -  L ^2 \right]$
$\frac{\sqrt{E_I^2 + E_Q^2} - \sqrt{L_I^2 + L_Q^2}}{\sqrt{E_I^2 + E_Q^2} + \sqrt{L_I^2 + L_Q^2}}$	$\frac{ E  -  L }{ E  +  L }$

In the dot product discriminator the complex prompt correlator is used to remove the remaining phase rotation in the early minus late term.  
In the last two discriminators the phase dependence is removed by the absolute value operator.

Joint Research Centre

30

## DLL Discriminator: S-Curve



31

## The Loop Filter

The discriminator outputs are noisy and vary with time (effect of dynamics). Loop filters are aimed at reducing the noise present at the discriminator output.

Loop filters have to average the noise effect and respond effectively to changes in the signal parameters.

Originally, loop filters were analog devices and implemented as the linear combination of analog integrators:

$$B(s) = \sum_{i=0}^{L-1} \frac{K_i}{s^i}$$

-  $1/s$  is the Laplace transform of the analog integrator  
-  $K_i$  are the integrator gains. The integrator gains are obtained in order to meet different design criteria (loop bandwidth).

An integrator-based structure is selected in order to avoid biases in the parameter estimates

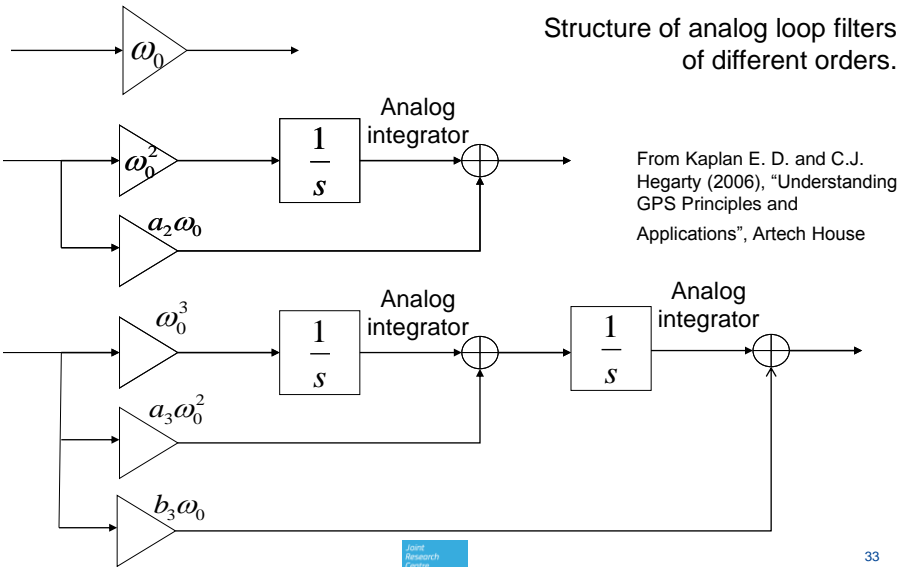
$L$  is the order of the filter (and of the loop). It determines the ability of the loop to respond to different types of dynamics.

Currently, most of the loop filters are implemented on digital platforms.

32



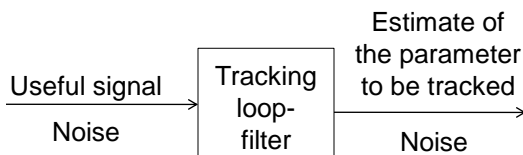
## Analog Loop Filters



Joint Research Centre

## Tracking Loop as Filters

Any tracking loop can be approximated by an equivalent linear device (filter). The approximation is valid for small tracking errors, i.e., when the discriminator acts in its linear region.



Tracking loops provide noisy estimates of the parameter that they are trying to estimate. This is due to the noise present in the input signal. The quantity of noise transferred from the input signal to the final estimate, determines the **loop bandwidth**

$$B_{eq} = \frac{1}{2T_c} \frac{\sigma_{OUT}^2}{\sigma_{IN}^2}$$

Coherent integration time

Variance of the output noise  
Variance of the input noise

Joint Research Centre

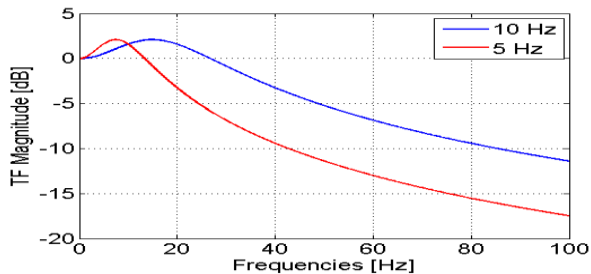
34



## Loop Bandwidth

The loop bandwidth is controlled by the loop filter and the discriminator gain.

The loop bandwidth is one of the main parameters for the loop filter design. Formulae for the loop filter design assume that the discriminator output has been opportunely normalized, such that the total discriminator gain is equal to 1.



Joint Research Centre

35



## Loop Filters: Standard Formulae

Loop Order	Noise Bandwidth $B_n$ (Hz)	Typical Filter Values	Steady State Error
First	$\frac{\omega_0}{4}$	$B_n = 0.25\omega_0$	Sensitive to velocity stress
Second	$\frac{\omega_0(1+a_2^2)}{4a_2}$	$B_n = 0.53\omega_0$ $a_2\omega_0 = 1.414\omega_0$	Sensitive to acceleration stress
Third	$\frac{\omega_0(a_3b_3^2 + a_3^2 - b_3)}{4(a_3b_3 - 1)}$	$B_n = 0.7845\omega_0$ $b_3\omega_0 = 2.4\omega_0$ $a_3\omega_0^2 = 1.1\omega_0^2$	Sensitive to jerk stress

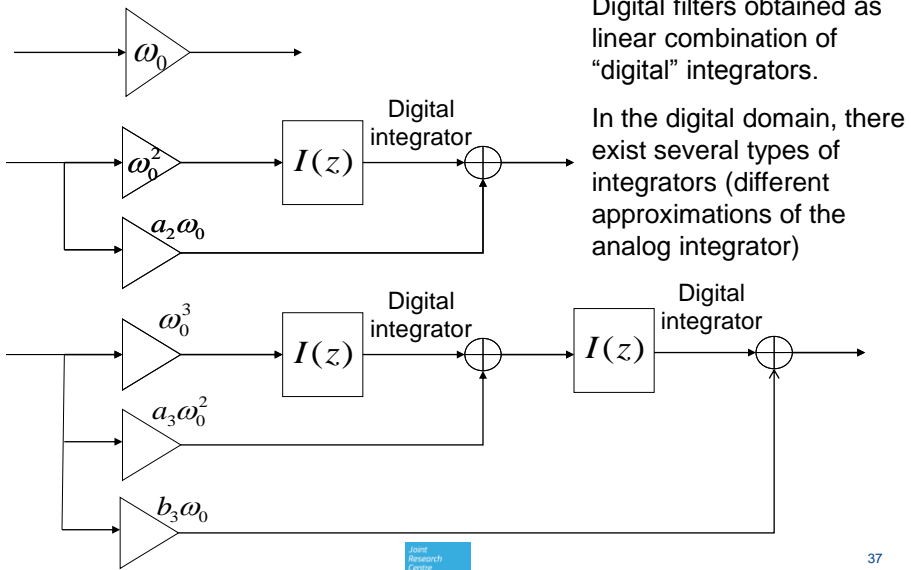
From Kaplan E. D. and C.J. Hegarty (2006), "Understanding GPS Principles and Applications", Artech House

Joint Research Centre

36



## Digital Loop Filters



## Loop Order and Dynamics

The filter order determines the ability of the loop to react to dynamics.

First order	Sensitive to velocity stress. Unconditionally stable for all noise bandwidths (the analog loop!) Used for aided code loops
Second order	Sensitive to acceleration stress. Unconditionally stable for all noise bandwidths (the analog loop!)
Third order	Sensitive to jerk stress. The loop remains stable for loop bandwidths less than 18 Hz. Used for unaided carrier loops

From Kaplan E. D. and C.J. Hegarty (2006), “Understanding GPS Principles and Applications”, Artech House



## Digital Filter Design: Transformation Methods

Several techniques can be adopted for the loop filter design in the digital domain. The most commonly used are based on transformation methods, i.e., the filter is designed in the analog domain and its digital counterpart is obtained by means of mapping functions.

In this way, different approximations for the analog integrator are obtained.

$$\text{Bilinear} \quad s \leftarrow \frac{2}{T_c} \frac{z-1}{z+1}$$

Transformation methods are effective only when

$$\text{Step Invariant} \quad s \leftarrow \frac{1}{T_c} \frac{z-1}{z}$$

$$B_{eq} T_c \ll 1$$

i.e., when the product between bandwidth and loop update rate is small.

- instability issues
- zero/pole displacement

$$\text{Impulse Invariant} \quad h[n] = h_a[nT_s]$$



39



## Digital Filter Design: Other Methods

The loop filters can be designed directly in the digital domain.

### Controlled-root Formulation

S. A. Stephens and J. Thomas, "Controlled-root formulation for digital phase-locked loops," IEEE Trans. Aerosp. Electron. Syst., vol. 31, no. 1, pp. 78 – 95, Jan. 1995.

The loop filter transfer function is still of the form:

$$B(z) = \frac{1}{T_c} \sum_{i=0}^{L-1} \frac{K_i}{(1-z^{-1})^i}$$

The integrator gains are determined by fixing the loop poles and loop bandwidth. This design guarantees a stable loop.

### Optimum filter

P. L. Kazemi, "Optimum Digital Filters for GNSS Tracking Loops," in Proc. of ION/GNSS'08, Savannah, GA, Sept. 2008.

The loop filter is designed such that the transfer function of the loop corresponds to the optimum filter for the input phase/delay. The filter is optimum in the sense that it minimizes the MMSE (Wiener filter).



40



## Numerically Controlled Oscillator

The NCO is used to generate the local code and carrier.  
It is usually made up of two parts:

- a phase (delay) accumulator

the tracking loops estimate the phase/delay rate and the NCO generates a phase/delay signal based on this estimate.

$$\text{phase}_{\text{NCO}} = \text{residual\_phase} + \text{phase\_rate}[0:(N - 1)]$$

- a phase (delay) to amplitude converter

that is used to generate the waveforms to be correlated by the incoming signal

$$\text{local\_carrier} = \cos(\text{phase}_{\text{NCO}}) + j \sin(\text{phase}_{\text{NCO}})$$



## Equivalent Models and Performance Analysis

A tracking loop is a complex device and the analysis is often limited to some aspects of the loops.

Use of

- computer simulations
- approximations

In the next slides

- linear theory of tracking loops:
  - + equivalent linear model
  - + transfer function and tracking jitter
- non-linear theory:
  - + mean time to lose lock
  - + mean cycle slip time



## Equivalent Model

The tracking loop is represented in the domain of the **quantity tracked** (parameter space)

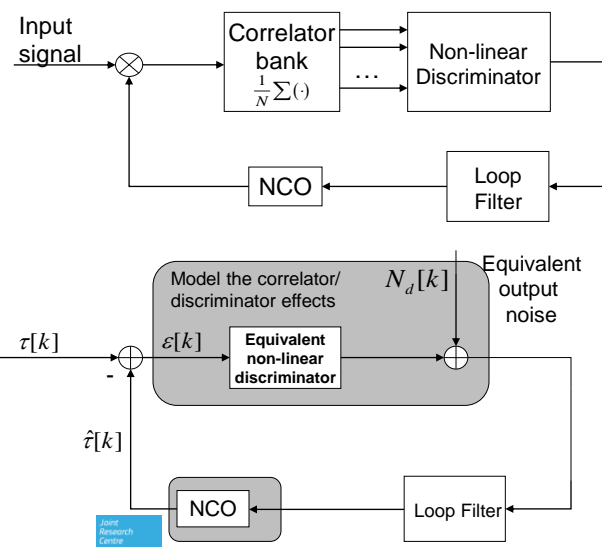
The loop filter already operates in the parameter space.

The NCO

- updates the estimate of tracked quantity (phase/delay)
- is an interface element: from the parameter to the signal domain

Correlators and non-linear discriminators are a second interface element: from the signal to the parameter domain

In the parameter space, the NCO is replaced by a model describing the update operations



## Correlator and Discriminator Output

The correlator outputs can be modeled as

$$\begin{aligned}
 P[k] &= \frac{\sqrt{2C}}{2} R_c(\varepsilon[k]) \frac{\sin(\pi \Delta F_d N T_s)}{N \sin(\pi \Delta F_d T_s)} \exp\{j\Delta\phi\} + N_p \\
 E[k] &= \frac{\sqrt{2C}}{2} R_c(\varepsilon[k] - d_s/2) \frac{\sin(\pi \Delta F_d N T_s)}{N \sin(\pi \Delta F_d T_s)} \exp\{j\Delta\phi\} + N_e \\
 L[k] &= \frac{\sqrt{2C}}{2} R_c(\varepsilon[k] + d_s/2) \frac{\sin(\pi \Delta F_d N T_s)}{N \sin(\pi \Delta F_d T_s)} \exp\{j\Delta\phi\} + N_l
 \end{aligned}$$

Noise components

The delay, frequency and phase information is embedded in the correlator outputs. In the following the DLL case is considered as an example, the effect of residual frequency errors is neglected.

The discriminator output is a function of the noisy correlators, but it can always be expressed as

$$D(P[k], E[k], L[k]) = D(S_p[k], S_e[k], S_l[k]) + N_d[k] = g(\varepsilon[k]) + N_d[k]$$

Signal components of  
the correlator outputs





## An Example: Dot-Product discriminator

Discriminator output:

$$D_{out} = \Re e \{ (E - L) P^* \} = \Re e \{ (S_E + N_E - S_L - N_L)(S_P + N_P)^* \}$$

$$= \Re e \{ (S_E - S_L) S_P^* \} + \Re e \{ (N_E - N_L) N_P^* \} + \Re e \{ (S_E - S_L) N_P^* + (N_E - N_L) S_P^* \}$$

**Signal component:**  
the discriminator  
output in the absence  
of input noise

Equivalent Output Noise

**Signal component:**

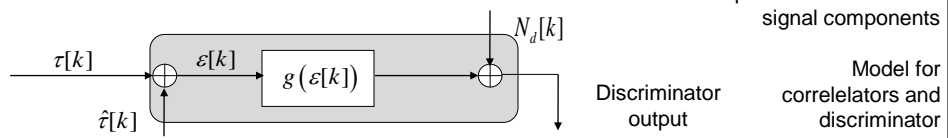
$$\Re e \{ (S_E - S_L) S_P^* \} = \frac{C}{2} (R_c(\varepsilon[k] - d_s/2) - R_c(\varepsilon[k]) + d_s/2) R_c(\varepsilon[k]) = g(\varepsilon[k])$$

Non-linear  
function of the  
delay error

**Noise component**

$$N_d[k] = \Re e \{ (N_E - N_L) N_P^* \} + \Re e \{ (S_E - S_L) N_P^* + (N_E - N_L) S_P^* \}$$

The equivalent output  
noise is usually  
dependent on the useful  
signal components

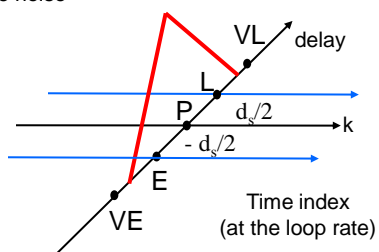


## Equivalent Output Noise

- ✓ The equivalent output noise is usually *non-Gaussian* and its probability density function (pdf) does not usually admit a closed-form expression.
- ✓ The analysis of the process pdf is usually too complex and only the noise variance is determined.
- ✓  $N_d[k]$  is, in general, a zero-mean white process. The whiteness of the process derives from the independence of the correlator outputs along the time dimension.
- ✓ When characterizing the equivalent output noise, it is important that to account for the statistical correlation between the noise components of the correlator outputs

$$C_{EPL} = \begin{bmatrix} 1 & R_c(d_s/2) & R_c(d_s) \\ R_c(-d_s/2) & 1 & R_c(d_s/2) \\ R_c(-d_s) & R_c(-d_s/2) & 1 \end{bmatrix}$$

$$= \begin{bmatrix} 1 & R_c(d_s/2) & R_c(d_s) \\ R_c(d_s/2) & 1 & R_c(d_s/2) \\ R_c(d_s) & R_c(d_s/2) & 1 \end{bmatrix}$$





## NCO Models

Due to the phase (delay) accumulation the NCO acts as an integrator

Different types and models:

Phase and phase-rate feedback

$$\hat{\phi}_{n+1} = \hat{\phi}_n + \hat{\dot{\phi}}_{n+1} T_c \xrightarrow{\text{Transfer function}} T_c \frac{z}{z-1} = \frac{T_c}{1-z^{-1}}$$

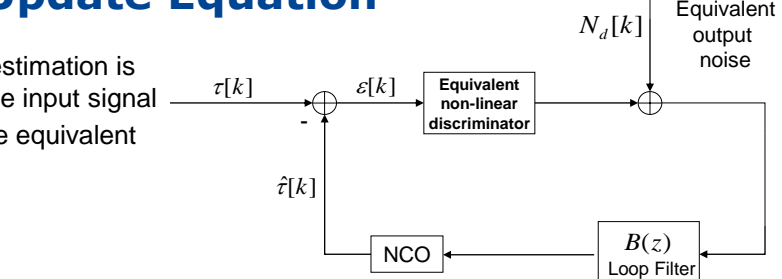
Rate only feedback

$$\hat{\phi}_{n+1} = \hat{\phi}_n + \frac{1}{2} \left( \hat{\dot{\phi}}_{n+1} T_c + \hat{\dot{\phi}}_n T_c \right) \xrightarrow{\text{Transfer function}} \frac{T_c}{2} \frac{z+1}{z-1} = \frac{T_c}{2} \frac{1+z^{-1}}{1-z^{-1}}$$

Joint Research Centre

## Loop Update Equation

The delay estimation is driven by the input signal  $\tau[k]$  and the equivalent noise  $N_d[k]$



Loop filter transfer function

convolution

Discriminator function

$$\hat{\tau}[k] = \hat{\tau}[k-1] + T_c b[k] * \left[ g(\epsilon[k-1]) + N_d[k-1] \right]$$

$$\epsilon[k] = \tau[k] - \hat{\tau}[k]$$

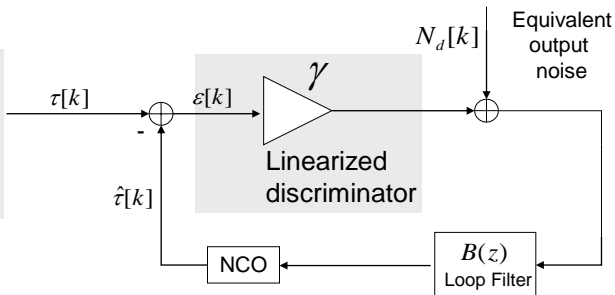
$$\hat{\tau}[k] = \hat{\tau}[k-1] + T_c b[k] * \left[ g(\tau[k-1] - \hat{\tau}[k-1]) + N_d[k-1] \right]$$

Joint Research Centre



## Linear Model

When the loop is locked the discriminator can be approximated by a constant gain



### Linear loop equation

$$\hat{\tau}[k] = \hat{\tau}[k-1] + T_c b[k] * [\gamma(\tau[k-1] - \hat{\tau}[k-1]) + N_d[k-1]]$$

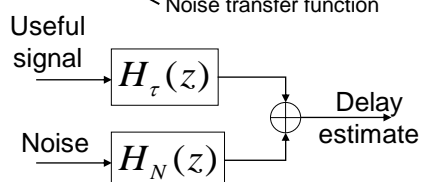
Joint Research Centre

## Loop Transfer Functions (I/II)

$$\hat{\tau}(z) = \frac{\gamma T_c B(z)}{z + \gamma T_c B(z) - 1} \tau(z) + \frac{T_c B(z)}{z + \gamma T_c B(z) - 1} N_d(z)$$

Signal transfer function

$$\hat{\tau}(z) = H_\tau(z) \tau(z) + H_N(z) N_d(z)$$



$$\varepsilon(z) = [1 - H_\tau(z)] \tau(z) + H_N(z) N_d(z) \quad \text{Error propagation}$$

$$H_\tau(z) = \left. \frac{\hat{\tau}(z)}{\tau(z)} \right|_{N_d(z)=0} = \frac{\gamma T_c B(z)}{z + \gamma T_c B(z) - 1} \quad H_N(z) = - \left. \frac{\hat{\tau}(z)}{N_d(z)} \right|_{\tau(z)=0} = - \frac{T_c B(z)}{z + \gamma T_c B(z) - 1}$$

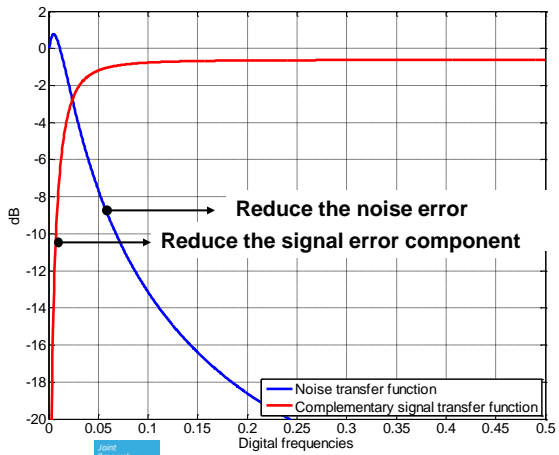
Joint Research Centre



## Loop Transfer Functions (II/II)

$$\varepsilon(z) = [1 - H_\tau(z)]\tau(z) + [H_N(z)]N_d(z)$$

- The error is given by a combination of signal and noise components
  - The noise is low-pass (LP) filtered, whereas the signal is high-pass (HP) filtered. The rejection bandwidth of the HP filter and LP filter are essentially the same
- Choose the loop bandwidth as a compromise between eliminating the noise and the signal components



## Equivalent Loop Bandwidth (I/II)

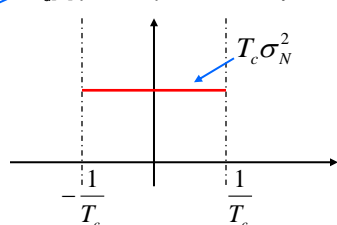
In the absence of signal, the error depends only on the noise process  $N_d[k]$

The variance of the error is given by:

$$\varepsilon(z) = H_N(z)N_d(z)$$

$$\begin{aligned} \text{Var}\{\varepsilon[k]\} &= \int_{-0.5}^{0.5} |H_N(e^{j2\pi f_d})|^2 G_N(f_d) df_d \\ &= T_c \int_{-0.5/T_c}^{0.5/T_c} |H_N(e^{j2\pi f T_c})|^2 G_N(f T_c) df \\ &= T_c \sigma_N^2 \int_{-0.5/T_c}^{0.5/T_c} |H_N(e^{j2\pi f T_c})|^2 df \end{aligned}$$

Coherent integration time       $N_d[k]$  variance





## Equivalent Loop Bandwidth (II/II)

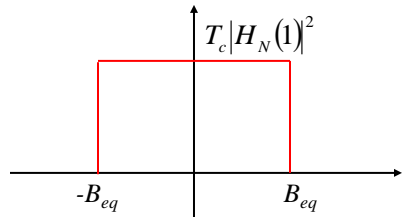
- The tracking loop transfers only a portion of the equivalent noise variance on the error signal

$$\frac{\text{Var}\{\varepsilon[k]\}}{\text{Var}\{N_d[k]\}} = T_c \int_{-0.5/T_c}^{0.5/T_c} |H_N(e^{j2\pi f T_c})|^2 df = 2T_c |H_N(1)|^2 B_{eq}$$

The equivalent loop bandwidth is a measure of the power transferred from the equivalent noise  $N_d[k]$  to the error process!

- If the tracking loop is replaced by an ideal low-pass filter of height  $H_N(1)$  and having the same effect on the error variance, then it is possible to define:

$$B_{eq} \triangleq \frac{1}{2} \int_{-\frac{1}{2T_c}}^{\frac{1}{2T_c}} \frac{|H_N(e^{j2\pi f T_c})|^2}{|H_N(1)|^2} df$$



Joint Research Centre

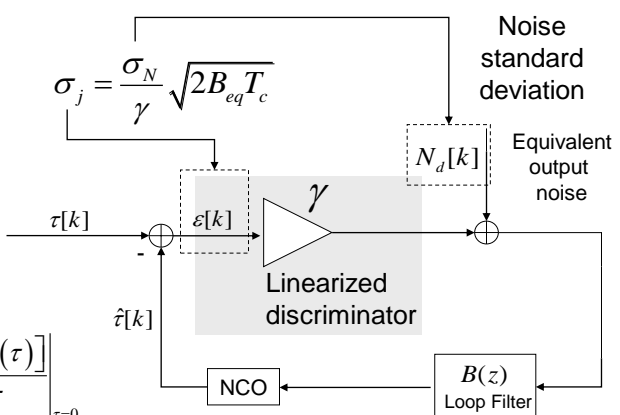
## Tracking Jitter (I/III)

A first measure of the loop performance is the tracking jitter that allows one to quantify the impact of thermal noise on the loop and it is defined as [VanD]:

The tracking jitter is a normalized version of the error standard deviation.

This standard deviation is normalized by the discriminator gain:

$$\gamma = \left. \frac{dE[g(\tau)]}{d\tau} \right|_{\tau=0}$$



[VanD] A. J. Van Dierendonck, P. Fenton, and T. Ford, "Theory and performance of narrow correlator spacing in a GPS receiver," NAVIGATION: Journal of The Institute of Navigation, vol. 39, no. 3, pp. 265 – 283, Fall 1992.

Joint Research Centre



## Tracking Jitter (II/III)

The tracking jitter measures the Root Mean Square (RMS) phase error of the loop and can be expressed as [Woo, Sim]

$$\sigma_j = \sqrt{\frac{C}{N_0 B_{eq}} S_L}^{-1}$$

↑ SNR

where  $S_L$  is the squaring loss. The last equation can be interpreted as follows: if the loop were a perfectly linear system, then the tracking jitter would be a measure of the SNR at the output of the loop. Since the PLL is a non-linear device, performance is degraded by the additional noise introduced by the non-linearities. This impact is measured by the squaring loss.

[Woo] K. T. Woo, "Optimum semi-codeless carrier phase tracking of L2," in Proc. of ION GPS'99, Nashville, TN, Sept. 1999, pp. 289 – 305.

[Sim] M. Simon and W. Lindsey, "Optimum performance of suppressed carrier receivers with costas loop tracking," vol. 25, no. 2, pp. 215 – 227, Feb. 1977.



## Tracking Jitter (III/III)

Coherent early minus late

$$\sigma_j = \lambda \sqrt{\frac{d_s}{C/N_0} \frac{B_{eq}}{2}} \quad [\text{m}]$$

DLL Non-coherent early minus late power

$$\sigma_j = \lambda \sqrt{\frac{d_s}{C/N_0} \frac{B_{eq}}{2} \left( 1 + \frac{2}{C/N_0 T_c (2 - d_s)} \right)} \quad [\text{m}]$$

Quasi-coherent dot product

$$\sigma_j = \lambda \sqrt{\frac{d_s}{C/N_0} \frac{B_{eq}}{2} \left( 1 + \frac{1}{C/N_0 T_c} \right)} \quad [\text{m}]$$

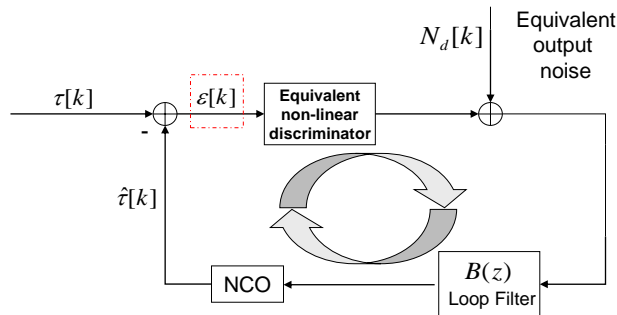
PLL Arctan discriminator

$$\sigma_j = \frac{\lambda}{2\pi} \sqrt{\frac{B_n}{C/N_0} \left( 1 + \frac{1}{2T_c C/N_0} \right)} \quad [\text{m}]$$





## Mean Time to Lose Lock (I/III)



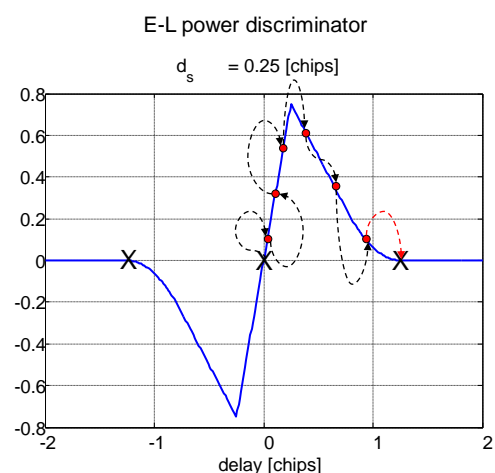
The error process  $\varepsilon[k]$  can be interpreted as a particle diffusing into a non-linear system.

$\varepsilon[k]$  enters the non-linear discriminator whose output depends on the S-curve.



## Mean Time to Lose Lock (II/III)

- The error process define a trajectory over the S-curve.
- The S-curve is characterized by stable points that are those values of delay that provide a zero control signal (discriminator output).
- Only one stable point is in the lock region and corresponds to the zero delay.
- When a stable point, different from (0, 0) is reached the loop is no longer able to track the signal and loss of lock occurs.





## Mean Time to Lose Lock (III/III)

- The time required by the error signal to reach a stable point different from (0, 0) defines the time to lose lock ( $T_{LL}$ ) that is in general a random variable.
- The mean value of  $T_{LL}$  corresponds to the mean time to lose lock (MTLL).
- The MTLL is evaluated by assuming that the particle,  $\varepsilon[k]$ , starts its trajectory in (0, 0).
- The MTLL is, in general, difficult to evaluate and simulations are often used.
- A tracking loop should be designed in order to guarantee a MTLL greater than the period of visibility of the satellite, under some minimal working conditions.

$$MTLL = E[T_{LL}] = E\{\min[k > 0] : g(\varepsilon[k]) = 0 \mid g(\varepsilon[0]) = 0\}$$

Joint Research Centre

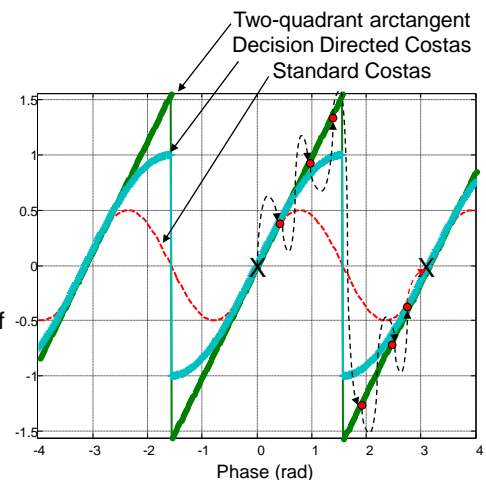


## Mean Cycle Slip Time

The mean cycle slip time (MCST) is defined in a similar way to the mean time to lose lock and apply to PLL.

The MCST is the mean time required by the error process for moving between two adjacent stable points.

The PLL S-curve is a periodic function of the input phase. Thus the MCST corresponds to the mean time required for covering a S-curve period.



Joint Research Centre



## Additional Error Sources

In previous slides only the effect of thermal noise was considered.  
However, tracking loops are affected by other error sources.

The most common are:

- Oscillator Phase Noise (PLL)

it is caused by the changes in the frequency reference provided by the local oscillator. It can be induced by oscillator instability, vibrations, change in temperature  
...

- Dynamic stress error (PLL)

it is due to the satellite/user dynamics. The loop should have an equivalent bandwidth large enough to accommodate the dynamic stress.

- Multipath (DLL)

the presence of reflected signal can introduce significant bias in the delay estimation (distortion of the correlation function)





## JRC GNSS Workshop

### Tracking Utilities

Cillian O'Driscoll



[www.jrc.ec.europa.eu](http://www.jrc.ec.europa.eu)

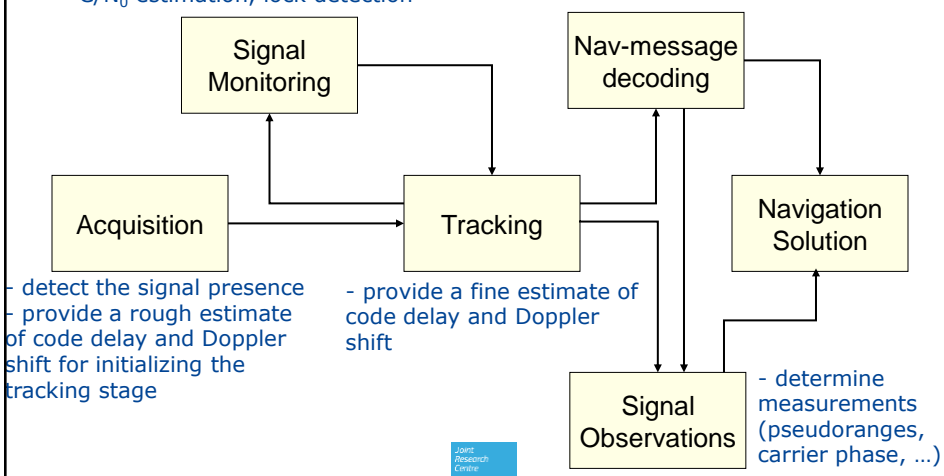
*Serving society  
Stimulating innovation  
Supporting legislation*



## Operations of a GNSS Receiver

- determine the measurement quality
- $C/N_0$  estimation, lock detection

- extract the navigation message
- satellite parameters





## Signal Monitoring

When a receiver is in tracking mode, it needs to know if a signal is actually tracked and that the estimated parameters (code delay, frequency and phase) are correct.

### Quality of the estimated parameters

Measurements from different satellites can have different accuracies (depending on the C/N0, elevation angle ...). An estimate of the quality of the signal parameter is required

### Tracking as a state machine:

Signal tracking is not limited to "static" tracking loops that operate always in the same way. The receiver has to change the tracking parameters (loop type, order, bandwidth, integration time), depending on the signal status.

E.g. if the signal frequency is known with a large uncertainty, the receiver should use an FLL with a large bandwidth for a fast pull-in

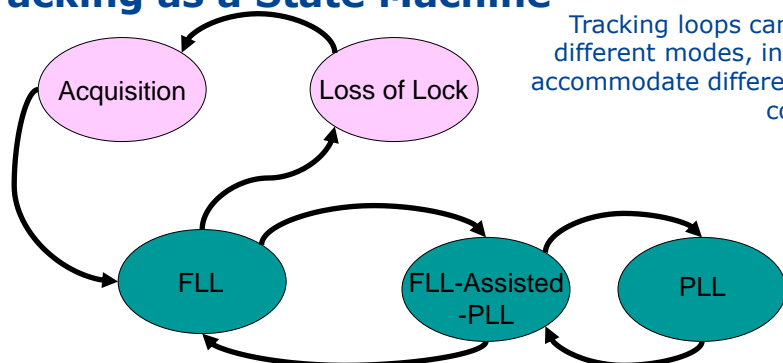
→ **The receiver needs to know what is the signal "status"**



**Need for a signal monitor**



## Tracking as a State Machine



Tracking loops can work in different modes, in order to accommodate different signal conditions

The receiver can:

- track the signal frequency or phase
- adjust the loop bandwidth and integration time
- assist the DLL with the Doppler measurements
- declare loss of lock and revert to acquisition

**Need for DECISION LOGIC**





## The Decision Process

### The receiver needs to determine

- if the phase and frequency are actually tracked
- how long the signal can be coherently integrated
- if the data demodulation process can start (bit synchronization)
- how good are the measurements.

### Decision process based on:

- Phase and Frequency Lock Indicators
- Bit synchronizer
- C/N<sub>0</sub> estimator

Receiver utilities

Input:  
correlator outputs (I & Q)

Sufficient statistics



decision statistics

Joint  
Research  
Centre

## Phase Lock Indicator (PLI)

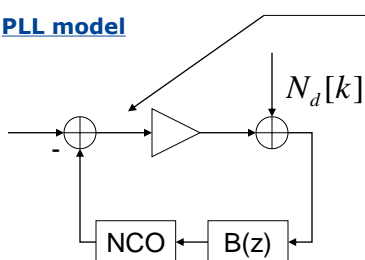
Used to answer to the following question:

$$|\Delta\theta| < T_\theta$$

Decision threshold

Residual phase tracking error committed by the PLL

### PLL model

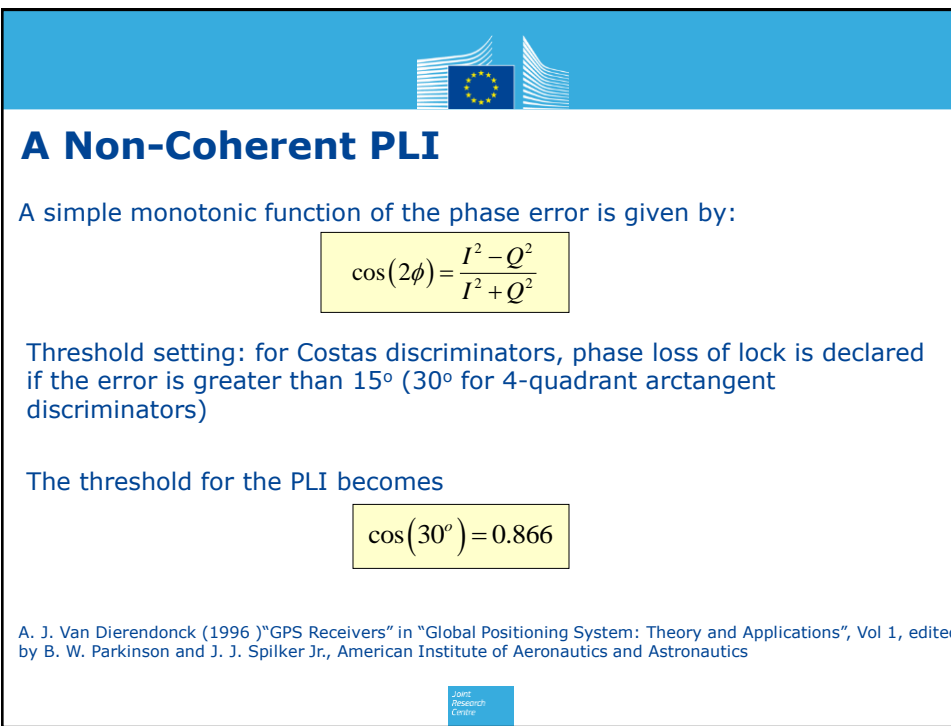
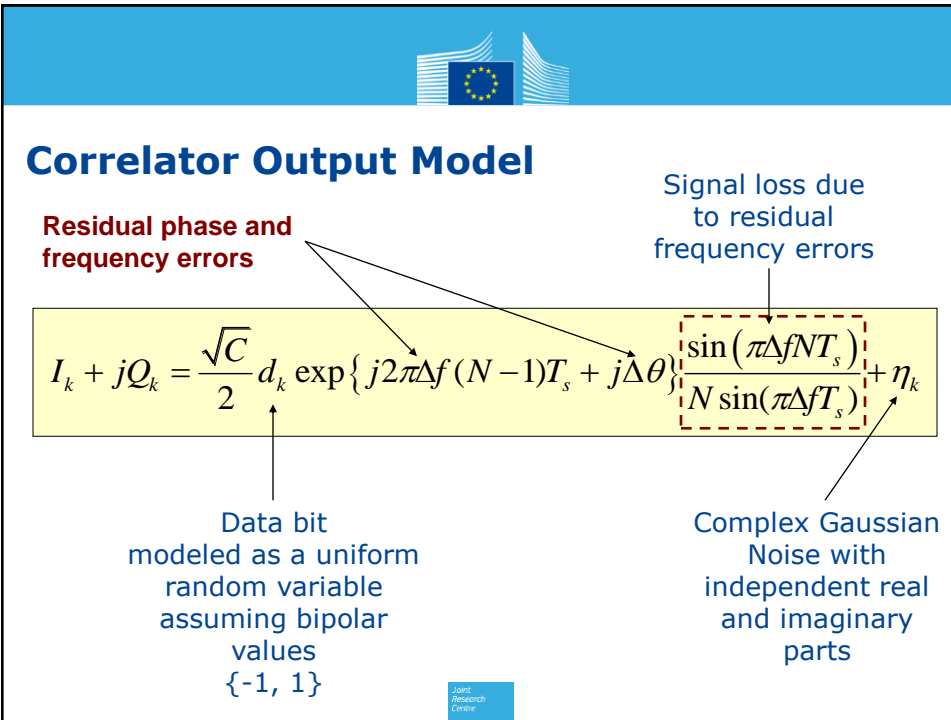


Phase error: difference between estimated and true phase

### Binary hypothesis testing

$$\begin{cases} H_0: & |\Delta\theta| > T_\theta; \\ H_1: & |\Delta\theta| < T_\theta; \end{cases}$$

Joint  
Research  
Centre





## Frequency Lock Indicator (I/II)

Frequency lock indicators can be derived using the same approach adopted for the PLI (LRT).

Any even function of the estimated frequency error can be used as FLI. If a frequency error is present, it can be estimated by differentiating the phase error:

$$\begin{aligned}\hat{\Delta f} &\approx \frac{\phi_k - \phi_{k-1}}{2\pi T_c} = \frac{1}{2\pi T_c} \left[ \arctan \frac{q_k}{i_k} - \arctan \frac{q_{k-1}}{i_{k-1}} \right] \\ &= \frac{1}{2\pi T_c} \arctan \frac{i_{k-1} q_k - q_{k-1} i_k}{i_k i_{k-1} + q_k q_{k-1}} = \frac{1}{2\pi T_c} \arctan \frac{\text{cross}}{\text{dot}}\end{aligned}$$

Analogy with Phase/Frequency discriminators

### Test:

$$|\hat{\Delta f}| < T_f$$

Rule of thumb:

$$T_f \leq \frac{1}{4T_c}$$

The maximum frequency error is inversely proportional to the coherent integration time

Decision threshold



## Equivalent FLIs

Equivalent FLIs can be obtained adopting any even functions of the estimated frequency error

An FLI analogous to the non-coherent PLI is obtained as follows

$$\cos(4\pi\hat{\Delta f}T_c) = \frac{\text{dot}^2 - \text{cross}^2}{\text{dot}^2 + \text{cross}^2}$$

The value of the thresholds for both PLI and FLI should be changed according to properties of the PLL and FLL in use. These threshold has to account for the pull-in capabilities and the bandwidth of the loop.

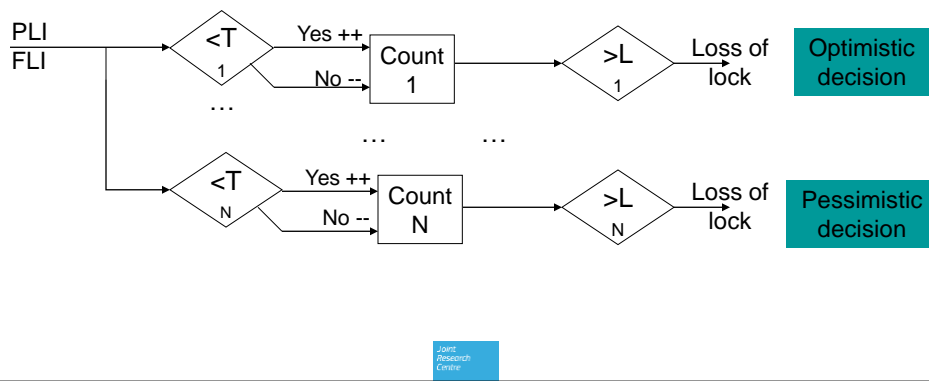




## A Non-Immediate Decision

PLI and FLI provide "instantaneous" information relative to frequency and phase errors. Moreover, PLI and FLI are noisy estimates and a decision based on single sample can easily be wrong.

### Decision based on several samples from the PLI and FLI:



Joint  
Research  
Centre



## Delay Lock Indicator and $C/N_0$ estimator

### **Code lock detection**

- can be inferred from frequency and phase lock
- is similar to estimating the  $C/N_0$  (code lock is required to obtain a good  $C/N_0$  estimation)

→  $C/N_0$  estimators as DLIs

The  $C/N_0$  is a property of the input signal and does not depend on the type of processing adopted by the receiver (receiver independent quantity).

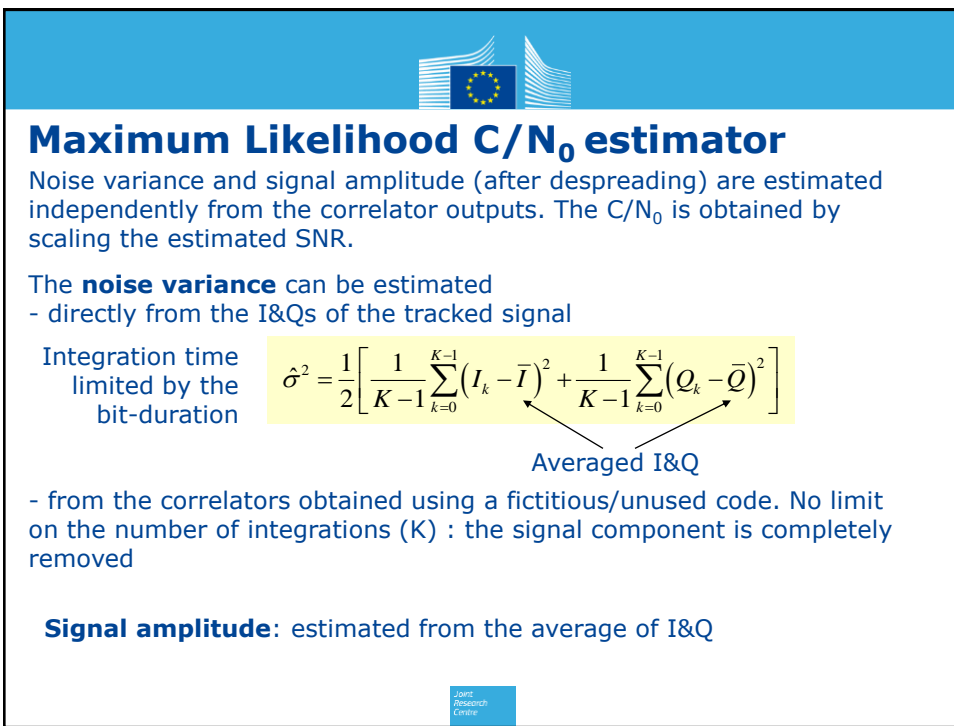
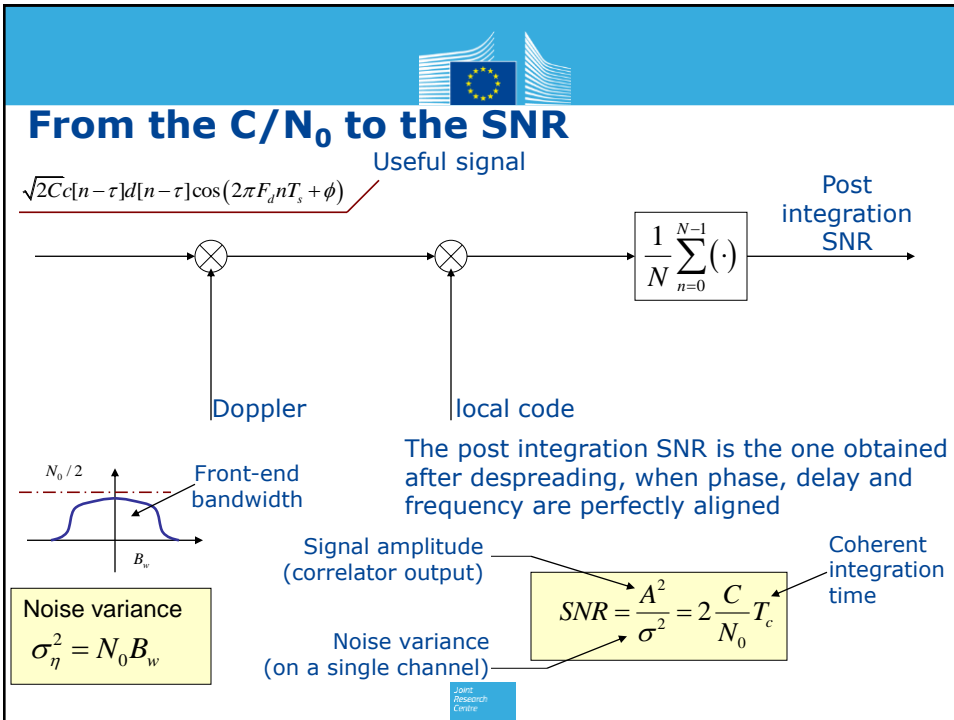
However:

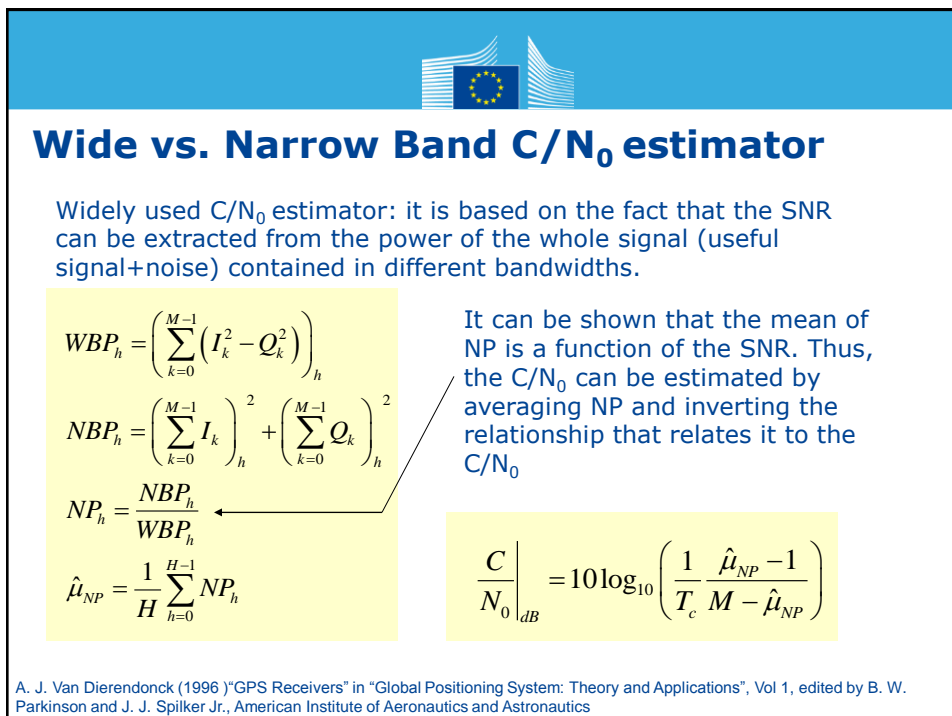
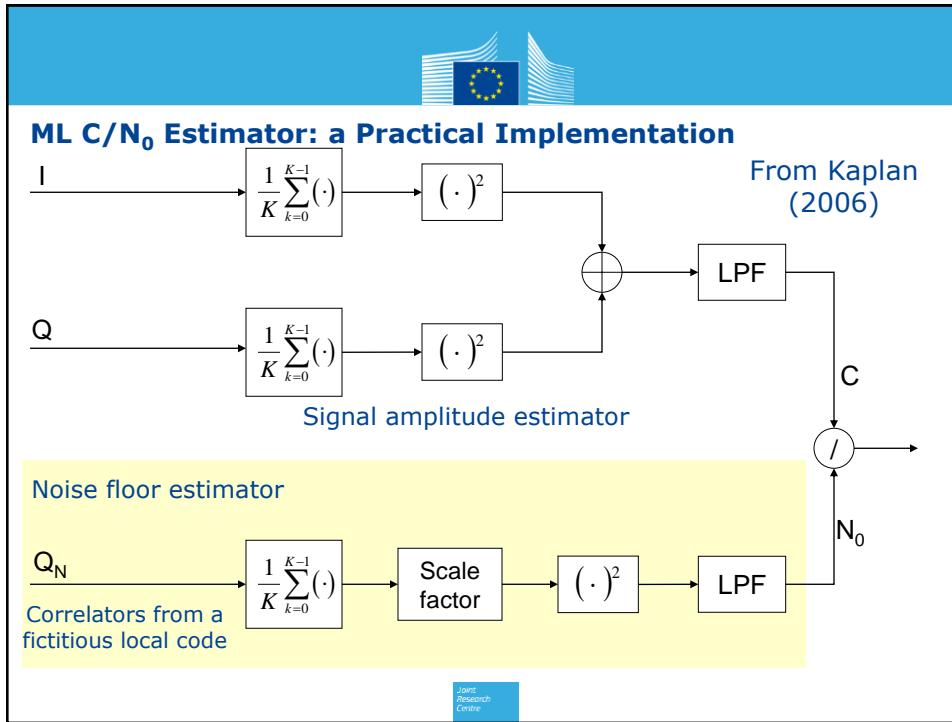
- the receiver can perceive only the quantity of noise power (variance) entering the front-end and not its power spectral density ( $N_0/2$ )
- when the signal enters the receiver, its power (C) is degraded by the front-end and reduced by several processing losses.

→ The  $C/N_0$  cannot be directly estimated!

All the  $C/N_0$  estimators determine the signal-to-noise (SNR) after despreading and evaluate the  $C/N_0$  from the SNR using an adequate propagation model.

Joint  
Research  
Centre







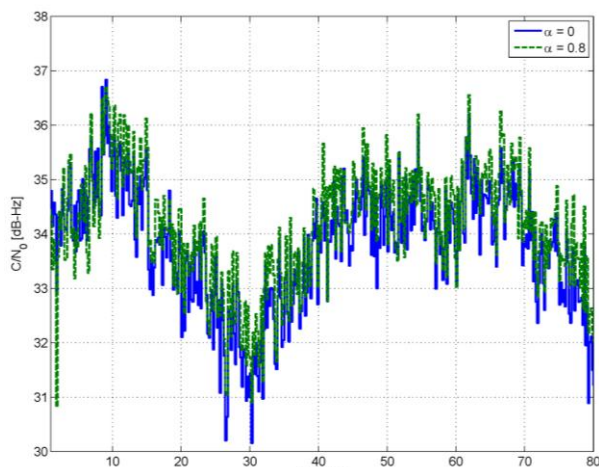
## C/N<sub>0</sub> Estimation: an example

C/N<sub>0</sub> estimates for an indoor dataset.

The C/N<sub>0</sub> estimates should be independent from the type of processing since it is a property of the input signal.

In practice, C/N<sub>0</sub> estimations depends on the different processing losses such as code and frequency misalignments.

C/N<sub>0</sub> estimations reflect the signal quality (similarly to the lock indicators): impact of signal fading

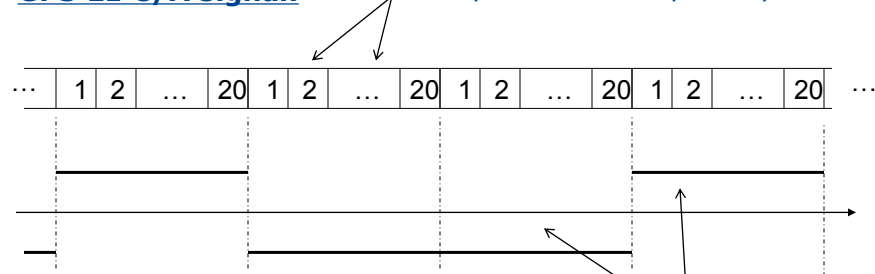


Joint  
Research  
Centre



## Bit Synchronization (I/II)

GPS L1 C/A signal: Periodic repetition of the primary PRN code



The L1 C/A signal is given by the periodic repetition of the PRN code modulated by the navigation message.

Each data bit last 20 ms, i.e., 20 primary code periods.  
The primary codes are thus grouped in blocks of 20 elements, each group is characterized by the same polarity (data bit)

Joint  
Research  
Centre

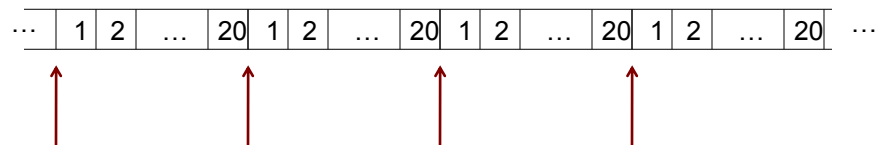


## Bit Synchronization (II/II)

### Bit synchronization:

Acquisition and tracking recover only the boundary of the primary PRN code.

Bit synchronization is aimed at determining the beginning of a data bit (a 20 element block characterized by the same polarity).



Bit synchronization is required:

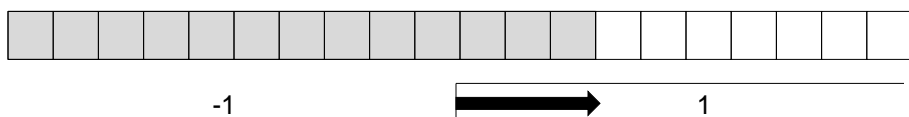
- for extending the coherent integration time (up to 20 ms). Long integration times further increase the de-spreading gain.
- to start the data demodulation process



## Maximum Likelihood Bit Syncher (I/II)

The I&Qs are modelled as Gaussian random variables whose means depend on the data bits. The data bits are assumed to be uniformly distributed on the set  $\{-1, 1\}$ .

Assume to have a block of 20 correlator outputs (1 ms) and that a data transition occurs:



The ML bit synchronizer requires the test of all possible alignments for the bit transition. The correlation between the 20 correlator outputs and the local sequence reproducing the bit transition is maximized when the bit alignment is matched.

P. A. Wintz and E. J. Luecke (1969) "Performance of Optimum and Suboptimum Synchronizer", IEEE Trans. On Comm. Technology, Vol. 17, n. 3, June, pp. 380-389

J. J. Spilker Jr. (1977) "Digital Communications by Satellites", Prentice -Hall, Englewood Cliffs, New Jersey. Chapter 14 "Bit Synchronizers for Digital Communication"





## Maximum Likelihood Bit Syncher (II/II)

If the phase is recovered, the ML bit syncher becomes:

$$\hat{\tau} = \arg \max_{\tau} \left\{ \log \cosh \left[ \sum_{i=0}^{19} I_i s(\tau) \right] \right\}$$

In-phase prompt correlator outputs      ↑      ↑

Sequence  
reproducing the bit  
transition,  $\tau$  controls  
the position of the  
transition

The “log cosh” emerges from the fact that the bits are randomly distributed.  
“log cosh” extracts the magnitude of the correlation and can be approximated by the absolute value (high SNR) or by squaring (low SNR).

Several blocks of 20 ms are needed

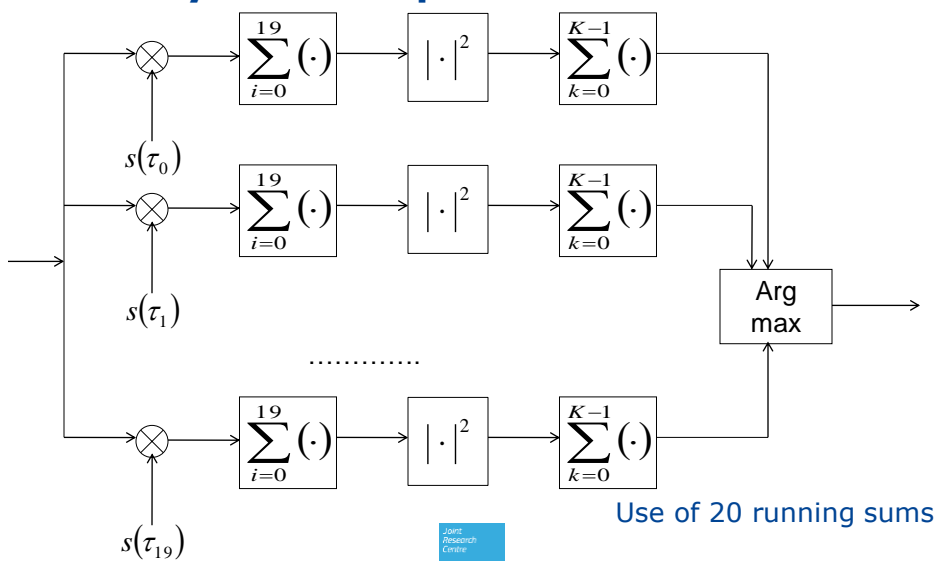
- since the transition does not always occur
- to increase the detectability of the bit boundary

$$\hat{\tau} = \arg \max_{\tau} \left\{ \sum_{k=0}^{K-1} \log \cosh \left[ \sum_{i=0}^{19} I_{i,k} s(\tau) \right] \right\} \approx \arg \max_{\tau} \left\{ \sum_{k=0}^{K-1} \left[ \sum_{i=0}^{19} I_{i,k} s(\tau) \right]^2 \right\}$$

Joint  
Research  
Centre



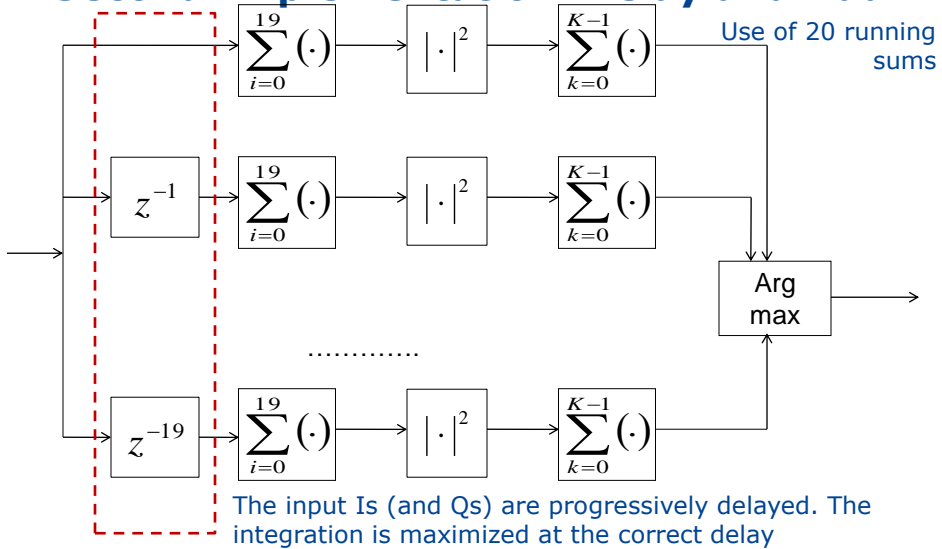
## ML Bit Syncher: Implementation



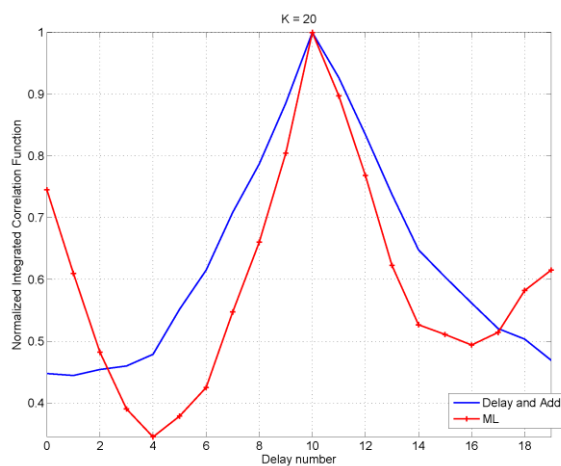
Joint  
Research  
Centre



## A Second Implementation: Delay and Add



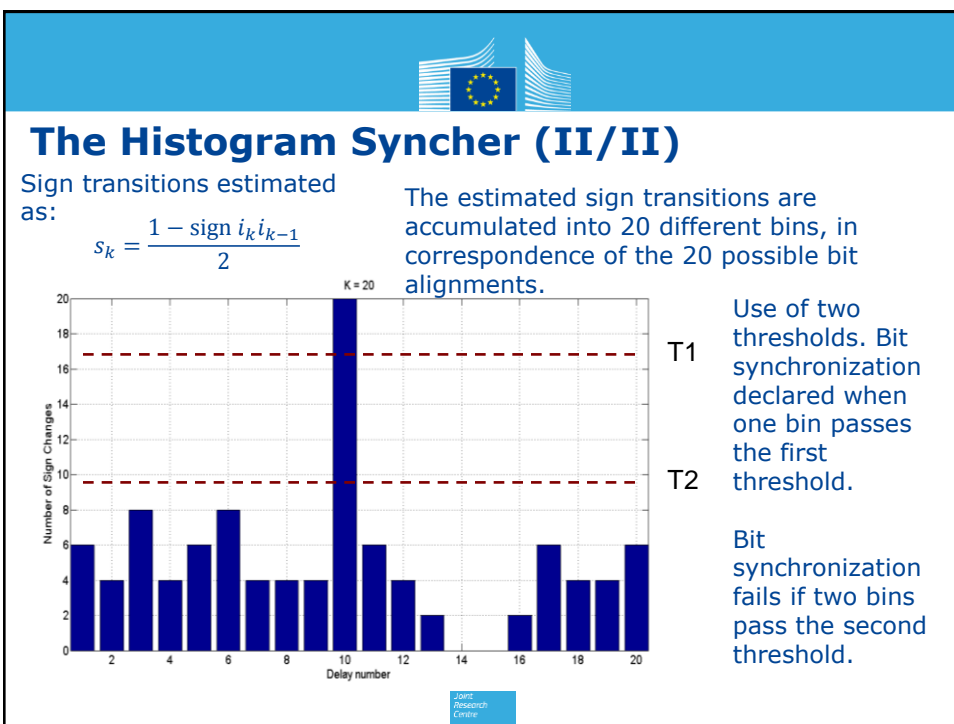
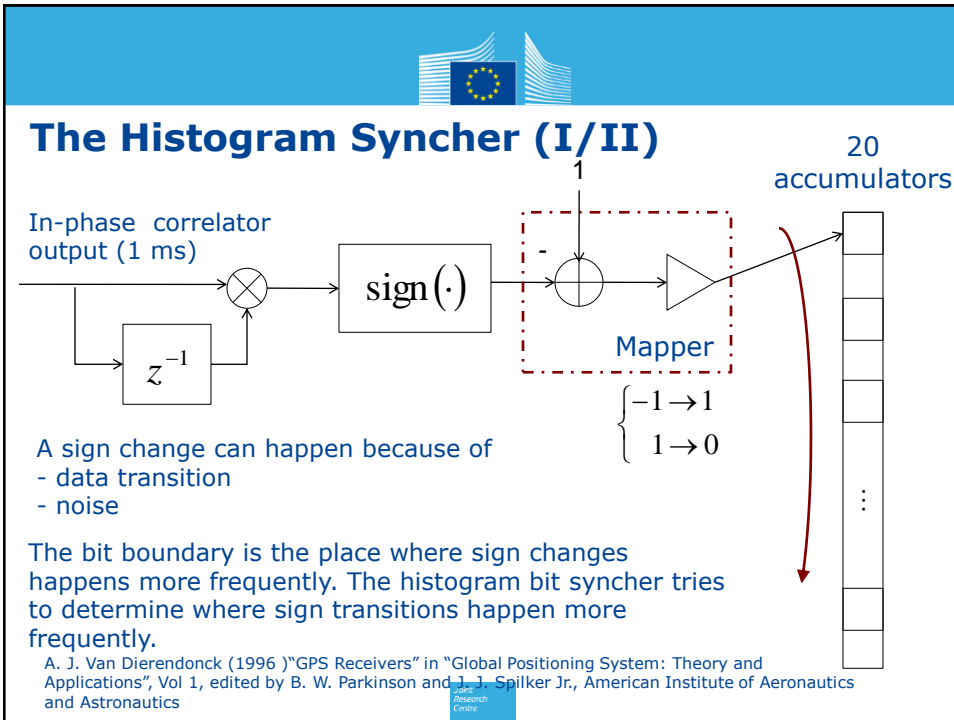
## ML Bit Syncer: an Example

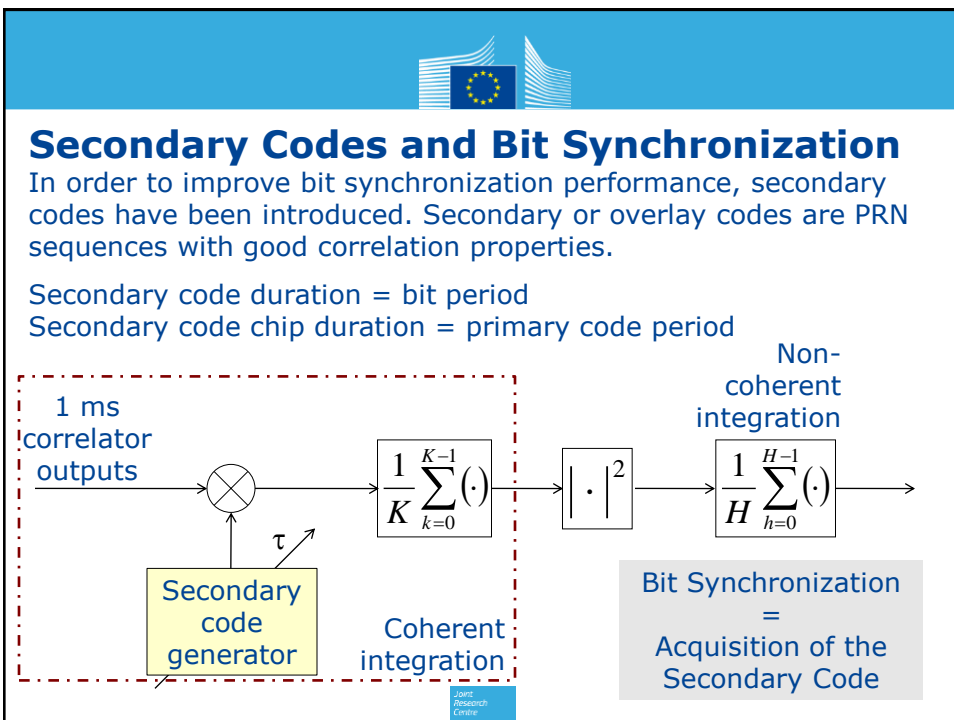
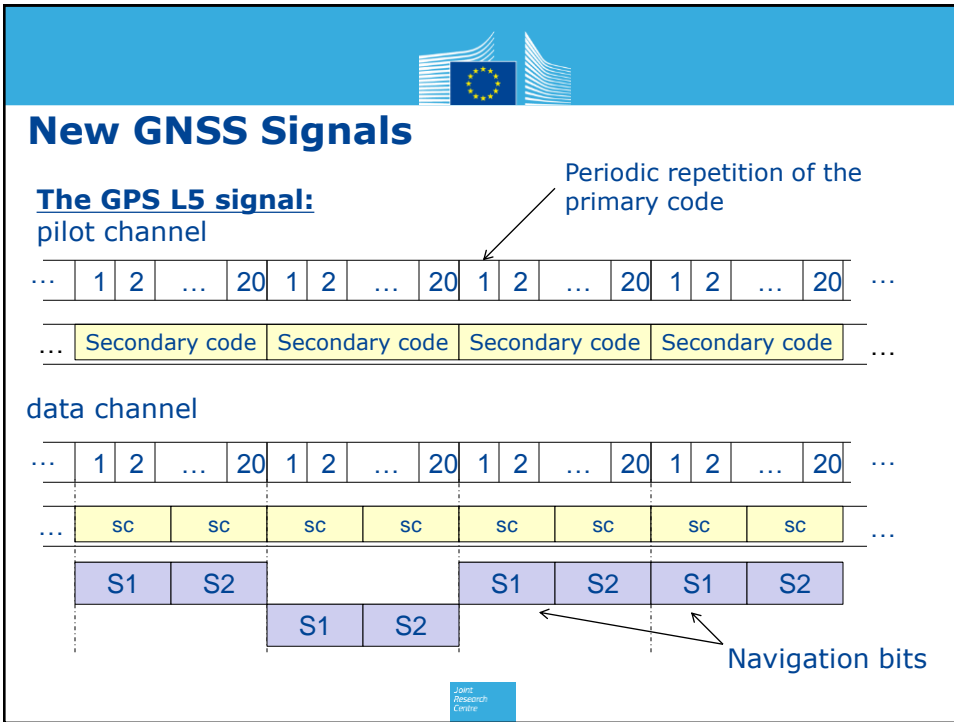


Bit synchronization results for an indoor data set (PRN 1),  $C/N_0 = 35$  dB-Hz

$K = 20$  non-coherent integrations, for a 400 ms total integration time.

The Delay and Add approach requires one more data block (19 additional correlator outputs) to allow the progress shift of the input data and the same integration time

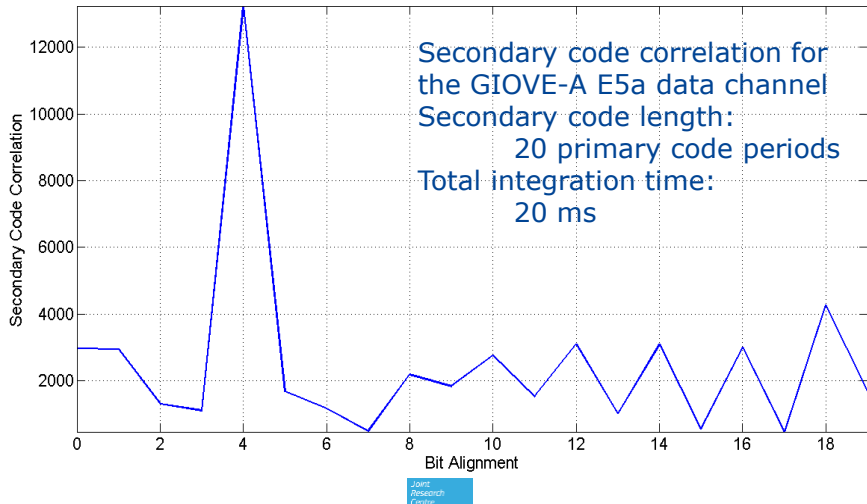






## Secondary Codes: an example

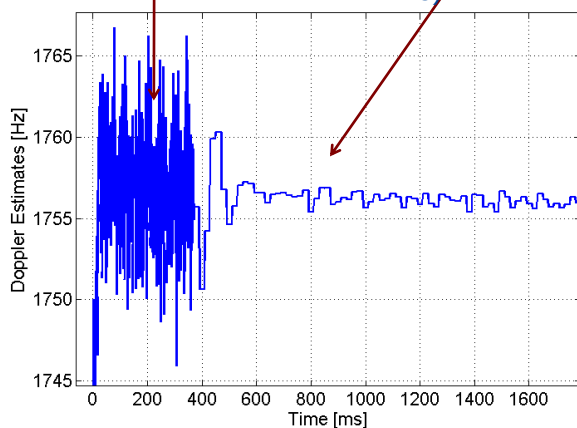
Giove-A E5a data channel -  $C/N_0 = 43 \text{ dB-Hz}$



## Impact of Bit Synchronization

Before bit synchronization:  
the coherent integration time  
is limited to 1 ms

After bit synchronization:  
the receiver can extend the coherent  
integration time up to a bit period (e.g. 20  
ms)



When the receiver is changing the integration time:  
- the loop filter coefficients need to be updated in order to accommodate the new integration time (bandwidth requirements and stability)  
- lower update rate, less noisy parameter estimates

The receiver can use more complex logics for gradually increase the integration time



## Navigation Message Decoding

After bit synchronization, the navigation message can be decoded.

- The bits of the navigation message are usually recovered using a hard decision process (sign of the in-phase correlator outputs accumulated over 20 ms).

- New GNSS signals can use more complex decision process (soft decision) with Forward Error Correction (FEC)

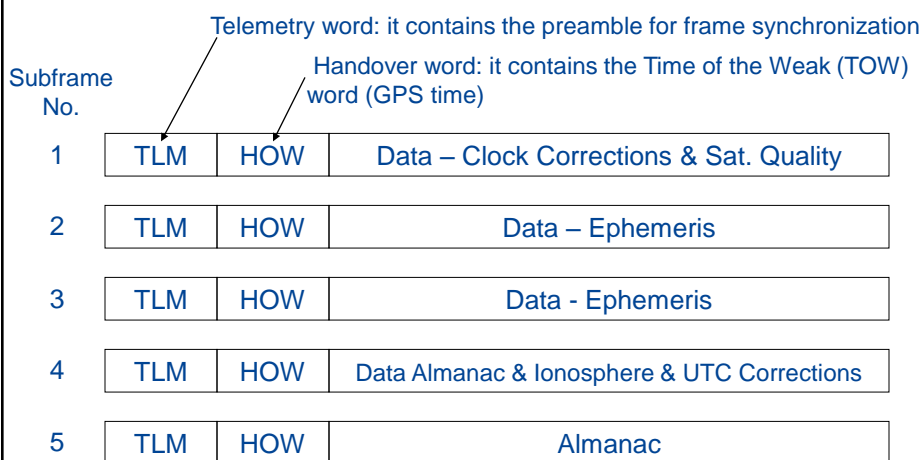
The navigation message contains:

- the **ephemeris**, with the modified Keplerian parameters describing the dynamic model of the satellite (it allows to recover the satellite position at a given time);
- bias - **clock corrections** allowing to compensate for the satellite clock bias and drift with respect to GPS (GNSS) time;
- **almanacs** for the approximate position of the other satellites
- ionospheric and other corrections.

This information is organized in master frame, frames, subframes and words. Each subframe is time-stamped, allowing the determination of the transmit time.



## Frame and Subframe Structure



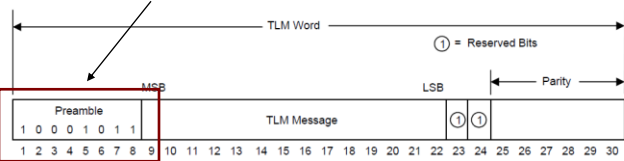
J. J. Spilker Jr. (1996) "GPS Navigation Data" in "Global Positioning System: Theory and Applications", Vol 1, edited by B. W. Parkinson and J. J. Spilker Jr., American Institute of Aeronautics and Astronautics



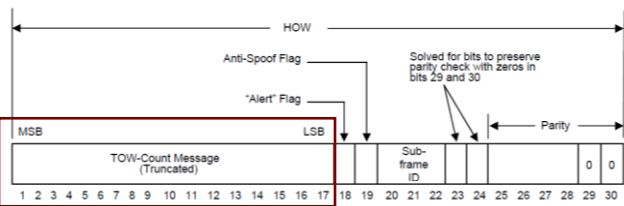


## Frame Synchronization and Z-count

8-bit modified Baker sequence  
for sub-frame synchronization



After bit synchronization, a GNSS receiver has to determine the beginning of a data subframe. This is achieved exploiting the correlation properties of a preamble inserted at the beginning of each TLM word.



After frame synchronization, the receiver can extract the time of the week (number of seconds from the beginning of the week). This information is in the HOW that contains part of the Z-count (29 bits).

17 bits corresponding to the TOW at the start (leading edge) of the next subframe

From ICD-GPS-200C-005R1 (2003), "Navstar GPS Segment/Navigation User Interface", 14 Jan 2003

Joint Research Centre



## Acknowledgement

These slides are based on those developed by Daniele Borio for the ENGO 638 course at the University of Calgary

Joint  
Research  
Centre



# From signal tracking to the navigation solution

Heidi Kuusniemi

*JRC Summer School on  
GNSS Core Technologies*

Ispra, Italy 2-4 July, 2012



FINNISH GEODETIC  
INSTITUTE

heidi.kuusniemi@fgi.fi

## Content

- ▶ Measurements
- ▶ Overview of estimating position, velocity and time
- ▶ Linear position estimation
- ▶ Velocity estimation
- ▶ Error sources
- ▶ Performance measures
- ▶ Summary

Slides partly based on:  
*GNSS Applications and Methods*, by S. Gleason  
and D. Gebre-Egziabher (Eds.),  
Artech House Inc., 2009  
<http://www.gnssapplications.org/>



2

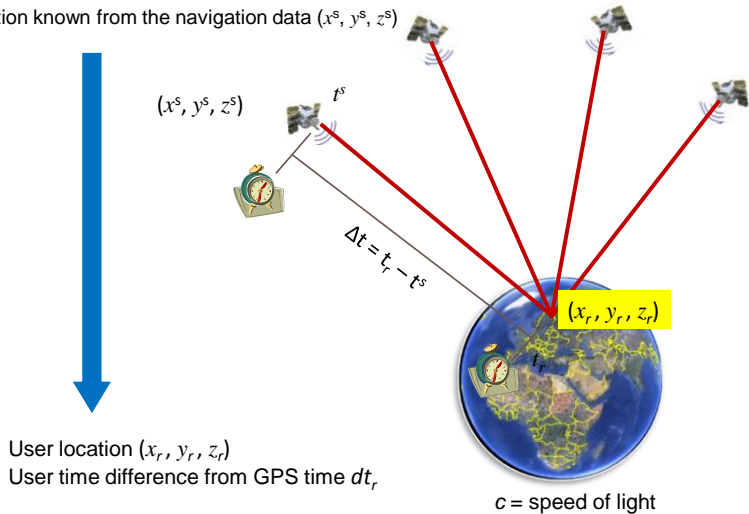
heidi.kuusniemi@fgi.fi



## Measurements – pseudorange (1)

Code range measurement =  $c \Delta t = c (t_r - t^s)$

Satellite location known from the navigation data  $(x^s, y^s, z^s)$



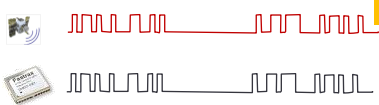
3

heidi.kuusniemi@fgi.fi

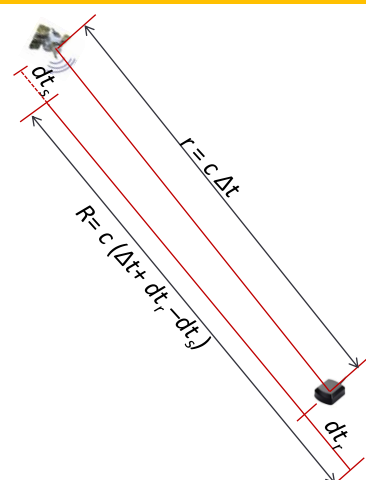


## Measurements – pseudorange (2)

$$\text{Pseudorange}$$
$$R = c (\Delta t + dt_r - dt_s)$$



- ▶ Satellite and receiver clocks are not synchronized or in GPS time
- ▶ Clock corrections are necessary to both clocks:
  - ▶ Satellite clock correction  $\underline{dt}_s$  is obtained from the navigation data (sent with the GPS-signal)
  - ▶ Receiver clock correction  $\underline{dt}_r$  is obtained/solved for in the receiver together with the user coordinates
    - ▶  $(x_r, y_r, z_r) \rightarrow (x_r, y_r, z_r, dt_r)$



4

heidi.kuusniemi@fgi.fi



## Measurements – carrier phase

Carrier phase measurement is a measure of the range between a satellite and a receiver expressed in units of cycles of the carrier frequency.

Carrier phase observation in unit of length:

$$L = \lambda\phi = r + N\lambda$$

Known satellite locations at time t:

$$(x^s, y^s, z^s)_t$$

Carrier wave length:

$$\lambda$$

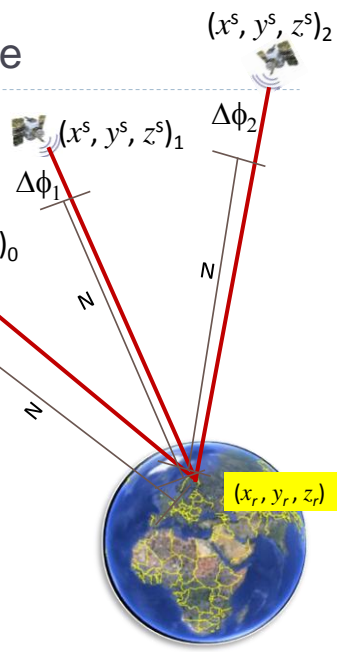


- 1) When a satellite is locked, the GPS receiver starts tracking the incoming phase
- 2) It counts the (real) number of phases as a function of time  
=  $\Delta\phi(t)$
- 3) The initial number of phases N is unknown
- 4) However, if no loss of lock, N is constant over an orbit arc

User location  $(x_r, y_r, z_r)$

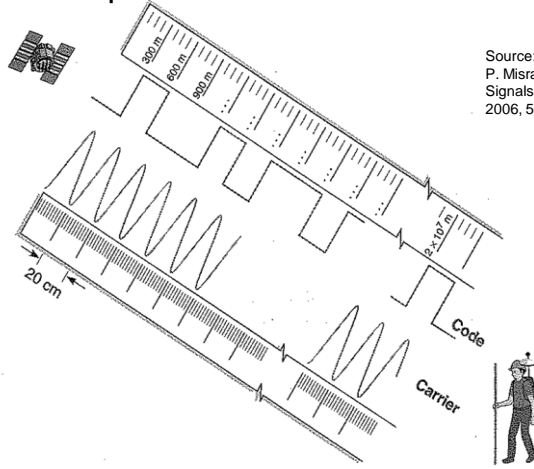
User time difference from GPS time  $dt_r$

Unknown initial number of phases N



## Measurements – code vs. carrier

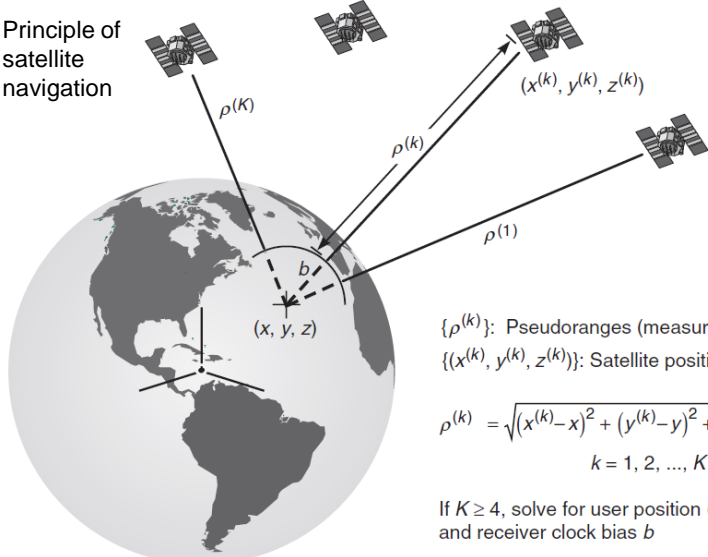
- ▶ Example on the difference between code and carrier phase measurements on GPS L1



Source:  
P. Misra, P. Enge, Global Positioning System; Signals, Measurements, and Performance, 2006, 569 s.

## GNSS navigation principle (1)

Principle of satellite navigation



$\{\rho^{(k)}\}$ : Pseudoranges (measurements)

$\{(x^{(k)}, y^{(k)}, z^{(k)})\}$ : Satellite positions (known)

$$\rho^{(k)} = \sqrt{(x^{(k)} - x)^2 + (y^{(k)} - y)^2 + (z^{(k)} - z)^2} - b$$

$$k = 1, 2, \dots, K$$

If  $K \geq 4$ , solve for user position  $(x, y, z)$ , and receiver clock bias  $b$



7

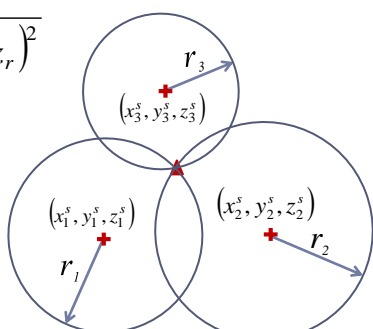
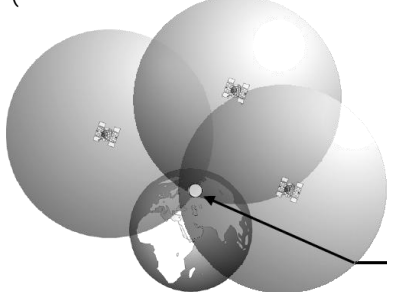
heidi.kuusniemi@fgi.fi



## GNSS navigation principle (2)

$$\begin{cases} r_1 = \sqrt{(x_1^s - x_r)^2 + (y_1^s - y_r)^2 + (z_1^s - z_r)^2} \\ r_2 = \sqrt{(x_2^s - x_r)^2 + (y_2^s - y_r)^2 + (z_2^s - z_r)^2} \\ r_3 = \sqrt{(x_3^s - x_r)^2 + (y_3^s - y_r)^2 + (z_3^s - z_r)^2} \end{cases}$$

Finding  $(x_r, y_r, z_r)$  so that these three equations stand, when  $r$  and  $(x^s, y^s, z^s)$  are known



▲ User position  $(x_r, y_r, z_r)$



8

heidi.kuusniemi@fgi.fi



## Overview of estimating PVT (1)

- ▶ The pseudorange measurement is the starting point

$$\rho^k(t) = r^k(t, t - \tau) + c[\delta t_u(t) - \delta t^k(t - \tau)] + I^k(t) + T^k(t) + \varepsilon^k(t)$$

$k$  is the individual identifier for the transmitting satellite.

$\rho^k(t)$  is the pseudorange measurement for satellite  $k$  (meters).

$t$  is the signal reception time (seconds).

$r^k(t, t - \tau)$  is the true or geometric range between the receiver at the time of reception,  $t$ , and the transmitting satellite  $k$  at time the time of transmission,  $t - \tau$  (meters).

$\tau$  is the time of flight (sometimes called delay) for the signal during its travel between the satellite and receiver (seconds).

$c$  is the speed of light in a vacuum (meters/second).

$\delta t_u(t)$  is the receiver clock offset relative to GPS time at the signal reception time (meters).

$\delta t^k(t - \tau)$  is the  $k$ th satellite's clock offset relative to GPS time at the time of transmission (meters).

$I^k(t)$  is the propagation delay caused by the Earth's ionosphere for satellite  $k$  (meters).

$T^k(t)$  is the propagation delay caused by the Earth's troposphere for satellite  $k$  (meters).

$\varepsilon^k(t)$  is the miscellaneous unmodeled range error for satellite  $k$ .

*uncertainty in the satellite position and clock offset as well as receiver noise and multipath*



9

heidi.kuusniemi@fgi.fi



## Overview of estimating PVT (2)

- ▶ Grouping all errors into a single term results in a best corrected pseudorange measurement from individual satellites

$$\rho_c^k = r^k + c\delta t_u + \tilde{\varepsilon}_T^k$$

with unknowns receiver clock offset  $\delta t_u$  and true range  $r^k$

- ▶ The magnitude and statistical nature of  $\tilde{\varepsilon}_T^k$  affects the quality of the PVT solution

- ▶ The smaller and more uncorrelated it is, the better the quality of the solution. Thus, it is normal to preprocess the GPS pseudorange measurements to reduce the magnitude of  $\tilde{\varepsilon}_T^k$  and make it as uncorrelated as possible

- ▶ GNSS satellites broadcast a message that allows the user to estimate  $\delta t^k$ ,  $I^k$  and  $T^k$  and, subsequently, remove them from  $\tilde{\varepsilon}_T^k$
- ▶ only remaining are the residuals from these corrections and other unmodelled errors



10

heidi.kuusniemi@fgi.fi



## Overview of estimating PVT (3)

- Using Cartesian coordinates for the user-receiver location at the signal reception,  $\mathbf{x}_u = [x, y, z]$ , and satellite positions at the time of transmission,  $\mathbf{x}^k = [x^k, y^k, z^k]$  the true/geometric range can be expressed as

$$r^k = \sqrt{(x^k - x) + (y^k - y) + (z^k - z)} = \|\mathbf{x}^k - \mathbf{x}_u\|$$

- both the position of the user receiver and the positions of the satellites are expressed in the same coordinate frame
  - WGS84 Earth-centered Earth-fixed coordinate frame most common in GPS applications
    - WGS84 standard also defines a surface geoid that is commonly used as a local Earth surface reference
  - Also a local coordinate frame utilized, East-North-Up

## Overview of estimating PVT (4)

- Simplifying the total receiver clock error term to  $b = c\delta t_u$  we obtain the pseudorange equation as

$$\rho_c^k = \|\mathbf{x}^k - \mathbf{x}_u\| + b + \tilde{\varepsilon}_T^k$$

- which relates the corrected pseudorange measurements for the  $k^{\text{th}}$  satellite in view to the WGS84 position coordinates for the user-receiver vector, the user receiver clock offset, and the pseudorange error term
  - the error term can be minimized to some extent using various techniques but never completely eliminated

## Linear Position Estimation (1)

- ▶ The standard approach for estimating the receiver position and clock offset is first to linearize the pseudorange measurements around a rough guess of the receiver position and clock bias and then to iterate until the difference between the guess and the measurements approaches zero
- ▶ A minimum of four measurements are needed to estimate the user receiver position and clock offset
- ▶ The rough guess of the receiver position can be very coarse, e.g. the centre of the Earth is adequate
- ▶ The initial rough guess for the receiver position and clock bias are expressed as  $\mathbf{x}_0 = [x_0, y_0, z_0]$  and  $b_0$

## Linear Position Estimation (2)

- ▶ Estimated pseudorange measurement for the  $k^{\text{th}}$  satellite can be expressed as

$$\rho_0^k = \|\mathbf{x}^k - \mathbf{x}_0\| + b_0$$

- ▶ The estimated pseudoranges based on the initial guess and the measured but corrected pseudoranges are related using a set of linear equations
  - ▶ First, expressing the true receiver position  $\mathbf{x}_u = [x, y, z]$  as  $\mathbf{x}_u = \mathbf{x}_0 + \delta\mathbf{x}$  and the true receiver clock offset as  $b = b_0 + \delta b$

## Linear Position Estimation (3)

- The difference between the estimated and the measured pseudoranges:

$$\delta\rho^k = \rho_c^k - \rho_0^k$$

$$\delta\rho^k = \|\mathbf{x}^k - \mathbf{x}_u\| + b + \tilde{\varepsilon}_T^k - (\|\mathbf{x}^k - \mathbf{x}_0\| + b_0)$$

Expansion with Taylor series:

$$\rho_c^k = f(x_u, y_u, z_u, b) = f(x_0 + \delta x, y_0 + \delta y, z_0 + \delta z, b_0 + \delta b) =$$

$$f(x_0, y_0, z_0, b_0) + \frac{\partial f(x_0, y_0, z_0, b_0)}{\partial x_0} \delta x + \frac{\partial f(x_0, y_0, z_0, b_0)}{\partial y_0} \delta y +$$

$$\frac{\partial f(x_0, y_0, z_0, b_0)}{\partial z_0} \delta z + \frac{\partial f(x_0, y_0, z_0, b_0)}{\partial b_0} \delta b + \frac{1}{2!} \frac{\partial^2 f}{\partial x^2} + \dots$$

► 15 truncated after the 1<sup>st</sup> order partial derivates

## Linear Position Estimation (4)

- With a Taylor series expansion about the approximate position and estimated receiver clock offset  $[x_0, y_0, z_0]$  and  $b_0$ , we get

$$\delta\rho^k = \rho_c^k - \rho_0^k$$

$$= \frac{\partial f(x_0, y_0, z_0, b_0)}{\partial x_0} \delta x + \frac{\partial f(x_0, y_0, z_0, b_0)}{\partial y_0} \delta y +$$

Line-of-sight unit vector  
between the estimated  
receiver location and  
satellite  $k$

$$\frac{\partial f(x_0, y_0, z_0, b_0)}{\partial z_0} \delta z + \frac{\partial f(x_0, y_0, z_0, b_0)}{\partial b_0} \delta b$$

$$L_{unit}^k$$

$$= -\frac{\mathbf{x}^k - \mathbf{x}_0}{\|\mathbf{x}^k - \mathbf{x}_0\|} \cdot \delta \mathbf{x} + \delta b + \tilde{\varepsilon}_T^k$$

► 16

## Linear Position Estimation (5)

- When measurements from more than one satellite are available ( $n$ ), the equation can be written compactly as

$$\delta\mathbf{p} = \begin{bmatrix} \delta\rho^1 \\ \delta\rho^2 \\ \dots \\ \delta\rho^n \end{bmatrix} = \underbrace{\begin{bmatrix} (-L_{unit}^1)^T 1 \\ (-L_{unit}^2)^T 1 \\ \dots \\ (-L_{unit}^n)^T 1 \end{bmatrix}}_{\text{Geometry matrix } \mathbf{G}} \begin{bmatrix} \delta\mathbf{x} \\ \delta b \end{bmatrix} + \begin{bmatrix} \tilde{\varepsilon}_T^1 \\ \tilde{\varepsilon}_T^2 \\ \dots \\ \tilde{\varepsilon}_T^n \end{bmatrix}$$

—————→  $\delta\mathbf{p} = \mathbf{G} \begin{bmatrix} \delta\mathbf{x} \\ \delta b \end{bmatrix} + \tilde{\boldsymbol{\varepsilon}}_T$

17

heidi.kuusniemi@fgi.fi



## Linear Position Estimation (6)

- The line-of sight vectors within the geometry matrix determine collectively the overall quality of the position estimation geometry
  - the matrix is used to calculate the dilution of precision (DOP) values, which give a good indication of the estimated position accuracy
- The estimation problem concerns the approximation correction values  $\delta\mathbf{x}$  and  $\delta b$ 
  - the convergence of the iterative solution depends on the geometry of the receiver-satellites system, which, in turn, affects the rank of matrix  $\mathbf{G}$ 
    - problems when all the satellites lie in or are very close to the same plane in a three-dimensional space
  - also Earth rotation needs to be taken into account
    - reference frame rotation during the signal propagation, i.e. the satellite position vector needs to be rotated by using an approximate transmission delay  $\tau$  and the rotation rate of the Earth  $\omega_E$  such that
$$\mathbf{x}^k = \begin{bmatrix} \cos(\omega_E \tau) & \sin(\omega_E \tau) & 0 \\ -\sin(\omega_E \tau) & \cos(\omega_E \tau) & 0 \\ 0 & 0 & 1 \end{bmatrix} \times \tilde{\mathbf{x}}^k$$
  - original estimate for satellite position vector is  $\tilde{\mathbf{x}}^k$

18

heidi.kuusniemi@fgi.fi



## Linear Position Estimation (7)

- ▶ The errors in the error vector  $\tilde{\varepsilon}_T$  are assumed to be zero-mean and uncorrelated
- ▶ Thus, the estimate in the least squares sense for  $\delta\mathbf{x}$  and  $\delta b$  is given by

$$\hat{\mathbf{x}} = \begin{bmatrix} \delta\mathbf{x} \\ \delta b \end{bmatrix} = (\mathbf{G}^T \mathbf{G})^{-1} \mathbf{G}^T \delta\mathbf{p}$$

- ▶ Least squares optimization when solution over-determined ( $n > 4$ )

- ▶ Least squares originally formulated by Gauss

- ▶ Iterative process updates the approximate initial guess each round  $\mathbf{x}_u = \mathbf{x}_0 + \delta\mathbf{x} = \mathbf{x}_{0,new}$

$$b = b_0 + \delta b = b_{0,new}$$

↑ Typically set to zero

## Linear Position Estimation (8)

- ▶ When the pseudorange measurements from different satellites are not of the same quality, the estimation procedure can be weighted
- ▶ If the user equivalent range errors for the visible satellites are given in an observation covariance matrix  $\mathbf{R}$

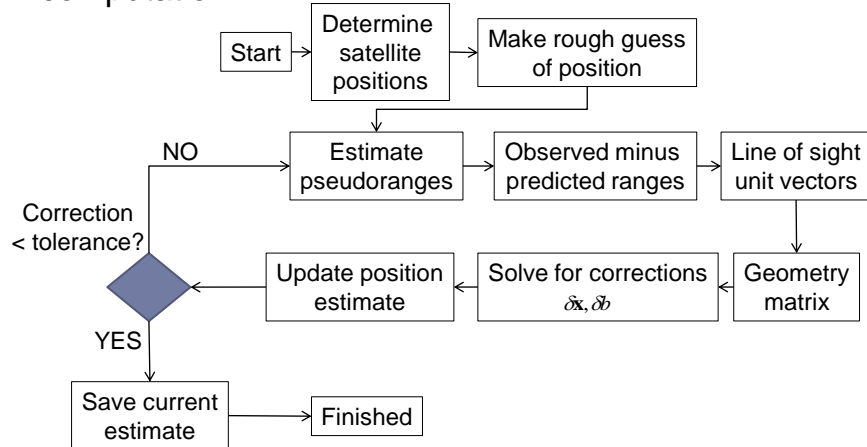
$$\mathbf{R} = \mathbf{C}_{\delta\mathbf{p}\delta\mathbf{p}} = \begin{bmatrix} \sigma_1^2 & 0 & 0 \\ 0 & \ddots & 0 \\ 0 & 0 & \sigma_n^2 \end{bmatrix}$$

the weighted least squares solution is

$$\hat{\mathbf{x}} = \begin{bmatrix} \delta\mathbf{x} \\ \delta b \end{bmatrix} = (\mathbf{G}^T \mathbf{R}^{-1} \mathbf{G})^{-1} \mathbf{G}^T \mathbf{R}^{-1} \delta\mathbf{p}$$

## Linear Position Estimation (9)

- Calculation steps in an iterative position computation:



## Linear Position Estimation (10)

- Covariance matrix of estimated parameters  $\hat{\mathbf{x}}$  and  $\hat{\mathbf{b}}$ :
- To compute the parameter estimate covariance, the covariance matrix of the measurements,  $\mathbf{R}$ , is needed
- Propagation of covariance can be applied to the weighted least squares problem:

$$\begin{aligned}
 \hat{\mathbf{x}} &= \begin{bmatrix} \hat{\mathbf{x}} \\ b \end{bmatrix} = (\mathbf{G}^T \mathbf{R}^{-1} \mathbf{G})^{-1} \mathbf{G}^T \mathbf{R}^{-1} \hat{\mathbf{p}} \\
 < \hat{\mathbf{x}} \hat{\mathbf{x}}^T > &= (\mathbf{G}^T \mathbf{R}^{-1} \mathbf{G})^{-1} \mathbf{G}^T \mathbf{R}^{-1} < \hat{\mathbf{p}} \hat{\mathbf{p}}^T > \mathbf{R}^{-1} \mathbf{G} (\mathbf{G}^T \mathbf{R}^{-1} \mathbf{G})^{-1} \\
 &= \mathbf{V}_{\hat{\mathbf{x}} \hat{\mathbf{x}}} = \mathbf{C}_{\begin{bmatrix} \hat{\mathbf{x}} \\ b \end{bmatrix} \begin{bmatrix} \hat{\mathbf{x}} \\ b \end{bmatrix}} = (\mathbf{G}^T \mathbf{R}^{-1} \mathbf{G})^{-1}
 \end{aligned}$$

## Linear Position Estimation (11)

- ▶ Covariance matrix of post-fit residuals
  - ▶ Post-fit residuals are the differences between the observations and the values computed from the estimated parameters,  $\mathbf{v}$
  - ▶ Because some of the noise in the measurements are absorbed into the parameter estimates, in general, the post-fit residuals are not the same as the errors in the data
    - ▶ In some cases, they can be considerably smaller
- ▶ The covariance matrix of the post-fit residuals can be computed using propagation of covariances:

$$\delta\mathbf{p} = \mathbf{G} \begin{bmatrix} \delta\mathbf{x} \\ b \end{bmatrix} + \tilde{\boldsymbol{\varepsilon}}_T$$

$$\begin{bmatrix} \delta\mathbf{x} \\ b \end{bmatrix} = (\mathbf{G}^T \mathbf{R}^{-1} \mathbf{G})^{-1} \mathbf{G}^T \mathbf{R}^{-1} \delta\mathbf{p}$$

$$\mathbf{v} = \delta\mathbf{p} - \mathbf{G} \begin{bmatrix} \delta\mathbf{x} \\ b \end{bmatrix} = \left[ \mathbf{I} - \underbrace{\mathbf{G}(\mathbf{G}^T \mathbf{R}^{-1} \mathbf{G})^{-1} \mathbf{G}^T \mathbf{R}^{-1}}_{\text{Amount error reduced}} \right] \tilde{\boldsymbol{\varepsilon}}_T$$

$$\mathbf{C}_{vv} = \langle \mathbf{v} \mathbf{v}^T \rangle = \mathbf{R} - \mathbf{G}(\mathbf{G}^T \mathbf{R}^{-1} \mathbf{G})^{-1} \mathbf{G}^T$$

- ▶ Post-fit residuals  $\mathbf{v}$  are suitable for checking the solution quality: receiver autonomous integrity monitoring

## Velocity Estimation (1)

- ▶ Velocity estimates can be generated using the same least squares approach
- ▶ The starting point for the velocity estimation is

$$\dot{\rho}_c^k = \dot{r}^k + \dot{b} + \dot{\varepsilon}_T^k$$

- ▶ When following the similar derivations as with the position estimation, we obtain

$$\dot{\rho}_c^k = (\mathbf{v}^k - \mathbf{v}_u) \cdot \mathbf{L}_{unit}^k + \dot{b} + \dot{\varepsilon}_T^k$$

Pseudorange rate from satellite  $k$ , m/s

Velocity vector for satellite  $k$ , m/s

Velocity vector for receiver, m/s

Receiver-to-satellite  
line-of-sight unit vector

Receiver clock drift, m/s

Pseudorange rate error, m/s

## Velocity Estimation (2)

- The equation for the receiver velocity and clock drift can be derived as

$$1. \dot{\rho}^k - (\mathbf{v}^k \cdot \mathbf{L}_{unit}^k) = -(L_{unit}^k \cdot \mathbf{v}_u) + \dot{b} + \dot{\epsilon}_T^k$$

$$2. \dot{\rho}^k + G_k \begin{bmatrix} \mathbf{v}^k \\ 0 \end{bmatrix} = G_k \begin{bmatrix} \mathbf{v}_u \\ \dot{b} \end{bmatrix} + \dot{\epsilon}_T^k$$

where  $G_k$  is the  $k$ th row of the  $\mathbf{G}$  matrix

$$\begin{bmatrix} \mathbf{v}_u \\ \dot{b} \end{bmatrix} = (\mathbf{G}^T \mathbf{G})^{-1} \mathbf{G}^T \mathbf{T}$$

where the  $k$ th row of  $\mathbf{T}$  is

$$T^k = \dot{\rho}^k + G_k \begin{bmatrix} \mathbf{v}^k \\ 0 \end{bmatrix}$$



25

heidi.kuusniemi@fgi.fi



## Velocity Estimation (3)

- Steps in deriving the receiver velocity

1. Calculate the  $\mathbf{G}$  matrix in the exact same manner as was done for the position solution

2. Build the satellite velocity matrix

3. Convert the raw receiver Doppler frequency measurements into pseudorange rates  $\dot{\rho}_c^k = \frac{cD}{f}$

Measured  
Doppler  
frequency

4. Calculate the  $T^k$  vector from individual satellite pseudorange rate, satellite velocity, and geometry

5. Estimate the receiver velocity and clock drift

- The precise GPS time of the receiver is solved as

$t = t_{ref} + b$  where  $t$  is the signal reception time,  $t_{ref}$  the GPS reference time decoded from the navigation data and  $b$  the receiver clock bias

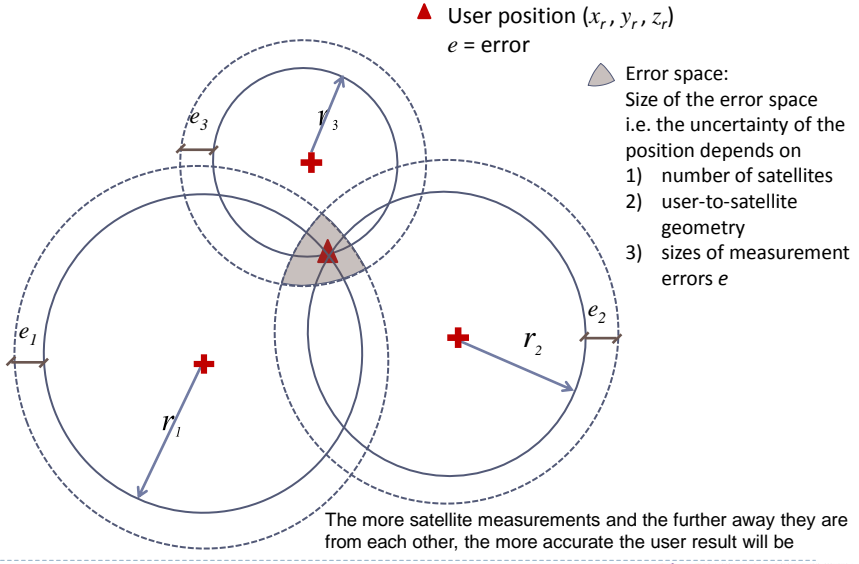


26

heidi.kuusniemi@fgi.fi



# Uncertainty in GNSS navigation



27

heidi.kuusniemi@fgi.fi



## Error sources (1)

- ▶ Significant errors present in pseudorange measurements

$$\rho^k(t) = r^k(t, t - \tau) + c[\delta t_u(t) - \delta t^k(t - \tau)] + I^k(t) + T^k(t) + \varepsilon^k(t)$$

include

- ▶ Orbital errors
  - Though the satellite orbits are modeled very precisely by the GPS control segment there are always still small errors remaining
- ▶ Satellite clock errors
  - The satellite clock corrections included in the GPS navigation message are still not perfect and a small error is resulting in the pseudorange measurement
  - Differential techniques improve the satellite clock error estimate
- ▶ Ionosphere errors
  - The ionosphere consists of the area between approximately 50 and 100 km above the Earth. A delay added to the code phase signal while it is traversing this region can vary considerably depending on the time of day and season
  - These delays can range up to and over 10 m in extreme conditions
  - The model developed by Klobuchar is a good first approximation for these delays (coefficients in the navigation message)
- ▶ Troposphere errors
  - The troposphere is everything under the ionosphere. In reality it is almost exclusively concentrated below 20 km and consists of dry gases and water vapor
  - The errors added to GNSS signals as they pass through the troposphere are less than those of the ionosphere but can still significantly impact the accuracy of the position estimation
  - The tropospheric error is a function of atmospheric temperature and pressure in the vicinity of the receiver. To some extent, it can also be mitigated with models (e.g. Saastamoinen)
- ▶ Receiver noise and multipath errors
  - Noise added as part of the down-conversion and tracking of the signals during measurements is inevitable. However, with modern receivers receiver noise can usually be kept to manageable levels
  - Multipath is the reflection of GNSS signals by an external reflector located near the receiver antenna. This reflected signal gets mixed with the direct signal. It enters the receiver processing chain and distorts the correlation tracking peak, thereby adding an error to the pseudorange measurement. These errors can be quite large in severe multipath environments (in dense urban areas for example), and there is no sure way to eliminate them

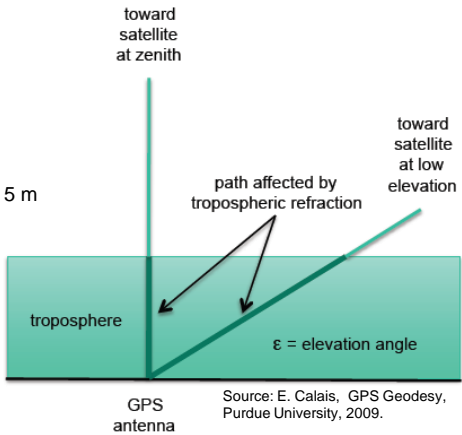
28

heidi.kuusniemi@fgi.fi



## Error sources (2)

- ▶ Measurements on all GNSS frequencies are affected by **atmospheric refraction**
  - ▶ Ray bending (negligible) & propagation velocity decrease (w.r.t. vacuum) ⇒ propagation delay
    - ▶ In the **ionosphere**: the delay is a function of the electron density, 0 to 50 m
    - ▶ In the **troposphere**:
      - Delay is a function of (P, T, H), 1 to 5 m
      - Largest effect due to pressure
  - ▶ Tropospheric delays increase with decreasing satellite elevation angle



Source: E. Calais, GPS Geodesy, Purdue University, 2009.

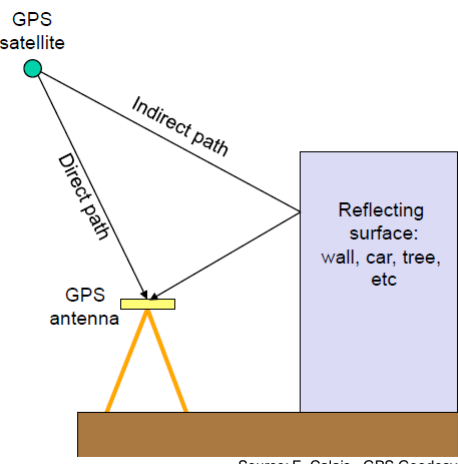
▶ 29

heidi.kuusniemi@fgi.fi



## Error sources (3)

- ▶ Multipath propagation:
  - ▶ A GPS signal may be reflected by surfaces near the receiver => direct and reflected signals
  - ▶ Echo-only signal reception pose a significant threat to position accuracy



Source: E. Calais, GPS Geodesy, Purdue University, 2009.

▶ 30

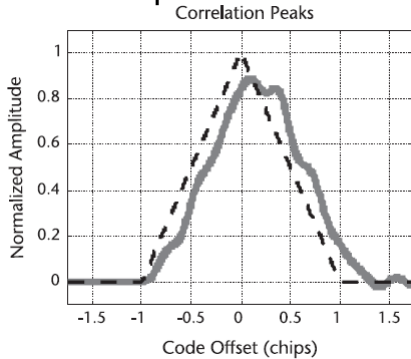
heidi.kuusniemi@fgi.fi



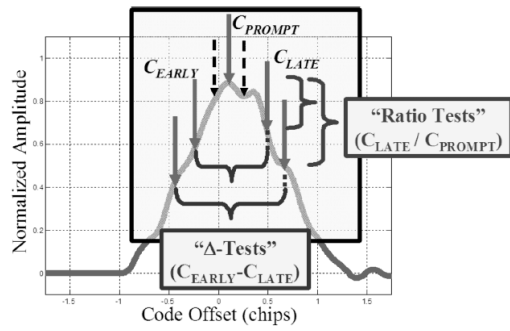
## Error sources (4)

### Multipath error mitigation

- ▶ Correlation peak deformation due to multipath:



- ▶ Multiple-correlator signal monitoring to fight against multipath



## Error sources (5)

- ▶ Ionosphere errors can be large, especially during times of high solar activity (now we are approaching a peak in 2013)
- ▶ By combining measurements made at different frequencies, the pseudorange errors due to the ionosphere on frequency L1 is

$$I_{f_1}^k = \frac{f_2^2}{(f_1^2 - f_2^2)} (\rho_{f_2}^k - \rho_{f_1}^k)$$

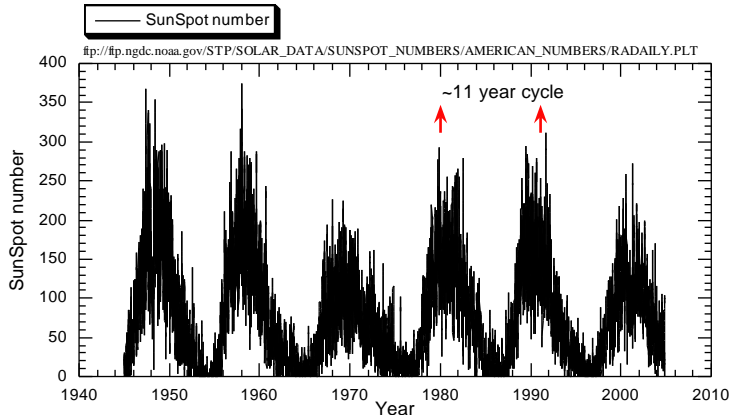
Pseudorange measurements at L1 and L2 for satellite k

Carrier frequencies at L1 and L2

- ▶ However, in single-frequency receivers, ionosphere is the major source of observation error

## Error sources (6)

### Sun Spot numbers



Source: T. Herring, Principles of the Global Positioning System, MIT, 2010.

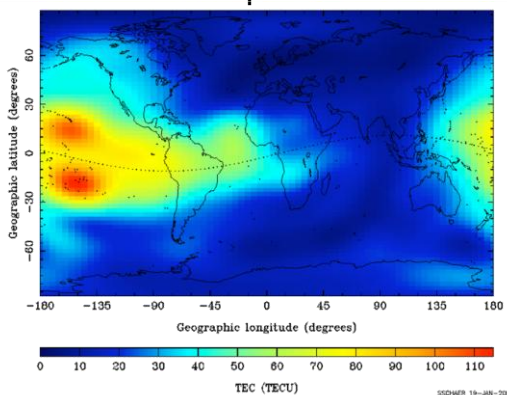
▶ 33

heidi.kuusniemi@fgi.fi



## Error sources (7)

### ► Global ionosphere variation



Global ionosphere info,  
13.1.2000, 23:00 UT

Source: E. Calais, GPS Geodesy,  
Purdue University, 2009.

Signal frequency

Elevation angle at  
ionospheric pierce point

### ► The relationship between the signal delay $\varepsilon_{iono}$ due to ionosphere and the total electron content (TEC) is

$$\varepsilon_{iono} = \frac{1}{\sin(\phi')} \frac{40.3}{f^2} TEC$$

▶ 34

heidi.kuusniemi@fgi.fi



## Error sources (8)

- ▶ Approximate errors for standalone GPS, total error budget

Error Source	<i>1σ Range Error for Stand-alone Users</i>
SV clock error	1–2m
SV ephemeris error	1–3m (corrected by single-frequency model)
Ionospheric delay error	1–7m
Tropospheric delay error	2–3m (uncorrected) 0.1–0.5m (corrected by atmospheric model)
Multipath (reference and user)	PR: 0.5–1.5m $\phi$ : 0.005–0.015m
Receiver noise (reference and user)	PR: 0.2–0.35m $\phi$ : 0.001–0.003m
<i>Totally: 6–20 m</i>	

Much larger in  
heavy-multipath  
environments



## Error sources (9)

- ▶ The satellite-to-user geometry can have a large impact on the accuracy of the position, velocity and time estimate
  - ▶ A metric normally used for measuring this impact is DOP, which represents the degree to which satellite-user geometry dilutes the accuracy of the solution
- ▶ Information about the DOP is encoded in the geometry matrix  $G$
- ▶ DOP-matrix  $H$  is denoted as

$$H = (G^T G)^{-1} = \begin{bmatrix} H_{11} & - & - & - \\ - & H_{22} & - & - \\ - & - & H_{33} & - \\ - & - & - & H_{44} \end{bmatrix}$$

The DOPs are the link between the pseudorange errors and the position, velocity and time (PVT) estimation errors



## Error sources (10)

- ▶ If operating in a local coordinate frame, the square root of the diagonal entries of the **H** matrix are called the east DOP (**EDOP**), north DOP (**NDOP**), vertical DOP (**VDOP**), and time DOP (**TDOP**).
  - ▶ These DOPs are sometimes combined to form new DOPs such as the total geometry DOP (**GDOP**), the three-dimensional position DOP (**PDOP**), and the two-dimensional horizontal positioning DOP (**HDOP**)

$$EDOP = \sqrt{H_{11}}$$

$$NDOP = \sqrt{H_{22}}$$

$$VDOP = \sqrt{H_{33}}$$

$$TDOP = \sqrt{H_{44}}$$

$$GDOP = \sqrt{H_{11} + H_{22} + H_{33} + H_{44}}$$

$$PDOP = \sqrt{H_{11} + H_{22} + H_{33}}$$

$$HDOP = \sqrt{H_{11} + H_{22}}$$

- ▶ In many land applications, when the receiver can be assumed to be on the ground and its height constrained, the HDOP will improve

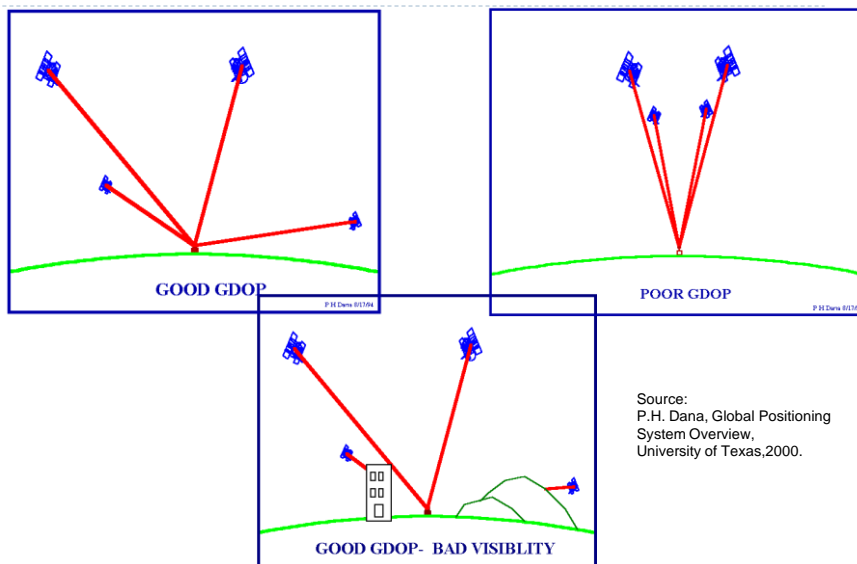


37

heidi.kuusniemi@fgi.fi



## Error sources (11)



38

heidi.kuusniemi@fgi.fi



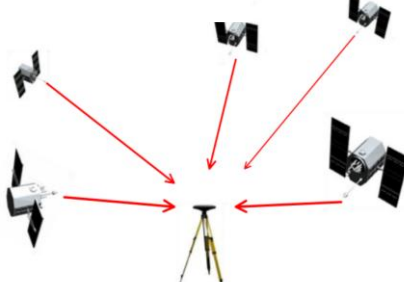
## Error sources (12)

- ▶ PDOP (position dilution of precision) reveals the user-satellite geometry
  - ▶ Typically:
    - ▶ < 3 = optimal
    - ▶ > 7 = poor geometry

Poor geometry



Good geometry



## Overview of Carrier Phase Positioning

- ▶ Precise positioning using carrier phase measurements provides positioning accuracy on the order of millimeters to decimeters, which is a great improvement over the code phase solution
  - ▶ The GPS carrier phase can be measured with accuracy on the order of millimeters to centimeters as opposed to the decimeters to meters accuracy of a code phase measurement
- ▶ The difficulty in performing a carrier phase based pseudorange measurement primarily lies in the challenge of a quick and robust determination of the carrier cycle ambiguity  $N$  for each satellite tracked
  - ▶ This ambiguity is conceptually equal to the exact number of carriers contained in the space between the receiver and the satellite at the initial signal lock
- ▶ Carrier phase positioning is performed in a differential mode (relative positioning with respect to a base station)
- ▶ The process of estimating and validating the correct estimate of the integers is a time consuming process
  - ▶ E.g. a typical method: the LAMBDA
- ▶ If the receiver makes a sudden move and the carrier phase lock is lost, even for an instant, the count is broken and the ambiguity must be recalculated

## Extended Kalman Filter (1)

- ▶ The estimate of the PVT can also be obtained by using an extended Kalman filter (EKF)
  - ▶ Is an implementation of a Bayes estimator
  - ▶ Basically, a weighted, recursive least squares estimator
  - ▶ The outputs from an EKF will often be better than those from the least squares method
- ▶ EKF assumes some knowledge of the receiver dynamics
  - ▶ When these assumptions are incorrect, problems can arise quickly
- ▶ Basic concept behind the EKF filter is that some of the parameters being estimated are random processes and as data are added to the filter, the parameter estimates depend on new data and the changes in the process noise between measurements

## Extended Kalman Filter (2)

- ▶ Formulation:
  - ▶ Measurements  $\mathbf{y}_t$  with noise  $\mathbf{v}_t$ , and a state vector  $\mathbf{x}_t$  with specified statistical properties (process noise  $\mathbf{w}_t$ )
$$\mathbf{y}_t = \mathbf{A}_t \mathbf{x}_t + \mathbf{v}_t \quad \text{Observation equation at time } t$$
$$\mathbf{x}_t = \mathbf{S}_t \mathbf{x}_{t-1} + \mathbf{w}_t \quad \text{State transition equation}$$
$$\langle \mathbf{v}_t \mathbf{v}_t^T \rangle = \mathbf{R}_t \quad \langle \mathbf{w}_t \mathbf{w}_t^T \rangle = \mathbf{Q}_t \quad \text{Covariance matrices}$$
  - ▶ Typically, the two phases alternate in a Kalman filter, with the *prediction* advancing the state until the next scheduled observation, and the *update* incorporating the observation
  - ▶ In the extended Kalman filter (EKF), the state transition and observation models need not be linear functions of the state

## Positioning performance measures

- ▶ **Accuracy:** measure of the level of positioning error
- ▶ **Integrity:** the measure of the likelihood of occurrence of an undetected navigation error that can be hazardous
- ▶ **Continuity:** the level of which the navigation function will continue without interruptions after an operation has been initiated
- ▶ **Availability:** fraction of time a navigation system is providing position fixes to the specified level of accuracy, integrity, and continuity
- ▶ **Reliability:** the combined level of accuracy, availability and integrity
- ▶ **Time-to-first-fix:** the time it takes for a navigation system to generate the first positioning solution (TTFF)

## Summary of GPS navigation (1)

- ▶ An estimate of the receiver position and velocity can be attempted if the following conditions are met:
  - ▶ 1. A minimum of four satellites are being tracked
  - ▶ 2. The transmission time for each satellite at the measurement data sample is known
  - ▶ 3. Ephemeris information for the tracked satellites is available
- ▶ Pseudorange =  $(\text{signal receive time} - \text{signal transmit time}) \times \text{speed of light}$ 
  - ▶ The signal receive time is taken from the internally maintained receiver clock
  - ▶ The signal transmit time is known with respect to the TOW reference time captured at the first subframe bit of the navigation data
    - ▶ time at last bit = TOW reference + number of bits since TOW reference
    - ▶ transmit time = time at last bit + ms since last bit + prompt code/1023

## Summary of GPS navigation (2)

- If differential corrections data is available it can be applied directly after the raw pseudorange measurement is made for individual satellites
- Satellite information including its position and velocity as a function of time and the estimated bias and drift rate of its clock are available in the navigation message
  - The orbit data is sent as a set of orbital elements, and the clock information as a simple polynomial correction model
  - As a channel receives its ephemeris data frames the values are decoded and stored
    - When it comes time to estimate the receiver position, these parameters are passed to the routine which processes the ephemeris to propagate the elements forward or backward returning the necessary information on the satellites themselves to be used during the PVT solution
- Satellite ephemeris data (and often timing information) can also be gathered by an external means
  - E.g. sp3 files from IGS

## Summary of GPS navigation (3)

- Estimation:
  - After all the necessary measurements and satellite information have been gathered together, it is possible to estimate the receiver position, velocity, and clock errors







# Carrier Phase Positioning

Gérard Lachapelle

Canada Research Chair in Wireless Location  
PLAN Group, University of Calgary

<http://PLAN.geomatics.ucalgary.ca>

JRC-ISPRA, Italy  
2-4 July 2012



## Contents

- Why high accuracy?
- Code and carrier phase measurements
- Errors and differential concept
- Carrier phase ambiguity resolution
- Example

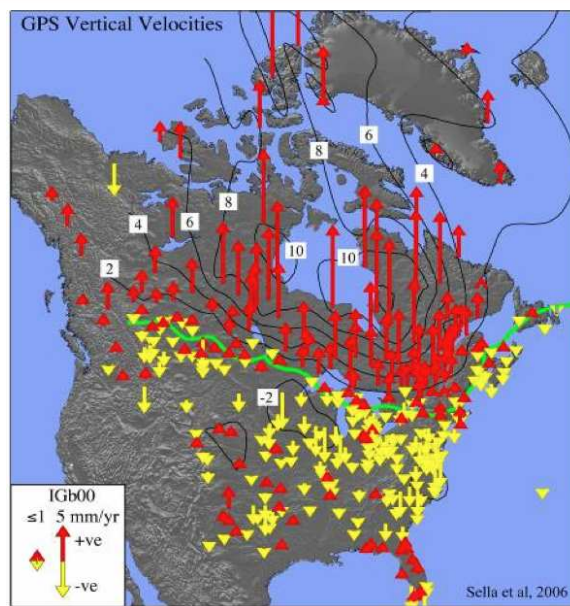
## Is High Accuracy Important?



3 G. Lachapelle Carrier Phase Positioning, JRC-ISPRA Summer School on GNSS Core Technologies, 2-4Jul12

PLN

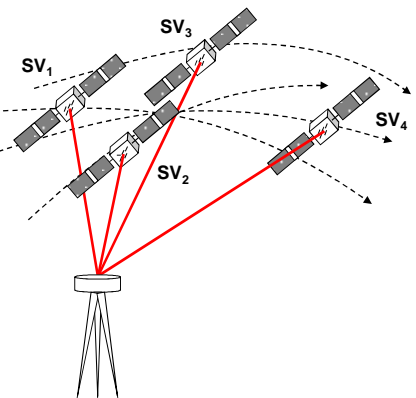
## GPS-Derived Crustal Motion



4 G. Lachapelle Carrier Phase Positioning, JRC-ISPRA Summer School on GNSS Core Technologies, 2-4Jul12

PLN

## Trilateration in Space



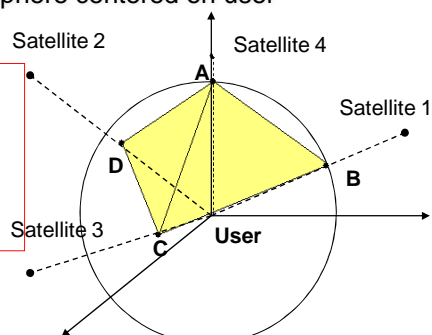
- Unknowns:
  - Latitude ( $\Phi$ )
  - Longitude ( $\lambda$ )
  - Height (h)
  - Receiver clock bias ( $dT$ )
- Observations:
  - At least four observations are required for a 3-D ( $\Phi, \lambda, h$ ) fix
- Two primary differences from terrestrial trilateration:
  - Targets (satellites) are moving (~4 km/s)
  - As a result, the geometry is changing as a function of time

## Dilution of Precision (DOP) – Measure of Geometry

- Geometry is measured through the Dilution of Precision (DOP)
- DOP is related to the volume formed by the intersection points of the user-satellite vectors, with the unit sphere centered on user

*Note<sup>1</sup>:* Larger volumes give smaller DOP  
*Note<sup>2</sup>:* Lower DOP values give better position accuracy:  

$$\text{Position Accuracy} = \text{DOP} \times \text{Range Accuracy}$$

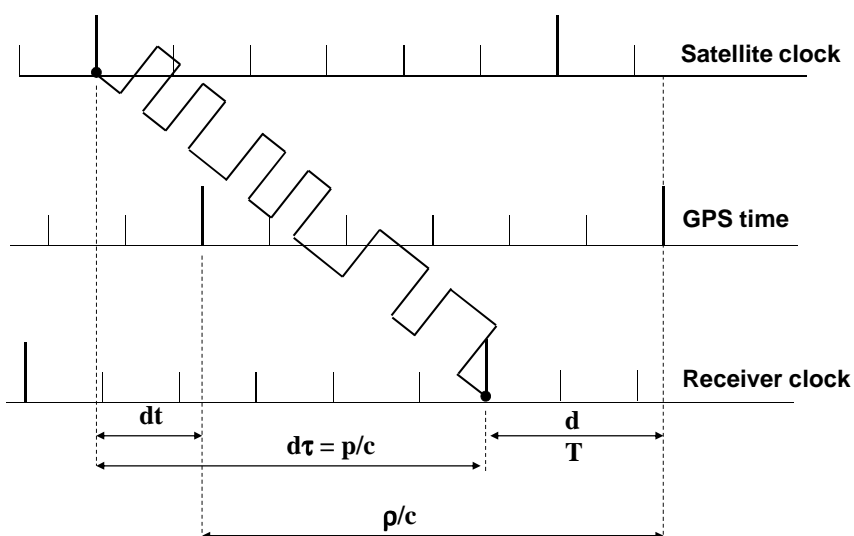


- For a four-satellite configuration, the best geometry is when there is one satellite at the zenith and the other three at elevation 0 and equally spaced in azimuth (i.e. every 120°)

## Overview of GPS Measurements

- A receiver channel typically provides the following:
  - Pseudorange measurement -  $P$  {Delay Lock Loop}
  - Doppler measurement
  - Carrier-phase measurement -  $\Phi$  {Phase Lock Loop}
  - Carrier-to-Noise density ( $C/N_0$ )
  - These measurements are *raw* measurements.
  - Most receivers generate navigation outputs (i.e. position, velocity, heading, etc.)
  - Most receivers take measurements on all channels simultaneously
  - The time at which a set of measurements is collected is called a *data epoch* – GPS time
  - Data rate - Up to 50 times per second

## Pseudorange (Code) Concept



## Pseudorange Observation Equation

- Observation equation (in units of length, e.g. m, here):

$$P = cd\tau = \rho + dp + c(dt - dT) + d_{ion} + d_{trop} + \varepsilon_P$$

where

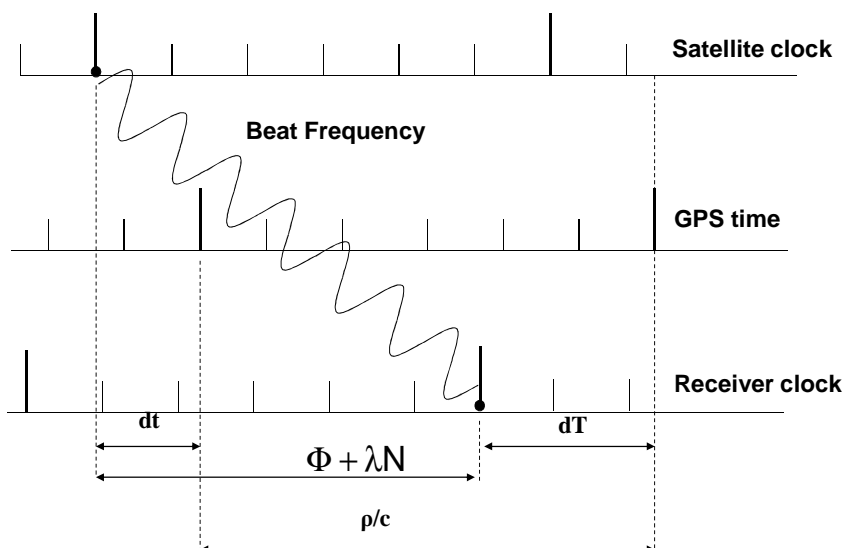
$P$  receiver measurement  
 $\rho$  geometric range (i.e.  $\| \mathbf{r}^s - \mathbf{R}_r \|$ )       $\{\rho = \sqrt{(x^s - x_R)^2 + (y^s - y_R)^2 + (z^s - z_R)^2}\}$   
 $dp$  orbital errors  
 $\mathbf{r}^s, \mathbf{R}_r$  position vector of SV (known) and rx (unknown)  
 $dt, dT$  satellite and receiver clock errors, respectively  
 $d_{ion}$  ionospheric delay  
 $d_{trop}$  tropospheric delay  
 $\varepsilon_P$  noise {function of  $\varepsilon$ (code noise) and  $\varepsilon$ (code multipath)}

$\varepsilon$  (C/A code noise)  $\approx 5 - 200$  cm for LOS measurements

$\varepsilon$  (P code noise)  $\approx 10$  cm

$\varepsilon$  (code multipath)  $\leq 1$  chip (non-Gaussian)

## Carrier Phase Concept



## Carrier Phase Observation Equation

- Observation equation (in unit of length):

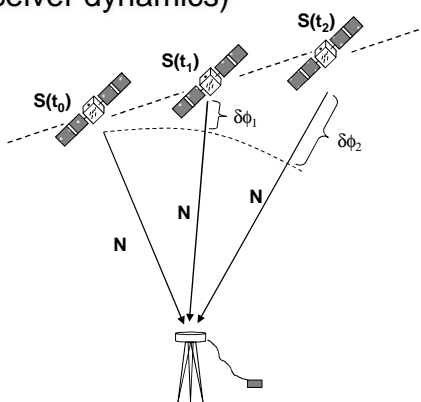
$$\Phi = \rho + dp + c(dt - dT) + \lambda N - d_{ion} + d_{trop} + \varepsilon_\Phi$$

where

- $\Phi$  receiver measurement  
 $\rho$  geometric range, namely  $\{[x_{s1} - x_g]^2 + [y_{s1} - y_g]^2 + [z_{s1} - z_g]^2\}^{1/2}$   
subscript si refers to satellite i and subscript g to antenna  
(unknown)  
 $dp$  orbital errors  
 $dt, dT$  satellite and receiver clock errors  
 $N$  cycle ambiguity (integer number)  
 $d_{ion}$  ionospheric delay  
 $d_{trop}$  tropospheric delay  
 $\varepsilon_\Phi$  noise {function of  $\varepsilon(\Phi)$  noise and  $\varepsilon(\Phi)$  multipath}}  
 $\varepsilon(\Phi \text{ noise}) \approx 1-5 \text{ mm (Lower than code measurements)}$   
 $\varepsilon(\Phi \text{ multipath}) \leq 0.25 \lambda \text{ (Lower than code measurements)}$

## Carrier Phase Ambiguities (1/2)

- At lock-on receiver measures fractional phase, integer number of cycles is unknown (integer ambiguity)
- If no loss of lock occurs, the ambiguity remains constant
- Receiver accurately measures changes in range over time (due to satellite-receiver dynamics)



## Carrier Phase Ambiguities (2/2)

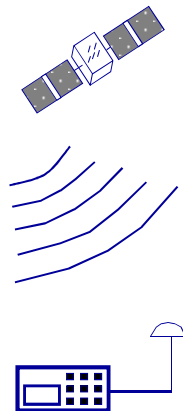
- Receiver measures the fractional phase difference between the incoming signal and the reproduced signal
  - Number of integer cycles between epochs are counted by integrating the Doppler (beat) frequency (Hz \* s)
  - Contains fractional + integer part (sometimes called accumulated phase or integrated Doppler)
- Carrier phase ambiguities are integer by definition and are defined at lock – on and are constant unless a cycle slip occurs
  - They are arbitrary (e.g. a few cycles or millions of cycles, + or -) and are different for each satellite-receiver measurement
- Example - approximate ambiguity derived from pseudorange (approximate since pseudorange is noisy – in reality it is constant)

GPS time (s)	Pseudorange (m)	Carrier phase ( $\phi$ cycles)	Ambiguity ( $\phi$ cycles - $p/\lambda$ )
387234	22441825.779	-975001.392	-118907592
387235	22441597.023	-976188.862	-118907577
387236	22441371.704	-977375.523	-118907580

## Use of Carrier Phase Observations

- **Velocity estimation**
  - Carrier phase differencing between epochs divided by time
  - Single point or between epochs, receivers and satellite differencing
  - No ambiguity resolution needed but phase lock/cycle slip free data required
- **Smoothing of code measurements**
  - Improves code based solution
  - Tolerant to cycle slips
- **Static and kinematic positioning**
  - Differential mode needed to reduce or remove clock, orbital and atmospheric errors
  - Continuous phase lock preferable
  - No or few cycle slips
  - Ambiguities to be resolved preferably as integer numbers and, if not, as real numbers

## Major Error Sources



- Satellite Errors ( $1\sigma$ ):  
Orbit & Clock: 1 - 2 m
- Propagation Errors:  
Ionosphere: 1-30 m  
Troposphere: 0.2 m
- Receiver Errors  
Code Multipath:  $\leq 1$  chip  
NLOS: Unlimited  
Code Noise: 5-200 cm  
NLOS: up to 25-30 m  
Carrier Multi.: 1-50 mm  
Carrier Noise: 0.2-2 mm

## Cycle-Slip Detection and Correction

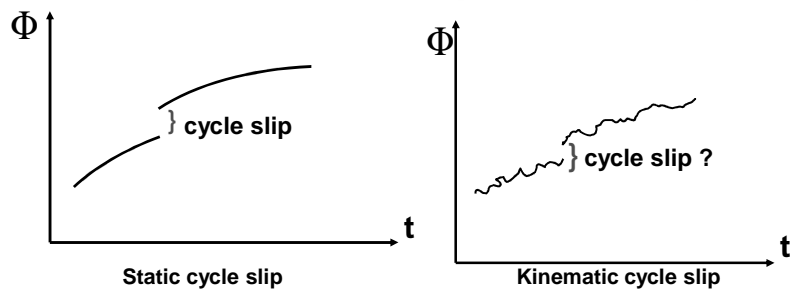
### Loss of Phase Lock

- Phase lock loops provide continuous carrier phase measurements
- However in case of signal interference, they are the first to malfunction
- Carrier phase measurement continuity is lost, resulting in a new unknown ambiguity on each satellite or satellite pair (for Double Diff)
- A discontinuity of phase measurements is called a cycle slip
- Cycle slips occur when a satellite signal is obstructed or attenuated by a certain amount and, in certain cases, when the unpredictable Doppler effect due to the antenna motion is too large
- In order to maintain the integrity of a carrier phase-based solution, cycle slips must be detected and, if possible, corrected. Otherwise the DGPS accuracy will degrade.
- Detection and correction can be done in undifferenced or differenced mode, depending on the approach

## Cycle Slip Detection

### Cycle Slip Overview

- Detection of carrier phase cycling slips is critical for cm – level positioning and for carrier smoothing
- More difficult for kinematic positioning than static additional Doppler shift is created in kinematic mode (difficult to predict)
- Options for cycle slip detection are dependent on mode (static vs kinematic) and receiver type (single vs dual frequency)



## Kinematic Cycle Slip Detection

### Kinematic Single Frequency Cycle Slip Detection (1/2)

- Phase Velocity Trend Method:
- $\Phi_k$  at  $t_k$  is predicted using  $\Phi_{k-1}$  and the phase rates at  $k$  and  $k-1$ :

$$\hat{\phi}_k = \phi_{k-1} + \frac{\dot{\phi}_k + \dot{\phi}_{k-1}}{2} \Delta t$$

- If  $|\hat{\phi}_k - \phi_k| <$  preset threshold, no cycle slip has occurred
- Threshold is a function of  $\Delta t$  and vehicle dynamics (assumes that phase velocity constant over  $\Delta t$ )
- Usually valid within 1 cycle if  $\Delta t \leq 1$  s
- Usable in kinematic mode but threshold may exceed 1 cycle in high dynamics (e.g., survey launch)

### Kinematic Cycle Slip Detection

#### *Kinematic Single Frequency Cycle Slip Detection (2/2)*

- Example: Cycle slips on PRN 12 at 154430 s

GPS Time (s)	$\phi$ (cycles)	$\dot{\phi}$ (Hz)	$\hat{\phi}$ (cycles)	$ \phi - \hat{\phi} $ (cycles)	Cycles Slip?
154426	4847.073	146.266	----	----	----
154427	4992.748	144.844	4992.628	0.120	no
154428	5136.899	143.688	5137.014	0.115	no
154429	5280.325	143.156	5280.321	0.004	no
154430	5452.985	142.032	5422.919	30.066	yes

### Kinematic Cycle Slip Detection

#### *Kinematic Dual Frequency Cycle Slip Detection*

- Need L1 and L2 data (through P code or cross-correlation)
- Over short interval ( $t_k, t_{k+1}$ ), form the following difference:

$$\delta\Phi_{L1} - \delta\Phi_{L2} = \delta d_{ion_{L1}} - \delta d_{ion_{L2}}$$

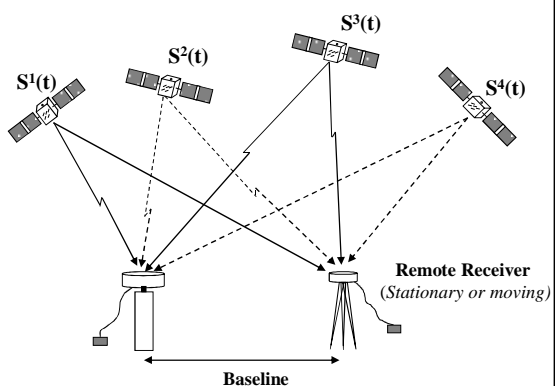
- Over a short time interval (e.g. 1 s),  $\delta\Phi_{L1} - \delta\Phi_{L2}$  will be  $\ll 1$  cycle because L1 and L2 are close and the dispersive effect of the ionosphere  $\ll 1$  cycle
- If  $\delta\Phi_{t_k, t_{k+1}} > 1$  cycle, a cycle slip has occurred
- Valid to detect a cycle slip within one L1 or L2 cycle
- Cannot determine whether slip has occurred on L1 or L2
- Works in both static and kinematic mode

## Differential Method Overview

- Differential methods are commonly used to eliminate or reduce errors that are spatially and/or temporally correlated
- For instance TDOA is a differential method in a sense as two pseudoranges (ranges with a common time bias – the receiver clock unknown) are differenced (one subtracted from the other)
- Differential methods are effective to remove timing biases, common propagation effects (e.g. Loran) and atmospheric effects (e.g. differential barometry) to eliminate effects of atmospheric pressure variations
- However, differential methods
  - Result in a loss of degrees of freedom
  - Thus, poorer geometry (higher Dilution of Precision)
  - Introduce serial correlations among derived measurements. The measurement covariance matrix of the derived measurements is a fully populated matrix
- Differential methods apply to other systems, e.g. GPS-ground-based RF

## Relative/Differential GPS Concept

- Measurements are assumed made at the same time - see previous discussion about measurement timing issues
- Position accuracy of 2<sup>nd</sup> receiver (Remote) with respect to that of 1<sup>st</sup> unit (Reference) is “better” because errors are reduced or eliminated
- 1<sup>st</sup> receiver can be mobile (relative GPS) or fixed (Differential GPS)
- Reduction or elimination of:
  - Orbital errors
  - Atmospheric errors
  - Satellite clock errors
- Remaining errors
  - Receiver noise
  - Multipath
  - Ionosphere ( $L_1$ )



### Carrier-Phase Relative Positioning

*Between Satellite-Receiver Double Difference ( $\Delta\nabla$ )*

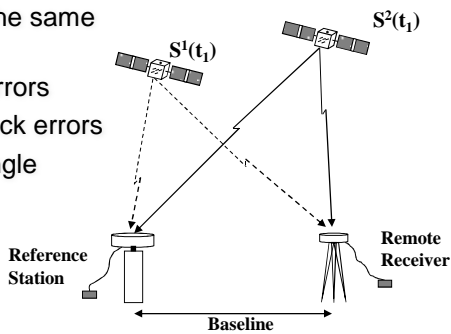
**Used for Carrier Phase Ambiguity Resolution**

$$\Delta\nabla = \left\{ (\bullet)_{\text{sat}_2} - (\bullet)_{\text{sat}_1} \right\}_{\text{rx}_2} - \left\{ (\bullet)_{\text{sat}_2} - (\bullet)_{\text{sat}_1} \right\}_{\text{rx}_1}$$

$$\Delta\nabla P = \Delta\nabla\rho + \Delta\nabla d\rho + \Delta\nabla d_{\text{ion}} + \Delta\nabla d_{\text{trop}} + \varepsilon_{\Delta\nabla\rho}$$

$$\Delta\nabla\Phi = \Delta\nabla\rho + \Delta\nabla d\rho + \lambda\Delta\nabla N - \Delta\nabla d_{\text{ion}} + \Delta\nabla d_{\text{trop}} + \varepsilon_{\Delta\nabla\Phi}$$

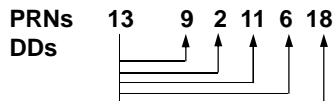
- Assumes that observations are at the same epoch
- Reduces orbital and atmospheric errors
- Eliminates satellite and receiver clock errors
- Increases noise 2x compared to single measurements



### Carrier-Phase Relative Positioning

*Between Satellite-Receiver Double Difference ( $\Delta\nabla$ ) Example*

- Given 6 satellites, the double differences (DDs) can be formed as follows:
  - (n-1) observations are formed where n is the number of satellites



- Satellite which is common to is called the 'base' satellite
  - Highest satellite is chosen as it is least susceptible to errors
- An example of  $\Delta\nabla\phi$  between PRN 13 and PRN 9 is given in the following table:

GPS Time (s)	Reference		Remote		$\Delta\nabla\phi$ (13-9) (cycles)
	$\phi_{13}$ (cycles)	$\phi_9$	$\phi_{13}$	$\phi_9$ (cycles)	
426916	-846502.672	627935.893	(627957.417)	622753.863	33094.715
426924	-819350.117	643767.629	-857378.431	638833.948	33094.633
426932	-792211.933	660393.255	-830781.263	654918.473	33094.548
426940	-765088.594	676990.342	-804160.483	671012.888	33094.435

## **Between Satellite-Receiver Double Difference Usage**

- Method is used for precise static & kinematic DGPS
- Ambiguities resolved either as integer or real numbers
- For short distances, errors are small
  - Correct integer ambiguities CAN be determined!
- For long distance, residual errors remain and limit the achievable accuracy, depending if integer ambiguities are resolved and the type of ambiguity resolved
- Number of unknowns in static double difference processing is  $3 + (n-1)$ :
  - 3 coordinate components (for remote X, Y, Z)
  - $+ (n-1)$  ambiguities, where n is the number of satellites
- For example, if 6 SV are tracked for 1 hour at a 15 s rate, there are only 8 unknown parameters
  - Good observability
  - Number of observations is  $(n-1)*m$ , where m is the number of epochs
  - Number of epochs (in this case) = 1200
- Cycle slips and satellite changes affect the number of ambiguities

## **Measurement Timing Issues**

- Carrier phase measurements are made at pre-determined epochs to be useful for precise DGPS
- Satellites are moving at a speed of 4 km/s
- Carrier phase rate can reach 5,000 cycles/s
- GPS time is estimated by the receiver with an accuracy of about 10-50 ns ( $1 \text{ ns} = 10^{-9} \text{ s}$ )
- But receivers do not readjust their clocks at every epoch and internal clocks may be readjusted only when the time misalignment is at the ms level ( $1 \text{ ms} = 10^{-3} \text{ s}$ )
- In 1 ms, the carrier phase can change by 5 cycles and the satellite positions by m along their orbits
- In differential mode, this is dealt with by calculating the satellite positions using the actual receiver times. A timing error of 10 ns results in a satellite position error of less than 1 mm

### Linear Combinations of Carrier Phase Observables

### Combinations of GPS L1 & L2 Phase Observables

- L1 and L2 data can be linearly combined to generate a new measurement

$$\varphi_{jk} = j\varphi_{L_1} + k\varphi_{L_2} \quad \lambda_{jk} = C/f_{jk}$$

- Most common are the widelane ( $j = 1, k = -1$ ), narrowlane ( $j = 1, k = 1$ ) and ionospheric-free ( $j = 1, k = -f_2/f_1$ )

Measurement	$j$	$k$	$\lambda(m)$	Ambiguity
Widelane WL	1	-1	<b>0.8619</b>	$\nabla\Delta N_{WL} = \nabla\Delta N_{L_1} - \nabla\Delta N_{L_2}$
Narrowlane NL	1	1	<b>0.1070</b>	$\nabla\Delta N_{NL} = \nabla\Delta N_{L_1} + \nabla\Delta N_{L_2}$
Ion-free IF	1	$-f_2/f_1$	<b>0.4844</b>	$\nabla\Delta N_{IF} = \nabla\Delta N_{L_1} - f_2/f_1 \nabla\Delta N_{L_2}$
Geometry-free GF	$\lambda_1$	$-\lambda_2$	$\infty$	$\nabla\Delta N_{GF} = \lambda_1 \nabla\Delta N_{L_1} - \lambda_2 \nabla\Delta N_{L_2}$
L1 only	1	0	<b>0.1903</b>	$\nabla\Delta N_{L_1}$
L2 only	0	1	<b>0.2442</b>	$\nabla\Delta N_{L_2}$

### Linear Combinations of Carrier Phase Observables

### Comparison of GPS L1 and WL Errors

Error	L1 Error (m)	WL Error (m)	Ratio $\frac{WL}{L1}$
SV Position	$\nabla\Delta\delta\rho_{SV}$	$\nabla\Delta\delta\rho_{SV}$	1
Receiver position	$\nabla\Delta\delta\rho_{rx}$	$\nabla\Delta\delta\rho_{rec}$	1
Troposphere	$\nabla\Delta\delta\rho_{tropo}$	$\nabla\Delta\delta\rho_{tropo}$	1
Ionosphere	$-\frac{1}{f_1^2} \nabla\Delta_{iono}$	$\frac{-\lambda_{WL}(f_1 - f_2)}{cf_1f_2} \nabla\Delta_{iono}$ $= \frac{1}{f_1f_2} \nabla\Delta_{iono}$	-1.283
Multipath	$\nabla\Delta_m$	$\frac{\lambda_{WL}}{\lambda_1} \nabla\Delta_m \sqrt{2}$	6.405
Noise	$\nabla\Delta_\epsilon$	$\frac{\lambda_{WL}}{\lambda_1} \nabla\Delta_\epsilon \sqrt{2}$	6.405

### Linear Combinations of Carrier Phase Observables

#### Comparison of GPS L1 and IF Errors

Error	L1 Error (m)	IF Error (m)	Ratio	$\frac{\text{IF}}{\text{L1}}$
SV Position	$\nabla\Delta\delta\rho_{\text{sv}}$	$\nabla\Delta\delta\rho_{\text{sv}}$	1	
Receiver position	$\nabla\Delta\delta\rho_{\text{rx}}$	$\nabla\Delta\delta\rho_{\text{rec}}$	1	
Troposphere	$\nabla\Delta\delta\rho_{\text{tropo}}$	$\nabla\Delta\delta\rho_{\text{tropo}}$	1	
Ionosphere	$-\frac{1}{f_1^2}\nabla\Delta\text{iono}$	0	0	
Multipath	$\nabla\Delta_m$	$\frac{\lambda_{\text{IF}}}{\lambda_1}\nabla\Delta_m\sqrt{\frac{f_1^2 + f_2^2}{f_1^2}}$	3.227	
Noise	$\nabla\Delta_\varepsilon$	$\frac{\lambda_{\text{IF}}}{\lambda_1}\nabla\Delta_\varepsilon\sqrt{\frac{f_1^2 + f_2^2}{f_1^2}}$	3.227	

### Linear Combinations

#### Geometry-Free (GF) Combination

- Used to obtained the double-difference ionospheric error. It is expressed in unit of length as

$$\Phi_{\text{GF}} = \lambda_1\phi_1 - \lambda_2\phi_2 = \Phi_1 - \Phi_2$$

- Neglecting carrier phase noise and multipath, one obtains the double difference ionospheric effect on L1

$$\nabla\Delta\text{IS}_{\text{L1}} = \left( \frac{f_2^2}{f_2^2 - f_1^2} \right) (\nabla\Delta\Phi_{\text{GF}} - \lambda_1\nabla\Delta N_1 + \lambda_2\nabla\Delta N_2)$$

- The measurement is free from tropospheric and orbital errors. It is slightly more than twice as noisy as L1 measurements.
- Used to assess the magnitude of the ionospheric effect on positioning (provided that the ambiguities can be resolved as integer values)

## GPS L1/L2 Linear Combination - Interpretation (1/2)

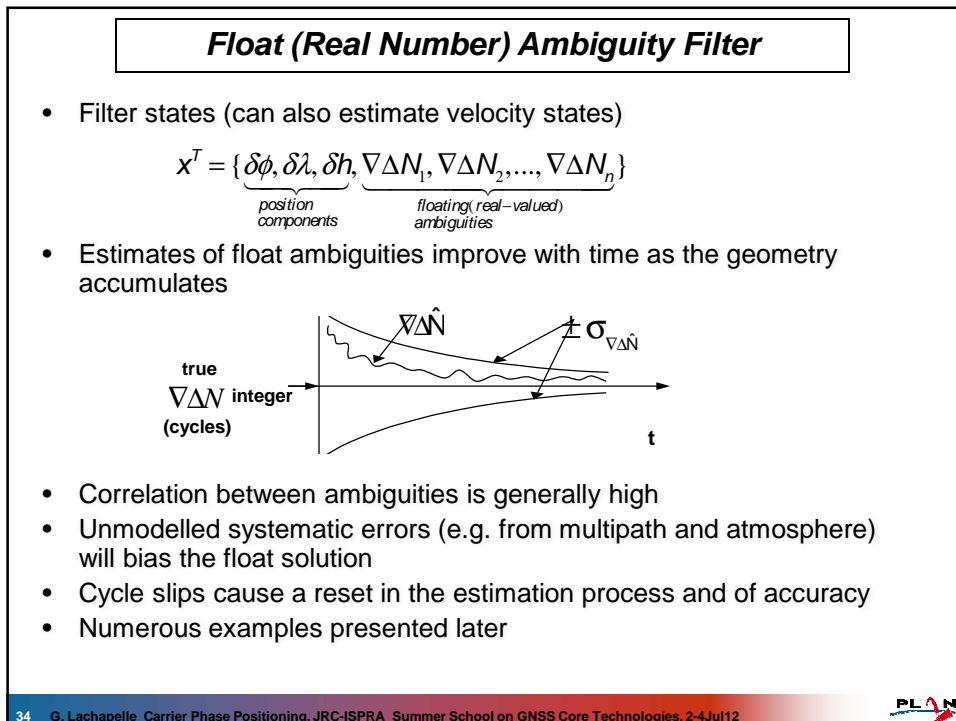
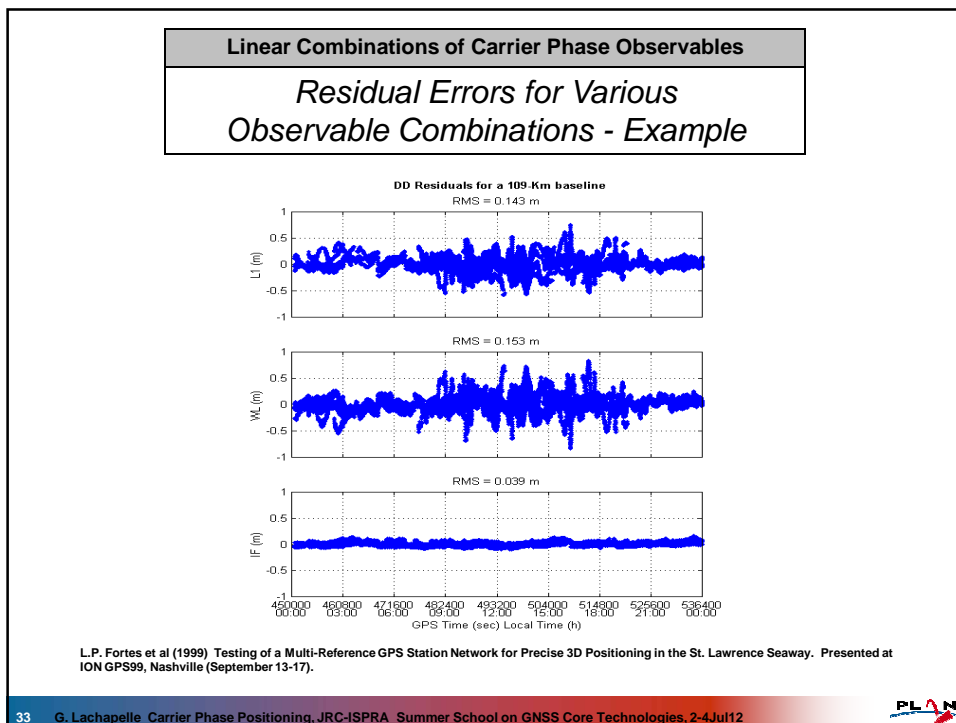
- The longer the wavelength of the derived ambiguities, the easier to find the correct integers
- WL is therefore the easiest to determine, but
- WL errors (ionosphere, multipath and noise) are amplified
- Therefore if only WL ambiguities are determined, the position solution will be affected by these errors. The effect of the ionosphere on a WL solution is great than that on a L1 solution!
- The IF ambiguities are free from the ionosphere but they are not integer. If the IF ambiguities are estimated directly, they therefore remain stochastic quantities and part of the state vector (referred to as real number or float solution – **Excellent choice if the differential ionosphere is significant and integer ambiguities cannot be determined**)
- However if WL and either L1 or L2 integer ambiguities can be determined, the other single frequency ambiguities can be derived using

$$\nabla \Delta N_W = \nabla \Delta N_{L1} - \nabla \Delta N_{L2}$$

## GPS L1/L2 Linear Combination - Interpretation (2/2)

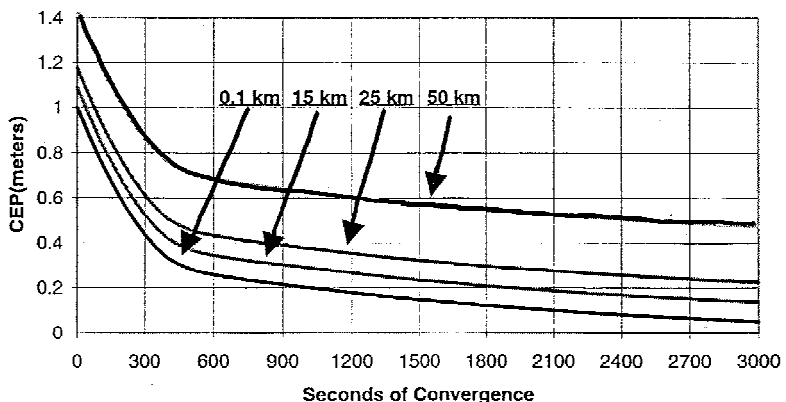
- The IF ambiguities can then be derived using the equation below. These ambiguities are no longer integer but it does not matter as they are derived from L1 and L2 integer ambiguities and they are still deterministic and are no longer part of the state vector – system observability improves
- The above is the best integer ambiguity solution that can be obtained when the effect of the ionosphere is significant – It is usually accurate to a few cm
- The others are affected by the ionosphere and can be in error by decimetres
- Remember: A position solution is calculated using the same carrier phase observable linear combination as that of the ambiguities
- **CONCLUSION: Beware - A “fixed ambiguity” solution does not mean high accuracy until the type of fixed ambiguities resolved is known**

$$\nabla \Delta N_{IF} = \nabla \Delta N_{L1} - \frac{f_2}{f_1} \nabla \Delta N_{L2}$$



### **Example of Float Solutions: RTK Positioning Performance – NovAtel RT20 (L1)**

- Typical horizontal accuracy convergence time



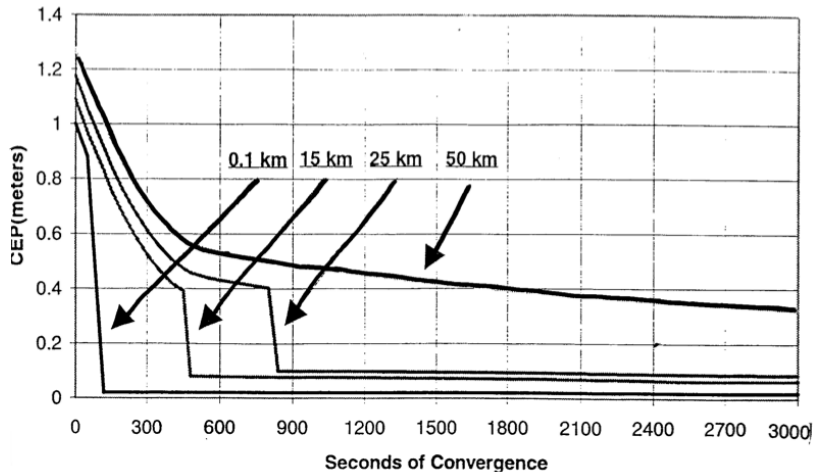
*NovAtel RT20 Manual*

### **Why is Accuracy Better when Ambiguities are Resolved as Integer Numbers?**

- When carrier phase measurements are used, ambiguities occur and have to be resolved either as real or integer values
- Initially, the ambiguities are part of the state vector. Thus, for 8 SVs, the state vector increases by 7 double differences ambiguities (from a minimum of 3 for the three position differences)
- If the correct integers are found (They always exist. The question is – Can they be found?), the state vector collapses, improving system observability substantially
- **If in doubt, resolve as real numbers (Float solution)**
- **Caution: Resolving the integer values does not necessarily yield a cm-level accuracy. Accuracy depends on the type of ambiguities resolved - How the ionosphere is dealt with...**

### Example (Float/Fixed): L1/L2 RTK Performance

- Typical horizontal accuracy convergence



NovAtel RT2 Manual

37 G. Lachapelle Carrier Phase Positioning, JRC-ISPRA Summer School on GNSS Core Technologies, 2-4Jul12



#### Introduction

### Factor Affecting Integer Ambiguity Resolution

- Static versus kinematic
  - Ambiguities are generally easier to resolve in static mode
- Baseline separation (correlated errors)
  - The closer the user is to the reference, the easier it is to resolve ambiguities because the correlated errors are reduced
- Multipath
  - Even if two points are close together, ambiguities will not be resolved if there is significant pseudorange multipath
- Length of data set and geometry
  - Information is gained through satellite geometry change – longer observation times give better opportunity for resolution
  - The more satellites tracked, the better
- Type of receiver
  - L1/L2 receivers can resolve ambiguities much faster than single frequency systems due to widelaning (WL) combination of  $L_1$  and  $L_2$
- Ambiguity algorithm
  - Some differences in performance are due to the algorithm used

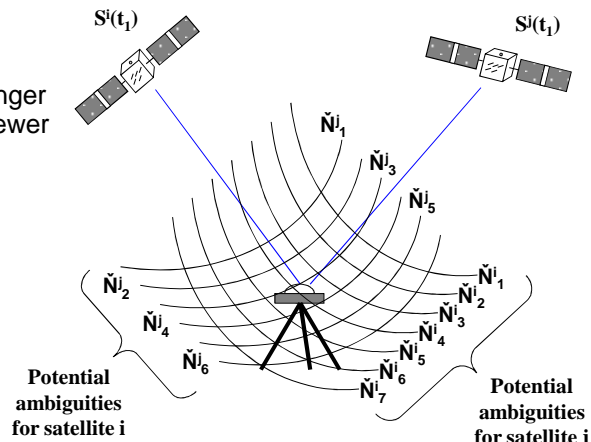
38 G. Lachapelle Carrier Phase Positioning, JRC-ISPRA Summer School on GNSS Core Technologies, 2-4Jul12



## Introduction

### Ambiguity Resolution (AR) Overview

- As more satellites are observed, there are fewer crossover points (i.e. valid combinations) to test
- As the wavelength gets longer (i.e. widelane), there are fewer crossover points to test



Ref: P. Alves, ENGO 625 Lead Discussion  
(2000)

39 G. Lachapelle Carrier Phase Positioning, JRC-ISPRA Summer School on GNSS Core Technologies, 2-4Jul12

PLN

## Ambiguity-Domain Approaches

### Overview of Search Strategies

- Some common methods for ambiguity-domain AR include
  - Rounding
  - Bank of Kalman Filters
  - Fast Ambiguity Resolution Approach (FARA)
  - Cholesky Search Technique
  - Fast Ambiguity Search Filter (FASF)
  - Least Squares Ambiguity Decorrelation Adjustment (LAMBDA)

40 G. Lachapelle Carrier Phase Positioning, JRC-ISPRA Summer School on GNSS Core Technologies, 2-4Jul12

PLN

### Ambiguity-Domain Approaches

#### *Least Squares Ambiguity Decorrelation Adjustment (LAMBDA)*

- Re-parameterization of the ambiguity states and covariance matrix
- Multi-dimensional confidence ellipsoid is severely elongated due to high correlation between ambiguities
- Transforms the ambiguity states to minimize correlation and reduce the search space
  - Minimizes the correlation in the transformed ambiguities
  - Integer transformation
  - Volume preserving (i.e., every transformed ambiguity set has a unique original set)
- Considers the full correlation between ambiguity states

**Decorrelate the second ambiguity from the first**

$$\begin{bmatrix} N_1 \\ N_{2''} \end{bmatrix} = \begin{bmatrix} 1 & 0 \\ \text{int}(-\sigma_{2,1}\sigma_1^{-2}) & 1 \end{bmatrix} \begin{bmatrix} N_1 \\ N_2 \end{bmatrix}$$

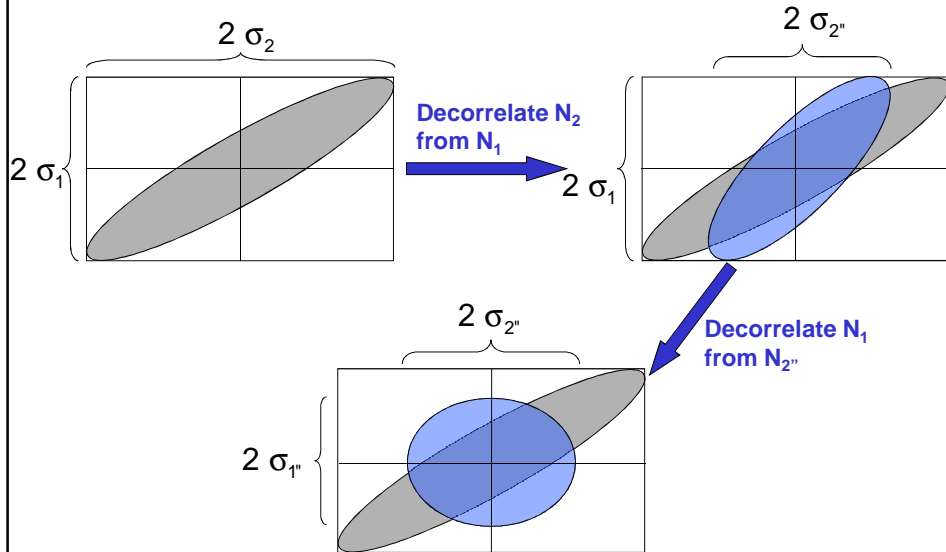
**Decorrelate the first ambiguity from the transformed second**

$$\begin{bmatrix} N_{1''} \\ N_{2''} \end{bmatrix} = \begin{bmatrix} 1 & \text{int}(-\sigma_{1,2}\sigma_2^{-2}) \\ 0 & 1 \end{bmatrix} \begin{bmatrix} N_1 \\ N_{2''} \end{bmatrix}$$

Reference: Teunissen, P.J.G. (1994), *A New Method for Fast Carrier Phase Ambiguity Estimation*, Proc. of IEEE PLANS, Las Vegas, pp. 562-573.

### Ambiguity-Domain Approaches

#### *LAMBDA Decorrelation Example*



### Ambiguity-Domain Approaches

#### LAMBDA Search

From a simplified Cholesky search: The sum of squared residuals is

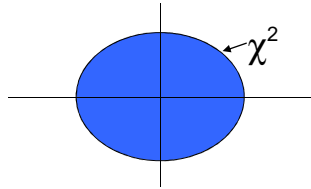
$$\Omega_{\text{fixed}} = \Omega_{\text{float}} + (\mathbf{N}_{\text{fixed}} - \mathbf{N})^T \mathbf{C}_N^{-1} (\mathbf{N}_{\text{fixed}} - \mathbf{N})$$

Minimizing  $\Omega_{\text{fixed}}$  as a function of  $\mathbf{N}_{\text{fixed}}$  is independent of  $\Omega_{\text{float}}$  therefore

To minimize  $\Omega_{\text{fixed}}$  we must minimize  $(\mathbf{N}_{\text{fixed}} - \mathbf{N})^T \mathbf{C}_N^{-1} (\mathbf{N}_{\text{fixed}} - \mathbf{N})$

**Search the ambiguities based on the function**

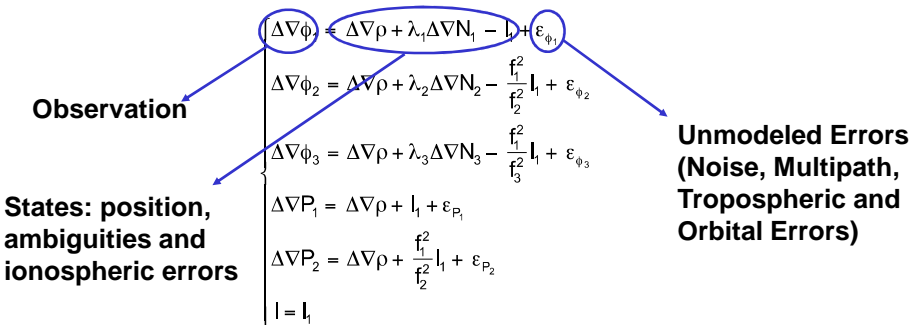
$$(\mathbf{N}_{\text{fixed}} - \mathbf{N})^T \mathbf{C}_N^{-1} (\mathbf{N}_{\text{fixed}} - \mathbf{N}) \leq \chi^2$$



Defining the search space by the minimum sum of squared residuals ensures that if only one ambiguity set is found then that set is the best because, by definition, all other ambiguity sets will have a higher sum of squared residuals.

### Stochastic Ionospheric Modeling (SIM)

- Use of an ionospheric weighted model:
  - Estimates ionosphere states using code and carrier phase measurements and
  - External ionospheric observations ('pseudo-observations')
  - System:



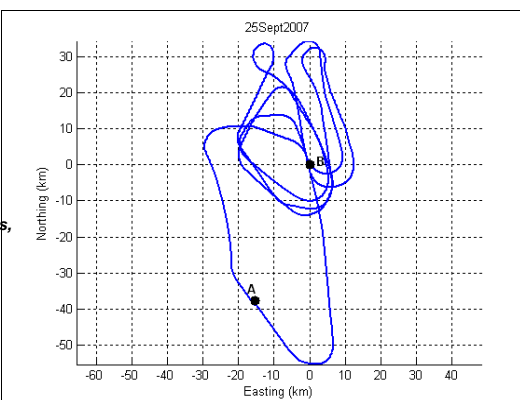
### **Partial Ambiguity Fixing**

- The method is conceptually simple:
  - Assume N satellites tracked, in which case there are N-1 DD ambiguities to resolve
  - For the simple case, the state (unknowns) vector consists of 3 position differences and N-1 ambiguities for a total of N+2 states
  - If all ambiguities can be resolved, the state vector reduces to 3 states, yielding maximum observability and best accuracy
  - During the ambiguity resolution process, some ambiguities are resolved earlier than others, depending on several factors, resulting in the reduction of the state vector
  - As the dimension of the state vector shrinks, observability and accuracy increase
  - In many situations (e.g. some satellites heavily impacted by the ionosphere), only ambiguity subsets can be resolved as integer. If the subset is deemed adequate, a solution based only on it can be selected or, alternatively, a mixed fixed/float integer solution is used.

### **Example 1: Carrier Phase Aircraft Testing**

- Light jet aircraft, up to 300 km/hr, 100 minutes, Sep07, period of low ionospheric activity, latitude of about 55 degrees.
- Dual-frequency high performance GPS receivers at two base stations (A and B) separated by 40 km. Data logged at 5 Hz.

*Data Courtesy of the Canadian Forces,  
Aerospace Engineering Test  
Establishment,  
Cold Lake, Alberta*



## Data Analysis Strategy to Demonstrate High Consistency/Accuracy

- Assess the GrafNav solutions by comparing their forward and reverse solutions using different combinations of base stations
- Assess the FLYKIN+™ solutions by comparing the results obtained with L1&L2 and widelane ambiguities using different base stations
- Compare the GrafNav and FLYKIN+™ solutions
- GrafNav solution had a “fixed” status throughout the entire kinematic portion of the data. Although no information is provided regarding the number or type of fixed ambiguities, the fact that the solutions were “fixed” is indeed promising

## Testing of Forward vs Backward vs two-base methods with Different Software

- Two independent GPS software used
  - NovAtel's GrafNav and University of Calgary's FLYKIN+.
  - Forward and reverse processing
  - One and two base stations

**GPS Processing Summary (FWD = Forward Processing, REV = Reverse Processing, CMB = Forward/Reverse Combined Processing)**

Software	Base Station		
	B	A	A & B
GrafNav	FWD, REV, CMB	FWD, REV, CMB	FWD, REV, CMB
FLYKIN+™ (L1&L2)	FWD	FWD	FWD
FLYKIN+™ (WL)	FWD	FWD	FWD

# GrafNav Consistency Statistics

RMS Position Agreement of Different Solutions Obtained using GrafNav and Different Combinations of Base Stations

Solution 1	Solution 2	RMS Agreement (m)		
		North	East	Vertical
GrafNav FWD B	GrafNav REV A	0.059	0.030	0.041
GrafNav FWD (A)	GrafNav REV (A)	0.019	0.052	0.033
GrafNav FWD (B + A)	GrafNav REV (B + A)	0.030	0.061	0.031
GrafNav FWD (B)	GrafNav FWD (A)	0.074	0.048	0.051

# FLYKIN+™ Consistency Statistics

RMS Position Agreement of Different Solutions Obtained using FLYKIN+™

Solution 1	Solution 2	RMS Agreement (m)		
		North	East	Vertical
FLYKIN+™ L1&L2 (B)	FLYKIN+™ L1&L2 (A)	0.013	0.005	0.026
FLYKIN+™ WL (B)	FLYKIN+™ WL (A)	0.040	0.014	0.039

## FLYKIN+™ vs GrafNav Solution Statistics

- The solutions are consistent to within 3 to 9 cm*

RMS Position Agreement Between FLYKIN+™ and GrafNav Solutions

Solution 1	Solution 2	RMS Agreement (m)		
		North	East	Vertical
FLYKIN+™ L1&L2 (B)	GrafNav CMB (B)	0.033	0.025	0.075
FLYKIN+™ WL (B)	GrafNav CMB (B)	0.027	0.031	0.083
FLYKIN+™ L1&L2 (A)	GrafNav CMB (A)	0.046	0.020	0.048
FLYKIN+™ WL (A)	GrafNav CMB (A)	0.026	0.026	0.078

<http://plan.geomatics.ucalgary.ca>

PLAN Students Win at Security Innovation Competition - April 30, 2012. Saeed Daneshmand and Ali Jafaria-Jahromi placed third in the 2012 National Security Innovation Competition, organized by the Defense Science and Technology Agency. Their entry describes a sophisticated technique to thwart interference attacks on GPS signals that lead to incorrect navigation data and misguided users. [Read More »](#)

The Position, Location And Navigation (PLAN) Group is dedicated to the research, development and improvement of wireless positioning and navigation technologies for outdoor and indoor use. To this end, most of our work is encompassed in the following research areas:

**GNSS Signal Processing**

- Signal acquisition and tracking algorithm development, including high accuracy phase lock loops
- Multi-frequency, multi-system signal processing enhancements
- Impact of signal attenuation and High Sensitivity GNSS, including Assisted GNSS (AGNSS)

**Sensor Augmentation**

- Tight and ultra-tight integration of GNSS with inertial sensors
- Impact of various oscillators on signal integration
- Multi-sensor augmentation
- Ground based RF ranging systems and augmentation

**Applications**

- Software GNSS receiver development
- Centimetre-level accuracy positioning and multi-frequency multi-constellation resolution
- Velocity and attitude determination
- Atmospheric propagation effects
- Indoor, pedestrian and vehicular navigation

Copyright © 2012 PLAN Research Group  
Department of Geomatics Engineering  
University of Calgary

2500 University Dr NW  
Calgary, Alberta  
T2N 1N4 Canada

# NEW GALILEO SIGNALS

Olivier JULIEN

Ecole Nationale de l'Aviation Civile (ENAC)

Toulouse, France

JRC GNSS Summer School on Core Technologies

2-4 July 2012

Ispra, Italy

## Introduction

- The objectives of this course is to provide the fundamental notions required to acquire and track the future Galileo signals. It is thus divided into 2 main sections:
  - The presentation of the signal-in-space innovations
    - BOC modulation
    - Secondary codes
    - Data/pilot components
  - The presentation of the Galileo signals based on these innovations

# Content

- I. Reminder on Receiver Signal Processing
- II. Binary Offset Carrier (BOC) Modulation
  - Description and characteristics
  - Impact on acquisition and tracking
- III. Secondary Code
  - Description and characteristics
  - Impact on acquisition and tracking
- IV. Data/Pilot Architecture
  - Description and characteristics
  - Impact on acquisition and tracking
- V. Galileo Signal Structure
  - Galileo services
  - Galileo civil signals' characteristics

# Content

- I. Reminder on Receiver Signal Processing
- II. Binary Offset Carrier (BOC) Modulation
  - Description and characteristics
  - Impact on acquisition and tracking
- III. Secondary Code
  - Description and characteristics
  - Impact on acquisition and tracking
- IV. Data/Pilot Architecture
  - Description and characteristics
  - Impact on acquisition and tracking
- V. Galileo Signal Structure
  - Galileo services
  - Galileo civil signals' characteristics

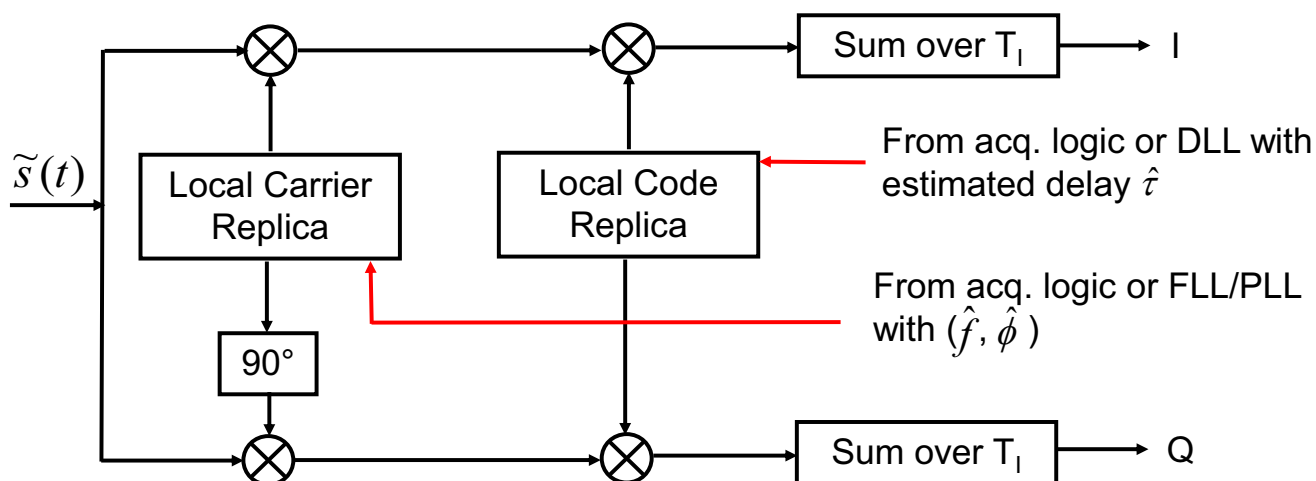
## 1. Typical GPS Legacy Signal

- The typical GPS L1 C/A legacy signal is composed of:
  - A low rate (50 Hz for GPS C/A) binary useful signal
  - A spreading code, using a Non-Return to Zero (NRZ) waveform, with a high chipping rate compared to the useful data rate (1.023 MHz for GPS C/A)
  - A carrier set at the desired frequency ( $L1 = 1575.42$  MHz for GPS C/A)
- In this case, the signal model is:

$$s(t) = Ad(t)c(t)\cos(2\pi f_{L_1}t + \varphi)$$

## 1. The Correlation Operation

- The correlation process consists in:
  - the carrier wipe-off,
  - the multiplication by a local replica, and
  - an integration over  $T_I$  (Integrate and Dump - I&D)



# 1. Correlator Output Model

- Assuming slowly varying signal dynamics and taking into account the front-end filter:

$$I(k) = \frac{A \sin(\pi \Delta f T_I)}{2 \pi \Delta f T_I} \tilde{R}_{I,L}(\Delta \tau) d(k) \cos(\Delta \phi) + n_I(k)$$

$$P_{n_I} = P_{n_Q} = \frac{N_0}{4T_I} \tilde{R}_{L,L}^2(0)$$

$$Q(k) = \frac{A \sin(\pi \Delta f T_I)}{2 \pi \Delta f T_I} \tilde{R}_{I,L}(\Delta \tau) d(k) \sin(\Delta \phi) + n_Q(k)$$

where

$\tilde{R}_{I,L}$  is the correlation function between the filtered incoming signal and the local replica

$\Delta f$  is the frequency tracking error (Hz)

$\Delta \tau$  is the code tracking error (in chips)

$\Delta \phi$  is the phase tracking error (in radians)

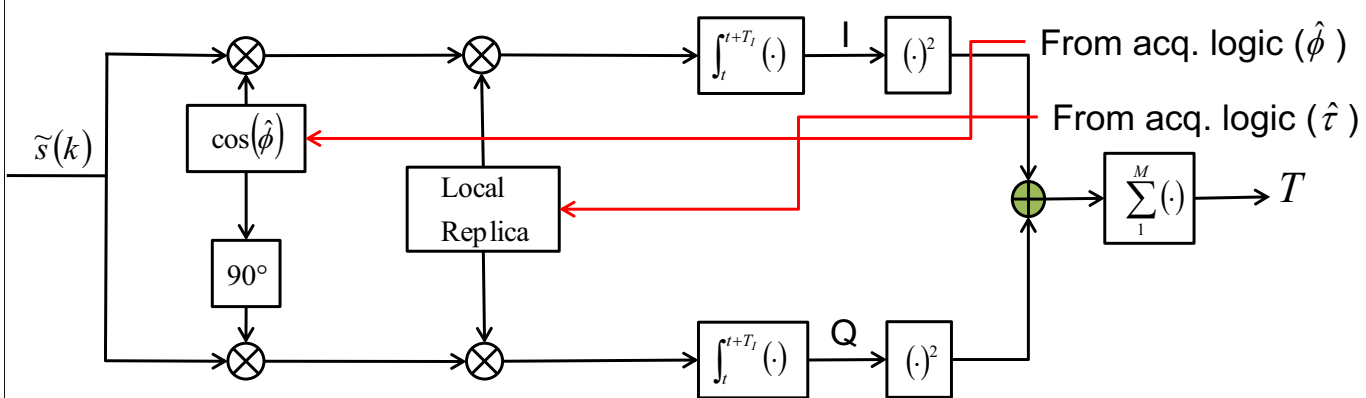
$d$  is the current navigation data bit

$T_I$  is the correlation integration time (in sec)

$n_I, n_Q$  are the I and Q post-correlation thermal noise components

# 1. Acquisition Architecture

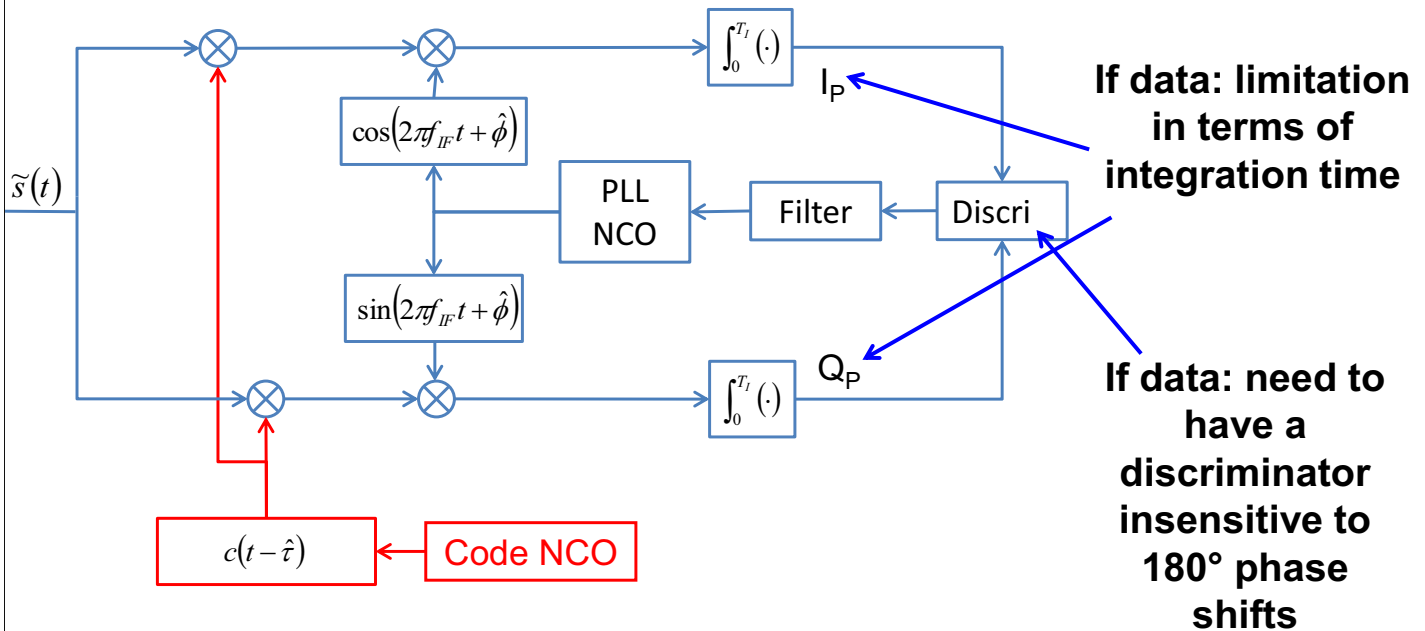
- Typical architecture for sequential acquisition



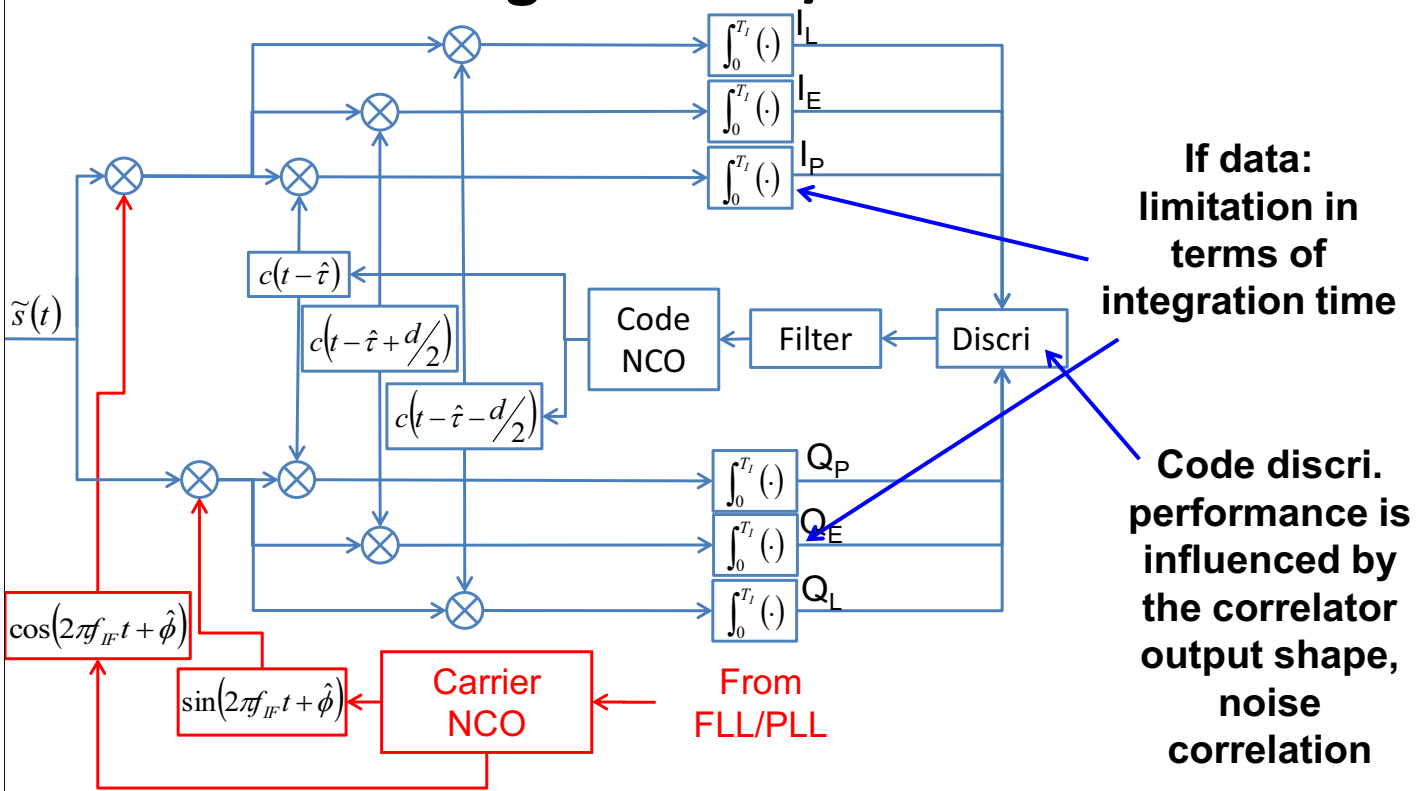
- Use of hypothesis test based on the following test detector:

$$T = \sum_{q=1}^M (I(q)^2 + Q(q)^2) \quad \text{where } M \text{ is the number of non-coherent integrations}$$

# 1. Phase Tracking of GPS C/A



# 1. Code Tracking of GPS C/A



# Content

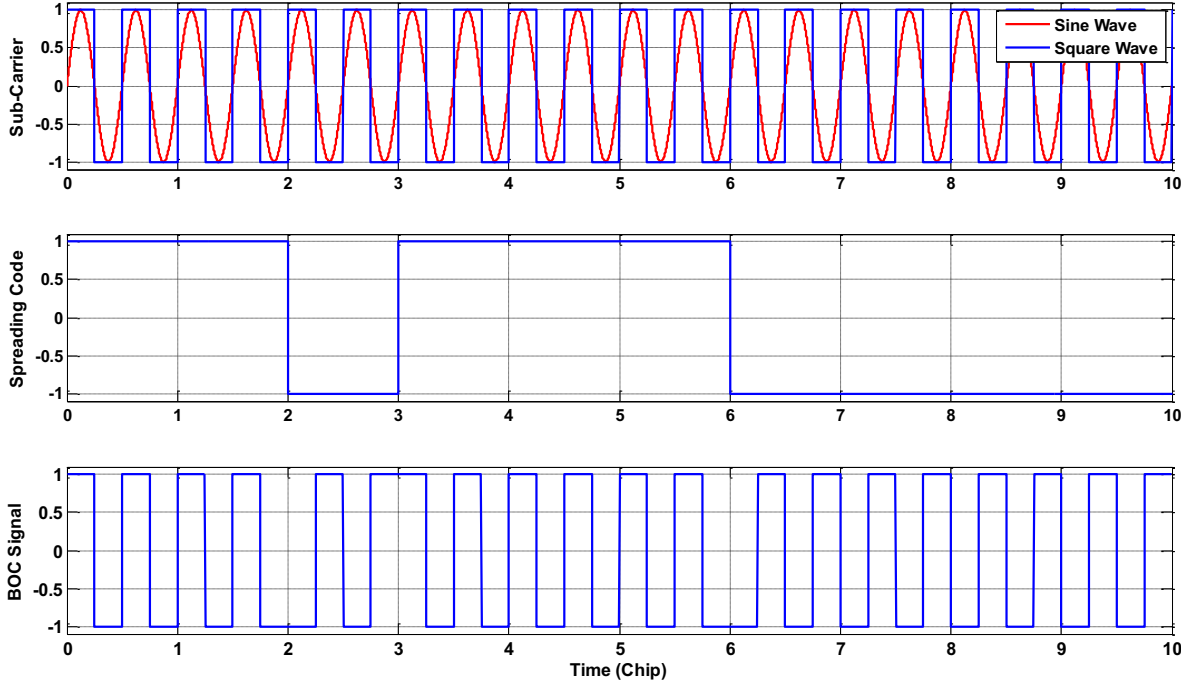
- I. Reminder on Receiver Signal Processing
- II. Binary Offset Carrier (BOC) Modulation
  - Description and characteristics
  - Impact on acquisition and tracking
- III. Secondary Code
  - Description and characteristics
  - Impact on acquisition and tracking
- IV. Data/Pilot Architecture
  - Description and characteristics
  - Impact on acquisition and tracking
- V. Galileo Signal Structure
  - Galileo services
  - Galileo civil signals' characteristics

## 2. BOC Description

- A square wave is a function representing the sign of a continuous wave
    - It can be derived from a sine or a cosine function
  - The BOC modulation consists in the multiplication of the spreading sequence with a square wave sub-carrier:
    - The sub-carrier is synchronized with the spreading code
    - Twice the frequency of the sub-carrier ( $f_{sc}$ ) divided by the spreading code rate ( $f_c$ ) is an integer ( $2.f_{sc}/f_c=r$ ). *In other words, the duration of one spreading code chip is equal to the duration of an integer number of half cycles of the subcarrier.*
- It is referred to as BOC(m,n) modulation where  $m=f_{sc}/f_{ref}$  and  $n=f_c/f_{ref}$ , with  $f_{ref}=1.023$  MHz

## 2. BOC Description

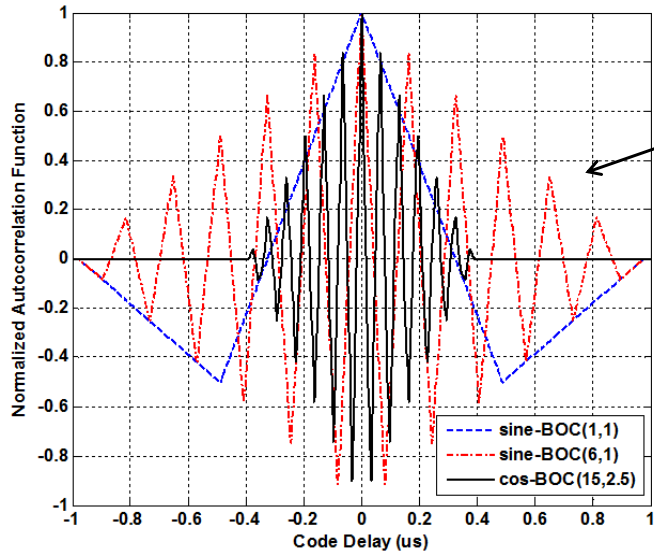
- Example of a sine-BOC(2,1)



## 2. BOC Reception

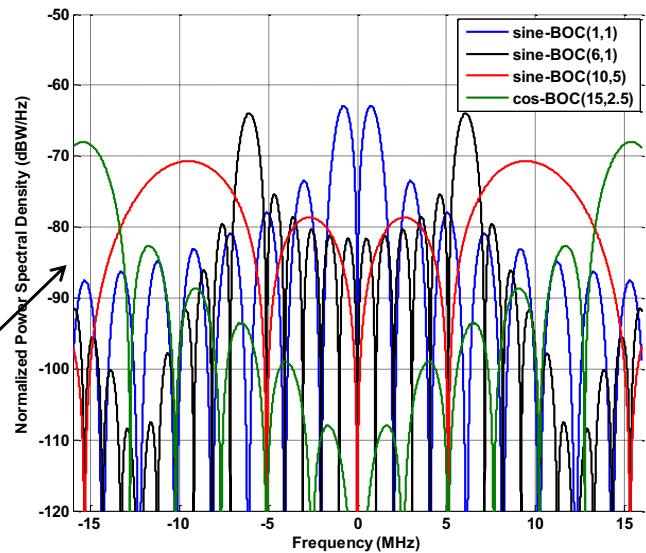
- The standard reception of a BOC signal implies the generation of a local BOC replica by the receiver with the same characteristics:
  - A sub-carrier, based on the same NCO as the code generator, has to be generated internally
- The presence of the sub-carrier affects the shape of the signal's auto-correlation function, and thus the shape of its Power Spectral Density (PSD).
- The characteristics of these 2 functions is critical to understand the benefits of such modulation.

## 2. BOC Correlation Function and PSD



The BOC(m,n) autoc. function has several peaks that are contained within the BPSK(n) autoc. function

The higher the ratio between m and n, the more peaks are present in the autoc. function



The BOC(m,n) PSD function has 2 main lobes offset from the carrier by approx.  $m^*1.023$  MHz.

The width of the main lobes are  $2m^*1.023$  MHz

## 2. BOC Correlation Function and PSD

- Theoretical expressions of the BOC(m,n) PSD:

$$G_{\text{sine-BOC}}(f) = f_c \left\{ \frac{\tan\left(\frac{\pi f}{f_c} \cdot \frac{n}{2m}\right) \sin\left(\frac{\pi f}{f_c}\right)}{\pi f} \right\}^2 \quad \text{if } \frac{2m}{n} \text{ is even}$$

$$G_{\text{sine-BOC}}(f) = f_c \left\{ \frac{\tan\left(\frac{\pi f}{f_c} \cdot \frac{n}{2m}\right) \cos\left(\frac{\pi f}{f_c}\right)}{\pi f} \right\}^2 \quad \text{if } \frac{2m}{n} \text{ is odd}$$

Sine-BOC(m,n)

$$G_{\text{cos-BOC}}(f) = f_c \left\{ \frac{\left(\cos\left(\frac{\pi f}{f_c} \cdot \frac{n}{2m}\right) - 1\right) \sin\left(\frac{\pi f}{f_c}\right)}{\pi f \cos\left(\frac{\pi f}{f_c} \cdot \frac{n}{2m}\right)} \right\}^2 \quad \text{if } \frac{2m}{n} \text{ is even}$$

$$G_{\text{cos-BOC}}(f) = f_c \left\{ \frac{\left(\cos\left(\frac{\pi f}{f_c} \cdot \frac{n}{2m}\right) - 1\right) \cos\left(\frac{\pi f}{f_c}\right)}{\pi f \cos\left(\frac{\pi f}{f_c} \cdot \frac{n}{2m}\right)} \right\}^2 \quad \text{if } \frac{2m}{n} \text{ is odd}$$

Cos-BOC(m,n)

The differences in the PSD function imply that the associated autocorrelation functions have different shapes

## 2. BOC Correlation Function and PSD

- Characteristics of the BOC( $m,n$ ) autocorr. function:
  - The number of peaks increases with the ratio  $r=m/n$
  - The slope of the autoc. main peak increases with the ratio  $r=m/n$
  - For a sine-BOC( $m,n$ )
    - There are  $2r-1$  peaks (main and secondary peaks)
    - The magnitude of the  $k^{\text{th}}$  peak (wrt the central peak) is  $(-1)^k(r-|k|)/r$
    - The 1<sup>st</sup> zero-crossing (the closest to 0) is located at  $1/(2r-1)$  chip
- Characteristics of the sine-BOC( $m,n$ ) PSD:
  - The main lobes are offset by  $f_{sc}$  from the carrier frequency
  - The width of the main lobes is  $2.f_c$
  - The width of the side-lobes is  $f_c$

## 2. Impact of BOC on Acquisition

- Presence of potentially high secondary peaks that could bias the acquisition
  - Should a specific acquisition strategy be used to avoid a biased acquisition, or should this be left to the tracking stage?
- The BOC( $m,n$ ) autocorrelation function has a narrow main peak compared to the standard BPSK( $n$ ) modulation
  - The acquisition search grid has to be adapted (more bins) in order to limit the correlation losses → longer acquisition required → this can be compensated by the use of a higher number of correlators working in parallel

## 2. Impact of BOC on Code Tracking

- For a common chipping rate, the BOC( $m,n$ ) signal will have a wider spectral occupation than BPSK( $n$ ).
  - It will require a higher sampling rate and more power
  - It will exhibit better performance against thermal noise, interference and multipath (at the expense of a higher required sampling rate and power).
- Performance against thermal noise:

$$\sigma_{DP}^2 = \frac{B_L d}{2\alpha \frac{C_P}{N_0}} \left( 1 + \frac{1}{\frac{C_P}{N_0} T_I} \right) \text{ (chips}^2)$$

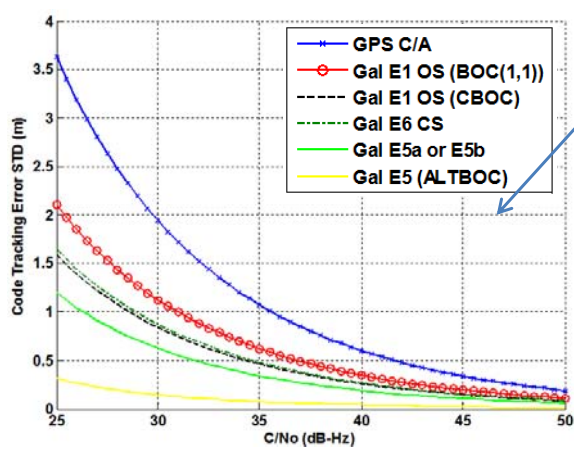
$$\sigma_{EMLP}^2 = \frac{B_L d}{2\alpha \frac{C_P}{N_0}} \left( 1 + \frac{2}{(2-\alpha d) \frac{C_P}{N_0} T_I} \right) \text{ (chips}^2)$$

$B_L$  is the DLL equivalent loop bandwidth

$d$  is the Early-Late spacing (chip)

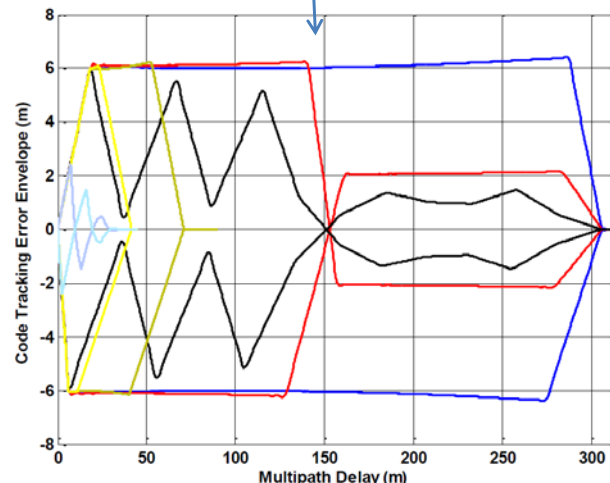
$\alpha$  is the slope of the main peak of the autocorrelation function

## 2. Impact of BOC on Code Tracking



Code Tracking Error Due to Thermal Noise

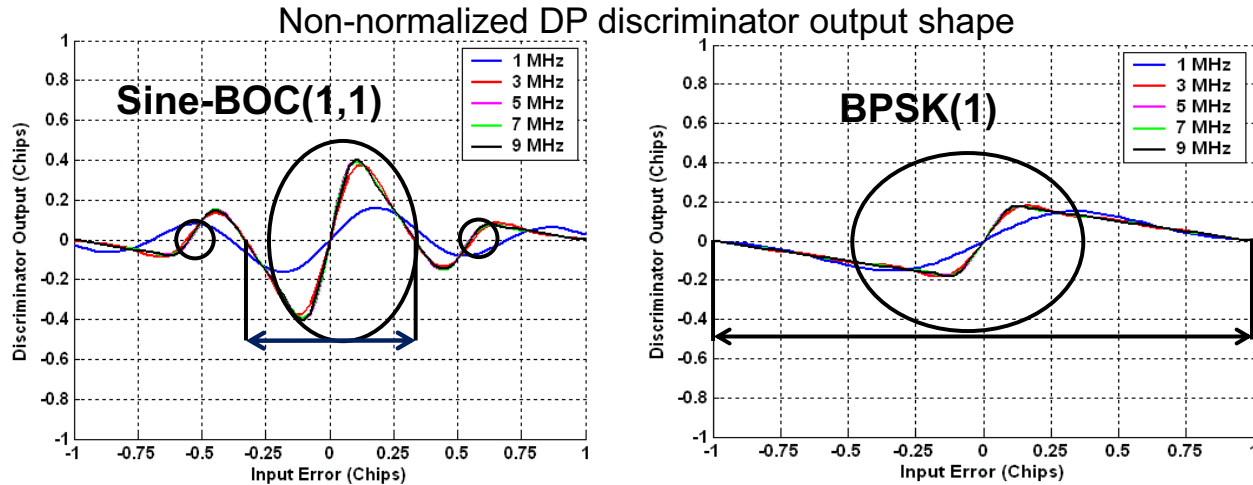
Multipath Error Envelope



Infinite Front-End Filter  
 $(d=1/12.2276e6 \text{ sec except for the ALTBOC where } d=1/40.92e6 \text{ sec}).$   
 $T_I=20 \text{ ms}, B_L=1 \text{ Hz}.$

## 2. Impact of BOC on Code Tracking

- Code Tracking Bias



- Narrower stability region → less stable for large errors
- Narrower operating region → cannot cope with large errors
- Higher slope around 0 → better suited for accurate tracking
- Several stability points → associated with peaks

## 2. Conclusions on BOC

- Advantages:
  - The BOC modulation allows a smart use of the frequency band
    - Limited overlap with other signals
  - BOC(m,n) provides better resistance against thermal noise and multipath compared to a BPSK(n)
  - No impact on carrier tracking
- Drawbacks
  - It has a wide spectral occupation
  - The autocorrelation function has several peaks, which can lead to ambiguous measurements

# Content

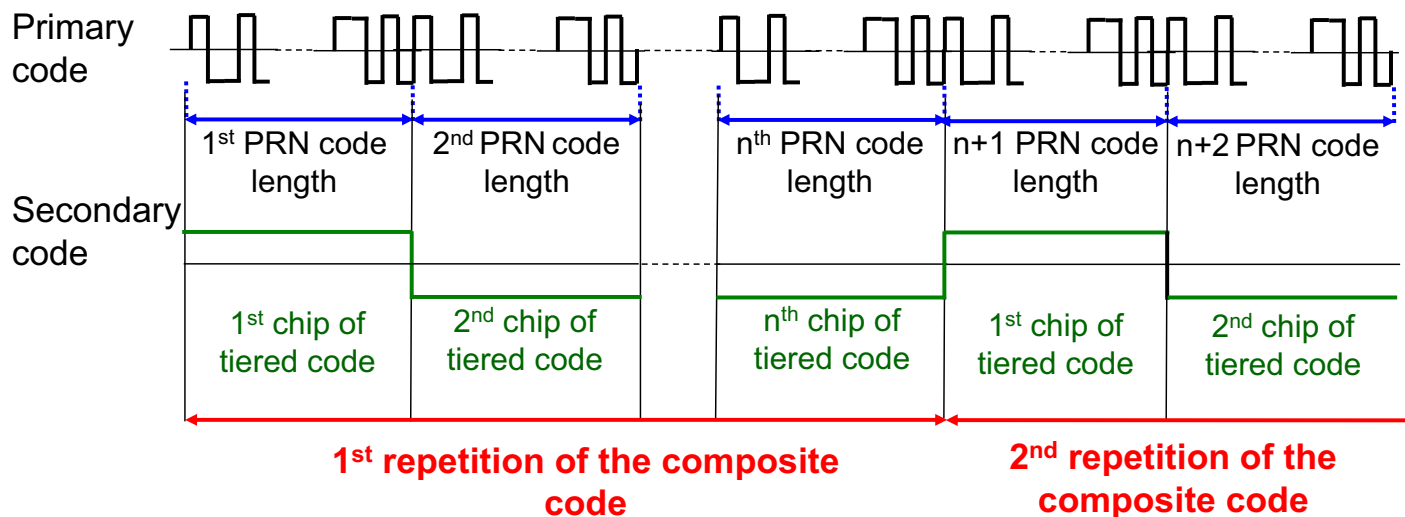
- I. Reminder on Receiver Signal Processing
- II. Binary Offset Carrier (BOC) Modulation
  - Description and characteristics
  - Impact on acquisition and tracking
- III. Secondary Code
  - Description and characteristics
  - Impact on acquisition and tracking
- IV. Data/Pilot Architecture
  - Description and characteristics
  - Impact on acquisition and tracking
- V. Galileo Signal Structure
  - Galileo services
  - Galileo civil signals' characteristics

## 3. Secondary Code Description

- In GNSS, secondary codes are usually:
  - Binary
  - Short (small number of chips)
  - One secondary code chip lasts the duration of the full (primary) spreading code
- The resulting sequence (product of secondary and primary codes) appears as a « long spreading sequence » → better correlation properties
- They are used to:
  - Improve the mitigation of narrow band interference
  - When included in a data bit, they help the data bit synchro

### 3. Secondary Code Description

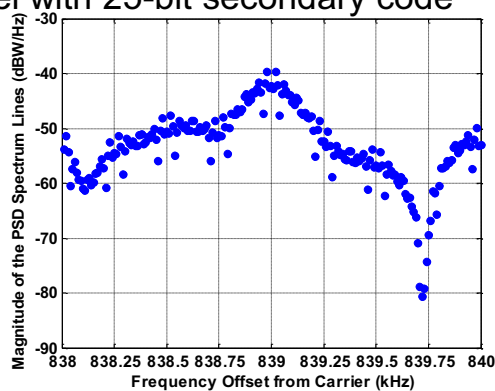
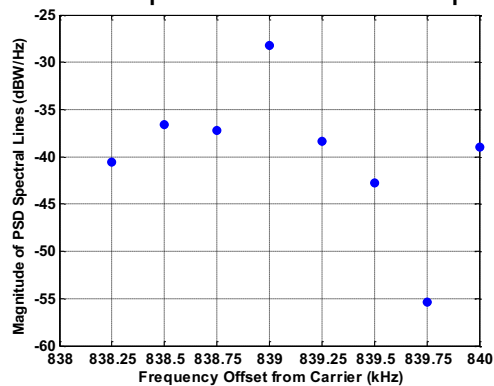
- Secondary codes “artificially” extend the length of the spreading code



### 3. Secondary Code Description

- A longer spreading sequence means that there will be more spectral lines composing the signal's PSD
- Since the signal carries the same power, each line has a lower magnitude than the PSD of the signal with the initial spreading sequence

Example: Galileo E1 OS pilot channel with 25-bit secondary code



### 3. Impact of Sec. Code on Acquisition

- It is necessary to acquire the secondary codes in order to start long coherent integrations over the secondary code
- Acquiring directly primary+secondary is usually difficult as
  - it represents a very long composite code (time consuming)
  - It induces long coherent integrations, thus narrow Doppler bins
- The secondary code is thus generally acquired after the acquisition of the primary code:
  - This can be done after tracking convergence by:
    - reading the « secondary chip sign » from the I channel of the pilot component ,and
    - Correlating it with the known sequence

### 3. Impact of Sec. Code on Tracking

- Two cases have to be distinguished:
  - The secondary code has not been acquired: in this case, the tracking is based on the primary code only in a standard way → no improvement of performance can be expected
  - The secondary code has been acquired: in this case, the receiver can decide if it is relevant to use it or not:
    - For carrier tracking, the integration time might be too long for the loop to be stable: it is important to know what are the expected signal dynamics and clock drift over the integration time
    - For code tracking, it is usually relevant as the signal dynamics are absorbed by the carrier tracking → the tracking performances can then be improved (reduced cross-correlation issues, improved resistance against thermal noise and narrow-band interference)

### 3. Conclusions on Secondary Codes

- Advantages:
  - Provides better resistance against narrow band interference
  - To be able to take full advantage of the secondary code, it is necessary to use a correlation over the whole secondary code
- Drawbacks
  - Complicates slightly the acquisition
  - Requires a long coherent integration

## Content

- I. Reminder on Receiver Signal Processing
- II. Binary Offset Carrier (BOC) Modulation
  - Description and characteristics
  - Impact on acquisition and tracking
- III. Secondary Code
  - Description and characteristics
  - Impact on acquisition and tracking
- IV. Data/Pilot Architecture
  - Description and characteristics
  - Impact on acquisition and tracking
- V. Galileo Signal Structure
  - Galileo services
  - Galileo civil signals' characteristics

## 4. Data/Pilot Architecture

- Legacy GPS signals use only one signal to carry the navigation data and the synchronization sequence to the user.
- It is well known that due to the navigation data, carrier tracking can only be done using a Costas loop rather than a true PLL
  - The PLL phase discriminator has to be insensitive to the data bit transition. This creates a reduction of the discriminator stable tracking region (lock points every 180°)
- The use of a data-less, or pilot, component would result in the use of a true PLL that increases the PLL tracking sensitivity by approx. 6dB

## 4. Data/Pilot Architecture

- Because the navigation message has to be transmitted, 2 components are then necessary: a data and a pilot signal
  - Two orthogonal spreading codes are used to be able to distinguish between the data and pilot components (and avoid interference).
  - The power of the overall signal has to be split between the 2 components
  - For a 50%/50% power split:
    - The carrier tracking is still improved (3dB loss due to the power split, but 6dB gain due to the use of a true PLL)
    - The data demodulation performance ( $E_b/N_0$ ) is decreased → in order to recover from this loss, the navigation data is usually better encoded
  - The signal model at baseband is then:

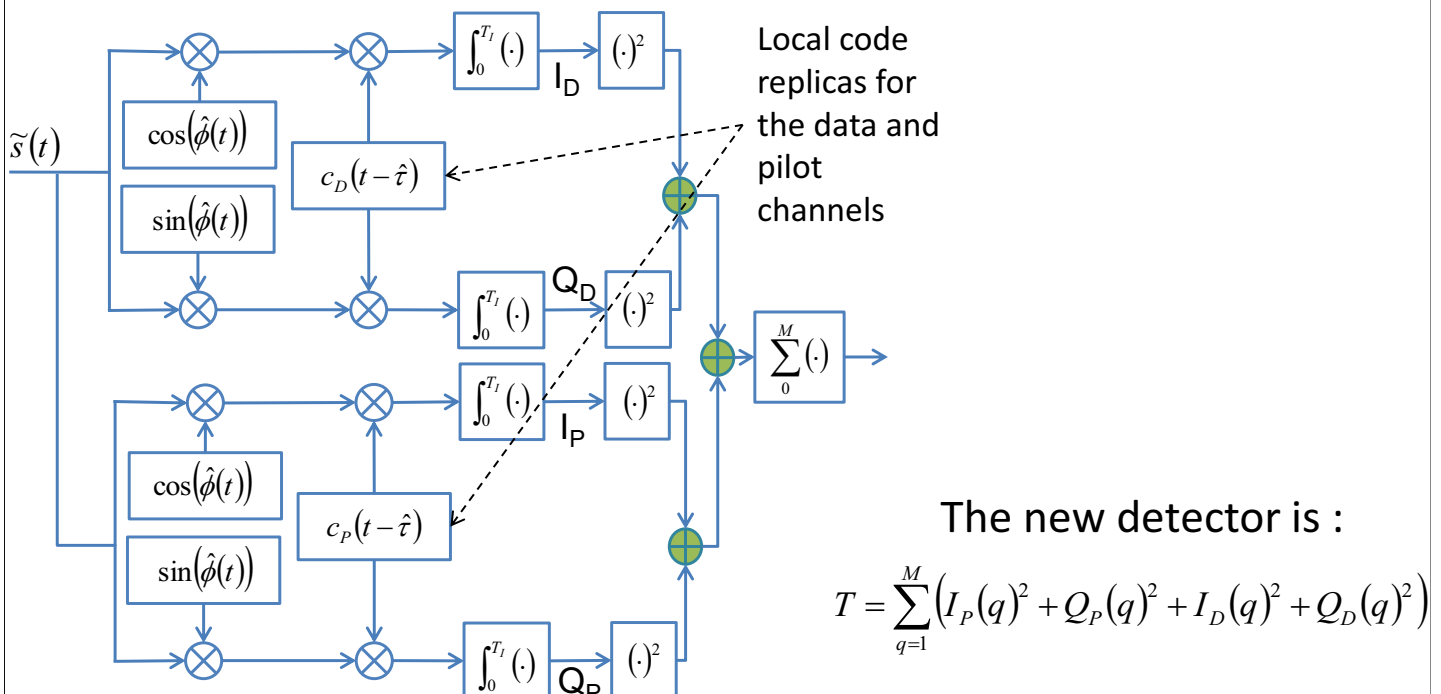
$$s_{BB}(t) = (\gamma d(t)c_D(t) + \beta c_P(t)) \text{ with } \gamma^2 + \beta^2 = 1$$

## 4. Impact of Data/Pilot on Acquisition

- Since the power is split between the data and pilot components, the receiver can:
  - acquire the signal based on both data and pilot components to gather the whole signal power
    - In order to combine both channels easily, the coherent integration is done over the length of one code repetition, or one data bit.
  - acquire the signal based only on the pilot component
    - Because there is no data, possibility to use longer coherent integrations. However, the pilot component almost always contains a secondary code that acts like unknown data before synchronization, thus limiting the coherent integration time.

## 4. Impact of Data/Pilot on Acquisition

- Combined Data/Pilot Acquisition



## 4. Impact of Data/Pilot on Carrier Tracking

- The presence of the pilot channel allows the use of a true PLL:
  - New phase discriminators can be used such as

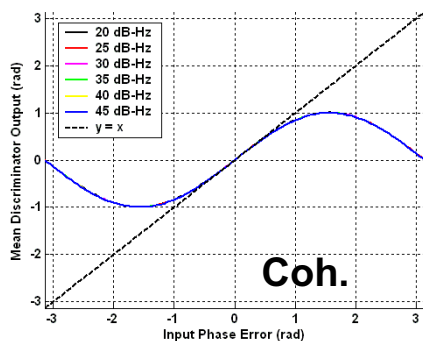
• Q

$$D_{Coh} = Q_P = \sqrt{\frac{C_p}{2}} \tilde{R}_{I,L}(\Delta\tau) \sin(\Delta\varphi) \xrightarrow{\varepsilon_\phi \rightarrow 0} \sqrt{\frac{C_p}{2}} \tilde{R}_{I,L}(\Delta\tau) \Delta\varphi$$

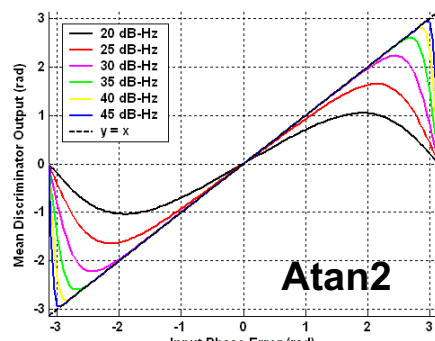
Power of the useful pilot channel  
 $C = C_D + C_P$

• Extended Arctangent

$$D_{\text{Atan2}} = \text{Atan2}(Q_P, I_P) = \Delta\varphi$$



Coh.



Atan2

Discriminator shape influences ( $T_I = 4$  ms)

Higher resistance to signal dynamics for pilot discriminator

## 4. Impact of Data/Pilot on Tracking

- The presence of a pilot channel allows the use of long coherent integrations:
  - Long coherent integrations help better filter thermal noise and slowly varying multipath and interf. from the correlator outputs
  - Reduction of the squaring losses in the code tracking jitter formula
- Even with a pilot channel, it is in general not possible to use long integration to track the phase (the tracking error due to the user/clock dynamics should not become too large during the correlation operation)
- In order to reduce receiver complexity, it is common to use only the pilot channel for phase tracking (pure PLL). The data demodulation is then done using only one correlator on the data channel

## 4. Conclusions on Data/Pilot Architecture

- Advantages:
  - Use of 1 signal that is dedicated to ranging. No drawback from the presence of the navigation data
  - The correlation time can be extended → better sensitivity of the receiver
- Drawbacks
  - The power is split between the 2 channels. Thus there is less power on each channel → a better encoding of the data is required in order not to increase the BER.

## Content

- I. Reminder on Receiver Signal Processing
- II. Binary Offset Carrier (BOC) Modulation
  - Description and characteristics
  - Impact on acquisition and tracking
- III. Secondary Code
  - Description and characteristics
  - Impact on acquisition and tracking
- IV. Data/Pilot Architecture
  - Description and characteristics
  - Impact on acquisition and tracking
- V. Galileo Signal Structure
  - Galileo services
  - Galileo civil signals' characteristics

## 5. Galileo Services

- 5 services will be provided by Galileo:

- **Open Service:**

- Provides PVT free-of-charge for mass market users
- Expected performances

	Single carrier			Dual carrier	
	L1 B/C	E5a	E5b	E5a - L1 B/C	E5b - L1 B/C
Positioning Horizontal accuracy (95%)	15 m	24 m	24 m	4 m	4 m
Positioning Vertical accuracy (95%)	35 m	35 m	35 m	8 m	8 m
Velocity accuracy (95%)	20 cm/s	20 cm/s	20 cm/s	20 cm/s	20 cm/s
Mean availability	99.5 %	99.5 %	99.5 %	99.5 %	99.5 %
Coverage	global				

- **Commercial Service:**

- Not yet fully defined. Trend is: Same as OS + encrypted signal providing higher accuracy and authentication;
- Not free-of-charge

## 5. Galileo Services

- **Safety-of-Life Service:**

- Same as OS + integrity service.
- This service will be offered to the safety-critical transport communities e.g. aviation.
- This service is currently being re-profiled

- **Public Regulated Service:**

- 2 specific signals providing PVT+integrity service+security service
- Signals are encrypted with controlled access for specific users like governmental bodies;

- **Search And Rescue Service:**

- Contribution to the international COSPAS-SARSAT cooperative system for humanitarian search and rescue activities
- Satellite-based transfer of the distress signals from the user to the Rescue Coordination Centre and acknowledging this action

## 5. Link Between Signals and Services

- 4 navigation messages:
  - F/NAV: basic parameters to support OS (only on E5a),
  - I/NAV: basic parameters + integrity to support SoL (on E1F and E5b),
  - C/NAV: includes commercial data to support CS (only on E6C),
  - G/NAV to support the PRS (only on E6P and E1P)

- 6 signals:

Signals	OS users	SOL users	CS users	PRS users
E1F	X*	X*	X	
E1P				X
E5a	X		X	
E5b	X*	X*	X	
E6C			X	
E6P				X

\* with no access to encrypted commercial data

## 5. Galileo E1F

- Designed for mass-market and safety critical applications
- Same carrier frequency as GPS L1 C/A (=1575.42 MHz).
- Part of an Aeronautical RadioNavigation Service (ARNS) band: can be used by civil aviation
- Multiplexed BOC modulation for compatibility with GPS L1c and minimal spectral overlap with existing signals. Galileo E1F uses a Composite BOC (CBOC) modulation as an implementation of the MBOC (GPS L1c uses TMBOC)
- 2 components in quadrature (CBOC modulation):
  - 1 data component (50%) that carries the navigation message.
  - 1 pilot component (50%) that includes a secondary code
- Participates to OS/SoL/CS services (carries the I/NAV)
  - Fast data rate (125 bps, 250 sps) in order to transmit the integrity message, which includes the use of a convolutional coding (rate ½ with a constraint length of 7)

## 5. Galileo E1F

Temporal expression:

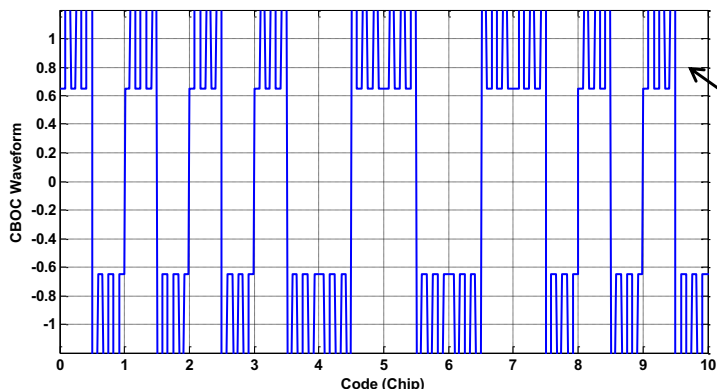
$$s_{E1}(t) = \frac{1}{\sqrt{2}} \left( c_{E1-B}(t) d_{E1-B}(t) CBOC_{(6,1,1/11^+)}(t) - c_{E1-C}(t) c_{Sec,E1-C}(t) CBOC_{(6,1,1/11^-)}(t) \right)$$

50%/50% data/pilot power share

where

$$CBOC_{(6,1,1/11^+)}(t) = \sqrt{10/11} BOC_{(1,1)}(t) + \sqrt{1/11} BOC_{(6,1)}(t)$$

$$CBOC_{(6,1,1/11^-)}(t) = \sqrt{10/11} BOC_{(1,1)}(t) - \sqrt{1/11} BOC_{(6,1)}(t)$$



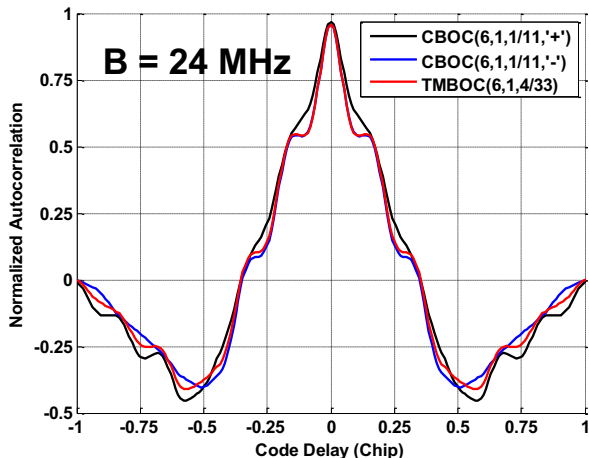
The BOC(6,1) sub-carrier modulates every chip of the data and pilot channels

4-level signal

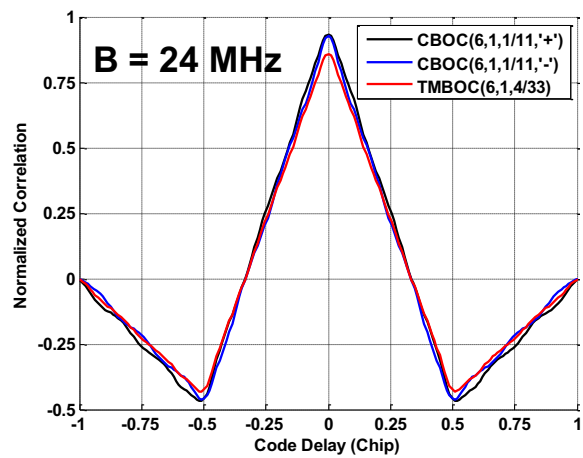
CBOC(6,1,1/11,'-) sub-carrier time representation

## 5. Galileo E1F

- Reception using a CBOC receiver → front-end filter with a minimum double-sided bandwidth of 14 MHz and a CBOC local replica
- Reception using a BOC(1,1) receiver → front-end filter with a minimum double-sided bandwidth of 4 MHz and a BOC(1,1)



Correlation Function (reception using CBOC)



Correlation Function (reception using BOC(1,1))

## 5. Galileo E5

- The E5a and E5b signals are wide-band signals transmitted in adjacent bands, supporting different services:
  - E5a is located at 1176.45 MHz (same as GPS L5) and supports the OS only (F/NAV)
  - E5b is located at 1207.17 MHz and supports the OS/SoL/CS (I/NAV)
- E5a and E5b are located in an ARNS band without exclusivity to GNSS (presence of pulsed interference: DME/TACAN, JTIDS/MIDS)
- E5a and E5b signals are transmitted coherently as one very wide-band (50 MHz) signal. This allows:
  - A simplified payload architecture (the signal uses only one transmission chain)
  - The possibility to process:
    - E5a and/or E5b separately if only one service is required
    - E5a and E5b (as one signal) together for enhanced performance
- E5a and E5b use an ALTernative BOC (ALTBOC) scheme

## 5. Galileo E5 ALTBOC

«sub-carrier» freq.  
chipping rate

- The Galileo E5 ALTBOC(15,10) baseband model is:

$$s_{ALTBOC(15,10)}(t) = \frac{1}{4} \left\{ \begin{array}{l} \left[ (c_{E5a}^D(t)c_{E5a,Sec}^D(t)d_{E5a}(t) + j \cdot c_{E5a}^P(t)c_{E5a,Sec}^P(t)) \cdot [sc_{as}(t) - j \cdot sc_{as}\left(t - \frac{T_s}{4}\right)] \right] \\ + \left[ (c_{E5b}^D(t)c_{E5b,Sec}^D(t)d_{E5b}(t) + j \cdot c_{E5b}^P(t)c_{E5b,Sec}^P(t)) \cdot [sc_{as}(t) + j \cdot sc_{as}\left(t - \frac{T_s}{4}\right)] \right] \\ + \left[ (c_1(t) + j \cdot c_2(t)) \cdot [sc_{ap}(t) - j \cdot sc_{ap}\left(t - \frac{T_s}{4}\right)] + (c_3(t) + j \cdot c_4(t)) \cdot [sc_{ap}(t) + j \cdot sc_{ap}\left(t - \frac{T_s}{4}\right)] \right] \end{array} \right\}$$

Useful signal

IM

where

$c_1, c_2, c_3, c_4$  are the product of several spreading codes

$sc_{as}, sc_{ap} \rightarrow$  see next slide

## 5. Galileo E5 ALTBOC Subcarriers

- The useful power is equally shared between the 4 components

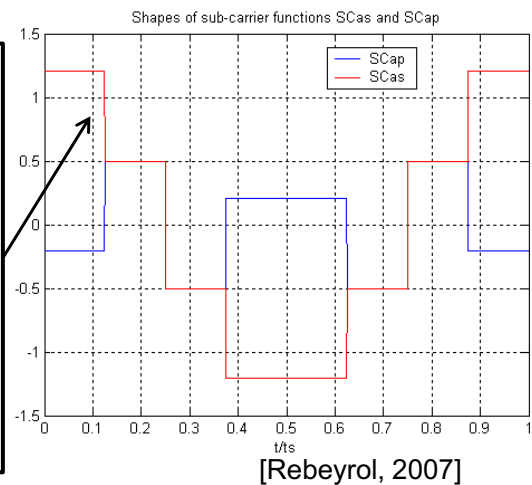
$SC_{as}$  looks like a quantized sine wave, thus

$$sc_{as}(t) - j \cdot sc_{as}\left(t - \frac{T_s}{4}\right)$$

approximation of an exponential function at frequency  $-f_s \rightarrow$  lower side-lobe

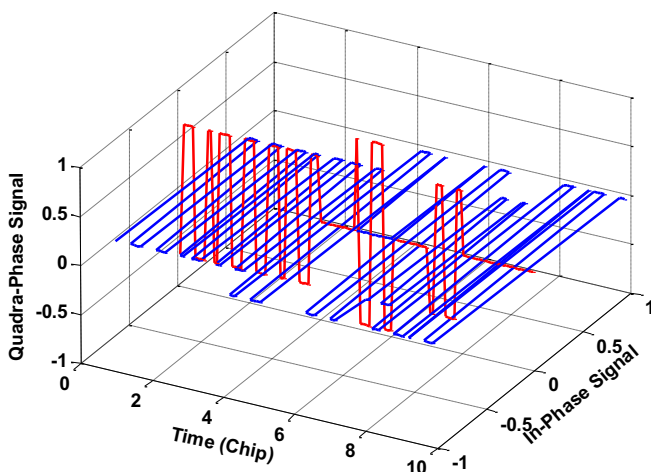
$$sc_{as}(t) + j \cdot sc_{as}\left(t - \frac{T_s}{4}\right)$$

approximation of an exponential function at frequency  $+f_s \rightarrow$  upper side-lobe

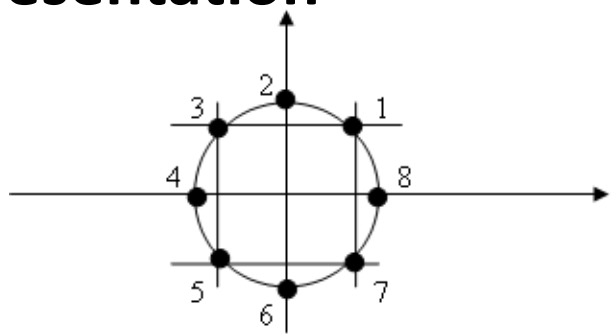


- The Inter-Modulation (IM) term is necessary to have a constant envelope signal  $\rightarrow$  It induces a loss of useful power

## 5. Galileo E5 ALTBOC Representation

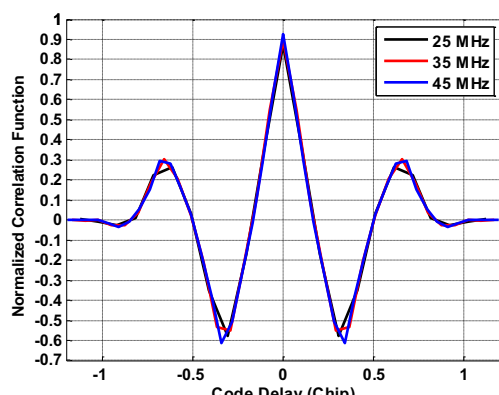


ALTBOC Time Representation



Constant Envelope ALTBOC  
(8-plot Constellation)

ALTBOC Correlation Function



## 5. Galileo Civil Signals Summary

Longer code length wrt GPS C/A for improved correlation isolation

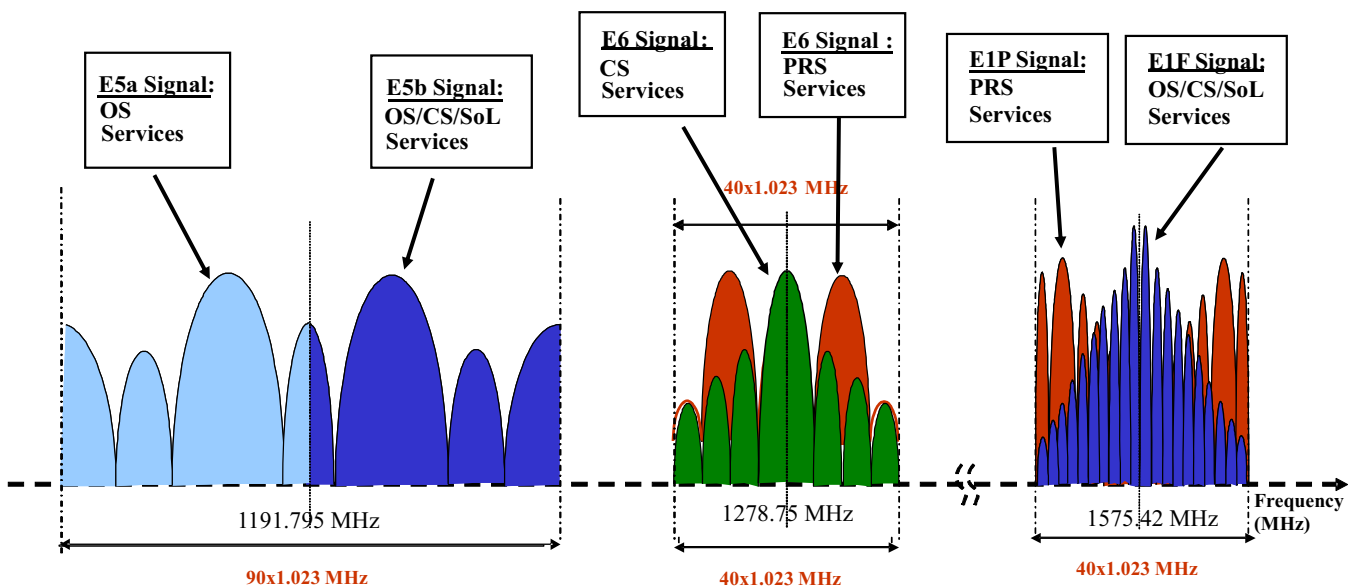
Chipping rate higher than that of GPS C/A for improved performance

Faster data rate than GPS C/A (use CC) and use of pilot

Use of secondary codes

Signal	Code Length	Chip Rate (Mcps)	Modulation	Navigation Data (sps)	Sec. code length	Total code (ms)
E5a-I	10230	10.23	AltBOC(15,10)	50	<b>20</b>	20
E5a-Q	10230	10.23		Pilot	<b>100</b>	100
E5b-I	10230	10.23		250	<b>4</b>	4
E5b-Q	10230	10.23		Pilot	<b>100</b>	100
E1F(B)	4096	1.023/6.138	CBOC(6,1,1/11)	250	<b>None</b>	None
E1F(C)	4096	1.023/6.138		Pilot	<b>25</b>	100
E6C-I	N/A	5.115	BPSK(5)	1000	<b>N/A</b>	N/A
E6C-Q	N/A	5.115	BPSK(5)	Pilot	<b>N/A</b>	N/A

## 5. Galileo Spectral Occupation



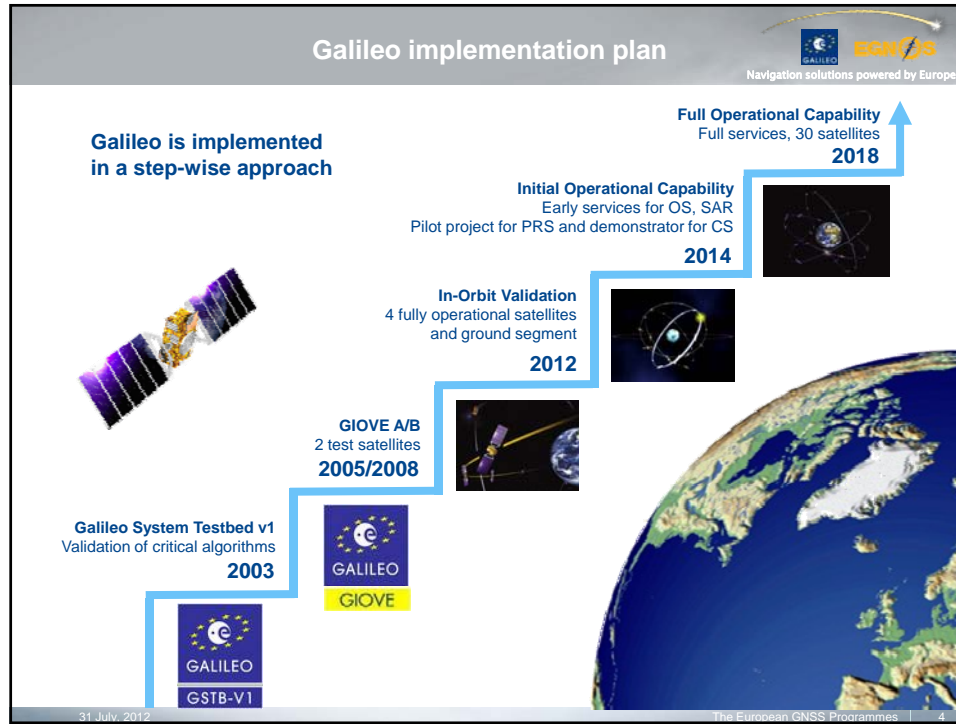
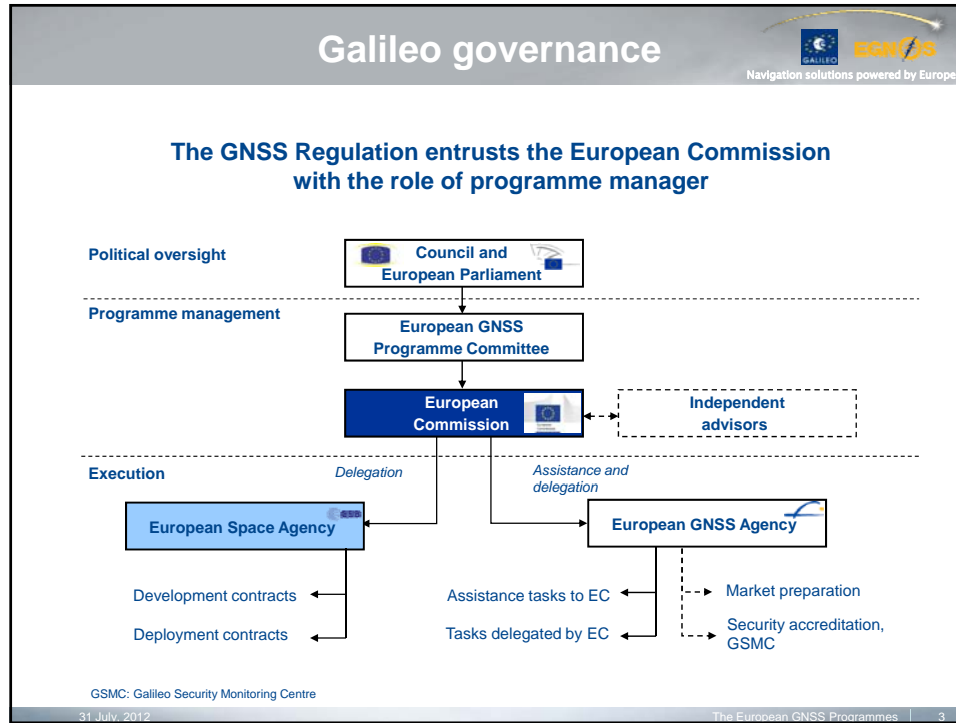


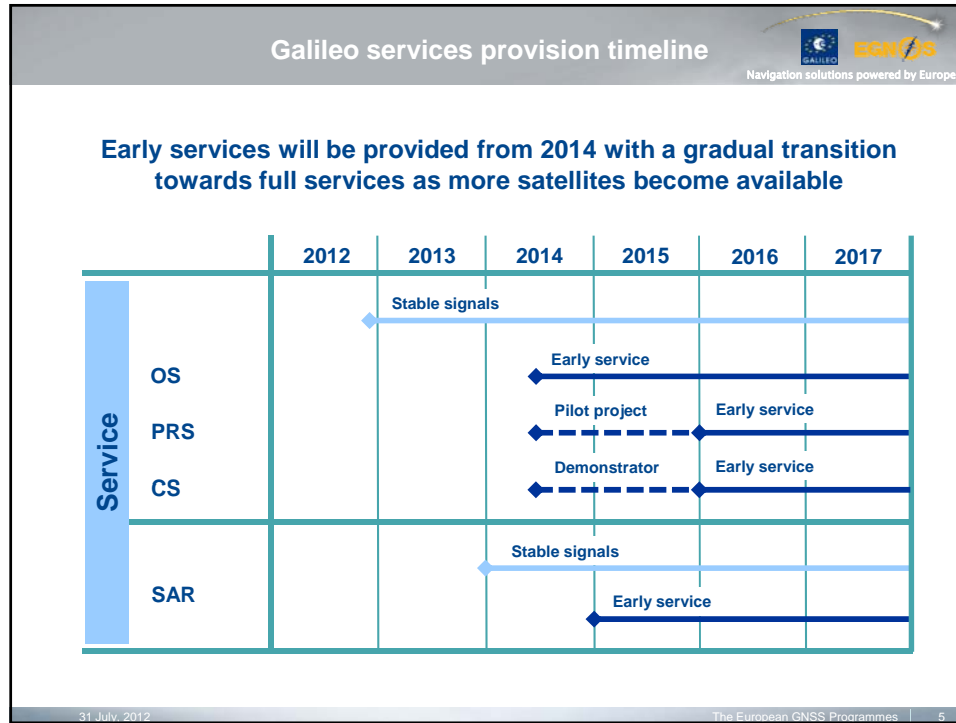


## The European Satellite Navigation Programmes

### EGNOS and Galileo







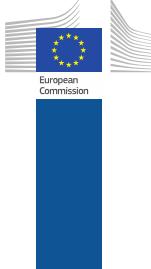
**Galileo is taking off**



**EGNOS**  
Navigation solutions powered by Europe

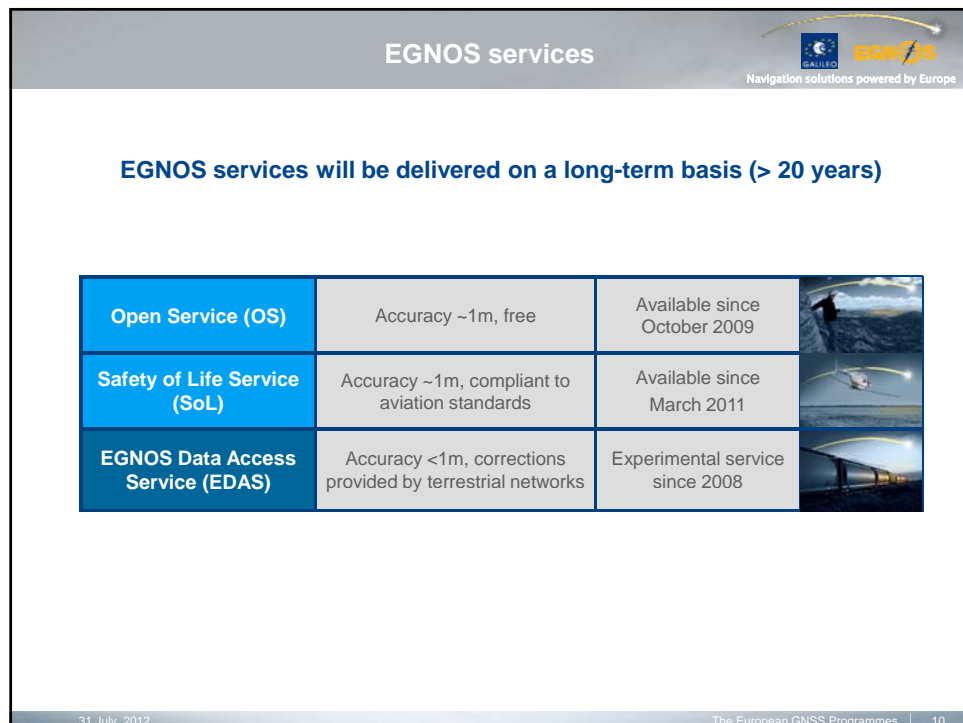
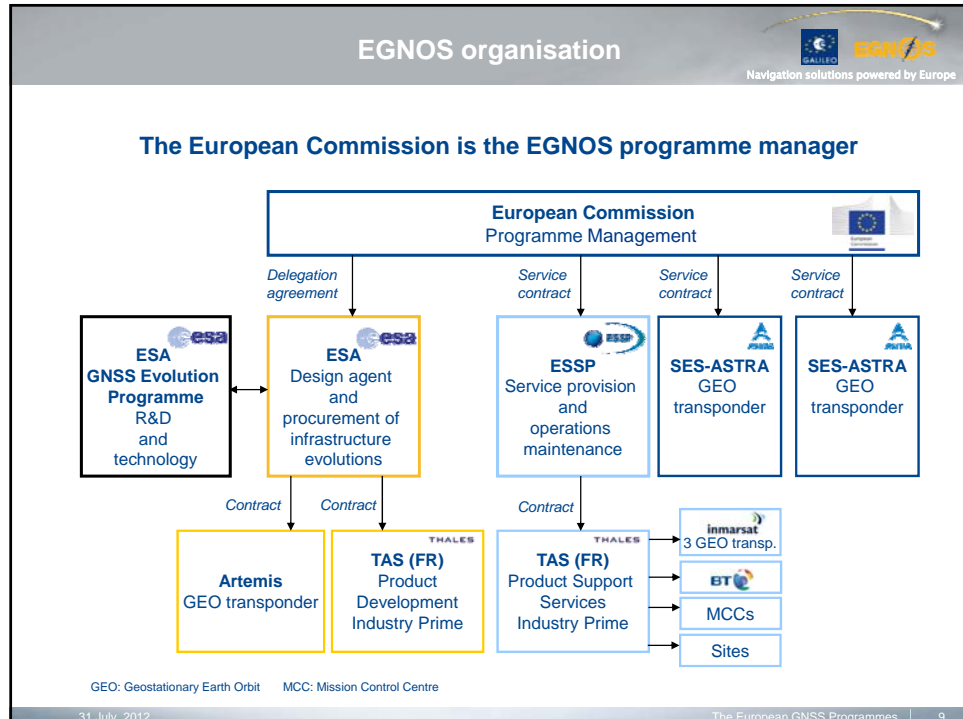
- ★ The first 2 **operational satellites** have been launched on 21 October 2011 (in addition to the two test satellites launched in 2005 and 2008)
- ★ The launch of the next two Galileo satellites, completing the IOV quartet, is scheduled for **September 2012**.
- ★ All **industrial contracts** necessary to ensure early Galileo services in 2014 have been signed
- ★ To **accelerate Galileo's deployment** and to further contain costs, the following contracts were signed on 2 February 2012:
  - ★ Additional order for 8 satellites
  - ★ Adaptation of Ariane-5 for Galileo
  - ★ Booking of one Ariane-5

31 July, 2012 | The European GNSS Programmes | 7



**EGNOS**  
*'It's there, use it'*

31 July, 2012 | The European GNSS Programmes | 8

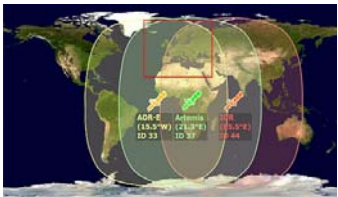


**EGNOS is fully operational**


  
Navigation solutions powered by Europe

- ★ **EGNOS open service is operational**  
since October 2009
- ★ Its **Safety of Life** service has been declared operational in March 2011
- ★ In May 2011, Pau Pyrénées airport (France) became **Europe's first airport to use the EGNOS Safety of Life service** to guide in aircraft for landing
- ★ Since December 2011, the EGNOS-based LPV procedures at Alderney airport (Channel Islands) are the first in Europe able to be used for **revenue services in commercial flights**
- ★ Around **100** EGNOS approach procedures for aircraft landings already published in Europe
- ★ 'Launch of the new EGNOS payload has been delayed (due to Proton failure) until late summer'



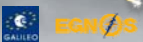


LPV: Localizer Performance with Vertical guidance

31 July, 2012

The European GNSS Programmes | 11

**EGNOS outlook**


  
Navigation solutions powered by Europe

**EGNOS services will further improve over time**

**2012**

- ★ Declare EGNOS coverage extension for 11 EU countries\*
- ★ Provide early EGNOS Data Access Service (EDAS)

**Medium term**

- ★ Implement LPV200 service level
- ★ Extend coverage to South Africa

**Long term**

- ★ Make use of E5a/E5b frequencies
- ★ Implement augmentation of Galileo and potentially other GNSS

LPV: Localizer Performance with Vertical guidance

\* CZ, EE, HU, IE, LV, LT, PT, RO, SK, ES, UK

31 July, 2012

The European GNSS Programmes | 12

# GNSS Interference

Heidi Kuusniemi

*JRC Summer School on  
GNSS Core Technologies*

Ispra, Italy 2-4 July, 2012



[Heidi.Kuusniemi@fgi.fi](mailto:Heidi.Kuusniemi@fgi.fi)

## Content



- Introduction
- GNSS vulnerabilities
- Types of interference
- GNSS jammers
- Effects of jammers on consumer receivers
  - Analysis of two jammers
  - Test results: performance of consumer-grade receivers in the presence of single- and dual-frequency jamming

## Introduction (1)



- **Deliberate and dangerous jamming:**

- In late 2009 engineers noticed that satellite-positioning receivers for navigation aiding in airplane landings at Newark airport were suffering from brief daily breaks
- It took two months for investigators from the Federal Aviation Authority to track down the problem
  - A driver who passed by on the nearby highway each day had a cheap GPS jammer (< 30 USD) in his truck
  - A jammer prevents a tracking device in the vehicle from determining and reporting location and speed, but it also disrupts GPS signals for others nearby
  - The driver objected his employers tracking his every move
  - Jammer ≈ “personal privacy device”?

*“GPS jamming: No jam tomorrow”,  
The Economist, 2011*



## Introduction (2)



- Using jammers is illegal in most countries
- Systems all over the world have been created to detect jamming/interference
  - e.g. GAARDIAN in Britain, JLOC in the US
- Interference in Newark airport is still observed as often as several times per day
  - the mitigations applied thus far have however reduced the frequency of incidents strong enough to affect navigation aiding in landings to several per week on average
- It has also been suggested that legislation is changed so that all smartphones would be required to search for jammers nearby and warn others in the vicinity
  - Crowd-sourcing for interference detection?
- Also terrestrial beacons, back-ups to GNSS, are again gaining importance



S. Pullen, G. Gao, “GNSS Jamming in the Name of Privacy”, Inside GNSS, March/April 2012, 34-43.

## GNSS vulnerabilities (1)

- The signals from GNSS satellites are very weak by the time that user equipment receives and processes them
  - they are especially vulnerable to radio frequency interference
- The minimum received power is

GPS L1 C/A code: -128.5 dBm

Galileo E1: -127 dBm

*F. Dovis, "Recent trends in  
Interference Mitigation  
and Spoofing Detection", ICL  
GNSS 2011, Tampere, Finland,  
30/06/2011*

## GNSS vulnerabilities (2)

- Unintentional interference
  - Free electrons in the ionosphere act as a retardant and accelerative force on the GPS code and carrier phase measurements respectively
    - Massive solar flares can cause GPS devices to lose signals
  - Terrestrial in-, near-, and out-of-band interference, as well as spurious emissions and/or harmonic interference from other systems, may disrupt GPS signal reception
    - TV and telecommunications signals
      - secondary harmonics from DVB-T (digital video broadcasting - terrestrial) might fall in the GNSS bands
    - the recent LightSquared Inc. incident in the USA (a 4G LTE wireless broadband network) that was finally banned due to GPS interference

## GNSS vulnerabilities (3)

Interference type	Telecommunication Systems	GNSS bands
Aeronautical communication systems	Distance measuring Equipment Tactical Air Navigation Secondary Surveillance Radar Multifunctional Information Distribution System Joint Tactical Information Distribution System Traffic Collision and Avoidance System Identity Friend and Foe Automatic Dependent Surveillance-broadcast	Galileo E5a E5b GPS L5
Radar	Air traffic control radar Solid state radar	Galileo E6 GPS L2
Satellite communication systems	Mobile Satellite Service	close to GPS L1
Secondary harmonics	TV channels Digital Video Broadcasting	Galileo E1 GPS L1
Other	Personal Electronic Devices Ultra Wide Band Systems VHF Omni-directional Range harmonics Instrument Landing System harmonics	all

F. Dovis, "Recent trends in Interference Mitigation and Spoofing Detection", ICL GNSS 2011, Tampere, 30/06/2011

## GNSS vulnerabilities (4)



### • Intentional interference

- Signals from such devices are regarded as intentional interference that intentionally send radio-frequency signals with high enough power and specific signal properties to prevent or hinder/complicate signal tracking in a specific geographical area
  - Jamming
    - any radio frequency interference signals that deteriorate GNSS reception and accuracy
  - Spoofing
    - attempts to deceive a GPS receiver by broadcasting a more powerful signal than that received from the satellites, structured to resemble a set of normal GPS signals
      - causes the receiver to determine its position to be somewhere other than where it actually is
  - Meacking or replay of recorded GNSS signals



## Interference classification (1)

- Interference signals can be classified according to their spectral and time features with respect to the GNSS signal
  - Continuous wave (CW) interference
  - Narrowband ( $B_{\text{interference}} \ll B_{\text{GNSS}}$ ) interference
  - Wideband ( $B_{\text{interference}} \approx B_{\text{GNSS}}$ ) interference
  - Pulsed interference
- The interference signal power should exceed the satellite signal power significantly in order to unbalance signal tracking
- Usage of jammers is illegal in almost all countries
- Typical use-cases of jammers are in cars, and they usually operate on the civilian L1/E1-band
  - Motivation behind: protection of location disclosure in e.g. road tolling, insurance billing, tracking of goods and people

## Interference classification (2)

- Typical jamming signal classification:
  - Class I: Continuous wave signal
  - Class II: Chirp signal with one saw-tooth function
  - Class III: Chirp signal with multi saw-tooth functions
  - Class IV: Chirp signal with frequency bursts
- The higher power jamming signal, the more damage will be caused and the further it will reach (typically  $> 30-40$  dB)

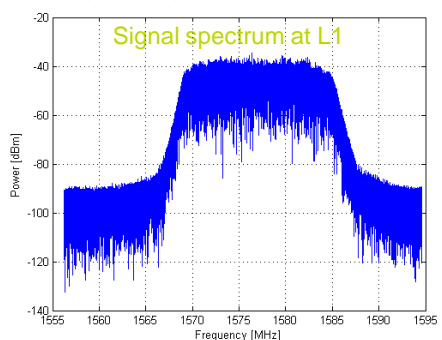
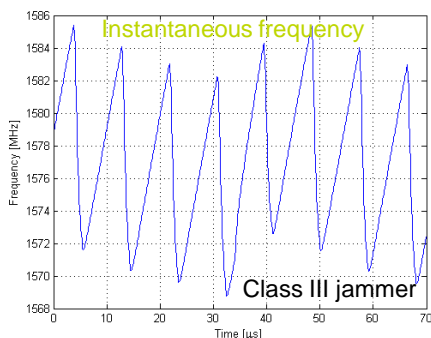


# Effects of jamming

- Jamming deteriorates the positioning solution accuracy or alternatively totally loses the satellite signals and thus impairs the positioning availability
  - Jamming affects the positioning receiver's carrier-to-noise ratio  $C/N_0$  (dBHz)
- The effect of jamming can resemble receiving attenuated and multipath-deteriorated signals of dense urban areas: the signal to noise ratio decreases and the GNSS signal to be received gets weaker and weaker
- GNSS receivers react differently to jamming
  - The basic principle of GNSS receivers are the same but their internal processes and filters may mitigate the effect of a jamming signal being present differently

## Analyzed jammers (1)

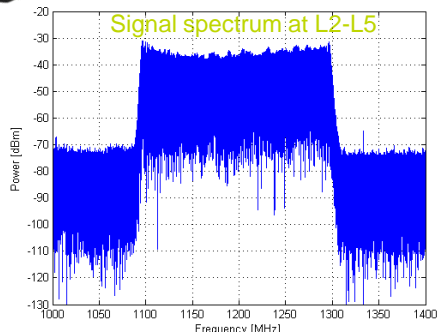
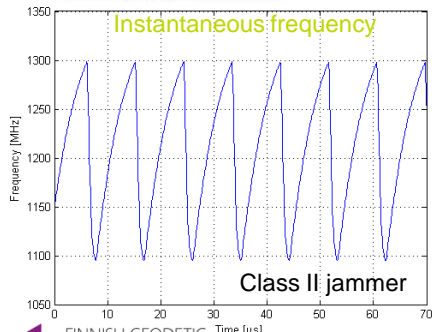
Covert GPS L1 jammer (14 \$):  
with special permission from the  
Finnish  
Communications Regulatory Authority,  
restricted to -30 dBm  
(nominal 13 dBm)



## Analyzed jammers (2)



GPS L2-L5 TG-120D jammer (130 \$):  
with special permission from the  
Finnish  
Communications Regulatory Authority,  
restricted to -30 dBm  
(nominal 33 dBm)



FINNISH GEODETIC  
INSTITUTE

Heidi.Kuusniemi@fgi.fi

13

## Test results (1)

- The effects of the jammers on consumer grade GPS receivers were analyzed in a confined navigation laboratory at the Finnish Geodetic Institute
- Positioning solutions were analyzed with and without the jammers on 24 hours consecutively in the single-frequency case, and in shorter time steps with a dual-frequency receiver
- GNSS receivers:
  - uBlox 5H and 5T
  - Fastrax IT500 and IT600
  - GPS inside Nokia N8
  - NovAtel OEM 4 (L1/L2)

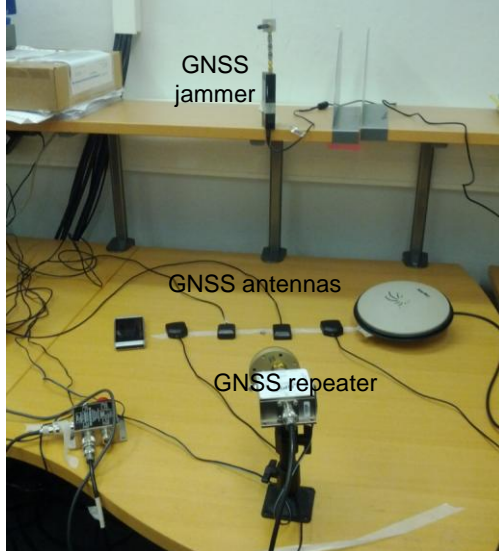


FINNISH GEODETIC  
INSTITUTE

Heidi.Kuusniemi@fgi.fi

14

## Test results – single-frequency (1)



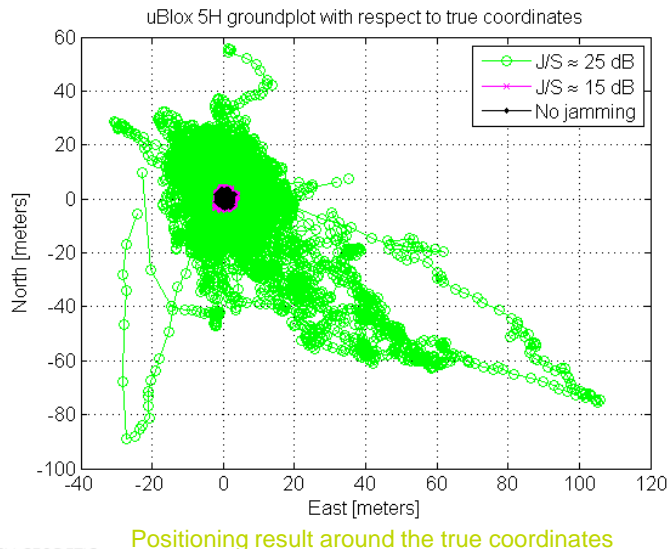
## Test results – single-frequency (2)

- Single-frequency L1
- 24-h static tests to assess the effects of the jamming signal on consumer grade receivers
- Jamming-to-signal ratio 15 dB and 25 dB
- The maximum horizontal error was increased and positioning solution availability decreased when the jamming signal power was increased

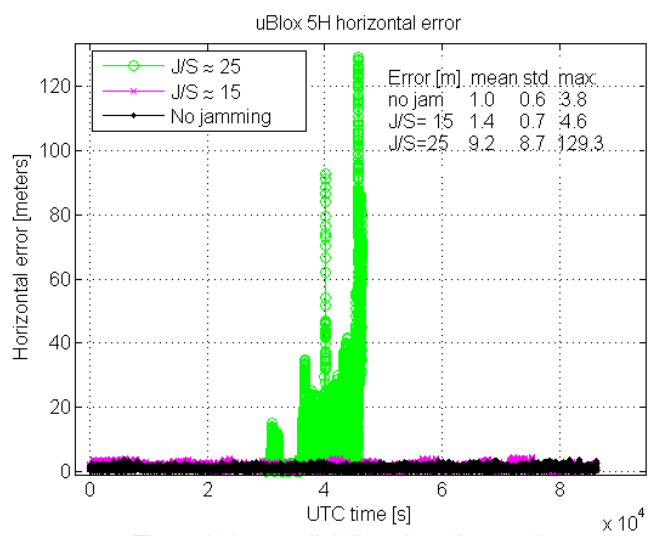


		Mean (m)	Std (m)	Max (m)	%
uBlox 5H	no jam	1.0	0.6	3.8	100
	max J/S≈15 dB	1.4	0.7	4.6	100
	max J/S≈25 dB	9.2	8.7	129.3	16
uBlox 5T	no jam	1.0	0.6	4.0	100
	max J/S≈15 dB	1.5	0.8	6.5	100
	max J/S≈25 dB	4.2	5.5	94	26
Fastrax IT500	no jam	2.2	1.0	5.3	100
	max J/S≈15 dB	2.3	1.0	6.5	100
	max J/S≈25 dB	3.7	5.2	85.4	16
Fastrax IT600	no jam	1.3	0.6	3.2	100
	max J/S≈15 dB	1.3	0.7	3.2	100
	max J/S≈25 dB	5.9	3.6	16.4	100
Nokia N8 GPS	no jam	2.6	2.4	32.4	100
	max J/S≈15 dB	3.1	3.8	34.0	100
	max J/S≈25 dB	3.9	2.2	22.4	16
NovAtel	no jam	1.0	0.7	4.8	100
	max J/S≈15 dB	2.4	3.9	90.5	30
	max J/S≈25 dB	5.4	7.3	92.1	8

## Test results – single-frequency (3)

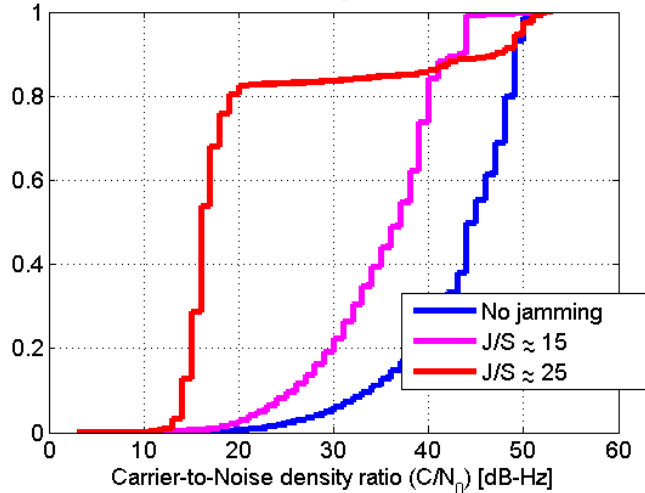


## Test results – single-frequency (4)



## Test results – single-frequency (5)

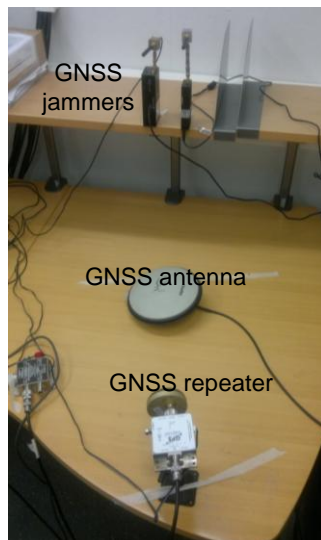
Cumulative distribution of signal-to-noise ratios, IT600



Similar performances were observed  
for the other tested receivers

19

## Test results – dual-frequency (1)



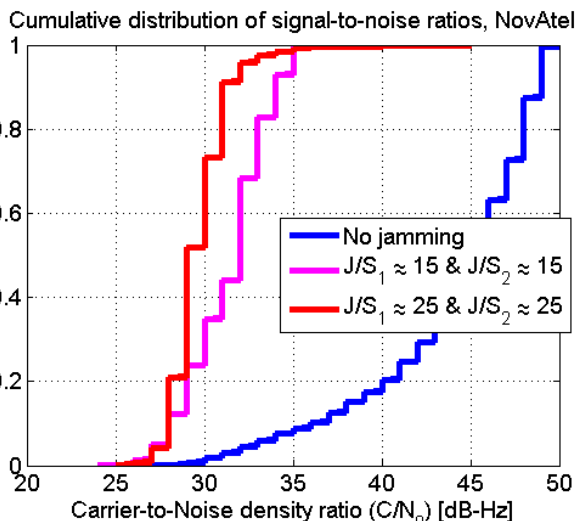
## Test results – dual-frequency (2)

- Both of the jammers were switched on, with a maximum J/S of around 15 dB and 25 dB in two consecutive tests
- The maximum horizontal error was increased and positioning solution availability decreased when the jamming signal powers were increased
- Only 1-hour datasets and code measurements only were, however, used in position computation

		Mean (m)	Std (m)	Max (m)	%
NovAtel L1 & L2	no jam	0.8	0.4	2.8	100
	max J/S≈15 dB	3.4	6.0	78.9	100
	max J/S≈25 dB	3.5	2.6	26.6	11



## Test results – dual-frequency (3)



Degradation in the C/N₀ of the dual-frequency signals in the dual-jammer test

## Jamming detection

- Typical mitigation approaches for civilian jamming mitigation include:
  - Antenna Solutions
    - Controlled Radiation Pattern Antenna
    - Adaptive Beamforming
  - Receiver Solutions
    - Adaptive Notch Filtering
    - Switching Frequencies (multi-GNSS / multi-frequency)
    - Integrating GNSS with INS (inertial navigation system)
    - Applying an interference suppression unit
- The jamming signals need to be detected first in order to mathematically model them and apply a mitigation approach
  - Adaptive filtering with respect to
    - Time (chirp signals)
    - Signal spectrum amplitude (narrow-band interference)

## Conclusions

- Reliable navigation functionality is imperative in more and more applications nowadays on land, sea, and air
- In-car, civilian jammers are a serious threat to the performance of consumer grade GPS receivers
  - steps must be taken against the use of jammers
- Accuracy and signal availability is significantly decreased when jamming is present
  - how much depends on what kind of a jamming signal is present and with what power
- Jamming signal detection crucial as well as reliability algorithms
- Weak signal tracking advantageous when interference present




  
**Interference Detection and Mitigation**
  
 Daniele Borio
   
 Joint Research Centre,  
 Ispra (VA), Italy



  
**GNSS SUMMER SCHOOL**  
**GNSS CORE TECHNOLOGY**  
 Summer School on  
**GNSS CORE TECHNOLOGIES**  
 July 2-4, 2012


  
**Introduction**

Strong RF interference can

- ✓ degrade the receiver performance: **increased variance** of the measurements and navigation solution, **biases** in the measurements
- ✓ **discontinue** receiver operations (frequent loss of lock)
- ✓ **prevent** the receiver to operate

**Countermeasures (at the receiver level):**

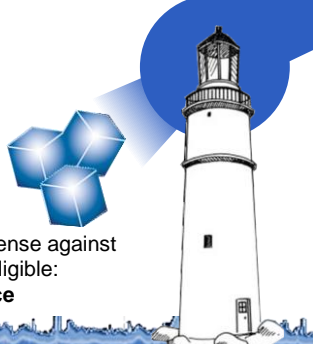
**Detection:** process of revealing the presence of interference

**Mitigation:** process of reducing the interference impact

Detection and mitigation are often implemented together

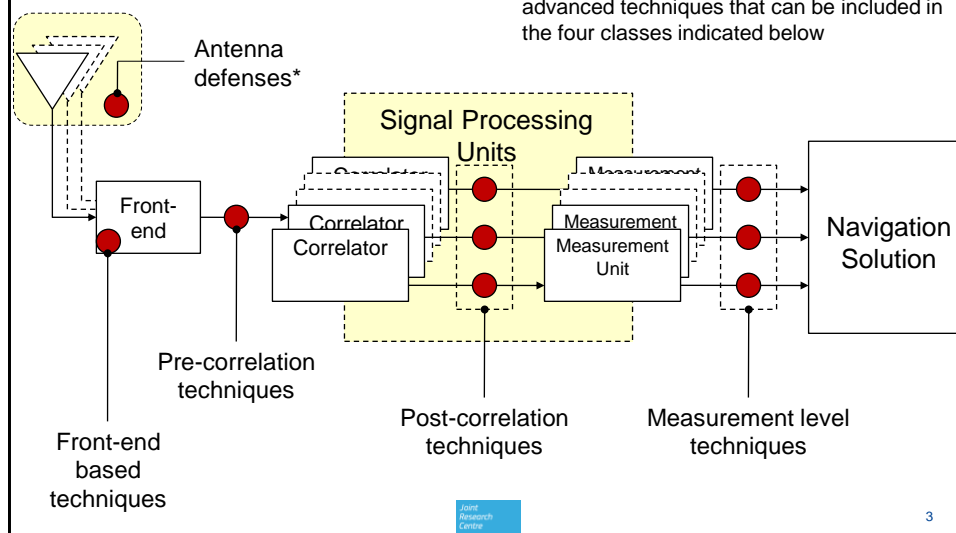
**Natural GNSS Signal Immunity:**

GNSS signals use DSSS modulations: de-spreading as natural defense against interference. Sometimes interference is present but its effect is negligible: detect (and mitigate) the interference **effect** rather than its **presence**



Joint Research Centre

## Classification (I/II)

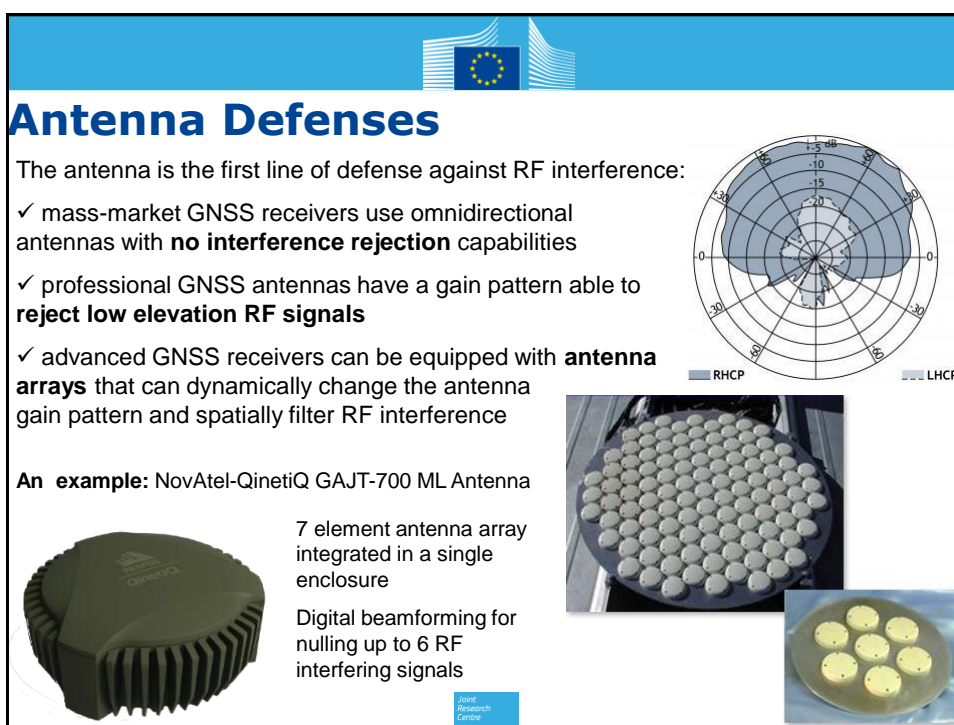
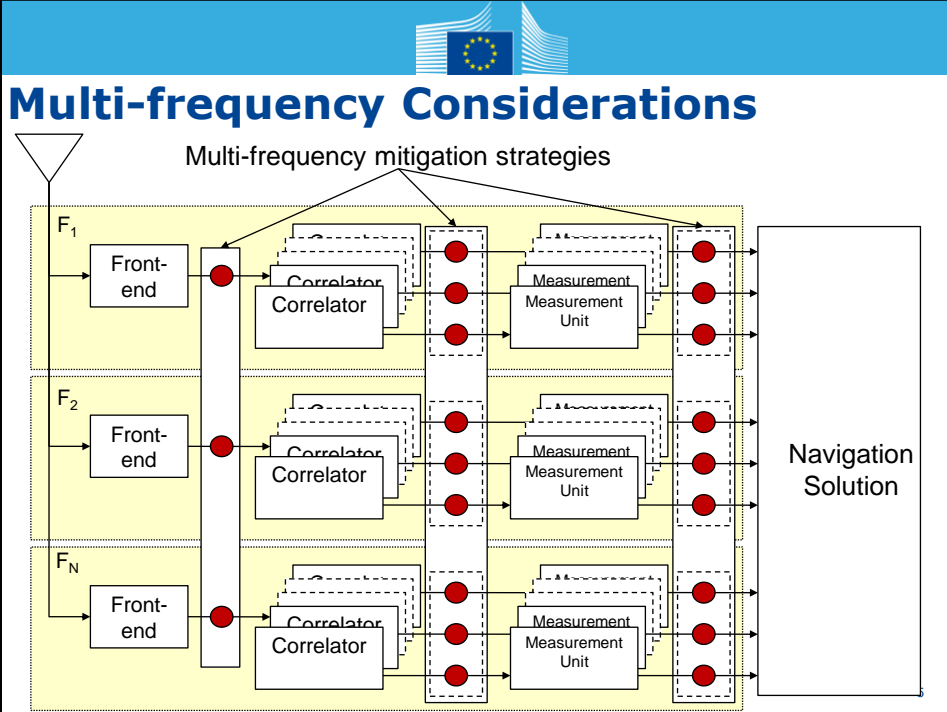


3

## Classification (II/II)

Interference detection/mitigation techniques can be implemented:

- at the **front-end level**, exploiting the characteristics of AGC and ADC
- at the **sample level** (pre-correlation techniques): the raw samples provided by the front-end are processed before entering the signal processing blocks of the receiver.
  - ✓ Notch Filter: for continuous wave removal
  - ✓ Pulse Blanking: for pulse interference removal
  - ✓ Null steering: when an antenna array is used
- at the **correlator output** (post-correlation techniques): the disturbing signal is removed at the correlator level. The same mitigation technique has to be replicated for each processing channel.
  - ✓ C/N<sub>0</sub> monitoring: the Carrier-to-Noise density power ratio of each received signal is monitored in order to detect interfering signals
  - ✓ Post-correlation beamforming when an antenna array is used
- at the **measurement level**: measurements corrupted by interference are rejected and not used in the navigation level (not considered here)
  - ✓ Reliability analysis





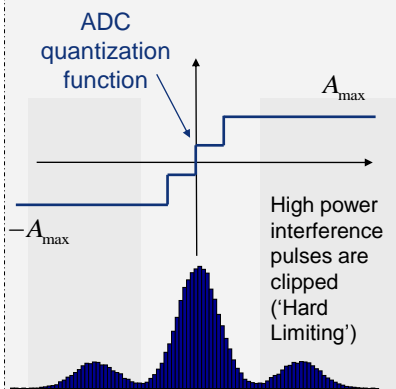
## Front-end vs. Interference

Interference can have a severe impact on the front-end

- ✓ mixing and down-conversion: spurious and inter-modulation products
- ✓ Quantization: generation of harmonics
- ✓ ADC saturation: the interfering signal is always represented using the highest/lowest level of the quantization function
- ✓ Front-end captured by a strong interfering signal

Conversely, a good filtering/ amplification chain can reduce the interference impact

In some cases, the receiver front-end can provide an additional 'natural immunity' against certain interference types: pulsed interference mitigated by ADC saturation



See JRC report "Impact of Pseudolite Signals on Non-Participating GNSS Receivers: Modeling Receiver Losses" <sup>7</sup>

Joint Research Centre

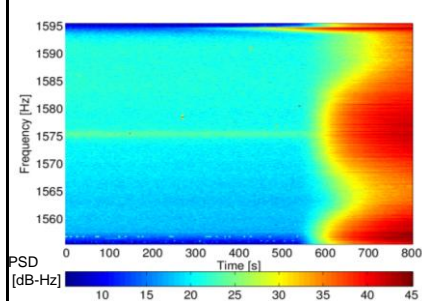
## Front-end: Non-linear Effects

The front-end functional blocks are non-linear in nature: difficulties in predicting the effects of an interfering signal. Non-linear effects worsen as the interference power increases.

**Real life example:** impact of a wide-band interference on a National Instrument (NI) PXI-e 5663 vector signal analyzer.

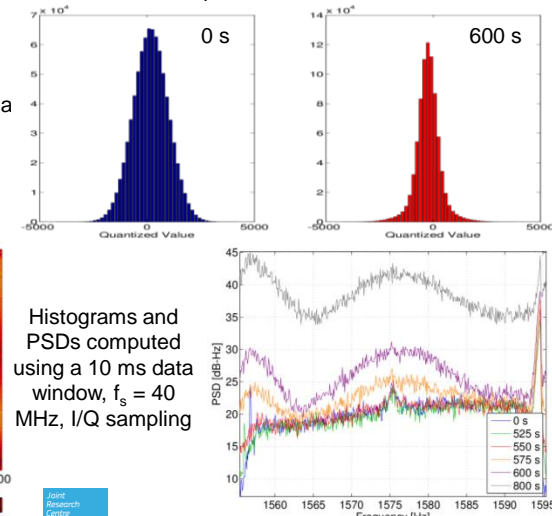
The interference power was increased as a function of time.

The pdf of the signal deviates from Normality



Histograms and PSDs computed using a 10 ms data window,  $f_s = 40$  MHz, I/Q sampling

Joint Research Centre





## Front-end Modifications

Some parts of the front-end can be directly used for interference detection and mitigation:

- ✓ **AGC gain** time series (Bastide et al 2003): AGC gain variations can indicate the presence of a disturbing signals (depends on the type of AGC)
- ✓ Distribution of the samples at the **ADC output**: deviation from Normality
- ✓ Increased sample variance (high number of samples represented with the highest/lowest levels of the quantization function)

Simple front-end modifications may improve receiver performance in the presence of interference (see for example Amoroso, 1983).

Current trend: use of high fidelity front-ends (8+ bits) able to properly represent the interfering signals that will be removed by the signal processing stages

Bastide, F., Akos, D., Macabiau, C., Roturier, B., "Automatic Gain Control (AGC) as an Interference Assessment Tool," *Proceedings of the 16th International Technical Meeting of the Satellite Division of The Institute of Navigation (ION GPS/GNSS 2003)*, Portland, OR, September 2003, pp. 2042-2053.

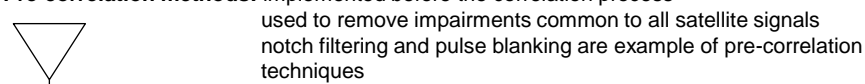
Amoroso, Frank; , "Adaptive A/D Converter to Suppress CW Interference in DSPN Spread Spectrum Communications," *Military Communications Conference, 1983. MILCOM 1983. IEEE* , vol.3, no., pp.720-728, Oct. 31 1983-Nov. 2 1983  
doi: 10.1109/MILCOM.1983.4794795

9



## Pre- and Post-Correlation Methods

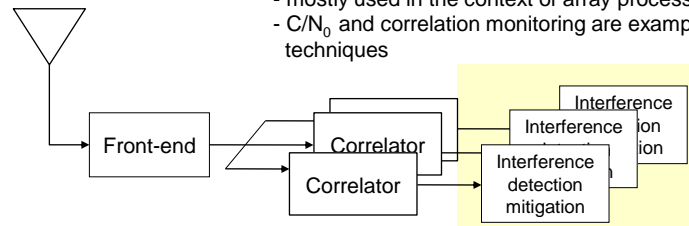
**Pre-correlation methods:** implemented before the correlation process



used to remove impairments common to all satellite signals  
notch filtering and pulse blanking are example of pre-correlation techniques

**Post-correlation methods:** implemented after the correlation process

- allow satellite specific processing
- mostly used in the context of array processing
- $C/N_0$  and correlation monitoring are example of post-correlation techniques



Post-correlation techniques can be integrated within the acquisition and tracking units

10



## Interference Detection

It is a **hypothesis testing problem** (as the acquisition process)

As already indicated, interference detection can be performed at almost all the receiver stages (front-end, pre- and post-correlation, measurements, ...)

When the detection is performed at the sample level (pre-correlation), the problem consists of choosing between the two hypotheses:

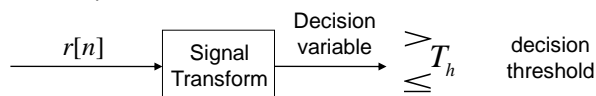
$$\begin{cases} H_0 : r[n] = y[n] + \eta[n] \approx \eta[n] \\ H_1 : r[n] = y[n] + i[n] + \eta[n] \approx i[n] + \eta[n] \end{cases}$$

The GNSS signal is usually neglected

As for the acquisition, the decision is not immediate and N samples can be used for the detection

A verification stage can be present

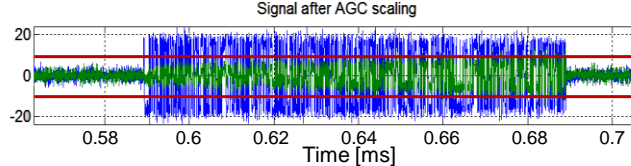
The general solution can be expressed as:



The 'signal transform' depends on the knowledge on the interfering signal (signal model). When the interference model is well defined, the signal transform is a form of **matched filter**.

The decision threshold can be set using the Neumann-Person criterion (false alarm probability) [11](#)

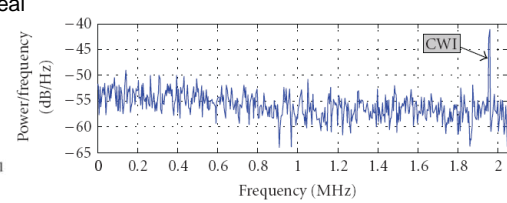
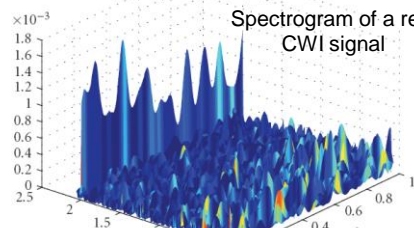
## Pulsed Interference and CWI Detection



Pulse from a GPS pseudolite with a 10% duty cycle

Interference pulses are detected by comparing the modulus of the received samples with a decision threshold ('null transform').

CWI are maximally concentrated in the frequency domain. The Discrete Fourier Transform (DFT) despread them reducing the impact of noise. The DFT of the input samples is compared with the detection threshold



From: Borio D. and L. Lo Presti "A Reconfigurable GNSS Acquisition Scheme for Time-Frequency Applications" [12](#)

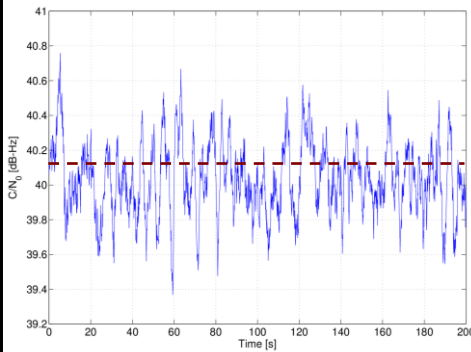


## C/N<sub>0</sub> Monitoring

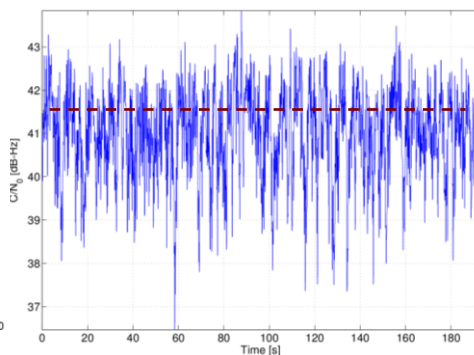
The estimated C/N<sub>0</sub> can reveal the presence of interfering signals

**Remark:** the estimation technique used to determine the C/N<sub>0</sub> can hide the interference presence

C/N<sub>0</sub> estimated in the absence of interference:  
small variations around the mean



C/N<sub>0</sub> estimated in the presence of pulsed interference: significant oscillations around the mean



Joint Research Centre

13



## Interference Mitigation

**Mitigation:** process of reducing the impact of RF inference

- ✓ Goal: enable receiver operation in the presence of interference
- ✓ Mitigation techniques: usually designed for a specific class of interfering signal. The '**universal**' mitigation technique still does not exist
- ✓ The '**perfect**' mitigation technique, i.e., a technique that leads to performance **identical** to the case of interference absence **does not exist** in practice (although in some cases, almost perfect interference cancellation can be achieved)
- ✓ Each mitigation technique has an impact on the useful signals as well:
  - SNR degradation (hopefully lower than in the presence of unmitigated interference)
  - Biases in the measurements (filtering for example can introduce a non-constant group delay)
- ✓ Enable interference mitigation only when **strictly necessary** (integration with interference detection units)
- ✓ Careful design: include **constraints** to **avoid biases** in the measurements

14



## The Interference Cancellation Principle

The problem of estimating the useful GNSS signal parameters can be reformulated in the presence of interference.

If the interference signal were known, then the MLE becomes:

$$(\hat{\tau}, \hat{f}_d, \hat{\phi}) = \arg \max_{\tau, f_d, \phi} \Re \left\{ \frac{1}{N} \sum_{n=0}^{N-1} \underbrace{[r[n] - i[n]]}_{\text{interference cancellation}} \underbrace{[c(nT_s - \tau)]}_{\text{local code}} \underbrace{\exp\{-j2\pi(f_{IF} + f_d)nT_s - j\phi\}}_{\text{local carrier}} \right\}$$

↑  
Interference is removed before applying standard correlation based processing

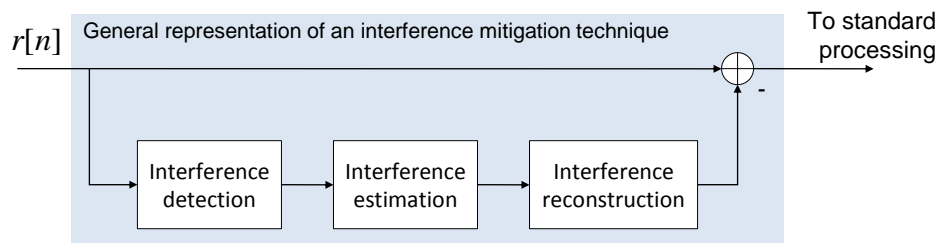
since  $i[n]$  is not known, it needs to be **estimated**.

Most of interference mitigation techniques can be interpreted as a form of interference cancellation.

Each interference mitigation technique is then characterized by the way it estimates the disturbing signal



## Mitigation as an Estimation Problem



The problem of interference mitigation reduces to the problem of estimating the interfering signal or its parameters.

E.g./ assume  $i[n] = A \exp\{j2\pi f_i n T_s + j\phi\}$  (continuous wave interference)

then the interference parameter MLEs are given by

$$\hat{f}_i = \arg \max_f \left( \left| \frac{1}{N} \sum_{n=0}^{N-1} i[n] \exp\{-j2\pi f n T_s\} \right|^2 \right) = \arg \max_f |I(f)|^2 \quad \hat{\phi} = \angle I(\hat{f}_i)$$

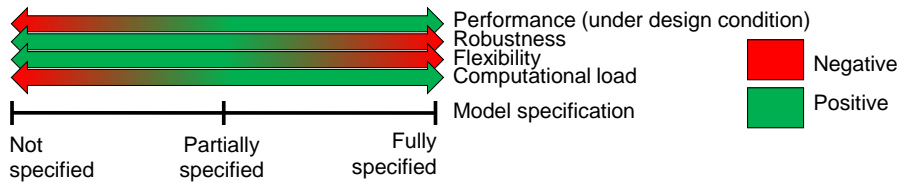
The ML estimation is one possible approach for reconstructing  $i[n]$ . It is particularly useful when a parametric model is available.



## Interference Model Dependence

The performance of a mitigation technique depends on the **model** adopted for designing the interference estimation block:

- ✓ **parametric** techniques: the functional form of  $i[n]$  is fully specified (low number of parameters)
- ✓ **non-parametric** techniques: generally based on the projection of the signal on a transformed domain (different base)



**Robustness** is defined here as the ability to cope with mismatches between the model specified and the real operating conditions. Model-based techniques tend to experience strong performance degradation in the presence of modeling errors.

**Flexibility** is the ability to deal with a wide class of interfering signals: model-based techniques are usually able to deal with a single type of interfering signal.

The level of model specification can be determined by comparing the **number of parameters** used for specifying the model and the number of samples used for estimating them.

17



## Transformed Domain Excision (I/III)

Form of non-parametric estimation technique where the signal is at first projected into a different representation **basis**

Original signal

$$i[n] = \sum_{k=0}^{N-1} i[k] \delta[n-k]$$

The time domain signal is expressed in a space defined by the **basis of shifted Kronecker's delta functions**

Transformed domain

$$i[n] = \sum_{k=0}^{N-1} I[k] f(k, n)$$

Signal coefficients in the transformed domain

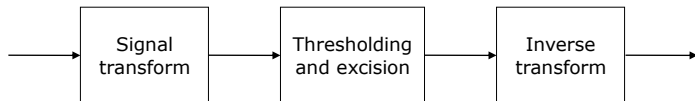
New basis used for the representation of the signal

'k' is just an index used for indicating the coefficient associated to the k-th basis function. Its physical meaning is determined by the set of basis functions. It can be replaced by an arbitrary number of indexes (e.g./ time-frequency, time-scale, ...)

The goal is to find a **sparse representation** of  $i[n]$ , i.e., find a basis leading to a set of coefficients,  $I[k]$ , with only a few elements significantly different from zero.



## Transformed Domain Excision (II/III)



It is assumed that in the transformed domain only the coefficients with a magnitude higher than a threshold belongs to the interference signal. These coefficients are zeroed before projecting back the signal in the time domain

This is equivalent to estimate the interference as

$$\hat{I}[n] = \sum_{k=0}^{N-1} \hat{I}[k] f(k, n) \quad \text{with} \quad \hat{I}[k] = \begin{cases} R[k] & \text{if } |R[k]| > T_h \\ 0 & \text{if } |R[k]| < T_h \end{cases}$$

Detection threshold ↓  
Transform of the input signal with noise and GNSS signal components ↑

White noise processes do not admit a **sparse representation**. It is expected that GNSS (and DSSS) signals do not admit a sparse representation similarly to white noise. Thus, if only a few coefficients are excised, the overall quality of the useful signal is not significantly affected.

- ✓ the performance of the algorithm depends on the basis: **sparsity of the interference representation**. The base needs to be **matched** to the interference signal



## Transformed Domain Excision (III/III)

These slides illustrate only the working principle. However, signal estimation using these techniques is usually quite complex:

- ✓ how to chose the **right transform**
- ✓ non-linear transforms: how to compute the **coefficients of the expansion**,  $I[k]$
- ✓ **over-specification** of the base in the transformed domain
- ✓ **invertibility** problems after excision
- ✓ **computational** load

Commonly used transforms are:

- ✓ Time-frequency distributions (linear and quadratic)
- ✓ Wavelet transform
- ✓ Radon transform
- ✓ Karhunen-Loëve transform (KLT)

### Further reading:

Franz Hlawatsch "Time-Frequency Analysis and Synthesis of Linear Signal Spaces: Time-Frequency Filters, Signal Detection and Estimation, and Range-Doppler Estimation"

Leon Cohen "Time Frequency Analysis: Theory and Applications"

Stephane Mallat "A Wavelet Tour of Signal Processing: The Sparse Way"



## DTF and STFT

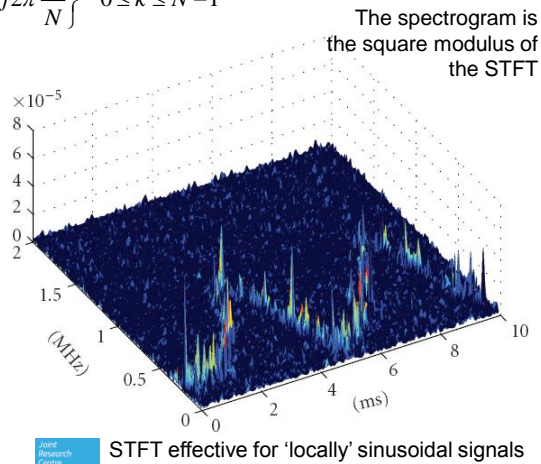
Discrete Fourier Transform (DFT) and its extensions (Short Time Fourier Transform and Spectrogram) use complex sinusoids as basis for the signal representation

$$f(k, n) = \exp\left\{j2\pi \frac{kn}{N}\right\} \quad 0 \leq k \leq N-1$$

- ✓ Particularly effective for identifying CWI and signals with a spectrum concentrated in the frequency domain
- ✓ Fast implementation using the FFT algorithm
- ✓ The Short Time Fourier Transform (STFT) is obtained by windowing the input signal and applying the DTF on the windowed signal

$$f(k, m, n) = h(n-m) \exp\left\{j2\pi \frac{kn}{N}\right\}$$

- ✓ Basis functions are indexed with respect to two parameters m and k



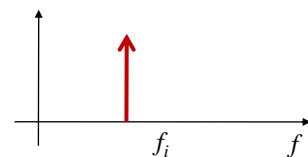
## Notch Filtering

**Notch Filter:** linear device the transfer function of which strongly attenuates only a single frequency. All the other signal components should be passed through the unchanged.

Parametric technique specific for **Continuous Wave Interference** (CWI), i.e., signals the power of which is concentrated around a single frequency.

**Real interference**  $i[n] = A \cos(2\pi f_i n T_s + \phi)$

**Complex interference**  $i[n] = A \exp\{j2\pi f_i n T_s + j\phi\}$



If the notch of the filter transfer function is placed in correspondence of the interference frequency, then the disturbing signal is essentially removed without significantly corrupting wideband GNSS signals



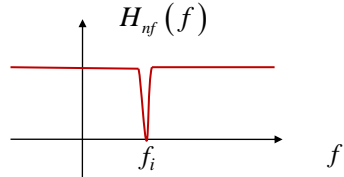
## Ideal Notch Filter

Ideally  $H_{nf}(f) = \begin{cases} 0 & \text{for } f = f_i \\ 1 & \text{otherwise} \end{cases}$

Theoretically, the ideal notch filter could be realized using the structure:

$$H_{nf}(z) = \frac{1 - e^{j2\pi \frac{f_i}{f_s} z^{-1}}}{1 - e^{j2\pi \frac{f_i}{f_s} z^{-1}}}$$

↑  
sampling frequency of  
the system



Transfer function with identical numerator and denominator (cancel out perfectly a part from the zero). The zero of the nominator is placed in correspondence of the notch frequency.

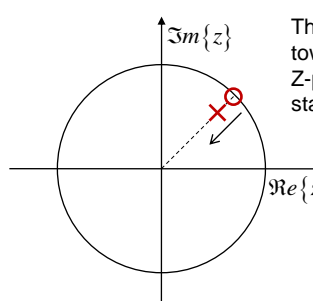
This type of structure is not physically realizable since the pole is on the unit circle.

**Several types of notch filters:** try to approximate with different approaches the ideal transfer function  $H_{nf}(z)$

- ✓ Finite Impulse Response (FIR)
- ✓ Infinite Impulse Response (IIR)
- ✓ Adaptive, static

In the next slides: special class of adaptive IIR notch filters

## Realizable Notch Filters



The pole is displaced towards the centre of the Z-plane to guarantee stability

$$0 \leq k_\alpha < 1$$

$$z_0 = A \exp \left\{ j2\pi \frac{f_i}{f_s} \right\}$$

Depending on the adaptation criteria, A may or not be constrained to unity

Notch filter zero

$$H_{nf}(z) = \frac{1 - z_0 z^{-1}}{1 - k_\alpha z_0 z^{-1}}$$

Pole contraction factor

In the case of a real interference, two frequency component  $\pm f_i$  have to be removed.

Real notch filter obtained by cascading two single pole notch filters:

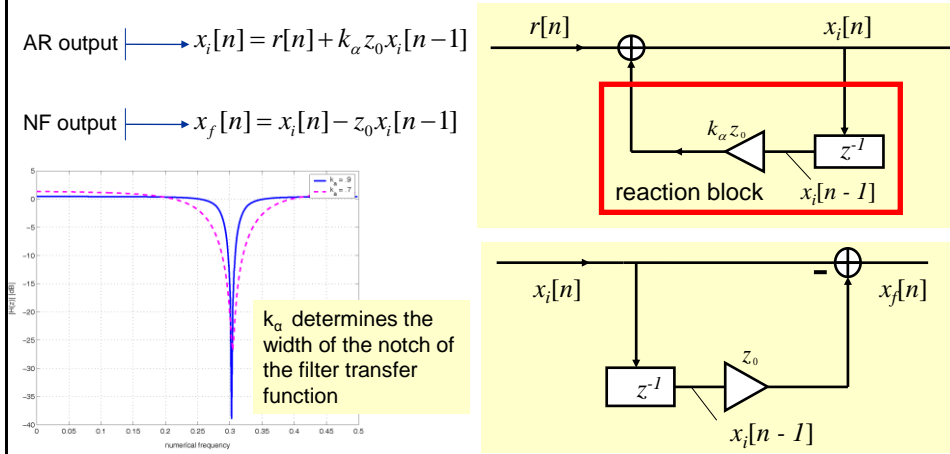
$$H_{rf}(f) = \frac{1 - z_0 z^{-1}}{1 - k_\alpha z_0 z^{-1}} \frac{1 - z_0^* z^{-1}}{1 - k_\alpha z_0^* z^{-1}} = \frac{1 - 2\Re{z_0} z^{-1} + |z_0|^2 z^{-2}}{1 - 2k_\alpha \Re{z_0} z^{-1} + k_\alpha^2 |z_0|^2 z^{-2}}$$



## Notch Filter Structure

The transfer function of the notch filter can be decomposed in two parts:

- ✓ **Auto-Regressive (AR)**: denominator of the transfer function
- ✓ **Moving Average (MA)**: numerator of the transfer function



## Adaptive Notch Filtering

The notch filter can be made adaptive by progressively adjusting the zero of the filter:

- ✓ useful when the frequency of the interfering signal is not known
- ✓ the frequency of the interference (and of the notch) can be estimated by minimizing a cost function

A simple criterion can be the **minimization of the energy** of the signal at the output of the filter. The energy of the output signal is minimized when interference is removed.

$$\text{Cost function} \quad J[n] = E[C[n]] = E\left[\left|x_f[n]\right|^2\right]$$

The zero of the notch can be updated using a **Least Mean Square (LMS)** approach:

**Stochastic gradient**

$$z_0[n] = z_0[n-1] - \mu \frac{\partial C[n]}{\partial z_0} \Bigg|_{z_0=z_0[n-1]}$$

The gradient of the cost function is progressively minimized (gradient descent algorithm) using the step  $\mu$

**Adaptation step**

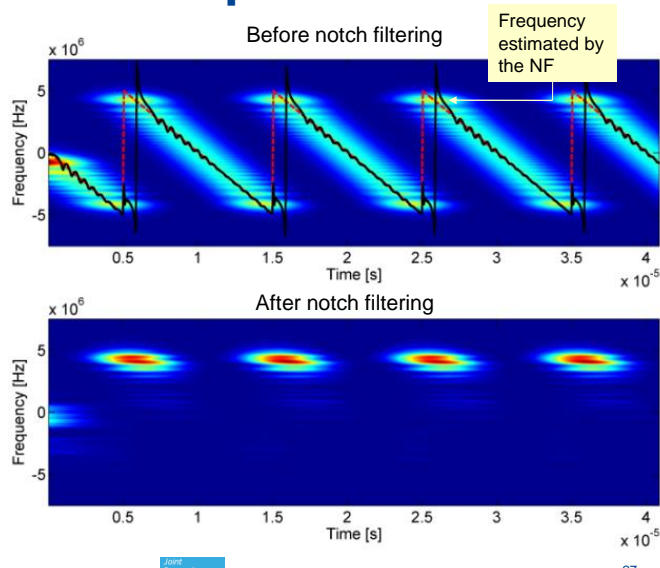
$$\text{Complex Notch Filter: } z_0[n] = z_0[n-1] + \mu \cdot x_f[n] x_i^*[n-1]$$



## Notch Filters vs. Swept Interference

Test conducted in the presence of swept interference (similar to the signal transmitted by a GNSS jammer)

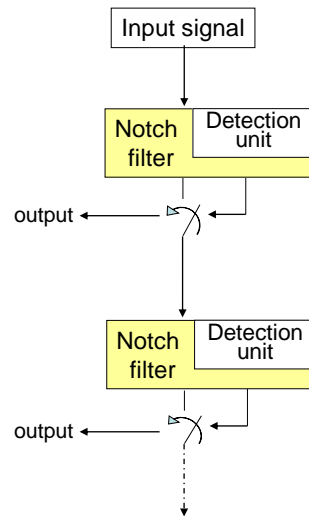
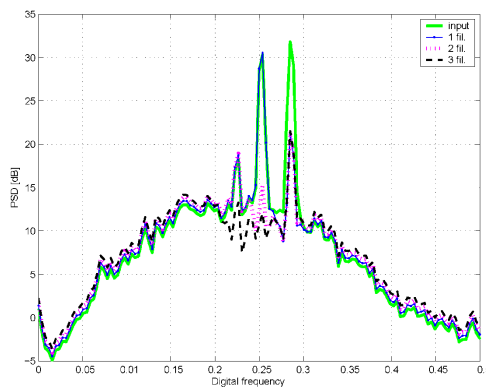
- ✓ Fast sweep rates challenge the adaptation algorithm of the notch filter
- ✓ Frequency jumps causes transients (biases) in the interference frequency estimated by the notch filter
- ✓ Residual interference power at the frequency transition edges



## Cascaded Notch Filters

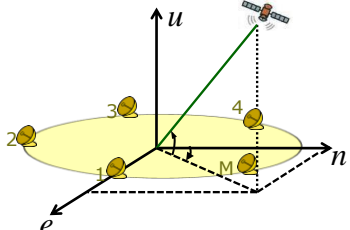
Several notch filters can be cascaded in order to remove several CWI signal

Notch filters introduce useful signal degradation depending on the notch frequency: it is necessary to introduce detection units to activate a notch filter only if residual interference is present





## Array Processing



**Working principle (simplified version):** signals from different directions are received by closely spaced antennas with different phases

Consider the case of two signals from two different directions received by two antennas:

$$r_0[n] = s_{0,0}y[n] + s_{0,1}i[n]$$

$$r_1[n] = s_{1,0}y[n] + s_{1,1}i[n]$$

Then it is possible to isolate the two signals:

$$y[n] = \frac{s_{1,1}}{s_{0,0}s_{1,1} - s_{1,0}s_{0,1}} \left( r_0[n] - \frac{s_{0,1}}{s_{1,1}} r_1[n] \right) \quad i[n] = -\frac{s_{1,0}}{s_{0,0}s_{1,1} - s_{1,0}s_{0,1}} \left( r_0[n] - \frac{s_{0,0}}{s_{1,0}} r_1[n] \right)$$

Array processing can be thus used for isolating and removing interfering signals coming from specific directions in space

$\begin{bmatrix} s_{0,0} \\ s_{1,0} \end{bmatrix}$  and  $\begin{bmatrix} s_{0,1} \\ s_{1,1} \end{bmatrix}$  are the steering vectors of the first and second signal and account for the

different signal phases due to the different propagation paths for the first and second antenna [29](#)



## Beamforming

Process of shaping the overall array beam pattern by linearly combining signals from different antennas

$$\tilde{r}[n] = \sum_{l=0}^{L-1} r_l[n] w_l^*$$

Going back to the previous example:

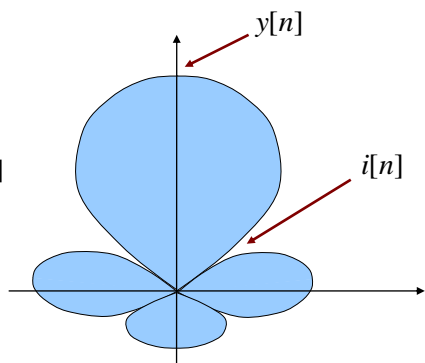
$$\tilde{r}[n] = \underbrace{\frac{s_{1,1}}{s_{0,0}s_{1,1} - s_{1,0}s_{0,1}} r_0[n]}_{w_0^*} + \underbrace{\frac{-s_{0,1}}{s_{0,0}s_{1,1} - s_{1,0}s_{0,1}} r_1[n]}_{w_1^*}$$

the array is providing a zero gain to signals coming from the same direction of  $i[n]$ .

A unit gain is provided to signals coming from the same direction of  $y[n]$ .

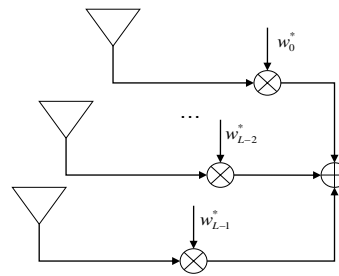
Array processing allows spatial filtering where the weights,  $\{w_l\}$ , define the spatial response of the array.

Several techniques exist for determining the weights: for example, it is possible to use all the adaptive techniques designed for standard filtering.



## Wide- and Narrow-band Beamforming

### Narrow-band beamforming



- ✓ The output is a linear combination of the signal from the different antennas
- ✓ The frequency response of the beamformer is flat
- ✓ Narrow-band because it is suitable for narrow-band signals

$$\tilde{r}[n] = \sum_{l=0}^{L-1} r_l[n] w_l^*$$

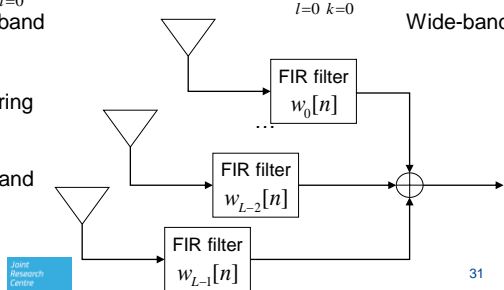
Narrow-band

$$\tilde{r}[n] = \sum_{l=0}^{L-1} \sum_{k=0}^{M-1} r_l[n-k] w_l^*[k]$$

Wide-band

### Wide-band beamforming

- ✓ Implements both spatial and frequency filtering
- ✓ It has a frequency selective response
- ✓ Wide-band because it is suitable for wide-band signals



Joint Research Centre

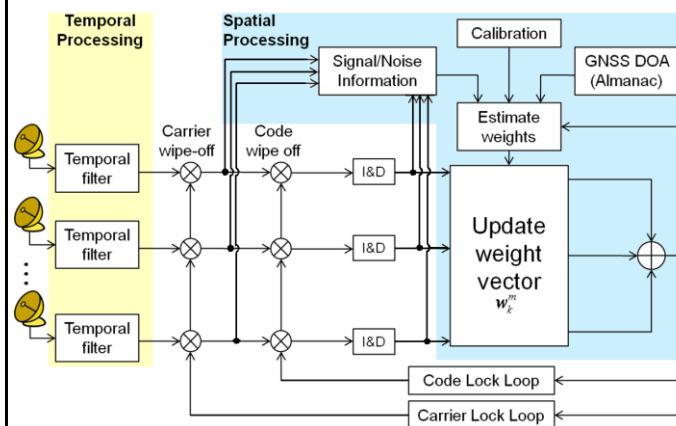
31

## Pre- and Post- Correlation Processing

Beamforming can be implemented on the raw samples (**pre-correlation**) or on the correlator outputs (**post-correlation**)

Post-correlation beamforming is particularly powerful since it allows **satellite specific** processing such as multipath mitigation

Weight adaptation and signal tracking can be performed jointly

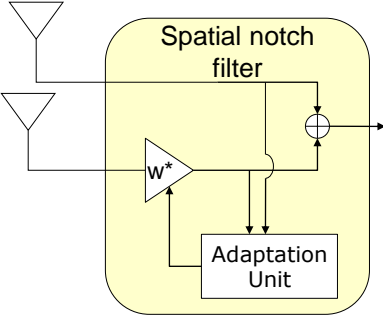


Pratibha B Anantharamu  
"Space-Time Equalization  
Techniques for New GNSS  
Signals" University of Calgary  
September 2011

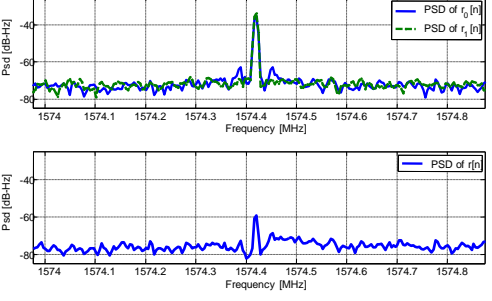
32



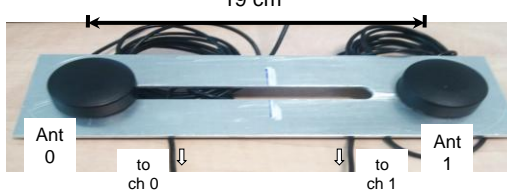
## Spatial Notch Filtering



The weight  $w$  is adapted in order to minimize the output energy



Dual channel GPS front-end providing synchronous samples through USB



## Final Remarks

Mitigation and detection techniques are powerful tools that can significantly improve the performance of a GNSS receiver in the presence of interference, however:

- ✓ they can be **prohibitively expensive** from a computational point of view
  - signal transform can be more computationally expensive than the process of correlation
  - “silicon is cheap” and “Moore law” are often excuses: many techniques can often be used for post-processing operations
  - balance between costs and benefits: a lot of computations for a gain of fractions of dB
- ✓ they can introduce **biases** in the measurements:
  - Design constraints: e.g./ linear or minimum phase filter response, minimum variance distortionless response beamforming, ...

All these factors have to be accounted for the design of interference detection/mitigation techniques.

Joint Research Centre

34





## GNSS Interference Source Localization

Jahshan Bhatti, Todd Humphreys, The University of Texas at Austin  
Brent Ledvina, Coherent Navigation

GNSS Summer School, Ispra (VA), Italy | July 4, 2012

## Outline

- I. Motivation and Prior Art
- II. Proposed Strategy
  - I. Sensor Network and Synchronization
  - II. TDOA Estimation
  - III. Emitter Identification and Localization
- III. Results

# Acknowledgement



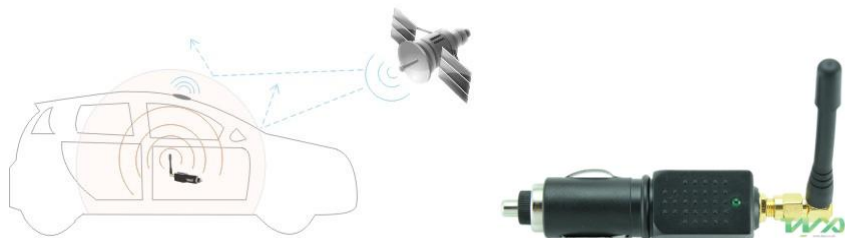
Members of the UT Radionavigation Laboratory



3

## Emitter Localization Motivation

- GPS jamming is a significant threat to US critical infrastructure.
- Increased use of personal privacy devices (PPDs) due to miniaturization and proliferation of GPS trackers.



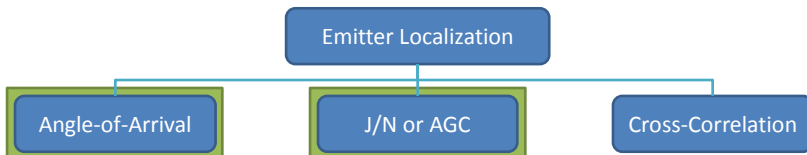
4

## Types of Emitter Localization Techniques



5

## Finding the Newark Jammer (2010)

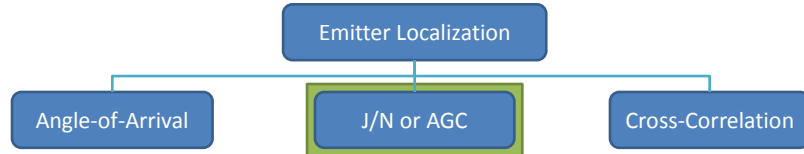


- Configuration
  - Relied on J/N readings and directional antennas to find jammer.
- Limitations
  - Lack of precision in lane.
  - Took team 4 months to find jammer.

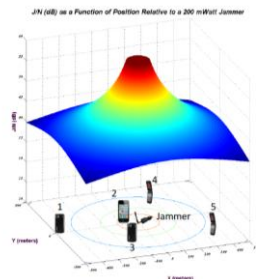


6

## J911 (Scott, 2010)

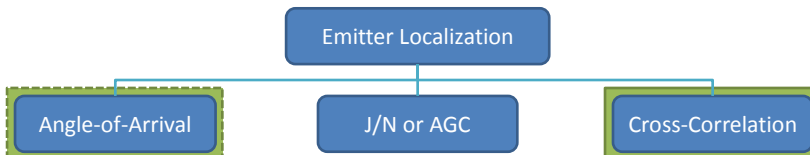


- Configuration
  - Cell phones report AGC values from GPS frontend to cellular network.
  - Relies on crowd-sourcing.
- Benefits
  - Brute-force density allows finding multiple emitters.
  - Low-bandwidth sensors.
- Limitations
  - Cannot guarantee availability.

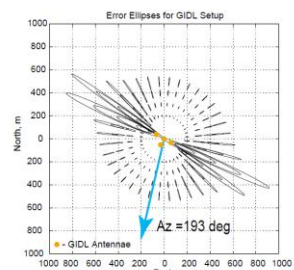


7

## GIDL (Gromov, 2002)



- Benefits
  - Estimator approaches CRLB for single-emitter TDOA precision.
  - Raw high-rate samples do not have to be transported across a network.
- Limitations
  - Cross-correlation TDOA estimation algorithm is limited to a single-emitter scenario.
  - Clock-sharing limits antenna baseline, yielding poor geometry and limited range precision.

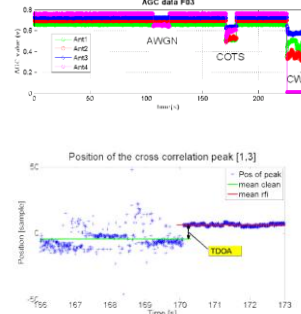


8

## Isoz and Akos Work (2010) on GPS Interference Localization

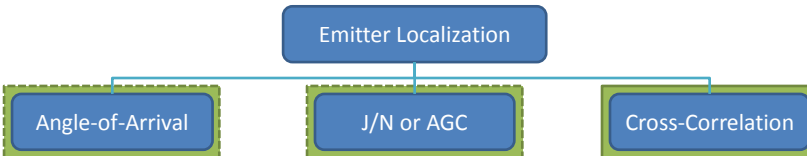


- Configuration
  - Collected data with miniature GPS digital frontend that produced AGC values and raw samples.
  - Performed AGC-based solution for strong emitters and cross-correlation-based solution for weak emitters.
- Benefits
  - Allows sparse network of sensors through synchronization.
  - Increased precision through cross-correlation-based solution.
- Limitations
  - Only considers single emitter.



9

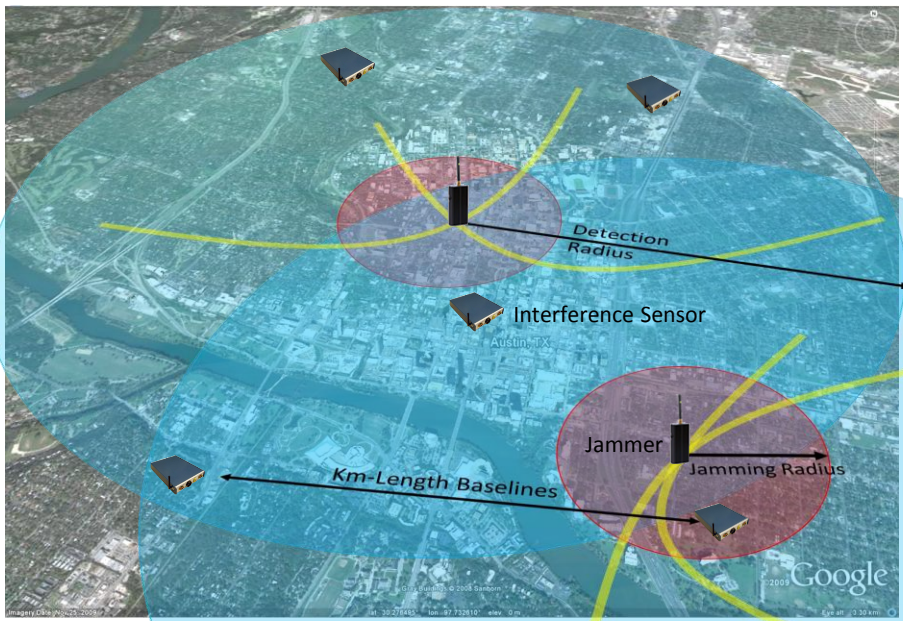
## Proposed Strategy for Emitter Localization



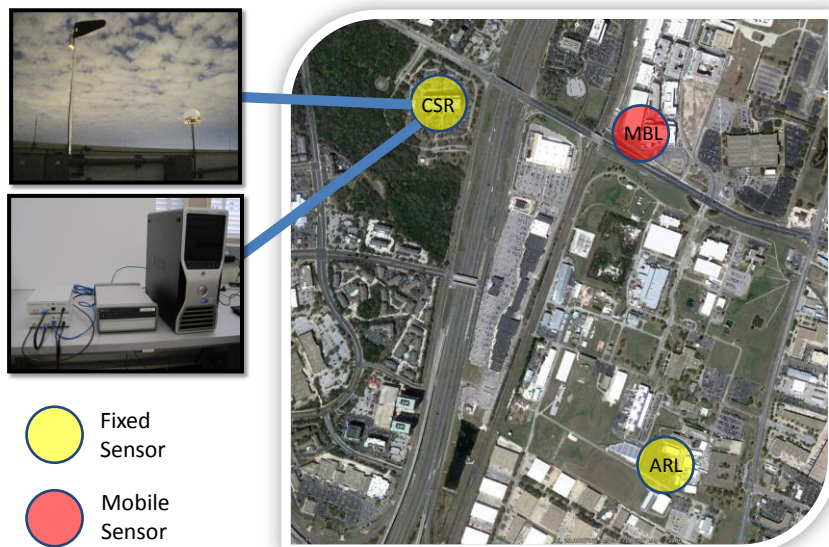
- Benefits
  - Sparse, scalable, synchronized sensor network.
  - Multiple-emitter TDOA estimation algorithms.
  - Fast, continuous, and accurate localization.
- Limitations
  - Limited by network throughput.

10

## Sensor Network Schematic



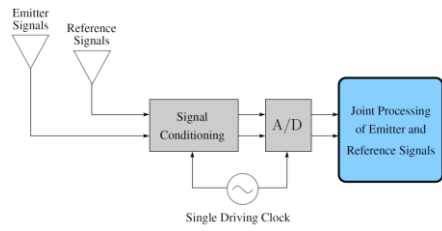
## UT Austin Prototype Emitter Localization Network



# Sensor Synchronization

- Work by Akos uses ambient GPS signals for sensor synchronization.
- Proposed strategy can use reference signals from any frequency band.
- Robust under intense GPS jamming.
- Emitter and reference signals are received in a tightly-coupled frontend architecture (Pesyna, 2011).

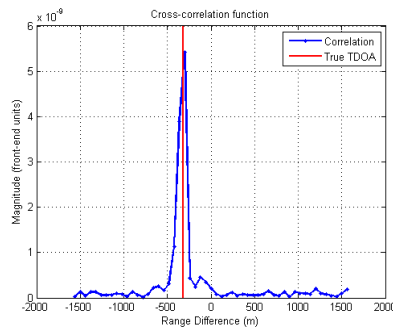
GRID: General Radionavigation Interfusion Device							
						Build ID: 1379	
Receiver time:		0 weeks 160.0 seconds		GPS time:		420794.0 seconds	
CH TXID	Doppler (Hz)	BGP (cycles)	PR (meters)	C/N0 (dB-Hz)	Az (deg)	El (deg)	Status
1 1u	430.75	-76149.17	20972553.14	46.3	301.7	12.9	6
2 2	-2337.63	372213.30	20793027.57	44.1	93.0	10.8	6
3 5	2814.11	449035.30	19188750.37	52.3	42.0	32.0	6
4 15	2320.50	342035.30	19188750.33	14.1	14.9	29.9	6
5 18	2228.97	-360186.88	19326452.99	48.6	243.3	29.8	6
6 21	2027.74	-324302.89	19403848.18	51.0	306.8	34.8	6
7 25	-2734.77	436530.00	20267387.49	47.7	218.6	19.7	6
8 26	140.77	-76149.17	20972553.14	46.3	301.7	47.0	6
9 29	338.14	-71226.59	16310240.92	52.1	287.2	79.5	6
10 30	-731.36	110014.30	20121635.89	46.5	282.3	18.5	6
11 --	--	--	--	--	--	--	--
CDMA_UHF_PILOT Channels--							
1 1	-0.59	91.58	7622658.88	62.0	0.0	0.0	5
---Navigation Data---							
X: -745467.86	Y: -5462657.31	Z: 3196401.16	dm1Rx: -3464662.39				
Xwell: 0.03	Ywell: -0.04	Zwell: 0.01	dm1RxDot1: 0.12				



13

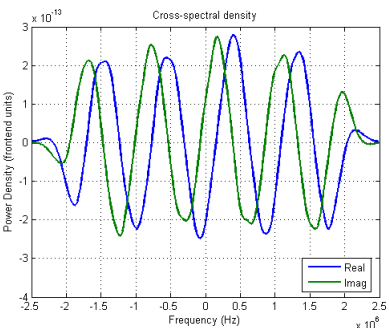
# Single-Emitter TDOA Estimation

How to estimate TDOA using cross-correlation?



Estimate location of peak in cross-correlation.

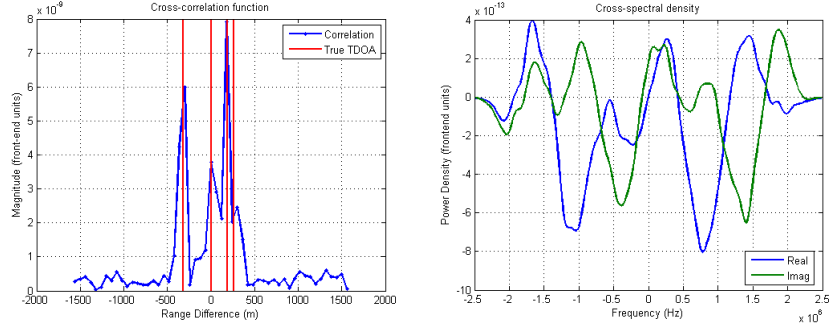
OR



Estimate frequency of complex sinusoid in cross-spectral density.

14

# Multiple-Emitter TDOA Estimation



Single-emitter estimation techniques break down. What can we do?

15

## Cross-Power Spectral Density Model

- Under the assumption of flat emitter power spectral densities, then the received cross-power spectral density can be modeled as

$$Y_{\tilde{r}_i \tilde{r}_k} (f) = \sum_{l=1}^M \alpha_{ik}^l \exp(-j2\pi\Delta_{ik}\tau_{m,0}^l f) + N(f)$$

where

$\alpha_{ik}^l$  is the complex attenuation factor  
 $\Delta_{ik}\tau_{m,0}^l$  is the apparent TDOA

- Subspace methods like MUSIC can be used to recover unbiased estimates of the frequency (TDOA) of the complex sinusoids assuming the number of emitters are known.
- Least-square fitting can be used to refine the MUSIC estimates.

16

## How Good Can We Get?

- The fundamental limit for single-emitter TDOA precision of wideband signals is given by the CRLB:

$$\sigma_{\tau_{ij}}^2 = \frac{3N_{0,i}N_{0,j}}{2\pi^2 TS_i S_j \Delta f^3} \left( 1 + \frac{S_i}{N_{0,i}} + \frac{S_j}{N_{0,j}} \right)$$

where

$T$  is the integration time

$\Delta f$  is the captured bandwidth

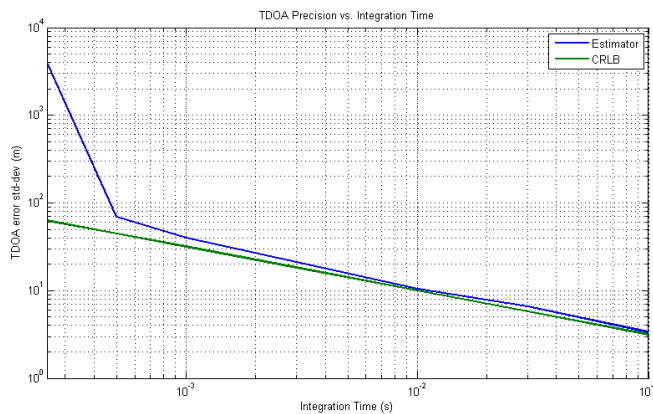
$S_i, S_j$  are the received signal power density

$N_{0,i}, N_{0,j}$  are the noise power density

- Practically limited by multipath and sensor synchronization errors.

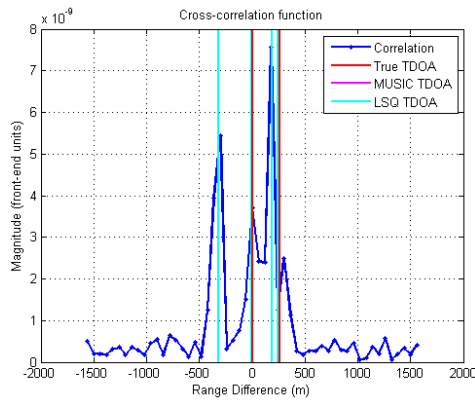
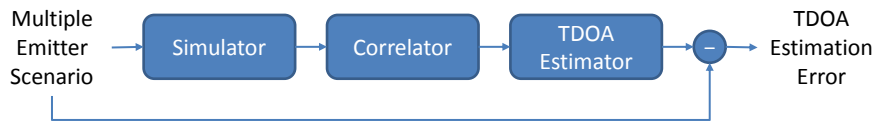
17

## Simulated Single-Emitter Estimator Performance



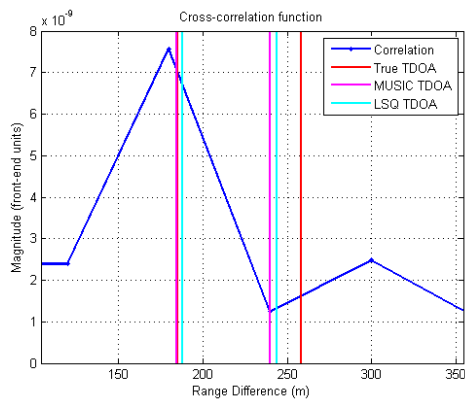
18

## Simulated Multiple-Emitter Scenario



19

## Simulated Multiple-Emitter Scenario



20

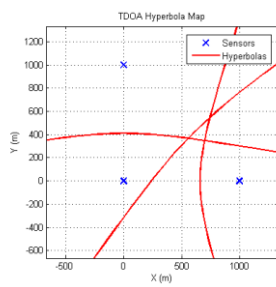
## Emitter Localization

- TDOA constrains the emitter position to a hyperbola of revolution.
- Once TDOA measurements are correctly associated, nonlinear least-squares algorithms can be used to estimate the emitter position.

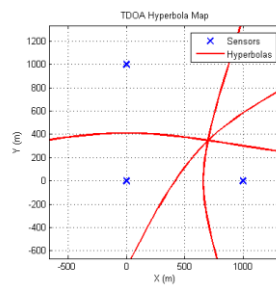
21

## TDOA Closure Metric

- In passive geolocation, the TDOA measurements from all sensor pairs must be associated with a particular emitter.
- The TDOA closure metric is defined as
$$\tau_c = \hat{\tau}_{ij} - \hat{\tau}_{ik} + \hat{\tau}_{jk}.$$
where  $\hat{\tau}_{ij}$  is a TDOA measurement between sensors  $i$  and  $j$
- If a triplet of TDOA measurements “close,” then geometrically, the three hyperbolas associated with the triplet intersect at a single point.



Not “Closed”

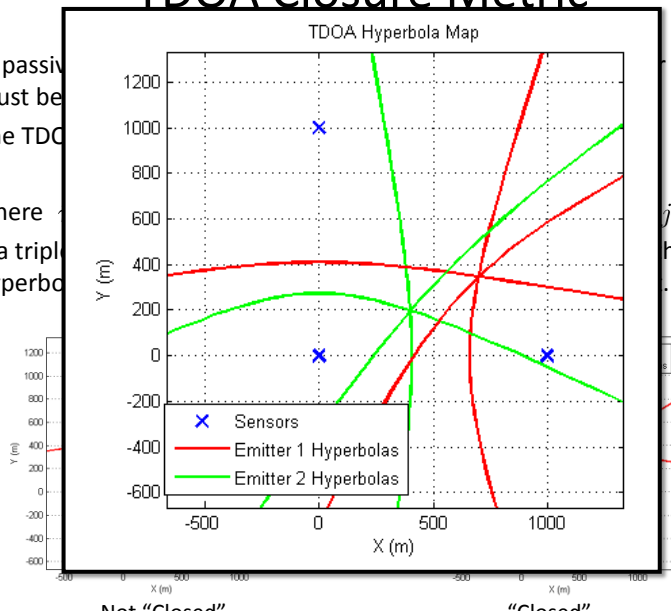


“Closed”

22

## TDOA Closure Metric

- In passive localization, the TDOA must be measured between pairs of sensors.
- The TDOA closure metric is given by the equation:
 
$$\text{Closure Metric} = \frac{\sum_{i,j} |d_{ij} - d_{ij}^{\text{true}}|}{\sum_{i,j} d_{ij}}$$
 where  $d_{ij}$  is the measured distance between sensor pairs  $i$  and  $j$ , and  $d_{ij}^{\text{true}}$  is the true distance between the same pair.
- If a triple closure condition is met, the three hyperbolas intersect at a single point.

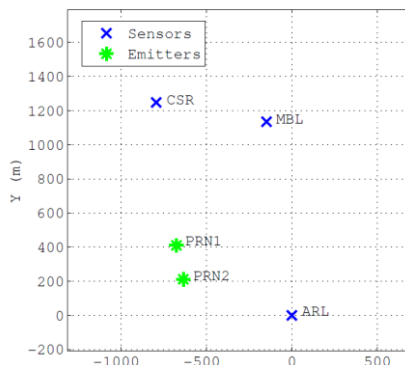


23

## 2.3 GHz Experimental Setup



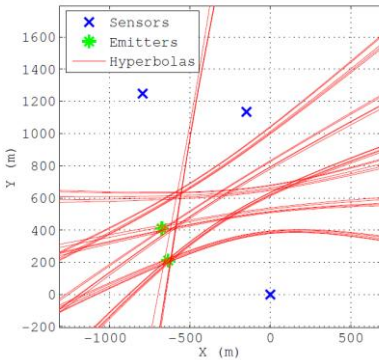
- 2 Emitters (USRP E100)
  - Transmitted GPS L1 C/A PRN codes
  - 1 Mcps
  - $\sim 10$  mW power
- 2 fixed sensors (ARL and CSR) and 1 mobile sensor
  - Receiving at 2 complex Msps (effective bandwidth of 1.5 MHz)
  - One-second coherent integration time
  - Synchronized with GPS



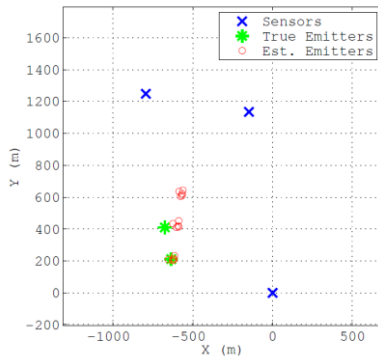
Emitter/Sensor Layout

24

## Results from 2.3 GHz Experiment



TDOA hyperbola map for the amateur band test exercise

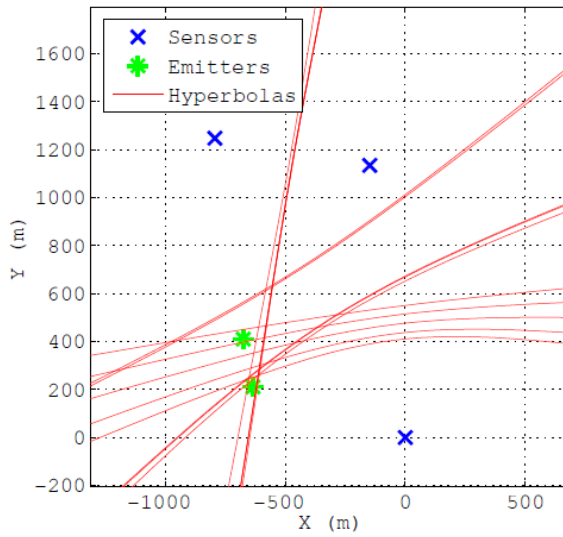


Estimated emitter locations for five independent runs

Note: Multipath creates false emitter position solutions!

25

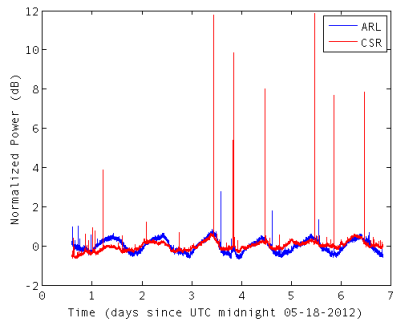
## Single-Emitter Assumption Results in Biased Estimate



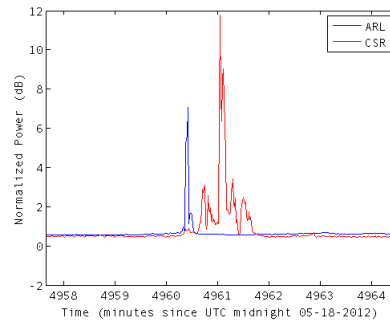
26

## Results from Operational GPS Jamming Detection Effort

- Continuously log received power in 10 MHz band centered at L1 averaged over one second at CSR and ARL stations using GPS antenna.



One week of logged data shows jamming patterns



Zoomed-in view of a jamming incident

27

## Future Work

- Proposed strategy is an “end-to-end” solution for fast and accurate multiple-emitter localization.
- Future work will
  - apply techniques in GPS bands.
  - jointly estimate TDOA and FDOA.
  - rigorously estimate number of emitters.

28



THE UNIVERSITY OF TEXAS AT AUSTIN  
**RADIONAVIGATION LABORATORY**



## GNSS Spoofing

Todd Humphreys, Kyle Wesson, Jahshan Bhatti, Daniel Shepard,  
The University of Texas at Austin

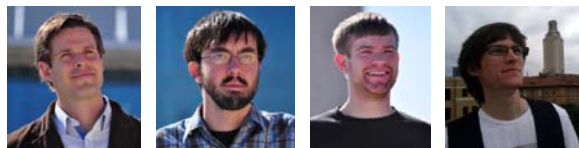
GNSS Summer School, Ispra, Italy | July 4, 2012

## Outline

- I. Civilian GPS Receiver-Spoofing
- II. Cryptographic Anti-Spoofing
- III. Vestigial Signal Defense

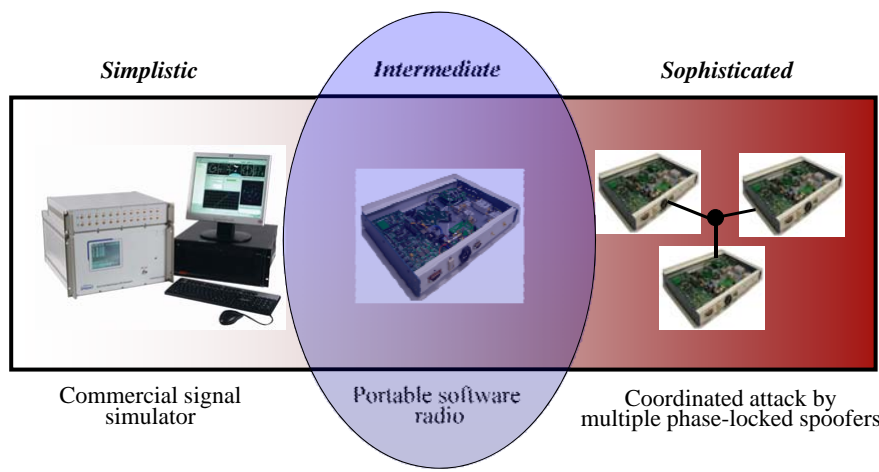
# Acknowledgement

Members of the UT Radionavigation Laboratory



3

# Spoofing Threat Continuum



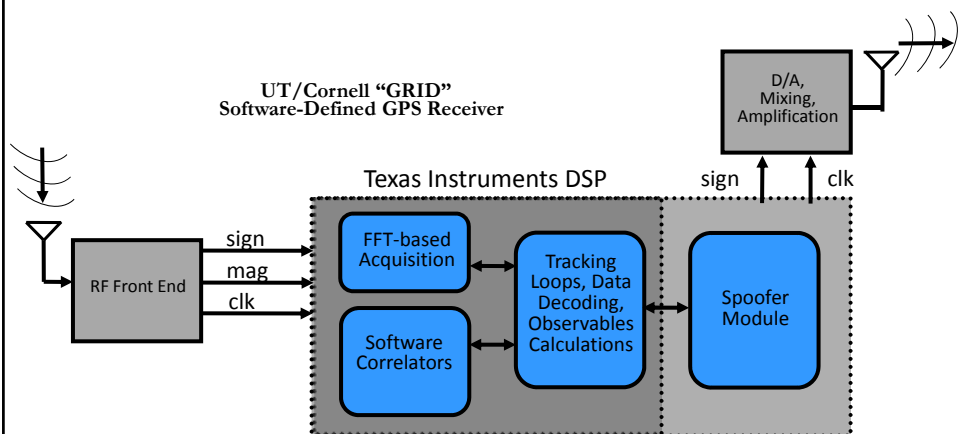
## The Civil GPS Spoofer

- Introduced in 2008 by Humphreys, et al.
- Improved spoofer capable of:
  - Tracking all L1C/A & L2C signals
  - Producing up to 10 L1C/A spoofed signals
  - Precise code phase alignment and frequency lock
  - Data bit prediction
  - Remote control of spoofer suggested position, velocity, and acceleration and signal power via internet



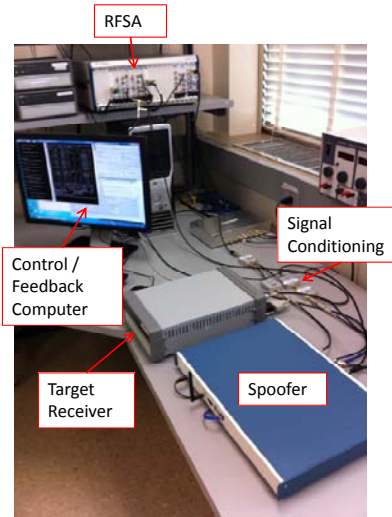
Humphreys, T.E., B.M. Ledvina, M.L. Psiaki, B.W. O'Hanlon, P.M Kintner, Jr., "Assessing the Spoofing Threat: Development of a Portable GPS Civilian Spoofer," Proceedings of ION GNSS, The Institute of Navigation, Savanna, Georgia, 2008.

## Receiver-Spoof Architecture

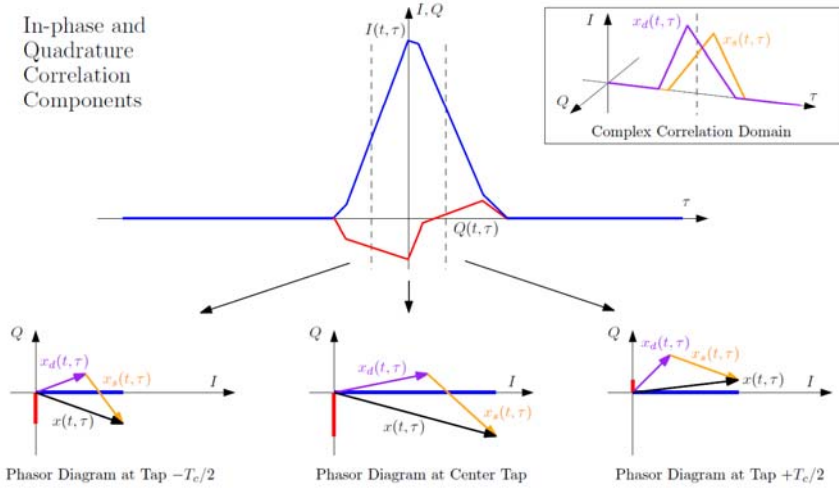


## Demonstration (over-wire)

- The spoofer receives authentic signals from rooftop antenna and generates spoofed signals.
- The spoofed signals are combined with the authentic signals and the combination is fed to:
  - the target receiver
  - a National Instruments Radio Frequency Signal Analyzer (RFSA) used for visualization



## Complex Correlation Domain Explanation

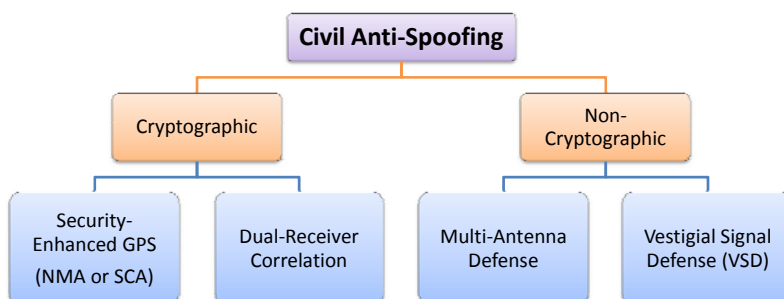


## Demonstration (over-the-air)

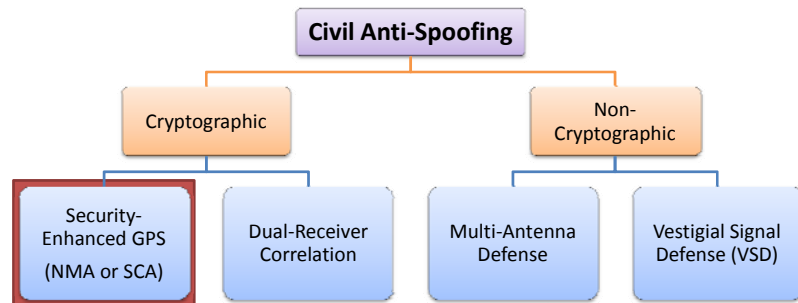


9

## Types of Civil Anti-Spoofing



## Types of Civil Anti-Spoofing



Why navigation message authentication?

- Offers significant protection against spoofing relative to additional cost and bulk required for implementation
- Practical and surprisingly effective
- Suggested by Logan Scott in 2003

Why cryptographic?

- Does not require additional hardware at receiver
- Can distinguish authentic from spoofed signal

## Security-Enhanced GNSS Signal Model

$$\begin{aligned} Y_k &= w_k c_k \cos(2\pi f_{IF} t_k + \theta_k) + N_k \\ &= w_k s_k + N_k \end{aligned}$$

- Security code  $w_k$ :
  - Generalization of binary modulating sequence
  - Either fully encrypted or contains periodic authentication codes
  - Unpredictable to would be spoofer

## Attacking Security-Enhanced GNSS Signals

1. **Meaconing:** Spoof records and re-broadcasts entire block of RF spectrum containing ensemble of GNSS signals

$$Y_k = \alpha w_{k-d} s_{k-d} + N_{m,k} + w_k s_k + N_k$$

2. **Security Code Estimation and Replay (SCER) Attack:** Spoof estimates unpredictable security code chips from authentic signals on-the-fly

$$Y_k = \alpha \hat{w}_{k-d} s_{k-d} + w_k s_k + N_k$$

Wesson, K., M. Rothlisberger, and T. E. Humphreys, "Practical cryptographic civil GPS signal authentication," NAVIGATION, Journal of the Institute of Navigation, 2012, to appear; available at <http://radionavlab.ae.utexas.edu/nma>.

Humphreys, T.E, "Detection Strategy for Cryptographic GNSS Anti-Spoofing," IEEE Transactions on Aerospace and Electronic Systems, 2012, to appear; available at <http://radionavlab.ae.utexas.edu/detstrat>

## What qualities should cryptographic civil GPS signal authentication have?

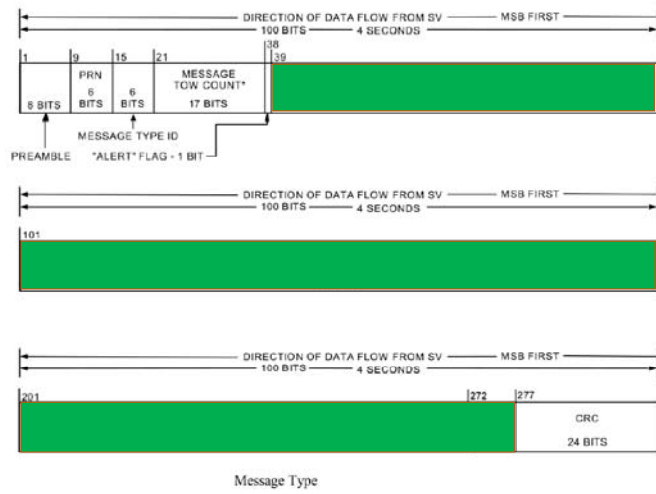
1. **Effective:** they make it difficult for a spoof to carry off a successful spoofing attack
2. **Practical:** they are likely to be implemented and adopted by the GPS community

## A strategy that meets these requirements:

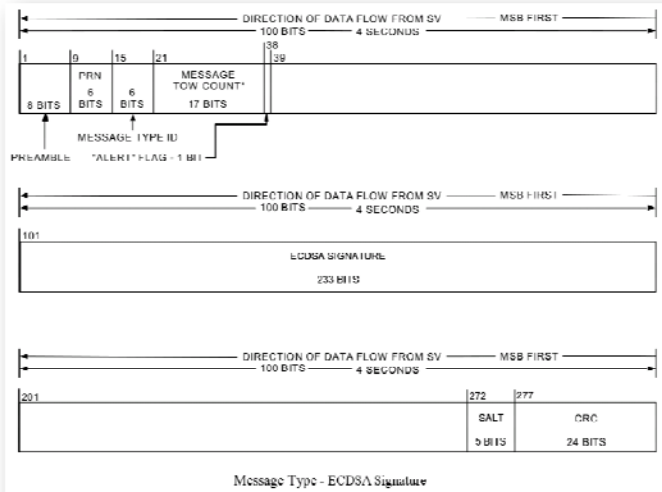
### Navigation Message Authentication (NMA):

- Forms  $w_k$  by making the navigation message periodically unpredictable
- Applies public-key cryptographic digital signature and verification techniques

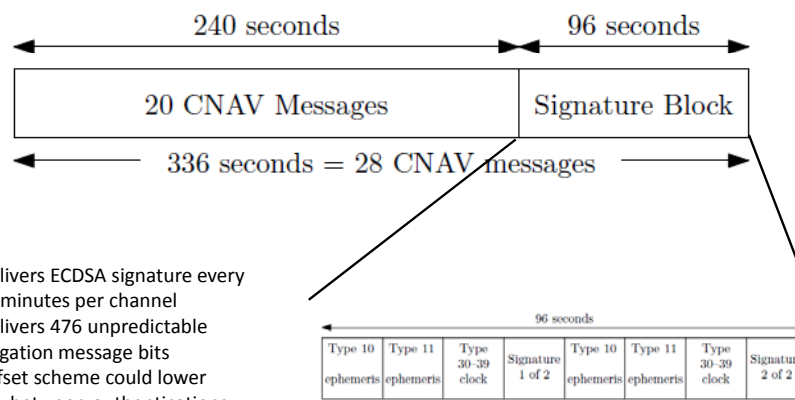
## CNAV Message



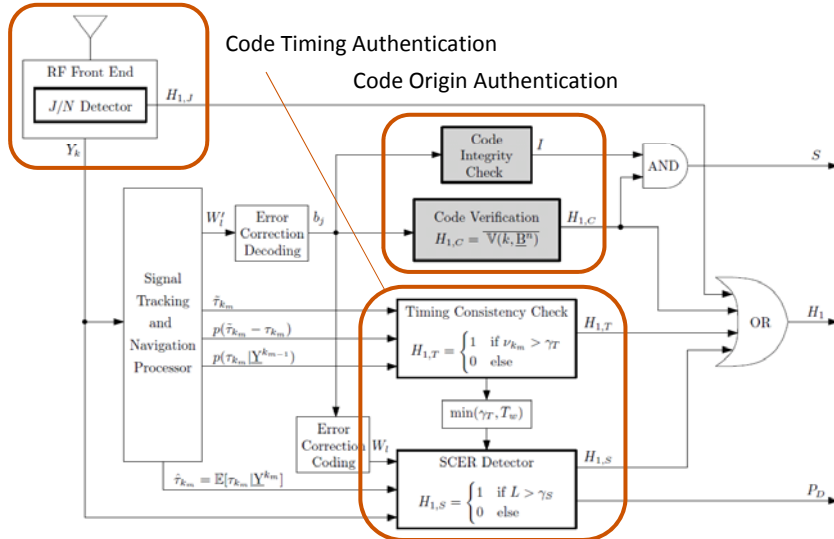
## CNAV ECDSA Message



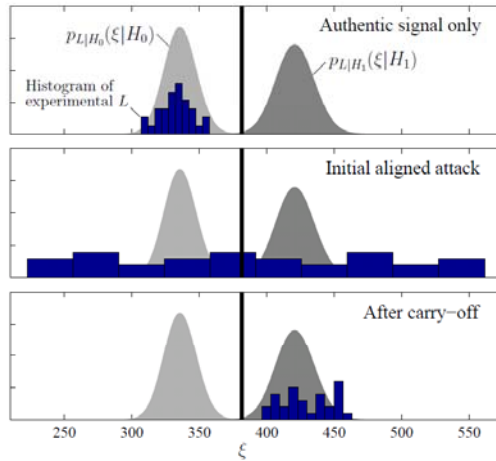
## Signing the CNAV Message



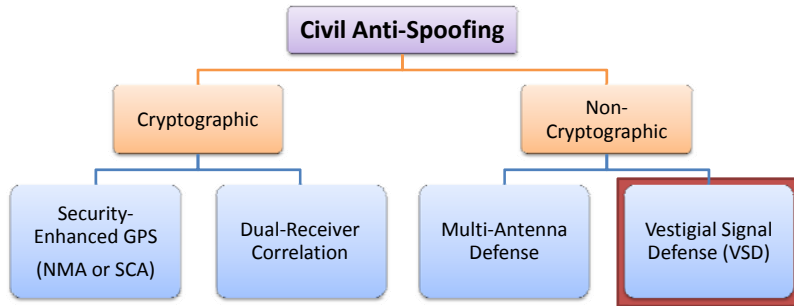
## What does it take to authenticate a GNSS Signal?



## Hypothesis Testing on Security Code



## Types of Civil Anti-Spoofing



Why not cryptographic anti-spoofing?

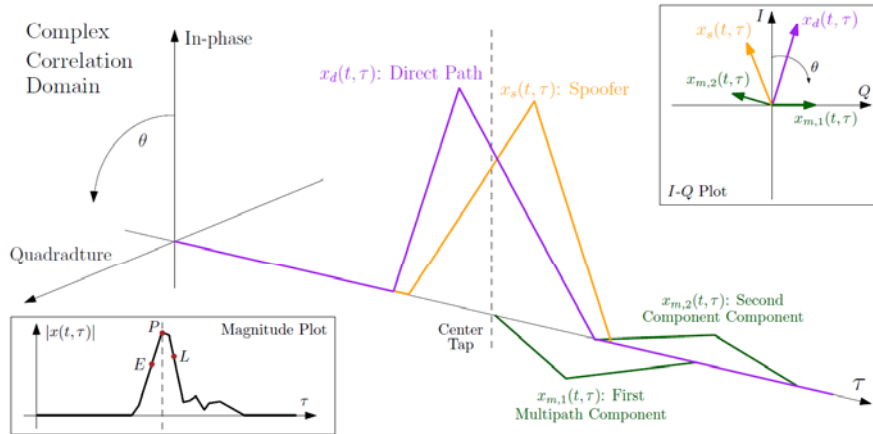
- Requires infrastructure and possibly changes to GPS IS
- Vulnerable to initial phase of spoofing attack

Why VSD?

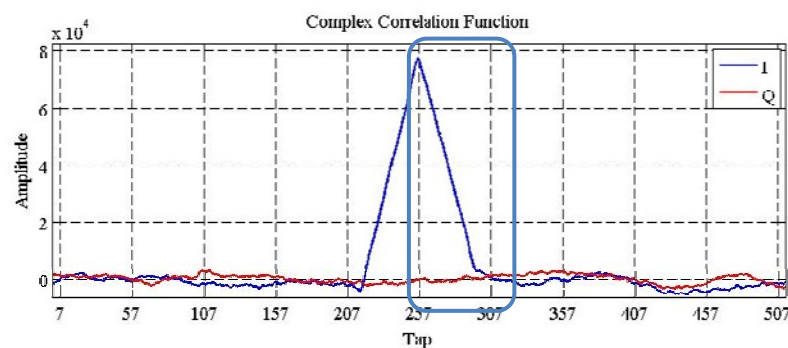
- Implementable today!
- Software-only defense; requires no additional receiver hardware

## Visual: Complex Correlation Domain

$$x(t) = x_d(t) + x_m(t) + x_s(t) + n(t)$$



## Is it Spoofing or Multipath?



## Observations

- Multipath can look like spoofing!
- Spoofing can look like multipath!
- Detecting the difference between spoofing and multipath is difficult!
- **Goal:** reduce the degrees-of-freedom available to a spoofer, making it mimic multipath

## Further Information

The University of Texas at Austin  
Radionavigation Lab Publications

<http://radionavlab.ae.utexas.edu/publications>





## GNSS Signals Workshop Pseudolites

Cillian O'Driscoll

[www.jrc.ec.europa.eu](http://www.jrc.ec.europa.eu)



*Serving society  
Stimulating innovation  
Supporting legislation*



## Pseudolites

Pseudolites, or **pseudo-satellites**, may be loosely defined as ground-based transmitters of GNSS like signals for the purpose of positioning or navigation.

Considered since the earliest days of GNSS, pseudolites (PLs) have the capacity to provide GNSS-like services in locations where GNSS is unavailable or insufficient

**However** there are a number of issues associated with the use of pseudolites which have held up their widespread deployment



## Overview

Pseudolite Applications

Issues

Pseudolite Signal Design

Impact on Non-Participating Receivers

Joint  
Research  
Centre

3



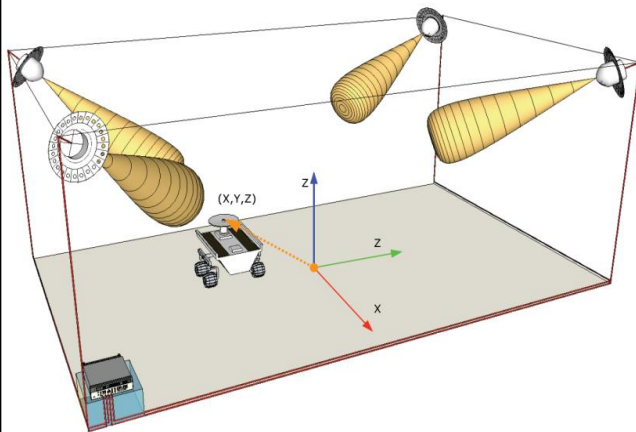
## PSEUDOLITE APPLICATIONS

Joint  
Research  
Centre

4



## Indoor Positioning



Four or more pseudolites are used to locate the user in an indoor environment.

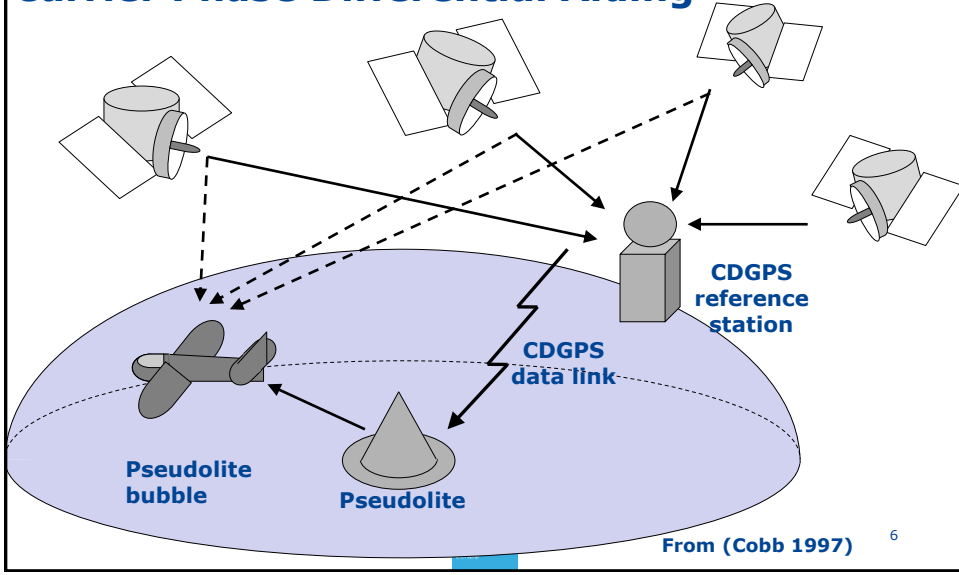
- GNSS augmentation
- Pseudoranges vs. Carrier Phase
- Synchronization

Joint Research Centre

5



## Carrier Phase Differential Aiding



From (Cobb 1997)

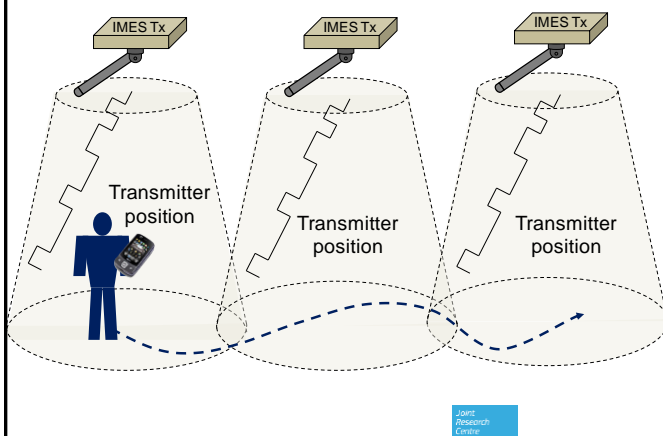
6



## Indoor Messaging System (IMES)

Part of Japanese Quazi-Zenith Satellite System (QZSS) ICD:

- simple concept, simple implementation
- accuracy  $\sim 10$  m



- IMES transmitters continuously broadcast their position
- Tx range is short
- User position approx. equals tx position

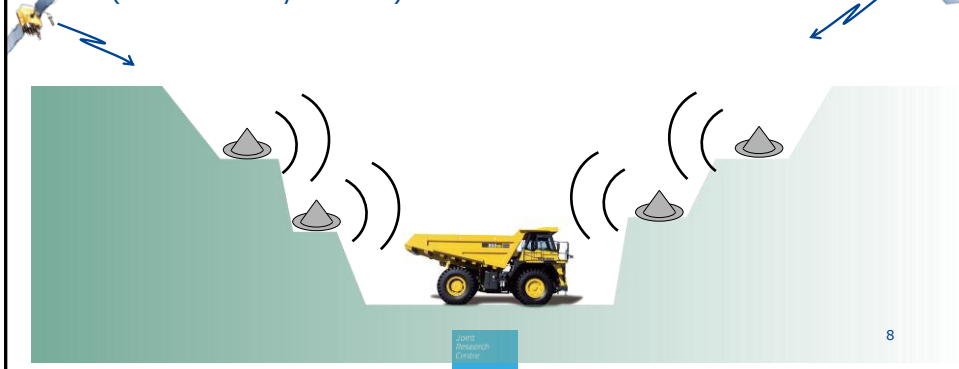
7



## Open Pit Mining

Satellite visibility is reduced  
PLs provide geometry improvements

Market pursued by Novariant Inc  
(now owned by Trimble).



8



## ISSUES



## Issues with PL deployment

- **Legal issues**
  - GNSS bands are reserved for Aeronautical use – not legal in all territories to broadcast ground based signals in these bands.
- **Interference with existing GNSS signals**
  - If GNSS bands are to be used – PLs act like jammers in those bands
- **The “near/far” problem:**
  - Received pseudolite signal powers vary greatly over their operational range
  - Requires large receiver dynamic range
- **Synchronisation**
  - some mechanism must be designed to account for asynchronicity between the pseudolite clocks
- **Monitoring:**
  - the GPS satellites are constantly monitored by a network of ground stations, problems can be quickly identified and isolated, how would the equivalent be managed for a network of pseudolites?



## Legal issues

Many PL proposals require broadcast in the existing GNSS bands

However, these bands are reserved for satellite navigation services

To use them for other purposes may require specific legislation

- In Europe, U.S. and Australia: **illegal** to broadcast in L1 band
- In Japan: **legal** broadcast in L1, provided power levels are below a threshold

Special rights can be granted to broadcast in L1 by regional authorities:

- In Germany a number of Galileo Test Environments (GATEs) have been designated
- In the U.S. during early stages of GPS, testing was performed by placing "satellites" on the ground facing up and flying receivers overhead in jet fighters



## GNSS Interference

If PLs are to transmit in the same bands as GNSS signals there will be some interference between the two systems

Potential ways to reduce this interference (Klein & Parkinson, 1984):

- Pulse the pseudolite signals: interference is limited to the pulse duration
- Frequency offset: either by a fraction of the signal bandwidth, or to an entirely new frequency band
- Alternative code structures: to reduce cross-correlation

Clearly the best method is to move completely out of the GNSS bands, but this complicates receiver designs

➔ Joint PL and GNSS receivers need two front-ends

**Pulsing** the signal is the best option in-band.



## The Near/Far Problem (I/II)

GNSS signals all come from > 20,000 km away



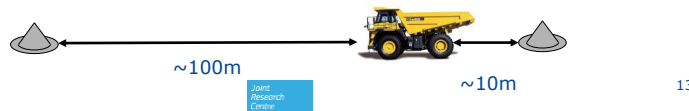
The **dynamic range** (range of largest to smallest received signal power) is low:

$$P \propto \frac{1}{r^2}$$

$$R_{dyn} = \frac{P_{max}}{P_{min}} = \left( \frac{r_{max}}{r_{min}} \right)^2 < 2 \text{ dB}$$

For PL systems, the **absolute range** to the transmitters is **small**, but the **dynamic range is large**:

- eg, for a minimum and maximum distance of 10 m and 100 m resp., the dynamic range is **20 dB**



13



## The Near/Far Problem (II/II)

What is the problem with having a large dynamic range?

Requires the **receiver** to have a large dynamic range

- ➔ Large number of bits in the ADC in order to represent the weakest signal accurately when the strongest signal is present
- ➔ More bits = more computation = more power = shorter battery life
- ➔ Existing GNSS receivers have low dynamic range (1 to 3 bits typically)
  - ➔ Problem for compatibility with GNSS signals, high power PL signals will completely dominate a non-participating receiver

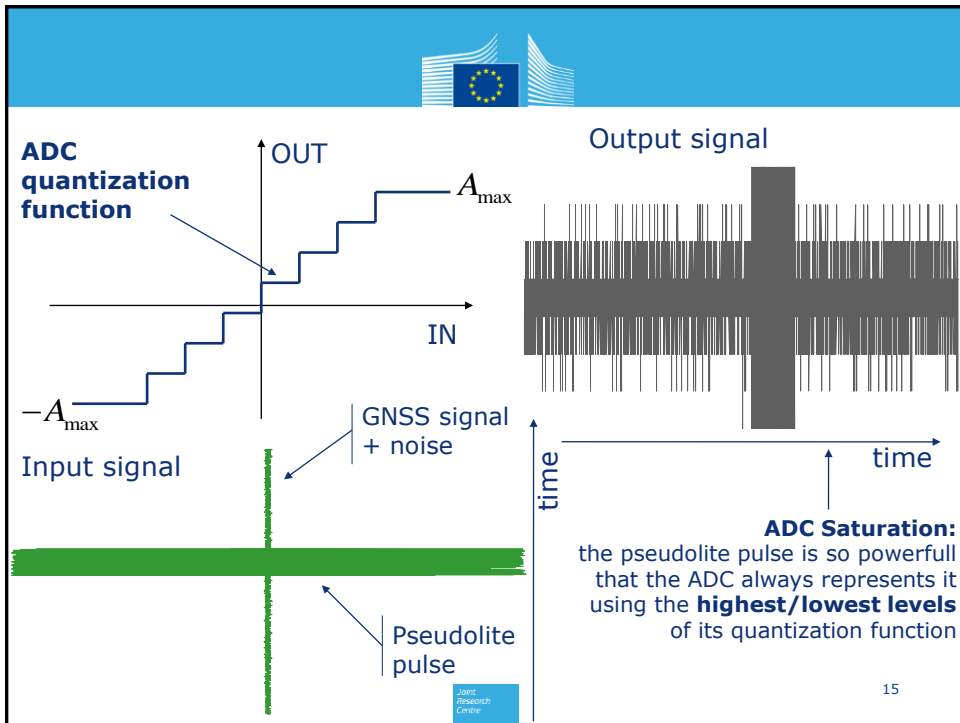
Again, **pulsing** can help overcome this problem

- ➔ During a pulse, strong signal saturates the ADC and weaker signals are completely masked
- ➔ Otherwise weak signals are represented as normal

Illustrated on following slide.



14



## Synchronisation

For one-way ranging synchronisation of the transmitters is vital

How to achieve this for a distributed network of ground based PLs?

- Co-locate PL and GNSS receiver → PL synchronises to GNSS time (e.g. RTCA, RTCM)
- Operate in differential mode: requires a reference receiver to determine and broadcast corrections (e.g. Novariant)
- Network synchronisation of PLs: arbitrary choice of “master” PL, other PLs synchronise to master or to any PL which is synchronised to the master (e.g. Locata)
- Use a completely asynchronous scheme (e.g. IMES)

Joint Research Centre

16



## Monitoring

As we have seen, GNSS typically have a network of ground stations constantly monitoring the satellites: noting errors, updating ephemeris and clock models and issuing commands

What is the equivalent for PLs?

Who monitors PLs for

- Accuracy of placement (equivalent to satellite ephemeris)
- Power levels – are the PLs meeting the regulations
- Total aggregate power – not just individual PLs but the sum total of all power from all PLs in a given geographic region

These issues are of particular concern for the case of broadcast in the GNSS bands



## PSEUDOLITE SIGNAL ASPECTS



## Requirements for PL Signals

PL signals must meet requirements for

- Ranging
- Data transmission
- Compatibility with existing services
- Near/far tolerance (limited receiver dynamic range)
- Multi-access

Signal model: very similar to GNSS with the (possible) addition of a pulse train

$$y_i(t) = \sqrt{2C_i} p_i(t) d_i(t) s_i(t) c_i(t) \cos(2\pi f_i t + \varphi_i) = p_i(t) s_{p,i}(t)$$



Joint Research Centre

19

## Impact on Non-participating Receivers

Simple model of the non-participating GNSS receiver:

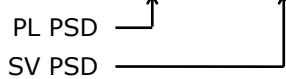
Receiver **correlates** received signal with local replica

Leads to an equivalent increase in the noise power spectral **density** of

$$I_0 = \kappa C_{PL}$$

Where:

- $\kappa = \int_{-\infty}^{\infty} G_{PL}(f - \delta f) G_{SV}(f) df$  - the **spectral separation coefficient** (SSC) between PL and SV



- $C_{PL}$  is the PL power

To limit impact on non-participating receivers → find ways to decrease SSC  $\kappa$

Joint Research Centre

20



## Aspects to Consider

Three primary considerations for PL signals

- Frequency band
- Code selection
- Pulsing scheme

Other considerations

- Power levels
- Polarization



## Choices of Frequency Band

Historically most commonly desired band for PL signals has been the GPS L1 band

- ➔ Ease of integration with existing GNSS receivers
- ➔ Seamless navigation between GNSS and PL

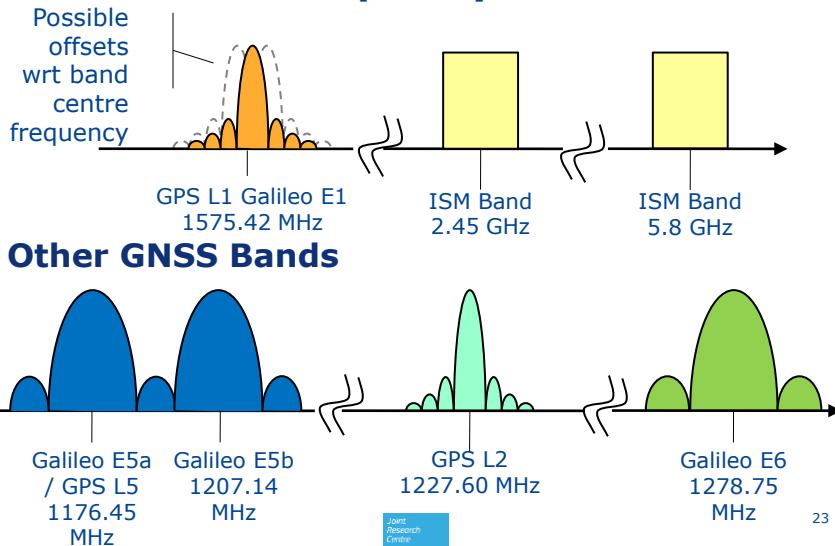
In recent years the Industrial, Scientific and Medical (**ISM**) bands have been increasingly considered

- ➔ No licensing requirements
- ➔ Avoid interference with existing GNSS receivers

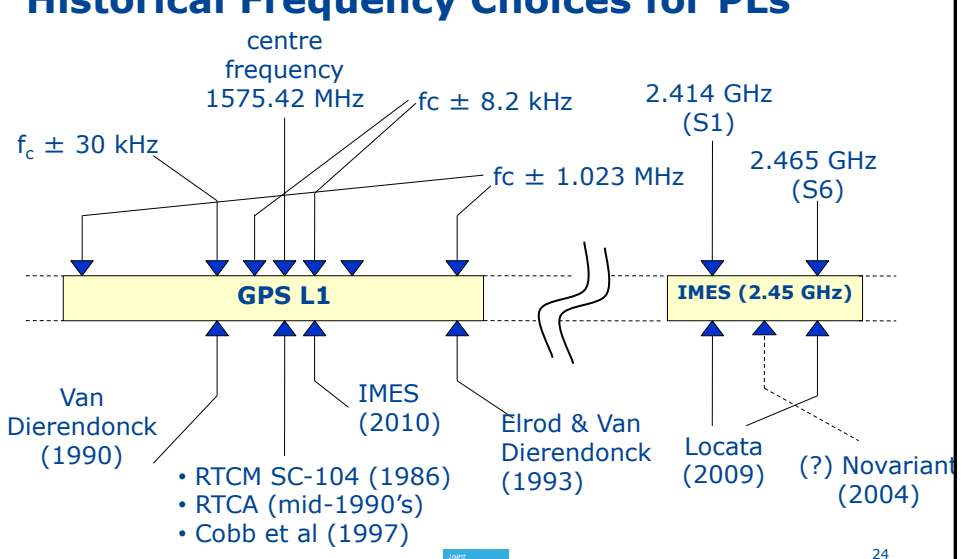
Even if a GNSS band is chosen a small **frequency offset** with respect to the GNSS centre frequency may be chosen to reduce the impact on GNSS signals



## Some Possible Frequency Bands



## Historical Frequency Choices for PLs

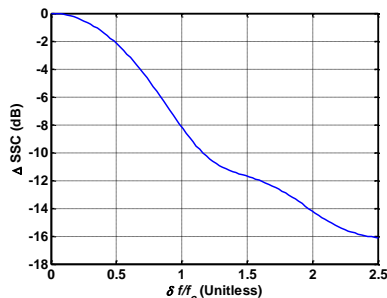




## Impact of In-Band Frequency Offsets

By offsetting the PL signal from the GNSS centre frequencies, three ends can be achieved:

1. Reduction in the SSC
2. Ensure that relative code phase changes rapidly → more "noise like" effect of the PL on the SV signal
3. Make it unlikely that false acquisitions occur



**Example:** Impact of frequency offset on SSC between two BPSK( $f_c$ ) signals

$$\Delta \text{SSC} = \frac{\text{SSC}(\delta f)}{\text{SSC}(0)}$$

Note that  $\delta f$  must be a significant fraction of  $f_c$  before the effect is noticeable

Joint Research Centre

25



## Signal Pulsing

Pulsing is the most effective way to limit the near/far effect

In essence the signal is transmitted for only a small percentage (the pulse duty cycle, PDC) of the full code period

Takes advantage of limited dynamic range of GNSS receivers:

- During the pulse: receivers saturate
- The saturation level determines the maximum PL power that enters the receiver
- Once the receiver saturates then further increases in PL power have no additional impact on the receiver
- Multiple PLs can operate with different pulse sequences: a form of **time-division multiple access (TDMA)**

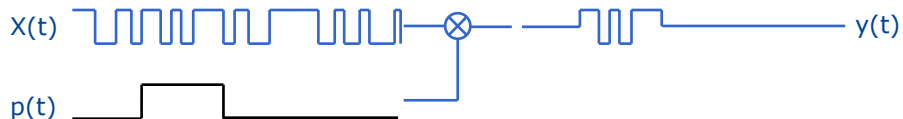
Joint Research Centre

26



## Overview of Pulsing

The basic idea is to multiply a **GNSS-like** signal by a pulse of short duration



A **pulsing scheme**, or pulse pattern, determines which subsequences of the spreading code get transmitted at any instant in time



Pulsing scheme must be carefully chosen to avoid altering the **spectrum** of the GNSS-like signal:

$$G_y(f) = G_X(f) * G_p(f)$$

**Goal:** To have an **impulse-like** spectrum for the pulse sequence



## Desirable Properties of a Pulsing Scheme

A good pulsing scheme should:

- Ensure minimal impact on the spectrum of the transmitted signal
- Ensure a sufficiently large subset of the spreading code is transmitted in each integration interval to minimise cross-correlation effects
- For multi-access: provide a family of pulsing schemes with low probability of pulse overlap
- For multi-access: ensure the maximum aggregate duty cycle does not exceed some threshold



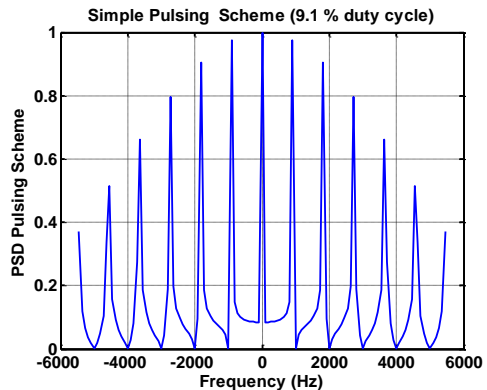
## Naïve Pulsing Scheme: GPS L1 C/A

C/A Code Cycles	Slot No.										
	1	2	3	4	5	6	7	8	9	10	11
1	X										Y
2		X									Y
3			X								Y
4				X							Y
5	Y			X							
6	Y				X						
7	Y					X					
8		Y					X				
9			Y					X			
10				Y					X		
11					Y					X	
12	X										Y
13	X										Y
14	X										Y
15		X									Y
16	Y			X							
17	Y				X						
18		Y				X					
19			Y				X				
20				Y				X			
21					Y				X		
22						Y				X	
23							Y				
⋮											

X = PL<sub>1</sub> Pulses, Y = PL<sub>2</sub> Pulses, etc.

Simple TDMA scheme: 11 slots (93 chips per slot) – only one slot “on” in each ms. Active slot increments by one each code period

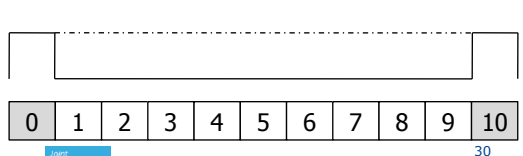
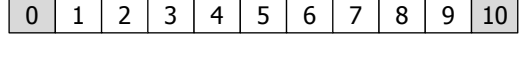
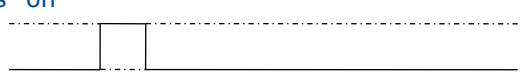
Very poor spectral properties



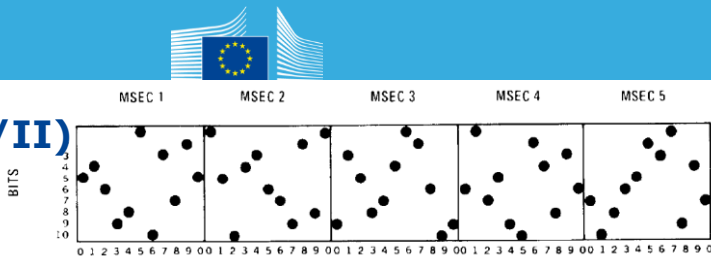
## RTCM: (I/II)

In the early to mid 1980's the Radio Technical Commission for Maritime Services (RTCM) in the U.S. defined a PL system based on the GPS L1 C/A code

- A 10 % duty cycle was proposed.
- Each 1 ms code period was divided into 11 **slots**, 93 chips per slot
- In each ms only one slot was “on”
- **Except** when slot 0 was on, at which time slot 10 was also transmitted
- Average duty cycle = 10 %
- The pulse pattern was pseudorandom
- Not designed for multi-access



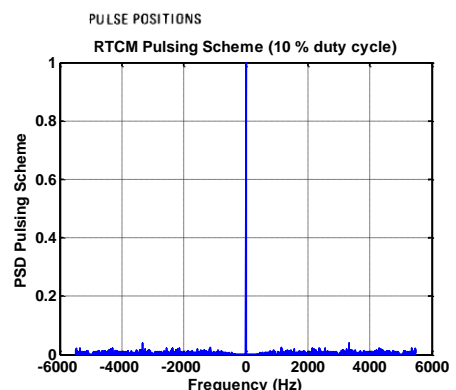
## RTCM: (II/II)



Sample pulse locations are shown above

The pseudorandom nature of the pattern leads to the PSD as shown on the right

Overall this was a good design  
But limited due to lack of multi-access considerations



From Thomas A. Stansell "RTCM SC-104 Recommended Pseudolite Signal Specification", NAVIGATION: Journal of The Institute of Navigation, Vol 33, No. 1, Spring 1986

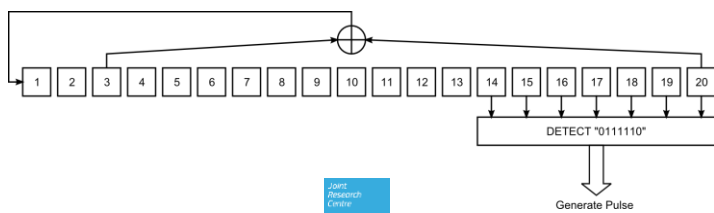
## RTCA: (I/II)

In the 1990's the Radio Technical Commission for Aeronautics started an investigation of Airport Pseudolites (APL) for Local Area Augmentation Systems (LAAS) in the L1 band

Based on a wideband BPSK(10) signal similar to the GPS P-code

Pulsing was proposed with a low duty cycle of between 2 and 4 %

Pulse pattern was based on a random stream generator, rather than on block method used for RTCM:



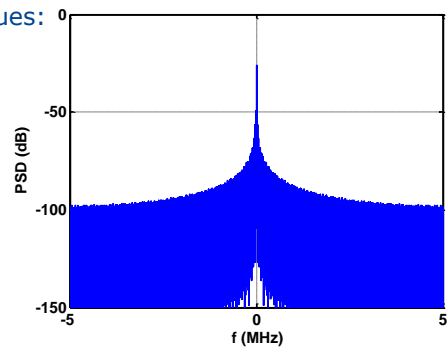
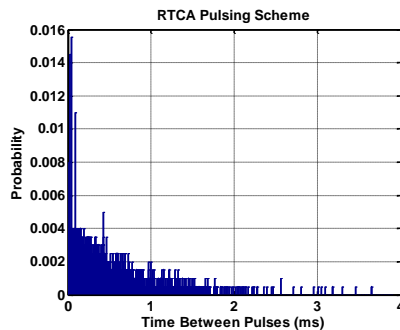


## RTCA: (II/II)

The sequence has excellent spectral properties

However, there were some serious issues:

- Frequent spells of > 1 ms with **no pulses**
- Longest period up to 3 ms without pulses



Ultimately RTCA abandoned the APL concept

33



## Locata

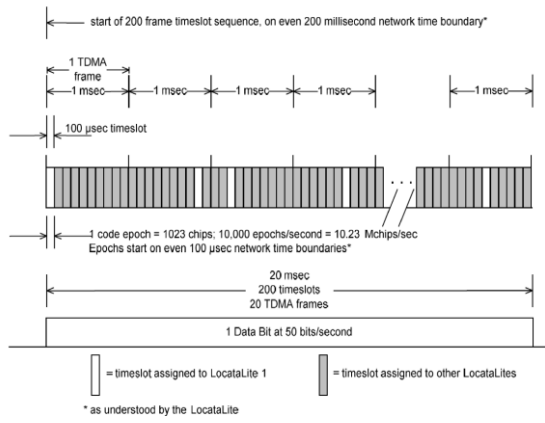
In 2011 Locata Corp of Australia released an Interface and Control Document (ICD) for their ground based GNSS Augmentation system

Locata signals are broadcast in the ISM bands

→ Avoid interference with GNSS

Signals are GPS C/A codes clocked at 10 times the chipping rate - BPSK(10)

A block pulsing scheme is applied: similar to RTCM **but** allowing for TDMA access of up to 10 "LocataLites" in each geographic region



Joint Research Centre

34



## RECEIVER ASPECTS

Joint  
Research  
Centre

35



## Overview

It is important to understand the impact the deployment of a PL system would have on:

- A. Existing (non-participating) GNSS receivers
- B. Receivers designed to process PL signals

To do so, we require a model of the receiver and a metric to use as an evaluation tool

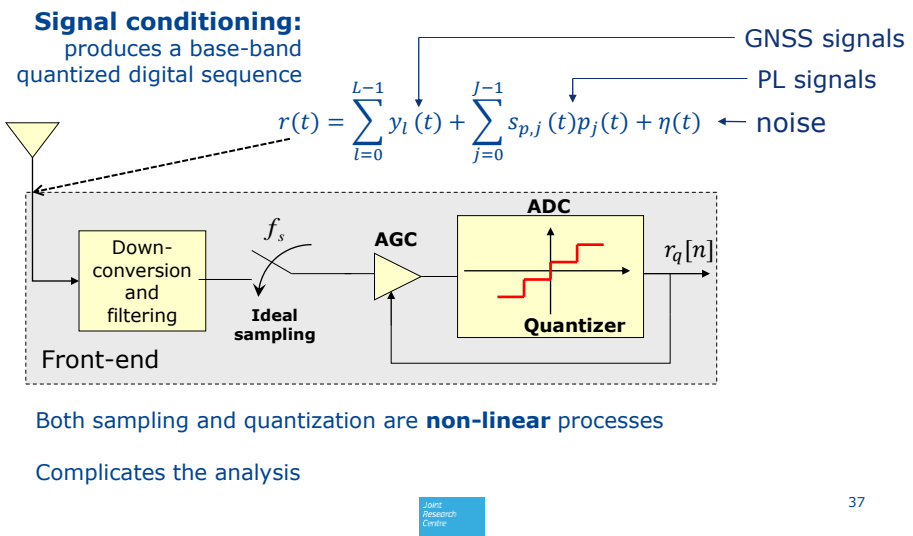
The  $C/N_0$  is a useful metric, though it must be remembered that this single number does not tell us everything, ultimately **navigation performance** is what is critical

Joint  
Research  
Centre

36



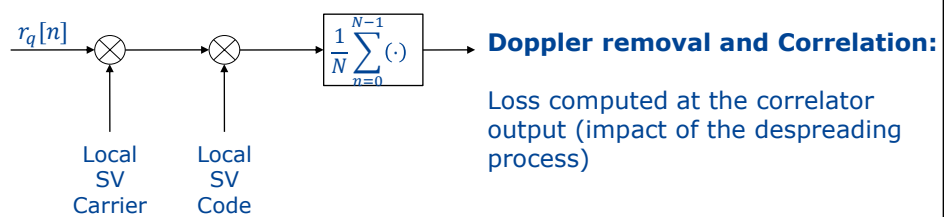
## Receiver Model: (I/II) The Front-End



## Receiver Model: (II/II) Correlation

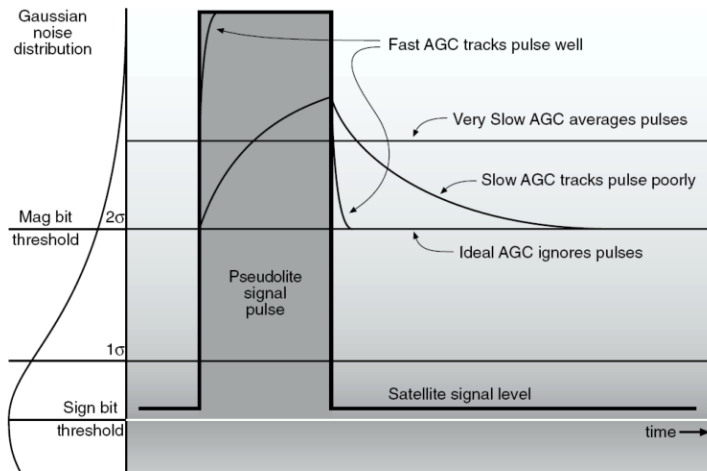
Once the signal has been down-converted and digitised, each tracking channel performs:

- A frequency shift to remove the carried Doppler
- Correlation with a local replica of the desired ranging code





## AGC Types



From H. Stewart Cobb. GPS pseudolites: Theory, Design and Applications. Phd thesis, Stanford University, 39  
<http://waas.stanford.edu/www/papers/gps/PDF/Thesis/StuCobbThesis97.pdf>, September 1997.



## Modelling the Quantizer

For simplicity we can assume there is only one GNSS signal and one PL signal.

Assuming an ideal or very slow AGC then the AGC gain can be assumed constant

Leading to the following non-linear model:

$$r_q[n] = Q_B(A_g y_{IF}[n] + A_g s_{p,IF}[n]p[n] + A_g \eta_{IF}[n])$$

Annotations for the equation:

- ADC quantization function
- AGC gain (**constant!**)
- Down-converted and sampled GNSS signal (**single component!**)
- Down-converted and sampled pseudolite signal
- Noise



## ADC Losses: Small Signal Model

In performing the conversion from analogue signal to digital there is inevitably some loss of information

Under the condition that the thermal noise at the input to the ADC is greater than all other signal components combined, it can be shown that this loss is given by an equivalent C/N<sub>0</sub> loss of:

$$L_q = \frac{2}{\pi} \frac{\left(1 + 2 \sum_{i=1}^{2^B-1} \exp\left\{-\frac{i^2}{2 A_g^2 \sigma_{IF}^2}\right\}\right)^2}{1 + 8 \sum_{i=0}^{2^B-1} i \operatorname{erfc}\left(\frac{i}{\sqrt{2} A_g \sigma_{IF}}\right)}$$

- $B$  is the number of bits in the ADC
- $A_g$  is the AGC gain (assumed constant – very slow AGC)
- $\sigma_{IF}^2$  is the noise power at IF =  $N_0 B_{eq}$



## Small Signal Model of Receiver Losses

When the PL signal power is much less than the noise power in the receiver front-end, then the small signal model applies

The quantization losses affect GNSS and PL signals in the same way

The excess loss in C/N<sub>0</sub> experienced by a GNSS signal in the presence of PL signal is given by:

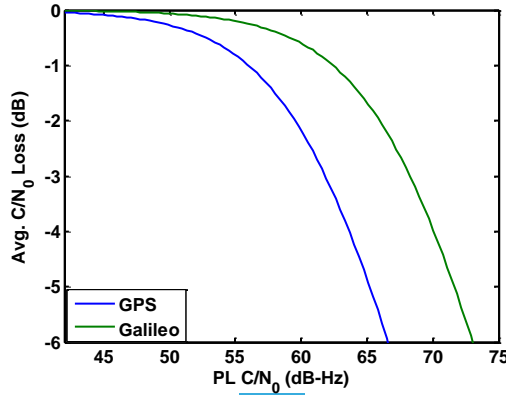
$$L_{ss} = \frac{1}{1 + L_q \left. \frac{C_p}{N_0} \right|_{eff} \kappa}$$

- $\left. \frac{C_p}{N_0} \right|_{eff} = d \left. \frac{C_p}{N_0} \right|_{peak}$  is the **effective** PL C/N<sub>0</sub> and  $d$  is the duty cycle
- $\kappa$  is the spectral separation coefficient as defined previously



## Example: GPS L1 C/A PL – 9.3 % duty cycle

The plot shows the modeled small signal losses for a receiver processing both GPS and Galileo signals – the difference arises due to difference in SSC



43

Joint Research Centre

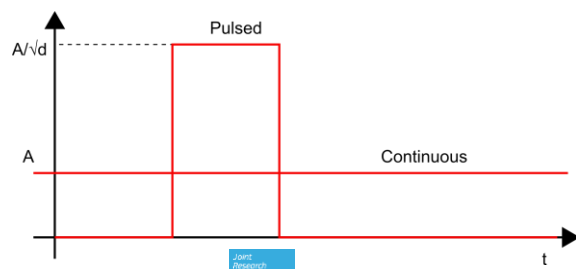


## A Note on Effective C/N<sub>0</sub>

Fair comparison between pulsed and continuous PLs requires use of effective pseudolite signal to noise density ratio (C/N<sub>0</sub>)

$$\left. \frac{C}{N_0} \right|_{\text{eff}} = d \left. \frac{C}{N_0} \right|_{\text{peak}}$$

The following signals have equal effective C/N<sub>0</sub>:



44



## Saturation Model: (I) - ADC

In saturation mode we have a two-part model

1. During the pulse the output of the ADC  $\in \{\pm A_{max}\}$
2. Otherwise the signal contains quantised signal plus noise as usual

$$r_q[n] = Q_B(A_g y_{IF}[n] + A_g \eta_{IF}[n])(1 - p[n]) + A_{max} \text{sign}(s_{p,IF}[n])p[n]$$

**Signal blanking:** useful signal and noise blanked by the pseudolite component

The pseudolite signal is effectively represented using a single bit

Note: during the pulse, the ADC output contains **no information** on the weaker signals → completely masked by the pulse



## Saturation Model of Receiver Losses

The following formula for the C/N<sub>0</sub> loss can be derived based on the previous model:

$$L_{sat} = \frac{(1-d)^2}{(1-d) + k_a \frac{1}{T_s} g(B, A_g) d}$$

**Noise Blanking:** Loss in noise power during pulse

**Effective PL Power:** On saturation: maximum PL power is clipped

**Signal Blanking:** Loss in carrier power during pulse

The **saturation** pseudolite C/N<sub>0</sub> is a function of the receiver front-end and the duty cycle. In general:

- More bits → greater C/N<sub>0</sub> loss
- More bandwidth  
→ greater C/N<sub>0</sub> loss

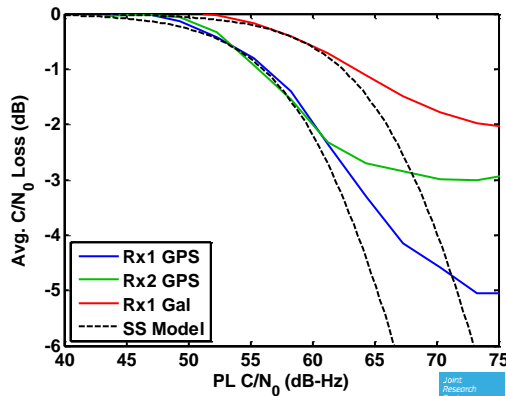
$$g(B, A_g) = \frac{(2^B - 1)^2}{1 + 8 \sum_{i=0}^{2^B-1-1} i \operatorname{erfc}\left(\frac{i}{\sqrt{2} A_g \sigma_{IF}}\right)}$$



## Example: GPS L1 C/A PL – 9.3 % duty cycle

Same as previous example. This time including data measured from two receivers:

1. Rx1 – GPS and Galileo capable – survey grade receiver
2. Rx2 – GPS only – high sensitivity receiver



### Notes:

- Pulsing **limits** maximum  $C/N_0$  loss
- Signal structure gives extra protection:
  - ➔ Galileo signal less affected
- Saturation loss greater for survey grade receiver
  - ➔ wider bandwidth?
  - ➔ more bits?

47



## SUMMARY



## Summary

Pseudolites have the potential to provide GNSS-like service in regions where GNSS is degraded or unavailable

However, there are many issues that need to be overcome, not least of which are regulatory issues, interference and the near/far effect

Careful signal design can help overcome some of the interference and near/far effect issues

However, in-band pseudolites **will** act as GNSS jammers, no matter how well designed the signal, there will be some deleterious effect



## REFERENCES



## Review References:

Cobb, H. S. (1997), 'GPS Pseudolites: Theory, Design, and Applications', PhD thesis, Stanford University.

Elrod, B. D. & Van Dierendonck, A. (1996), Pseudolites, *Chapter 2 in Bradford W. Parkinson & James J. Spilker, Jr., ed., 'Global Positioning System: Theory and Applications'*, vol II, AIAA, , pp. 51--80.

Kanli, M. O. (2004), Limitations of Pseudolite Systems Using Off-The-Shelf GPS Receivers, in '*Proceedings of the 2004 International Symposium on GNSS/GPS*'.

O'Driscoll, C.; Borio, D. & Fortuny-Gausch, J. (2011), 'Scoping Study on Pseudolites'(JRC64608), Technical report, Joint Research Centre (JRC) of the European Commission.

Rizos, C. (2005), Pseudolite Augmentation of GPS, in '*Workshop on Geolocation Technology to Support UXO Geophysical Investigations*'.



51



## References for Specific PL Systems

### RTCM:

Stansell, Jr, T. A. (1986), 'RTCM SC-104 Recommended Pseudolite Signal Specification', *Navigation: Journal of the Institute of Navigation* **33(1)**, 42--59.

### RTCA:

Van Dierendonck, A. J.; Fenton, P. & Hegarty, C. (1997), Proposed Airport Pseudolite Signal Specification for GPS Precision Approach Local Area Augmentation Systems, in '*Proceedings of ION GPS 97*'.

### Novariant:

Zimmerman, K. R.; Cohen, C. E.; Lawrence, D. G.; Montgomery, P. Y.; Cobb, H. S. & Melton, W. C. (2000), Multi-Frequency Pseudolites for Instantaneous Carrier Ambiguity Resolution, in '*Proceedings ION GPS 00*', pp. 1024 -- 1033.

### Locata:

Locata Corp (2011), 'LocataNet Positioning Signal Interface Control Document', Technical report, Locata Corporation. <http://www.locatacorp.com/icd/>



52



## References on the Signal Model

- Borio, D.; O'Driscoll, C. & Fortuny-Gausch, J. (2011), Pulsed pseudolite signal effects on non-participating GNSS receivers, *in 'Proceedings of IPIN 2011'*.
- Borio, D.; O'Driscoll, C. & Fortuny-Gausch, J. (2011), Impact of Pseudolite Signals on Non-Participating GNSS Receivers, *in 'Proceedings of ENC 2011'*.
- Van Dierendonck, A. J.; Fenton, P. & Hegarty, C. (1997), Proposed Airport Pseudolite Signal Specification for GPS Precision Approach Local Area Augmentation Systems, *in 'Proceedings of ION GPS 97'*.